

BOEING

CR-151666
D180-22876-2

NAS9-15196
DRL T-1346
DRD MA-664T
LINE ITEM 3

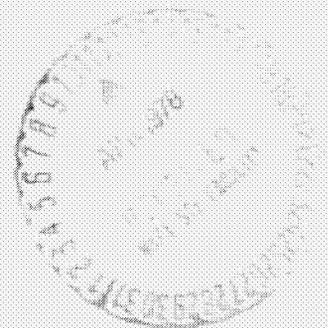
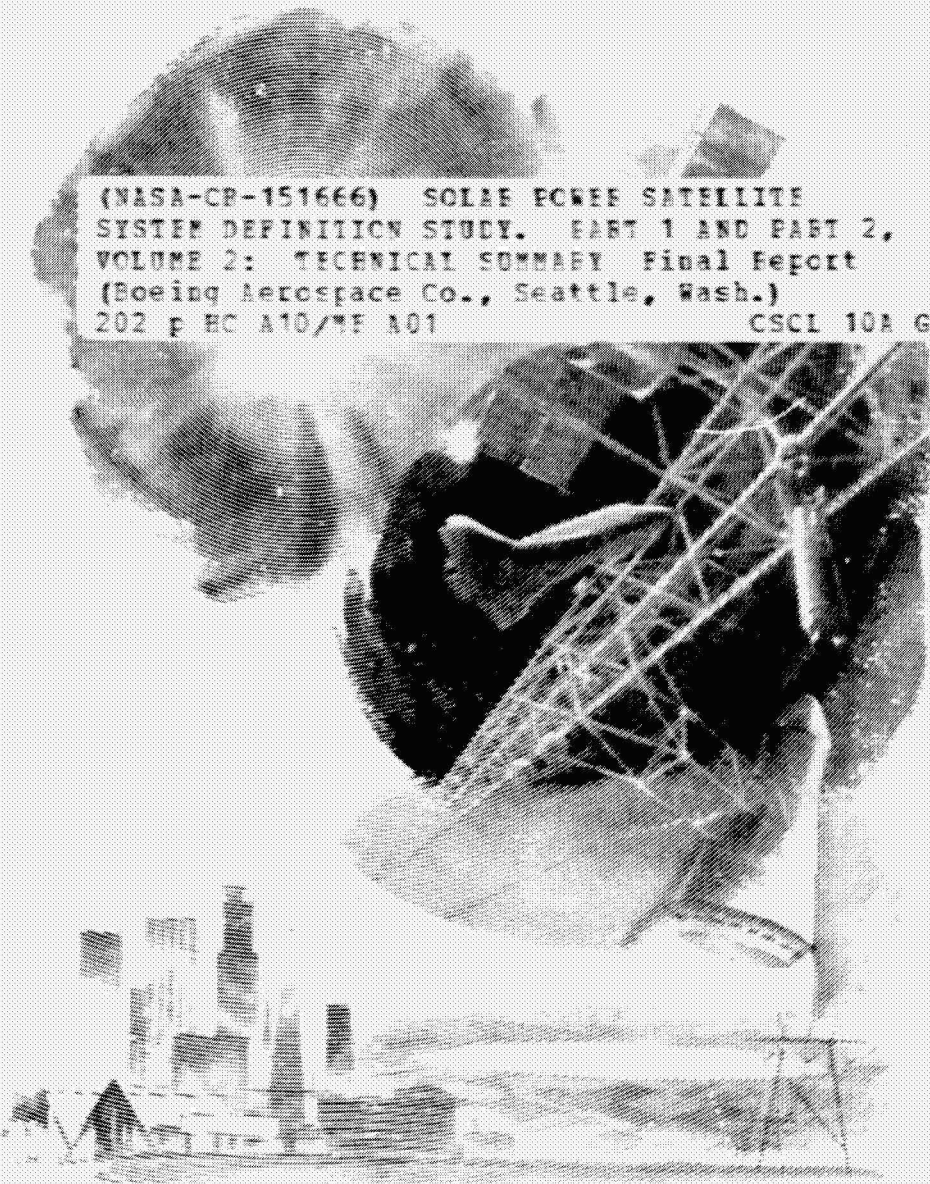
**Volume II
Technical Summary**

(NASA-CR-151666) SOLAR POWER SATELLITE
SYSTEM DEFINITION STUDY. PART 1 AND PART 2,
VOLUME 2: TECHNICAL SUMMARY Final Report
(Boeing Aerospace Co., Seattle, Wash.)
202 p HC A10/TF A01

N78-20156

Unclass
09493

CSCI 10A G3/15



Solar Power Satellite

SYSTEM DEFINITION STUDY
PART I AND PART II

D180-22876-2

CONTRACT NAS9-15196
DRL T-46
DRD MA-664T
LINE ITEM 3

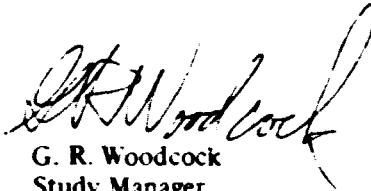
Solar Power Satellite

SYSTEM DEFINITION STUDY PART I AND PART II

VOLUME II
TECHNICAL SUMMARY
D180-22876-2
DECEMBER 1977

Submitted To
The National Aeronautics and Space Administration
Lyndon B. Johnson Space Center
in Fulfillment of the Requirements
of Contract NAS9-15196

Approved:


G. R. Woodcock
Study Manager

BOEING AEROSPACE COMPANY
MISSILES AND SPACE GROUP—SPACE DIVISION
P.O. BOX 3999
SEATTLE, WASHINGTON

FOREWORD

The SPS system definition study was initiated in December 1976. Part I was completed on May 1, 1977. Part II technical work was completed October 31, 1977.

The study was managed by the Lyndon B. Johnson Space Center (JSC) of the National Aeronautics and Space Administration (NASA). The Contracting Officer's Representative (COR) was Clarke Covington of JSC. JSC study management team members included:

Dickey Arndt	Microwave System Analysis	Andrei Konradi	Space Radiation Environment
Harold Benson	Cost Analysis	Jim Kelley	Microwave Antenna
Bob Bond	Man-Machine Interface	Don Kessler	Collision Probability
Jim Cioni	Photovoltaic Systems	Lou Leopold	Microwave Generators
Hu Davis	Transportation Systems	Lou Livingston	System Engineering and
R. H. Dietz	Microwave Transmitter and Rectenna	Jim Meany	MPTS Computer Program
Bill Dusenbury	Energy Conversion	Stu Nachtwey	Microwave Biological Effects
Bob Gundersen	Man-Machine Interface	Sam Nassiff	Construction Base
Alva Hardy	Radiation Shielding	Bob Ried	Structure and Thermal Analysis
Buddy Heineman	Mass Properties	Jack Seyl	Phase Control
Lyle Jenkins	Space Construction	Bill Simon	Thermal Cycle Systems
Jim Jones	Design	Fred Stebbins	Structural Analysis
Dick Kennedy	Power Distribution		

The study was performed by the Boeing Aerospace Company. The Boeing study manager was Gordon Woodcock. Boeing Commercial Airplane Company assisted in the analysis of launch vehicle noise and overpressures. Boeing technical leaders were:

Ottis Bullock	Structural Design	Don Grim	Electrical Propulsion
Vince Caluori	Photovoltaic SPS's	Henry Hillbrath	Propulsion
Bob Conrad	Mass Properties	Dr. Ted Kramer	Thermal Analysis and Optics
Eldon Davis	Construction and Orbit-to-Orbit Transportation	Frank Kilburg	Alternate Antenna Concepts
Rod Darrow	Operations	Walt Lund	Microwave Antenna
Owen Denman	Microwave Design Integration	Keith Miller	Human Factors and Construction Operations
Hal DiRamio	Earth-to-Orbit Transportation	Dr. Ervin Nalos	Microwave Subsystem
Bill Emsley	Flight Control	Jack Olson	Configuration Design
Dr. Joe Gauger	Cost	Dr. Henry Oman	Photovoltaics
Jack Gewin	Power Distribution	John Perry	Structures
Dan Gregory	Thermal Engine SPS's	Scott Rathjen	MPTS Computer Program Development

The General Electric Company Space Division was the major subcontractor for the study. Their contributions included Rankine cycle power generation, power processing and switchgear, microwave transmitter phase control and alternative transmitter configurations, remote manipulators, and thin-film silicon photovoltaics.

Other subcontractors were Hughes Research Center—gallium arsenide photovoltaics; Varian—klystrons and klystron production; SPIRE—silicon solar cell directed energy annealing.

D180-22876-2

This report was prepared in 8 volumes as follows:

- | | | | |
|------------|---|-------------|---|
| I | - Executive Summary | V | - Space Operations |
| II | - Technical Summary | VI | - Evaluation Data Book |
| III | - SPS Satellite Systems | VII | - Study Part II Final Briefing Book |
| IV | - Microwave Power Transmission Systems | VIII | - SPS Launch Vehicle Ascent and Entry Sonic Overpressure and Noise Effects |

D180-22876-2

Table of Contents

Section	Page
1.0 INTRODUCTION	1
1.1 ENERGY NEEDS	1
1.2 THE SPS CONCEPT	2
1.3 SPS STATUS	5
1.4 STUDY DESCRIPTION	-
1.4.1 Division of Effort	7
1.4.2 Study Objectives	7
1.4.3 Guidelines & Assumptions	8
2.0 SYNOPSIS OF STUDY RESULTS	9
2.1 FINDINGS	9
2.2 DESIGN EVOLUTIONS	9
2.2.1 Configurations	9
2.2.2 Mass Histories	12
3.0 STUDY ACCOMPLISHMENTS & RESULTS	15
3.1 PART I ISSUES	15
3.1.1 Energy Conversion	15
3.1.2 Construction Location	21
3.1.3 Part II Findings Relative to Part I Issues	22
3.2 MAIN PART II RESULTS	23
3.2.1 Microwave Power Transmission	23
3.2.2 Photovoltaic SPS Designs	50
3.2.3 Thermal Engine SPS's	83
3.2.4 Space Construction & Transportation Operations	103
3.2.5 Uncertainty Analyses	146
3.2.6 SPS Costs	155
4.0 TECHNOLOGY VERIFICATION NEEDS	181
4.1 GROUND-BASED (NONFLIGHT) TECHNOLOGY VERIFICATIONS	181
5.0 DISCUSSION OF SPS PLANNING ISSUES	193

D180-22876-2

List of Figures

Figure	Title	Page
1-1	Applicability: The U.S. Can Effectively Electrify.....	3
1-2	Energy Problems Are Causing a U.S. Economic Crisis.....	4
1-3	Space Solar Power Concept.....	4
1-4	Major Program Elements.....	6
2-1	SPS System Definition Study Design Evolutions.....	10
2-2	Reference Photovoltaic SPS Estimate History.....	13
2-3	Reference Thermal Engine SPS Mass Estimate History.....	14
3.1-1	Energy Conversion Comparison SPS Size.....	16
3.1-2	Energy Conversion Comparison SPS Mass.....	16
3.1-3	Reduction in Gallium Required for CR> 2 System.....	18
3.1-4	Cost Differential Factors as Determined by Study Part I.....	20
3.1-5	Photovoltaic Preference is Sensitive to Solar Blanket Costs.....	24
3.2.1-1	Transmitter Beam Spatial Distribution.....	26
3.2.1-2	Spacetenna Size & Power Density Required for Fixed Rectenna Size & Power Output.....	28
3.2.1-3	Sidelobe Distributions for Fixed Rectenna Constraints.....	28
3.2.1-4	The Microwave Beam: A Safe Power Carrier.....	29
3.2.1-5	Spacetenna Pattern.....	29
3.2.1-6	Microwave Power Transmitter Design Concept.....	31
3.2.1-7	70 Kw Klystron.....	33
3.2.1-8	Cathode Emission Data.....	33
3.2.1-9	Waveguide.....	35
3.2.1-10	Power Taper Integration.....	35
3.2.1-11	MPTS Power Distribution System Block Diagram.....	36
3.2.1-12	Alternate Array Candidates.....	36
3.2.1-13	MPTS-Reference 10 dB Taper.....	38
3.2.1-14	MPTS- 17 dB Power Density Taper.....	38
3.2.1-15	MPTS-Array Pattern Roll-Off Characteristics.....	39
3.2.1-16	MPTS-Spacetenna Section with One DC-DC Converter Failure.....	39
3.2.1-17	SPS High Level Systems Model ISAI AH Implementation Diagram.....	43
3.2.1-18A	Transmitter Average-to-Peak Power Ratio.....	44
3.2.1-18B	Receiver Average-to-Peak Ratio.....	45
3.2.1-19	Beam Spread Factor.....	46
3.2.1-20	Maximum Thermal Load.....	47
3.2.1-21	Peak Beam Power Density.....	48
3.2.1-22	SPS System Performance Sidelobe Limits 100 W/cm ²	49
3.2.1-23	Transmitter Constraints Determine Minimum Cost Design Point.....	49

D180-22876-2

List of Figures

Figure	Title	Page
3.2.2-1	Annual Power Variation	51
3.2.2-2	Spectrum of Protons Incident on Solar Cells.	53
3.2.2-3	Reducing Cover Thickness Increases Damage	53
3.2.2-4	Effect of Cover Thickness on Power Mass Ratio 30 Year Degradation	54
3.2.2-5	Thin Cells Exhibit Lower Radiation Degradation	54
3.2.2-6	Comparative Radiation Characteristics	57
3.2.2-7	Attitude Control Propellant –Photovoltaic POP	59
3.2.2-8	Photovoltaic Reference Configuration.	62
3.2.2-9	Low Cost Annealable Blanket Structure	64
3.2.2-10	Photovoltaic Reference Configuration Solar Array	65
	Fundamental Element “Blanket Panel”	
3.2.2-11	Photovoltaic Reference Panel to Array Assembly	67
3.2.2-12	Photovoltaic Reference Solar Array Arrangement & Attachment	67
3.2.2-13	Photovoltaic Reference Power Collection	70
3.2.2-14	Photovoltaic Reference 20 Meter Beam Structure.	70
3.2.2-15	Continuous Beam Configurations	73
3.2.2-16	Antenna Support & Mechanical Joint Weights.	75
3.2.2-17	Electrical Rotary Joint and Mass.	76
3.2.3-1	Reference Rankine SPS Design	85
3.2.3-2	Rankine Cycle Schematic	85
3.2.3-3	Modules Consist of Concentrator & Focal Point Assemblies	88
3.2.3-4	Concentrator Frame Element	88
3.2.3-5	Facet Support Structure	89
3.2.3-6	Reflector Facet 1000 M ² of Reflecting Area.	89
3.2.3-7	Reflector Facet Mounting.	90
3.2.3-8	Cavity and Compound Parabolic Concentrator (CPC)	92
3.2.3-9	CPC Aperture “Door” Maintains Correct Cavity Temperature	92
	Despite Varying Power Output	
3.2.3-10	Focal Point Assembly	93
3.2.3-11	System Flow Schematic	93
3.2.3-12	Alkali Metal Vapor Turbine.	96
3.2.3-13	Generators.	97
3.2.3-14	Turbogenerator Pallet	97
3.2.3-15	Primary Radiator System	99
3.2.3-16	Antenna Joint for “P.E.P” SPS	96

D180-22876-2

List of Figures

Figure	Title	Page
3.2.4-1	LEO Construction Integrated Operations	104
3.2.4-2	Self Power Configuration Photovoltaic Satellite	106
3.2.4-3	Integrated GEO Construction Operations Concept	106
3.2.4-4	Thermal Engine SPS Construction Concept	108
3.2.4-5	Beam Assembly Concept	110
3.2.4-6	Beam Machine	110
3.2.4-7	LEO Base Construction Tasks	112
3.2.4-8	LEO Base Construction Tasks Thermal Engine Satellite	112
3.2.4-9	LEO Construction Base Photovoltaic Satellite	113
3.2.4-10	LEO Construction Base Thermal Engine Satellite	115
3.2.4-11	GEO Base Construction Tasks	116
3.2.4-12	Orbital Bases GEO Construction	116
3.2.4-13	Major Construction Equipment Photovoltaic Satellite	118
3.2.4-14	Antenna Subarray Installation Construction Operations	118
3.2.4-15	Module Construction Sequence Photovoltaic Satellite	120
3.2.4-16	Antenna/Yoke/Module Assembly Photovoltaic Satellite	120
3.2.4-17	GEO Berthing Concept Photovoltaic Satellite	121
3.2.4-18	Antenna Final Installation Photovoltaic Satellite	123
3.2.4-19	Photovoltaic Satellite LEO Construction Timeline	123
3.2.4-20	Crew Size and Distribution LEO Construction	124
3.2.4-21	Construction Mass Summary	124
3.2.4-22	Construction Base ROM Cost First Set	125
3.2.4-23	HLLV Two-Stage Configuration	127
3.2.4-24	Component Packaging Characteristics	132
3.2.4-25	Component Mix Per Delivery Flight	133
3.2.4-26	Component Packaging Density Impact	133
3.2.4-27	SPS Launch Vehicle—Cargo Version	135
3.2.4-28	Personnel Launch Vehicle	136
3.2.4-29	Space Based Common Stage OTV GEO Construction	138
3.2.4-30	Transportation Cost Sensitivity Interest Rate	138
3.2.4-31	Self Power Configuration Photovoltaic Satellite	140
3.2.4-32	Crew Size and Distribution	140
3.2.4-33	Collisions with Man Made Objects	142
3.2.4-34	Transportation Requirements LEO vs GEO	144
3.2.4-35	Number of HLLV Launches	144
3.2.4-36	Transportation Cost LEO vs GEO	145

D180-22876-2

List of Figures

Figure	Title	Page
3.2.5-1	Past Program Growth Distribution	147
3.2.5-2	Uncertainty Analysis Methodology	149
3.2.5-3	Photovoltaic SPS Efficiency: Relative Uncertainty Contributions	151
3.2.5-4	Photovoltaic SPS Mass/Size Uncertainty Analysis Results	153
3.2.5-5	Rankine Thermal Engine Size/Mass Uncertainty Analysis Results	153
3.2.5-6	Mass/Cost Uncertainty Analysis Results	154
3.2.6-1	Program Cost Baseline	157
3.2.6-2	Mature Industry: Production Rate Curve	157
3.2.6-3	Cost Analysis Methodology	158
3.2.6-4	Energy Costs and Payback for Silicon Solar Cells	162
3.2.6-5	Silicon Solar Cell Manufacture	164
3.2.6-6	Photovoltaic Preference is Sensitive to Solar Blanket Cost	164
3.2.6-7	Unit Klystron Cost vs Manufacturing Rate for Large Volume Manufacture	165
3.2.6-8	Moving Rectenna Factory – Artists Concept	167
3.2.6-9	Rectenna Cost Estimates Span Wide Range	168
3.2.6-10	Rectenna Size Optimization	168
3.2.6-11	LEO Transportation Costs for 14 Year Program at 4 Satellites/Year	171
3.2.6-12	Flight Vehicle Production Hardware Costs	172
3.2.6-13	Major Manpower Cost Data and Comparisons	172
3.2.6-14	Propellant Cost Basis	174
3.2.6-15	HLLV Launch Costs	174
3.2.6-16	Production Cost Results Summary	175
3.2.6-17	Predicted Busbar Power Cost and Uncertainties	177
3.2.6-18	Projections Indicate SPS Power will be Economically Attractive	177
3.2.6-19	Total Costs Through #1 SPS Photovoltaic System	179
4-1	Interferometer Spacecraft Concept	191
4-2	The Verification Phase: First Step to SPS	192

D180-22876-2

LIST OF TABLES

Table		Page
1-1	Energy Equivalents	3
1-2	Guidelines and Assumptions	8
2-1	Principal Findings	10
3.1-1	Operations Cost Drivers Favor Photovoltaics	23
3.1-2	LEO Versus GEO Construction Summary of Differences	24
3.2.1-1	Power Transmission System Highlights	31
3.2.1-2	Nominal Efficiency Chains Photovoltaic SPS	41
3.2.2-1	Part II Reference System Energy Conversion/Sizing	57
3.2.2-2	Structural Design Criteria	62
3.2.2-3	Photovoltaic Blanket Weight Buildups	68
3.2.2-4	Qualitative Comparison of Structural Options	72
3.2.2-5	Continuous Beam Characteristics	74
3.2.2-6	Reference Photovoltaic Instrumentation and Controls	76
3.2.2-7	Control Stability Analysis Results	78
3.2.2-8	Control Stability Analysis Results	79
3.2.2-9	Photovoltaic Reference Configuration Nominal Mass Summary – Weight in Metric Tons	81
3.2.2-10	Satellite Weight Delta GEO vs. LEO Construction	82
3.2.3-1	Data Base Draws Heavily on Demonstrated Technology (General Electric Data) ...	86
3.2.3-2	Material Availability	86
3.2.3-3	Radiator Mass	100
3.2.3-4	Power Budget	100
3.2.3-5	System Efficiency Chain	100
3.2.3-6	Perpendicular-to-Ecliptic Plane Orientation	102
3.2.3-7	Potassium Rankine SPS Mass Statement	102
3.2.4-1	Satellite Design Impact Summary LEO Construction	142
3.2.5-1	Photovoltaic End-to-End Efficiency Worksheet	150
3.2.6-1	Mature Industry Methodology Confirmation	160
3.2.6-2	Solar Cell/Blanket Costs	162
3.2.6-3	Rectenna Nominal Cost Estimate @ 1 SPS/Yr	169
3.2.6-4	Cost/Flight WBS	171
3.2.6-5	Cost Summary	175
4-1	SPS 5 Year Technology Development Plan	185
4-2	Recommended Technology Studies	185

1.0 INTRODUCTION

1.1 ENERGY NEEDS

The production and utilization of energy on a significant scale is a relatively recent occurrence in human history. It began with the industrial revolution. Industry utilizes energy and employs machines to increase human productivity. The advent of industrialization demarcates an economic condition of scarcity from one of plenty. Today we use the terms "industrialized" and "non-industrialized" almost synonymously with rich and poor.

The development of industry has been fueled by the rapid consumption of fossil fuels that were formed over time periods of geologic extent. (In 1976, the world consumed approximately 1% of its total remaining proven reserves of fossil resources.) Within the past generation the finiteness of these resources has become of more than philosophical interest; within the past five years it has become a pressing problem popularly dubbed the "energy crisis." If mankind is to continue to enjoy the benefits of industrialization, alternative sources must be developed. There are several potential options: singly or in some combination. These future energy systems should satisfy the following ten requirements:

- (1) The source of the energy should be non-depletable over time scales of at least hundreds of years.
- (2) The system should not be capacity-limited, i.e., it should be possible to install as much capacity as is desired.
- (3) The system should permit installation of generating capacity at a rate sufficient to meet the combined demand for new capacity and for replacement of obsoleted capacity.
- (4) The system should be usable for baseload, i.e., continuous service.
- (5) The system should produce much more energy over its lifetime than is invested to create and operate the system.
- (6) The system should have acceptable economics. In the simplest terms, it should produce electric power that consumers and industry can afford to buy.
- (7) The system should be environmentally acceptable in all respects, including air pollution, water pollution, thermal pollution, hazards, land use, and any other unique factors associated with the particular nature of the system.
- (8) The system should not require excessive consumption of critical resources even to install the greatest plausible total capacity.

D180-22876-2

- (9) The system should have the potential for compatibility with power grids as regards reliability, availability, power characteristics, plant size, and ability to serve all regions of the world.
- (10) The system should admit to an orderly, manageable development program without excessive risk, cost or calendar time required to reach initial commercial status.

Most of these requirements are self-evident but elaboration of potential capacity requirements is important because the scale of these requirements is often not appreciated. The United States in 1975 consumed a total of 71 Quads, or 2370 Gw-years (see Table 1-1). Of this, 668 Gwy equivalent thermal energy was used to generate 217 Gwy of electric power (some electric power comes from hydroelectric sources, so that the actual thermal energy consumption is less than 668 Gwy).

The conversions from thermal to electric power in Table 1-1 used the national average heat rate (thermal/electrical equivalence) of $3.04 \text{ kWh}_{\text{th}}/\text{kwhe}$ (10,389 Btu/kwh). This applies to conversion of thermal energy to electric energy but not necessarily to the reverse. Conversion of electric energy to low grade heat energy for space heating can approach this figure, but conversion of electric energy to high-grade heat is likely to occur at the energy equivalence of 3413 Btu/kwh. A more probable overall average electrical equivalence is about $2 \text{ kWh}_{\text{th}}/\text{kwhe}$ (7000 Btu/kwh).

The distribution of energy consumption by use in 1975 is shown in Figure 1-1. The figure also illustrates the degree to which the nation could electrify if primary energy sources were basically electrical in nature. The distribution of energy supplies by source for the year 1976, is shown in Figure 1-2. The fraction of our total energy supplies that is imported is large and increasing.

The development of new energy sources to fill this need will be a massive undertaking. Relatively few alternatives now known offer any hope of meeting the requirements summarized above. One of the more promising is the solar power satellite.

1.2 THE SPS CONCEPT

An SPS system for utility electric power would include a number of satellites in geosynchronous orbit, each with one or two associated power receiving stations on the ground. Receiving stations can be located near load centers (weather is not a significant factor). Each will provide at least 1000 megawatts and possibly up to 10,000 megawatts of baseload electrical output. A satellite system is pictorialized in Figure 1-3. Power is transferred from the satellites to the ground stations by high-precision electromagnetic beams. The transmissions would presumably use the industrial microwave band at 2.45 GHz; an alternative industrial allocation available at 5.8 GHz could be used but has received comparatively little attention.

Table 1-1 Energy Equivalents

1 quad thermal is equal to:	U.S. consumption in 1975 was equivalent to:
3342 Gwy _{th}	2370 Gwy _{th} , or
10.8 Gwy electric	766 Gwy electric, or
1.8 x 10 ⁸ Bbl oil	12.5 x 10 ⁹ Bbl oil, or
45 x 10 ⁶ metric tons coal	3.2 x 10 ⁹ metric tons coal

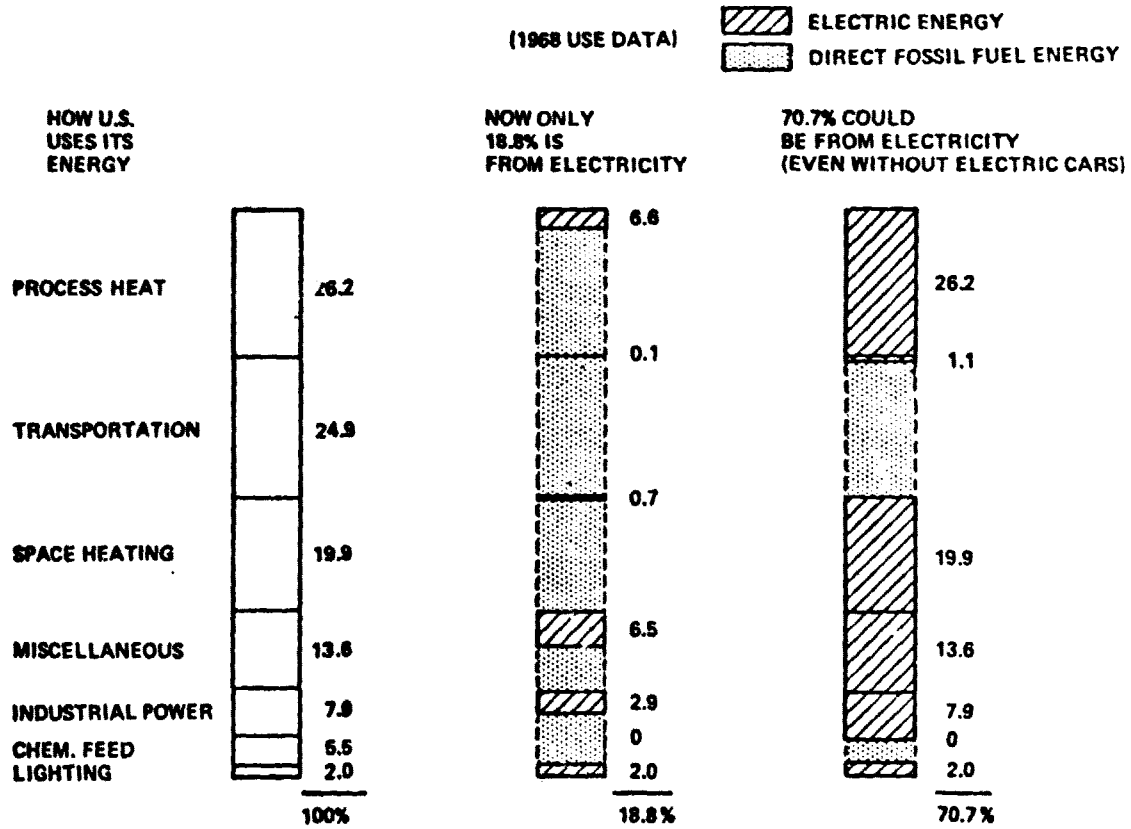


Figure 1-1 Applicability: The U.S. Can Effectively Electrify

**ORIGINAL PAGE IS
OF POOR QUALITY**

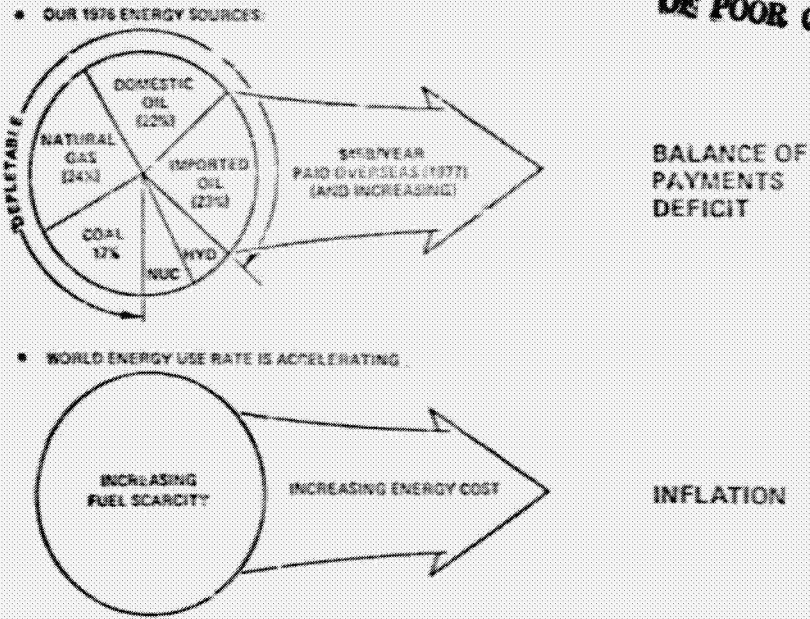


Figure 1-2 Energy Problems Are Causing a U.S. Economic Crisis

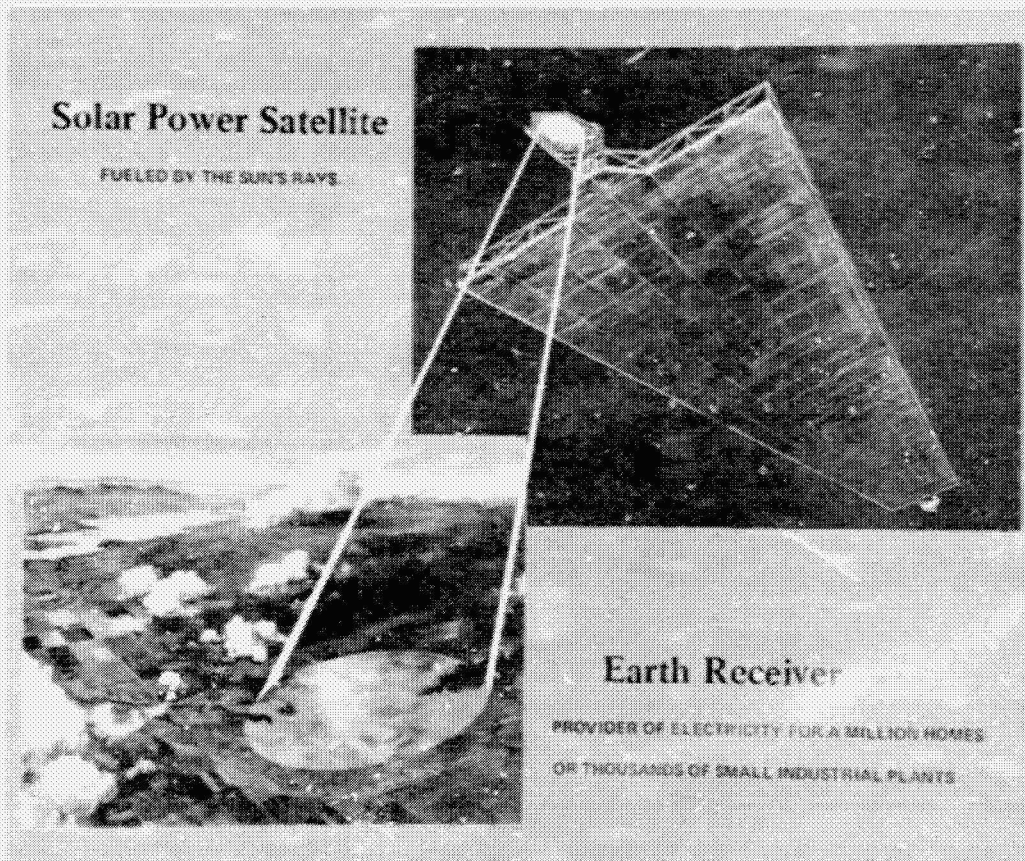


Figure 1-3 Space Solar Power Concept

D180-22876-2

A complete SPS operational system is symbolized in Figure 1-4. In addition to the satellites and their ground systems it will include:

A space transportation system capable of delivery of the SPS's to geosynchronous orbit and capable of supporting all required space operations needed to establish and maintain the SPS system.

One or more construction bases, located either in geosynchronous orbit or low Earth orbit, capable of constructing the satellites. Satellite hardware delivered to the construction bases will be prefabricated to the extent practicable.

Maintenance and service bases capable of supporting the maintenance operations required to keep the SPS's operating.

One or more Earth-based space transportation ports (launch sites) capable of supporting space transportation operations.

One or more space-based space transportation operations support bases, capable of supporting space transportation operations. This function could conceivably be combined with that of either a construction base or a maintenance base.

Earth-based manufacturing facilities capable of producing the hardware and consumables necessary to transport, construct and maintain the SPS system.

1.3 SPS STATUS

The concept of the space-based power station is now about a decade old, the first publications by Peter Glaser having appeared in 1968. The early years of concept evaluation and development were marked by the virtually single-handed dedication of Glaser and the almost universal ridicule which greeted his relatively sober quantitative analyses of potentialities and fundamental feasibility. Primarily through his efforts, the concept slowly gained first the recognition and eventually the concurrence and support of a portion of the aerospace profession, as represented by its inclusion in the AIAA's Assessment of Solar Energy for Earth, several Congressional hearings, and the NASA "Outlook for Space" in which it was identified as one of the major potential future space activities.

During this period a number of different technical approaches were suggested, including modifications of Glaser's original photovoltaic scheme: an active solar-thermal-electric concept and a passive satellite relay concept to transmit Earth-generated power over intercontinental distances. All these schemes utilized a common mode of power transmission: microwaves. A primary limiting factor on all of them was identified very early as the cost of transportation into geosynchronous orbit.

ORIGINAL PAGE IS
OF POOR QUALITY

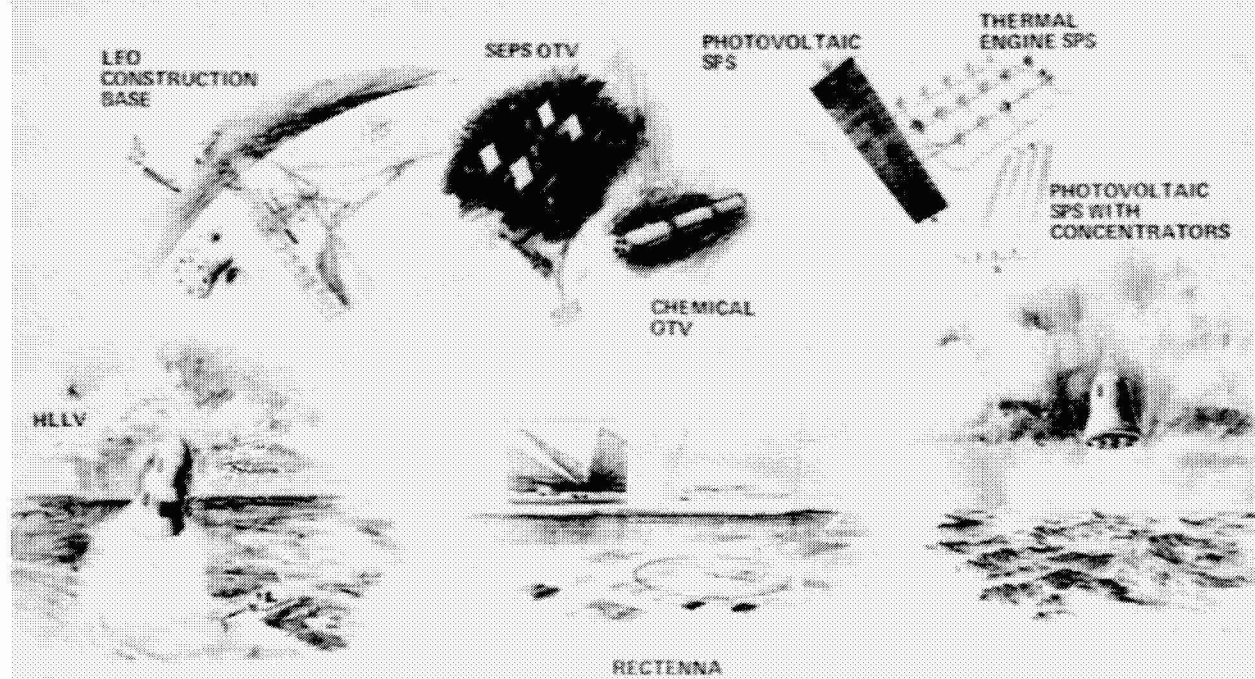


Figure 1-4 Major Program Elements

D180-22876-2

The early studies also identified the feasibility of efficient long-range transmission of power by microwaves as the most prominent issue affecting eventual feasibility of the concept. Accordingly, proof-of-principle tests were planned by NASA and conducted at JPL in 1975. The test results confirmed the physical principles involved, demonstrating that efficient transfer of energy is physically achievable.

At about this same time (1975-76), space transportation system studies funded by NASA were indicating that unit transportation costs, e.g., in dollars per kg, would reduce to surprisingly low values through the benefits of scale and through complete vehicle reusability, if a job of the magnitude of SPS were undertaken. Thus one of the chief cost barriers to SPS began to appear surmountable.

These events led to further NASA and industry studies. Two contracted "SPS Systems Definition Studies" were conducted in 1977 under NASA sponsorship; this report summarizes results of the JSC-managed Boeing effort. These efforts have more thoroughly defined and evaluated the SPS concepts, including support systems. SFS advocates are now arguing that this concept has potential as a non-depletable energy source, as good as or better than ground-based solar power or thermonuclear fusion. NASA and DOE are developing a plan to continue exploration and evaluation of the concept over the next three years. The plan primarily includes paper studies of SPS systems and their potential environmental and social impacts.

1.4 STUDY DESCRIPTION

1.4.1 Division of Effort

The study was divided into Part I and Part II efforts. The first part was conducted from December 1976 through April 1977 and the second part from May 1977 through December 1977.

1.4.2 Study Objectives

The objectives of the study were as follows:

Part I

"Issues--To derive specific, comprehensive supporting data necessary for NASA evaluation of the following two major SPS system issues:

- (a) What is the overall most effective means of accomplishing solar energy-to-electrical energy conversion on an SPS in geosynchronous orbit?
- (b) At what location (or locations) in space could the various phases of SPS construction and assembly be done?

Transportation--To increase the scope and depth of understanding of the space transportation systems necessary to support an SPS program."

Part II

“The objective of Part II of this study is to define the overall SPS system in more detail in order to achieve, as a goal, somewhere on the order of a factor of two reductions in the uncertainty of the weight and cost estimate ranges resulting from the JSC study.”

1.4.3 Guidelines and Assumptions

Guidelines and assumptions used during the course of the study are summarized in Table 1-2. It is emphasized that the approach taken to this study was to maximize confidence in results, rather than to minimize mass and cost projections by using optimistic or far-future technology extrapolations. This is reflected in the selection of energy conversion systems, in the selection of transportation systems, in the mass and cost estimating techniques, and in the uncertainty analyses approach.

A significant factor in overall cost characteristics is the maximum ionosphere beam intensity stated. This intensity limit strongly influences the cost characteristics of the ground receiving system by establishing maximum total power that can illuminate a given receiver area. The ground receiver is estimated to represent 25% of total costs.

Table 1-2 Guidelines & Assumptions

SPS 1050

GUIDELINES

- JSC INHOUSE STUDY (JSC-11568, THE “GREEN BOOK”) SHOULD BE USED AS A POINT OF DEPARTURE.
- SPS SYSTEM DESIGNED AND ANALYZED SHOULD REPRESENT THE EARLY PART OF A MATURE OPERATIONAL PROGRAM.
- SPS SYSTEM DESIGNS SHOULD MAXIMIZE CONFIDENCE IN RESULTS RATHER THAN MINIMIZING MASS AND COST THROUGH MAJOR TECHNOLOGY EXTRAPOLATIONS.

ASSUMPTIONS

- INITIAL SPS'S DEPLOYED IN 1990'S
- 1977 DOLLARS THROUGHOUT
- SPACE TRANSPORTATION OPERATIONS KSC-BASED
- SPS'S OPERATE AT GEO
- NOMINAL DESIGN OUTPUT 10,000 MEGAWATTS THROUGH TWO MICROWAVE LINKS AT 2.45 GHz
- MAXIMUM INOSPHERE BEAM INTENSITY 23 MW/CM²

2.0 SYNOPSIS OF STUDY RESULTS

2.1 FINDINGS

The most significant study results are summarized in Table 2-1. The study concentrated on maximum confidence system designs with the result that the SPS, rather than being a mid-21st-century system, should be achievable by the year 2000. The base technology is in hand. After a modest technology verification effort of 3 to 5 years duration, full scale development could begin and would provide a mainstream energy system of great potential.

2.2 DESIGN EVOLUTIONS

2.2.1 Configurations

Figure 2-1 illustrates the design evolutions in the two principal types of SPS systems and space support systems.

The photovoltaic SPS began with the JSC truss configuration, employing a geometric concentration ratio 2 as defined by JSC-11568. This configuration was designed on the basis of beginning-of-life output capability. The initial step was to resize the configuration to allow maintenance of output capability throughout its thirty-year design life. The resulting configuration (shown next in the figure) employed periodic array addition to maintain output.

At the completion of Part I of the study, a total of 10 photovoltaic configurations had been defined as shown. These included silicon and gallium arsenide energy conversion at concentration ratios 1 and 2, using various power maintenance methods. Significant risks associated with gallium availability were identified for the gallium system, therefore, the lowest cost silicon system was selected for continuance into Part II. This configuration employed concentration ratio 1 and in situ annealing of the solar cells for power maintenance.

Further analyses of the interactions of the various sizing limitations and of array performance allowed a slight reduction in system size for the final configuration. Division of the satellite into 8 modules is also indicated in the figure. The system output, with the optimum rectenna size, was reduced to 9.3 GW as a result of final definitions of the efficiency chain. (For convenience in finalizing the point design data, the configuration was frozen with a given amount of electrical power crossing the rotary joint. When the efficiency chain analyses were completed, including a 95% power interception efficiency for the optimum rectenna size, the resulting output was 9.3 GW total.)

Table 2-1 Principal Findings

- POWER TRANSMISSION**
 - PRACTICAL DESIGNS IDENTIFIED THAT MEET REQUIREMENTS AND CONSTRAINTS
 - DETAILED MICROWAVE LINK ERROR ANALYSIS CONFIRMED ATTAINABILITY OF ACCEPTABLE LINK EFFICIENCY
- ENERGY CONVERSION**
 - SILICON PHOTOVOLTAIC BEST OVERALL CHOICE
 - POTASSIUM RANKINE BACKUP CHOICE
- SPACE TRANSPORTATION OPERATIONS**
 - LOW COST DUE TO TRAFFIC LEVEL, NOT NEW TECHNOLOGY
 - PAYLOAD VOLUME IS LAUNCH VEHICLE DESIGN DRIVER
- SPS SYSTEM COSTS**
 - POWER COST 4 TO 5 ¢/kwh; COMPETITIVE WITH FOSSIL SOURCES BY YEAR 2000
 - SYSTEM DESIGN FLEXIBILITY KEY TO COST CONFIDENCE

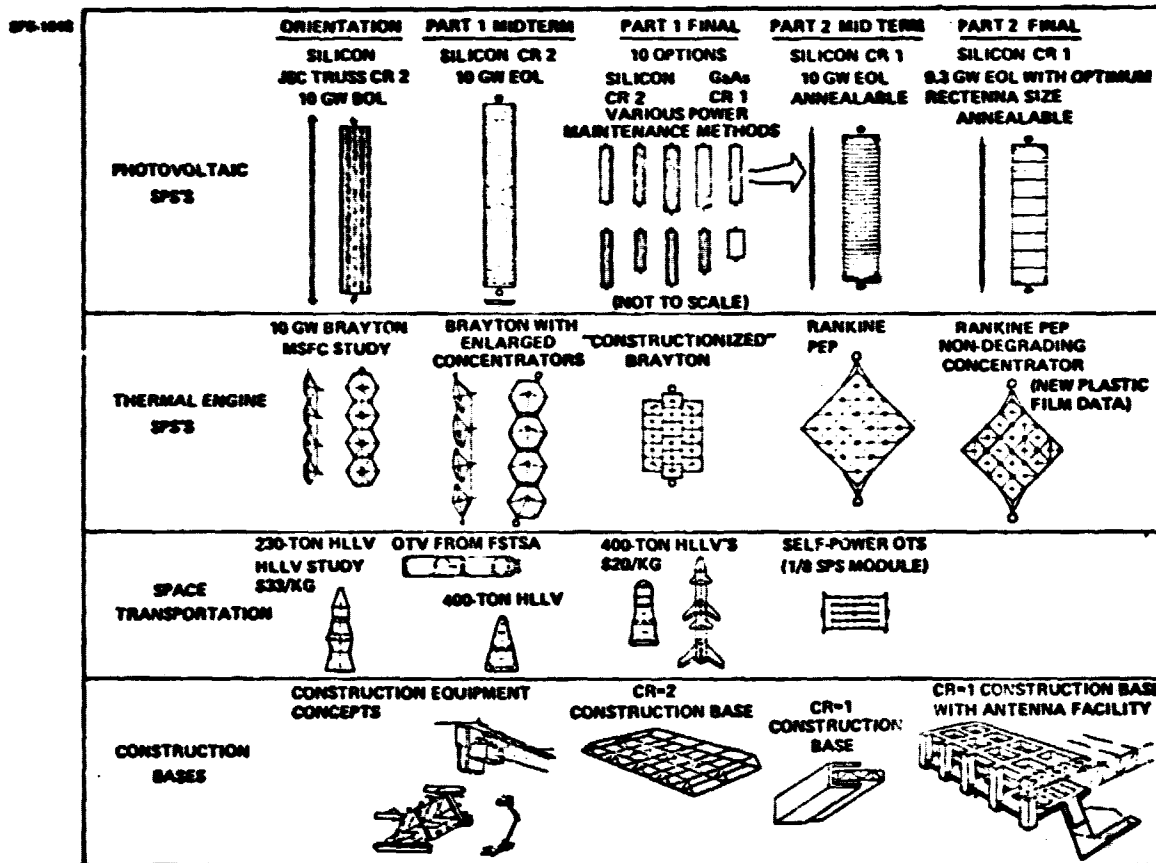


Figure 2-1 SPS System Definition Study Design Evolutions

D180-22876-2

The thermal engine analyses began with the 10 GW Brayton system as defined under an earlier contract. Early in this study, an analysis of available (but old) data on plastic film reflector degradation in the space environment suggested that a 30% degradation might occur. Consequently, the concentrators were enlarged. The configuration was also geometrically changed to improve the efficiency slightly. As the Part I study proceeded, significant difficulties were encountered with development of a construction concept for the large 4-module Brayton SPS. The configuration was divided into 16 modules of trough-shaped concentrators as shown under "constructionized Brayton."

During Part I, Rankine and Thermoinic systems were also evaluated. Thermoinic systems were soon dropped because of excessive mass and consumption of scarce resources. The Rankine systems evaluated many potential working fluids and finally selected potassium as the most practical. Initial evaluations indicated the potassium system to be more massive than the Brayton system. However, a cycle temperature ratio optimization indicated that the Rankine system could operate at considerably lower temperatures than the Brayton system while still exhibiting a lower overall mass. The penalty paid for this operating characteristic is a somewhat lower end-to-end system efficiency, resulting in a larger concentrator. Since the concentrator unit mass is relatively small, even though the system is larger, it is less massive overall than the equivalent Brayton system. Additional design changes introduced at this point involved the elimination of steerable facets from the concentrator. By flying the system perpendicular to the ecliptic plane, i.e., always exactly facing the sun, it is possible to use reflector facets that are aligned on initial installation without further adjustment or active steering.

Toward the end of the study, new information became available on plastic film reflectors indicating that degradation would not occur and the final system configuration was, therefore, resized to reflect nondegradation of the concentrator.

The principal evolution of space transportation systems concepts was in the launch vehicle element. The study began with the 230-ton payload heavy lift launch vehicle at a projected cost for transportation to orbit of \$33 per kilogram. This cost included an expendable shroud. Packaging studies conducted during the study indicated that payload densities of approximately 75 kilograms per cubic meter could be achieved, making possible a reusable shroud. Staging optimization studies also led to a larger booster for the upper stage resulting in a 400-ton heavy lift launch vehicle that went through the evolution shown: Initially, a conical vehicle, later a more cylindrical vehicle, with the addition of a two-stage winged vehicle option based on earlier JSC studies of a very similar configuration.

Studies of chemical orbit transfer vehicles included space-based and Earth-launched options, but the orbit transfer option taken from the Future Space Transportation System Analyses study, a two-stage fully reusable space-based option, was indicated to be least cost and was retained. Resizing from the FSTSA study was accomplished to match the payload capability of the OTV to the HLLV.

D180-22876-2

Considerable investigation of the means of moving the SPS hardware itself from low Earth orbit to geosynchronous orbit continued to indicate a significant cost advantage to the self-power concept. Shown at the end of the space transportation configuration evolution is a 1/8 size photovoltaic module with 25% of the solar cells deployed for power generation, and equipped with propellant tanks and electric thruster systems to allow this module to transport itself from low earth orbit to geosynchronous orbit in approximately 6 months.

The evolution of construction concepts began with equipment concepts for structure construction, installation of solar cells, and installation of power conductors. The initial construction base concept was for construction of a concentration ratio 2 satellite and included rather little detail other than overall size and shape. As a result of the configuration selection for Part II of the study, the construction base was altered for construction of concentration ratio 1 satellites. This construction base concept went through further evolution to the arrangement shown at the lower right hand corner of the figure. In this illustration, most of the structure is shown blocked in with structural detail shown only on one small portion of the construction base. This construction base includes capabilities to construct satellite modules and transmitter antennas. Analogous construction base concepts were developed for the thermal engine system also, but are not shown.

2.2.2 Mass Histories

The mass estimate history for the photovoltaic SPS, through the conduct of the system definition study, is shown in Figure 2-2. (SPS-1399) The point of departure estimates came from the JSC "green book", (JSC-11568). Energy conversion system detailed mass estimates were available by the Part I mid-term. The principal reason for increase was the addition of borosilicate glass covers on the solar cells, increasing the unit mass of the solar blankets substantially.

Some reduction of structure mass for the energy conversion system resulted in the values shown for the Part I final. During this time, an arbitrary 50% mass growth allowance was carried. With initiation of Part II of the study, effort was begun on the power transmission system. By the mid-term of Part II, detailed mass estimates were available. These mass estimates resulted in a significant increase in the power transmission system mass primarily due to requirements determined for thermal control systems. At this time also, a mass properties review suggested that with the availability of comparatively detailed mass estimates and the general lack of escalating factors internal to the SPS design, a 25% mass growth allowance would be more appropriate. During the final part of the Part II effort, a detailed uncertainty analyses was conducted and predicted a mass growth of 26.6%. This growth allowance was incorporated in the final mass statement.

SPS-1300

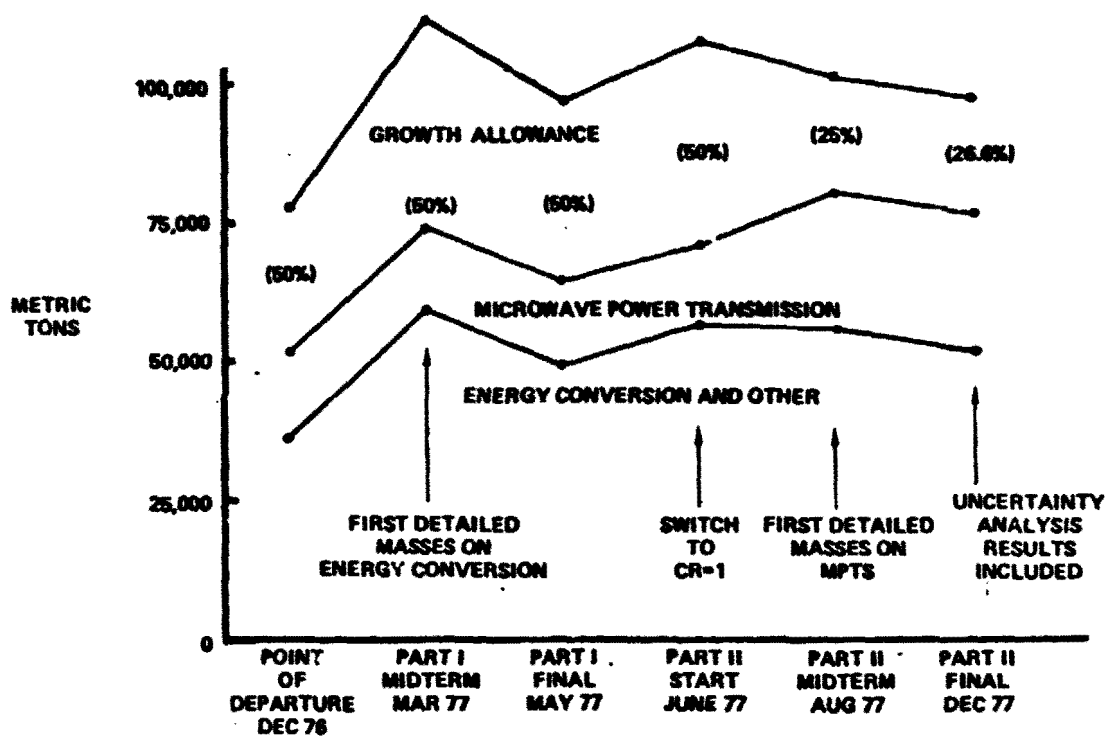


Figure 2-2 Reference Photovoltaic SPS Mass Estimate History

The thermal engine mass estimate history shown in Figure 2-3 (EPS-1398) goes back to Boeing IR&D work conducted beginning in 1972. The specific values shown for 1973 and 1975 come from Boeing papers published in the technical literature. These papers did not address the mass of microwave power transmission systems and early estimates available from the literature were quite optimistic.

The point-of-departure mass estimate represented the first completely integrated thermal engine design with all interrelationships in this complex system properly represented. The power transmission system mass at that time was taken from Raytheon publications. Brayton system cycle optimization brought the mass down slightly by the Part I mid-term, where also the JSC microwave power transmitter mass was adopted. By the Part I final, additional mass reductions resulted from the adoption of the 16-module configuration as compared to the 4-module configuration.

The continuing reduction in energy conversion mass was due to first, the switch to the Rankine system and secondly, elimination of the oversized concentrator originally thought necessary to compensate for the degradation of plastic film reflectors. The power transmission system masses for the thermal engine and photovoltaic systems are equivalent. The uncertainty analysis predicted a 20% mass growth for the thermal engine system, less than for the photovoltaic system, as might be expected due to the somewhat greater maturity of the technology.

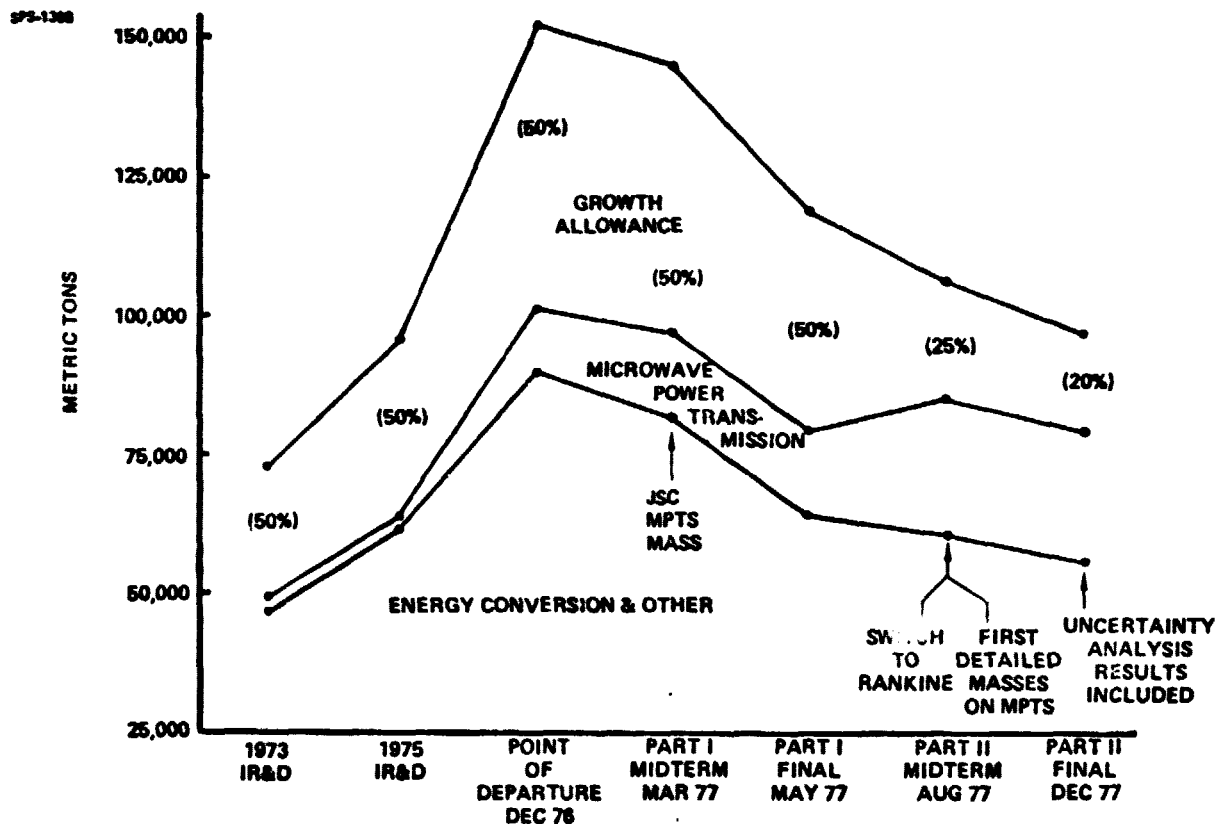


Figure 2-3 Reference Thermal Engine SPS Mass Estimate History

3.0 STUDY ACCOMPLISHMENTS AND RESULTS

3.1 PART I ISSUES

3.1.1 Energy Conversion

The evaluation effort included all energy conversion options known to be of potential interest for the SPS applications:

- (1) Silicon single crystal photovoltaics;
- (2) Gallium arsenide single crystal and thin-film photovoltaics;
- (3) Other thin-film photovoltaics;
- (4) Thermal engine Rankine closed-cycle vapor turbines, with several working fluids under consideration;
- (5) Thermal engine Brayton closed cycle gas turbines;
- (6) Thermionic direct thermal conversion.

Certain known options were not included:

- (1) Thermoelectrics--rejected on elementary considerations of efficiency, materials consumption, and waste heat rejection.
- (2) Magnetoplasmadynamics rejected on grounds of problems in attaining the necessary working fluid temperatures by solar heating.
- (3) Direct thermal conversion by electrostatics--insufficient data available for this recently-proposed thermal engine.
- (4) Thermophotovoltaics--rejected on consideration of *overall* efficiency and problems of waste heat rejection.

The principal energy conversion conclusions at the completion of Part I were as follows:

- (1) Conversion efficiency and resulting SPS size (at fixed output) tended to favor the Brayton gas turbine and gallium arsenide photovoltaic options. A size comparison of the options investigated is shown in Figure 3.1-1 (Part I, Vol. I, Fig. 1-9). Size, however, was not seen as a primary decision factor.
- (2) Much more important was mass. It is a significant cost factor, especially for hardware that must be delivered to space. Here again, gallium arsenide looked good, with all of the options except thermionics in an acceptable range, as shown in Figure 3.1-2 (Part I, Vol. I, Fig. 1-10). Of the various Rankine cycle working fluids, only the alkali metals were compatible with the high cycle temperatures essential to neat rejection system mass in the acceptable range. (Water, i.e., steam Rankine, is compatible from the fluid thermal stability standpoint, but a steam system operated in the minimum-mass temperature range is essentially a Brayton gas cycle.)

D180-22876-2

SIZE FAVORS GALLIUM ARSENIDE & BRAYTON BUT IS NOT A STRONG DISCRIMINATOR

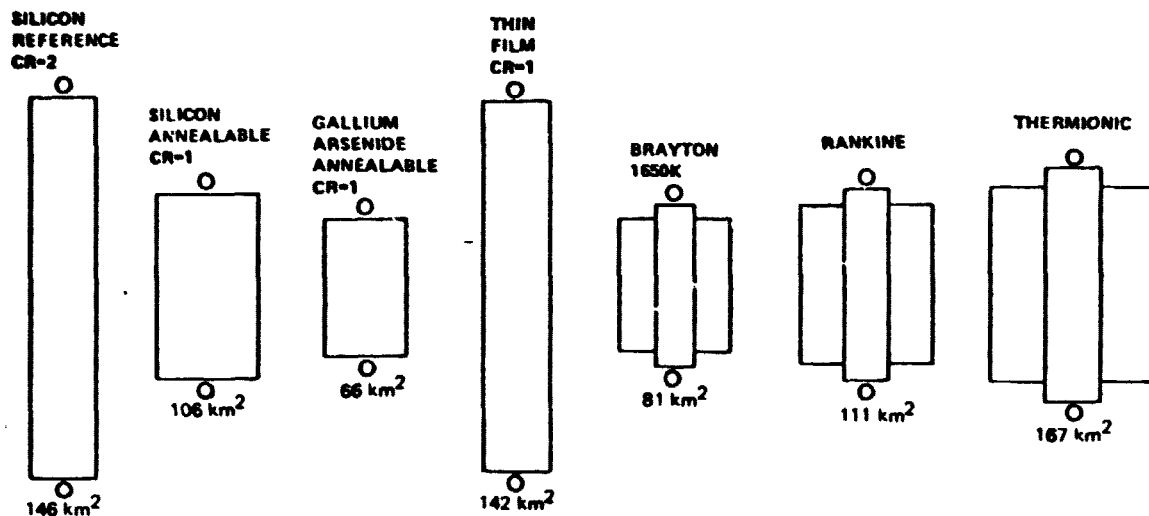


Figure 3.1-1 Energy Conversion Comparison SPS Size

MASS COMPARISON INDICATES ELIMINATION OF THERMIONICS

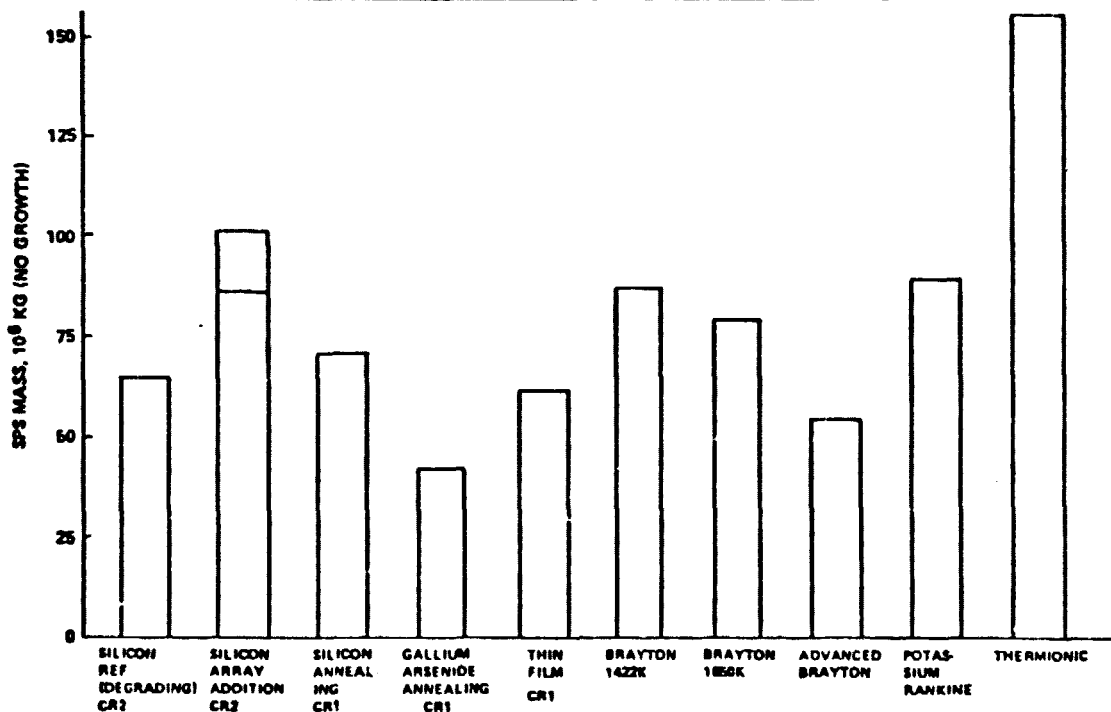


Figure 3.1-2 Energy Conversion Comparison SPS Mass

D180-22876-2

- (3) Radiation degradation of solar cells, especially silicon, was known to be a serious problem. The amount of degradation depends on the amount of shielding provided, e.g., by coverglasses. (Attempts to provide lighter weight plastic coverglasses have to date been unsuccessful because the plastics become opaque in the geosynchronous combined radiation and uv environment.)

It has long been known that radiation damage in silicon solar cells can be largely annealed out by heating to $\sim 500^{\circ}\text{C}$. This normally would be done by bulk heating. Recent developments had indicated, however, that directed energy pulse heating could be effectively used. As a part of this study, under subcontract, Simulation Physics (now SPIRE, Inc.) conducted exploratory laser and electron beam annealing tests on severely irradiated solar cells provided by Boeing. Approximately 50% of the cells' lost performance was recovered in these tests. It is believed that further development and optimization of the process could approach 90% recovery. Accordingly, an annealable blanket design (compatible with annealing temperature) was selected as the reference design for Part II.

- (4) The more complex thermal engine systems were found to be more difficult to construct, but at this point in the study, differences in constructability were not viewed as particularly significant - all configurations were constructable. These differences were later to emerge as a strong decision factor.
- (5) If SPS's are to be installed on a large scale, availability of raw materials could be a significant issue. Materials availability was a strong negative factor for the thermionics option. Considered together with excessive mass, the negative factors were judged to be a conclusive reason to discard thermionics. Materials availability also imposed significant design constraints on the other thermal engine options, which benefit from the use of exotic metals at high temperatures. Tungsten, tantalum, and molybdenum were eliminated. Molybdenum itself is not particularly scarce, but must be alloyed with rhenium for ductility; rhenium is very scarce. Materials issues were primary in the ultimate selection of potassium Rankine as the preferred thermal engine. This selection, however, did not occur until Part II.

The availability of gallium also emerged as a major issue. This controversy continues to the present day, with gallium arsenide advocates insisting that there is "no problem" and skeptics arguing that the problem is insurmountable. Our evaluation is as follows. *If* thin film gallium arsenide cells, e.g., on a sapphire substrate, are used with moderate sunlight concentration, and *if* moderately optimistic gallium availability estimates are used, the problem is at least workable, as illustrated in Figure 3.1-3. (The cells must be about $5\ \mu\text{m}$ thick on a substrate of some other material. The physics of gallium arsenide photovoltaics does not preclude such cells being efficient. Gallium arsenide cells presently in experimental production are conventional in thickness, e.g., $100\ \mu\text{m}$ or more.) In view of this issue and the associated technology advancement requirements, this study backed away from gallium arsenide as a primary candidate. It is still so regarded, however, by some investigators. In summary, from the resources

SPS-1020

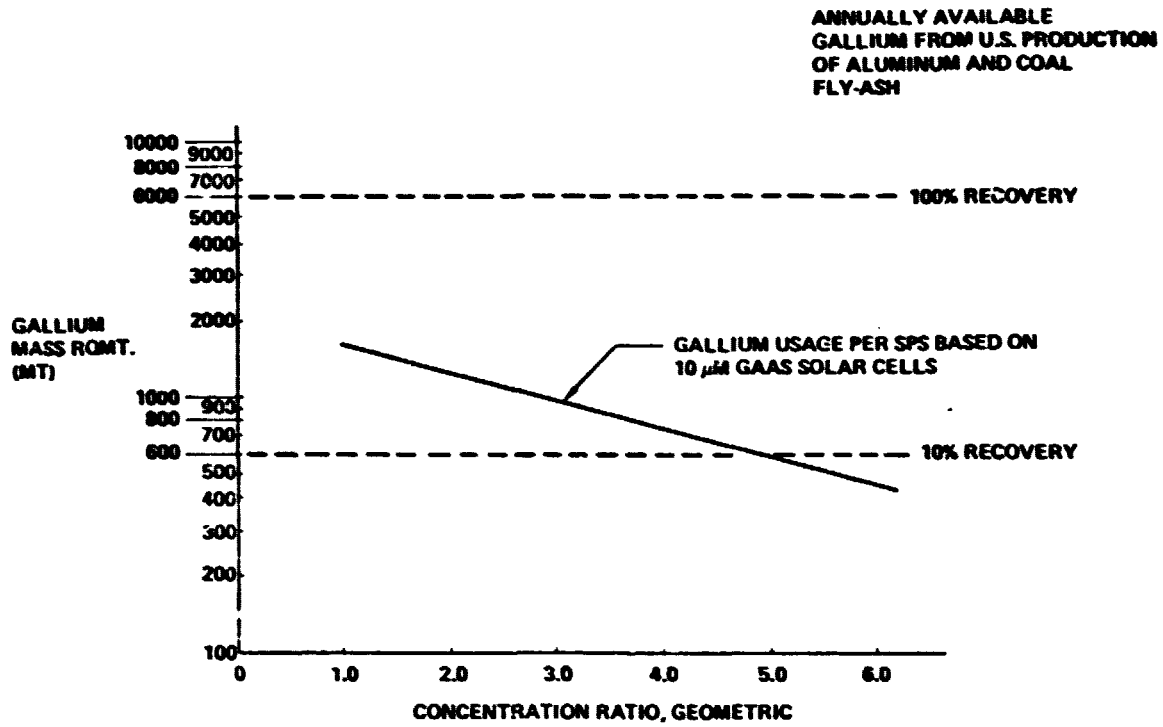


Figure 3.1-3 Reduction in Gallium Required for CR > 2 System

standpoint, the silicon system was most favored, thermal engines were readily workable with appropriate design constraints, and gallium arsenide was probably workable with advanced technology. Some of the other thin-film photovoltaic approaches (e.g., copper indium selenide) were rejected due to resources considerations as was the thermionics thermal engine.

- (6) Technology advancement requirements figured importantly in the eventual selection of preferred systems as well as in the Part I screening stage. A major increase in the scale of space operations must be brought about to install SPS's at a rate of practical interest. Although the technical advancements required in systems and subsystems are quite modest, the required advances in operations technology may be compared to the advances in aircraft operations technology that occurred with the introduction and expansion of the jet age. It is prudent to restrict areas of major technology advance to as few as possible to maximize chances of program success. There was, therefore, a strong motivation to minimize the technological advance required in energy conversion. Silicon photovoltaics and the turbogenerator options fitted this prescription; the other options did not.
- (7) Cost is the overriding factor in design selection for any system intended for commercial application, with financial risk a close second. All other parameters are of little significance. (Most of the foregoing factors appear on the cost-risk balance sheets.) At the conclusion of the Part I effort, the silicon photovoltaic and Brayton thermal engine were judged to be essentially equal in cost (Figure 3.1-4) and, as noted above, quite comparable in risk. The gallium arsenide option exhibited appreciable potential cost advantages, mainly resulting from mass and size reductions, but these potentials were heavily overshadowed by the materials availability and technological risk concerns already discussed.

Silicon systems at concentration ratio 1 (i.e., no concentration) and 2 were evaluated. Because concentration is relatively ineffective with silicon due to temperature effects the simpler no-concentration configuration was found to be least cost. Higher solar cell costs improve the benefits of concentration, but these benefits are net positive only when solar cell costs are high enough to make the thermal engine option a relatively uncontested winner. This conclusion does not necessarily apply to advanced-technology gallium arsenide options.

The net result of these considerations was a decision to carry the silicon CR=1 and Brayton energy conversion options into Part II as primary candidates. General Electric, our major sub-contractor in this study, expressed the strong opinion that the Brayton-versus-potassium-Rankine tradeoff had not been adequately worked. It was therefore agreed that this matter would be re-examined in greater depth as a priority item early in Part II.

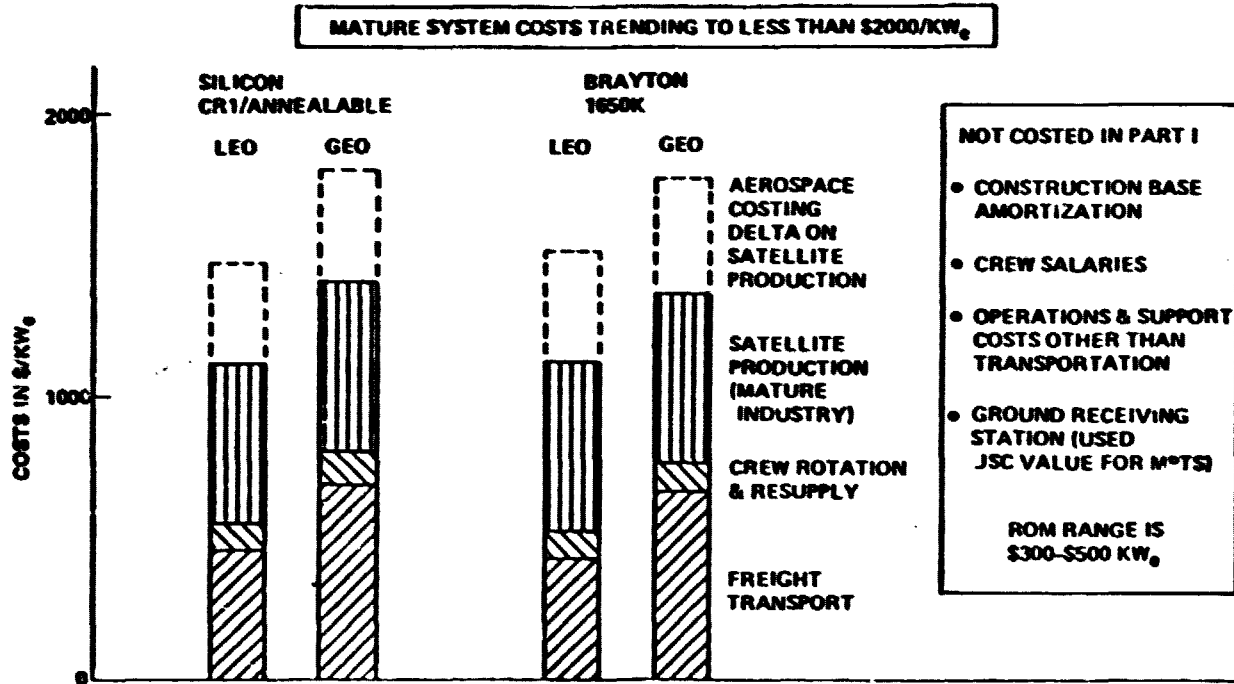


Figure 3.1-4 Cost Differential Factors as Determined by Study Part I

3.1.2 Construction Location

The principal construction location conclusions at the end of Part I were as follows:

- (1) **The primary component of the issue was transportation related. The payoff for low Earth orbit (LEO) construction is the enabling of the self-powered mode for LEO to geosynchronous Earth orbit (GEO) transportation at the very high specific impulse available through electric propulsion. The propellant requirement for LEO-GEO transportation shrinks from the predominant requirement to a relatively incidental requirement, from 2.1 tons per ton delivered to GEO to about 0.25 tons per ton.**

- (2) **The essence of the tradeoff was a factor of 2 reduction in launches to low Earth orbit for LEO construction as compared to GEO construction, versus an array of difficult-to-quantify operational complexities and concerns.**

- (3) **Most important of the problematical operational factors associated with the electric propulsion mode are:**
 - (a) **Trip times on the order of six months, compared with less than one day for the high-thrust LO_2/LH_2 systems associated with GEO construction.**

 - (b) **Radiation degradation of the SPS from exposure to the van Allen belts during the slow transfer.**

 - (c) **Modularization of the SPS, necessary for attitude control authority in the presence of the strong gravity gradients at LEO.**

 - (d) **Conversion of the SPS modules into powered spacecraft capable of executing the transfer.**

 - (e) **The risks of collisions with man-made orbiting objects during the LEO construction operations and during the slow spiraling transfer from LEO to GEO.**

 - (f) **Upper atmosphere drag affecting the LEO construction operations.**

 - (g) **Operational hardware and software complexities ensuing from low-thrust orbit transfer operations.**

At the conclusion of the Part I effort, the reduction in LEO transportation cost was judged to overwhelm all other factors. The overall reduction in *system* cost, however, was on the order of 10%. The predominant penalty on LEO construction was the added interest cost chargeable to total capital cost as a result of the six month transit times. The investigations of collision hazards was incomplete at this point.

3.1.3 Part II Findings Relative to Part I Issues

The issues addressed during Part I of the study are fundamental and permeate all aspects of system design and selection.

As a result, although narrowing of options, clarification of sub-issues, and focusing of attention was achieved, complete answers were not obtained during Part I. As an example, complete definition of hardware packaging densities and transportation/construction operations options was not achieved until the power transmitter (excluded from Part I) was taken into account.

During Part II, the following major conclusions were obtained relating to the Part I questions:

- (1) Continuing comparative evaluation of potassium-vapor Rankine cycle systems versus inert gas Brayton systems led to a preference for the Rankine system because:
 - (a) The Rankine system mass-optimizes at somewhat lower mass and much-reduced radiator area.
 - (b) The Rankine system is practical, e.g., in terms of hardware mass, at cycle temperature limits generally in the superalloy range, whereas the Brayton systems were dependent on refractory metals or ceramics. Strong implications are present here for technology advancement requirements and resource consumption.
 - (c) The Rankine system exhibited good performance at relatively low (circa 30 megawatts) per-engine power ratings. By way of contrast, the Brayton engines are sensitive due to blow-by tolerances on turbomachinery and needed to be sized greater than 300 megawatts per engine. The higher temperatures and power levels required for the Brayton engines have significant cost implications regarding developmental test facilities.

As a result, and due in no small way to the General Electric Subcontract effort, the Rankine potassium vapor cycle was selected as the preferred engine.

- (2) Further analysis of transportation and construction operations differences between the thermal engine and photovoltaic options began to reveal significant differences in operations cost. Although differences in satellite mass and cost continued to be unimportant, differences in construction crew size, facility cost, and payload packaging densities emerged as decision drivers as synopsized in Table 3.1-1. Consequently, an overall preference for the silicon photovoltaic system gradually became quantifiable.

**Table 3.1-1
Operations Cost Drivers Favor Photovoltaics**

	SILICON PHOTOVOLTAIC	RANKINE THERMAL ENGINE
Construction Crew Size	540	815
Space Construction Base Cost	8.2 Billion	12.4 Billion
Net Packaging Density	95 kg/m³	65 kg/m³

This preference is small, however, with respect to possible uncertainties in solar cell costs, as shown in Figure 3.1-5. Therefore, although we recommend the silicon photovoltaic system for preferred concept selection, the Rankine thermal engine should be carried as a backup to hedge against solar cell cost uncertainties.

- (3) Construction in low Earth orbit continued to show a ten percent cost advantage. Practical measures were found to avoid collision with any observable man-made objects for which epermerides are predictable. A refined analysis of system degradation during one 180-day transfer through the van Allen belts revealed no substantive differences from the earlier more parametric analyses. All operational and other LEO/GEO differences were at least roughly quantified as summarized in Table 3.1-2. LEO construction offers recurring and nonrecurring cost advantages and is recommended as the preferred concept selection.

3.2 MAIN PART II RESULTS

The primary objective of Part II was to accomplish as much system definition as possible within the available study resources. As much reduction as possible in mass and cost uncertainty was the desired outcome of the effort. Dr. George Hazelrigg of ECON has observed that reduction of uncertainty can be economically more important than the projections of low mass and cost that can be derived by adoption of advanced-technology assumptions. An economic determination of next program steps can best be made when uncertainties are minimized.

3.2.1 Microwave Power Transmission

The interface requirements and performance of the microwave power transmission system are the keys to an integrated system definition. The performance of the power transmission system establishes overall system sizing and output; the electric power condition requirements of the RF power amplifiers determine the voltages and currents to be produced by the energy conversion system.

D180-22876-2

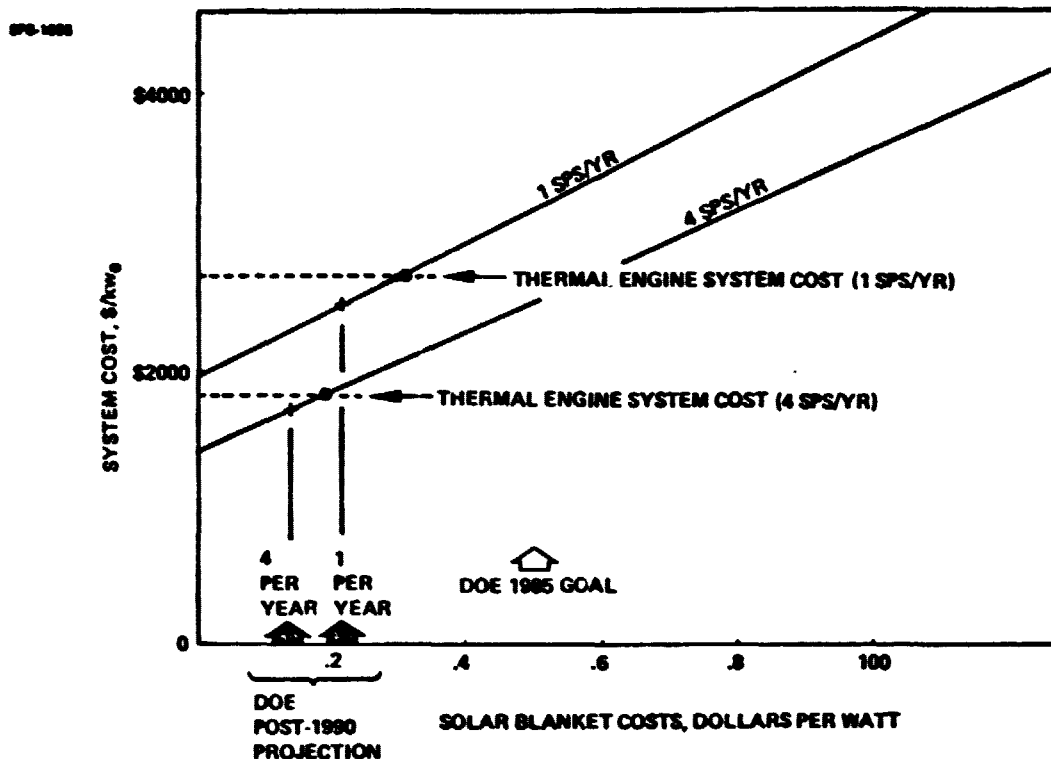


Figure 3.1-5 Photovoltaic Preference is Sensitive to Solar Blanket Costs

Table 3.1-2 LEO Versus GEO Construction Summary of Differences

RFP REF	DESCRIPTION	DELTA COST IN MISSIONS PER SPS (GEO - LEO)	
		RECURRING (4 SPS/YR)	INITIAL NON-RECURRING
A)	TRANSPORTATION REQUIREMENTS (INCLUDES CREW)	HLLV = 2,548 OTV = -205	2,223 (FLFET INVESTMENT) -1,431 (OTS)
B)	CONSTRUCTION REQUIREMENTS	24 -9 9	530
C)	SPS DESIGN REQUIREMENTS	-139 -70	-350 -175
D)	DEGRADATION POTENTIAL		
E)	LAUNCH SITE DIFFERENTIAL EFFECTS	-	1,715 LAUNCH FACILITY COSTS
F)	STARTUP	-303	
G)	OPERATIONS CONSIDERATIONS	-10	
H)	COLLISION	-1 -5	
I)	COST DIFFERENTIALS	156	
J)	ORBIT TRANSFER	-	
TOTAL COST DIFFERENTIALS		1,995	2,512

3.2.1.1 Power Transmission: Principles of Operation

The long-range transfer of power from the SPS at geosynchronous orbit to a receiving station on Earth employs the principles of free-space propagation of electromagnetic waves. Narrow beams are more familiar in terms of light sources than in terms of radio-wavelength sources. With large aperture RF sources, however, narrow beams can be created.

Effective production of a narrow beam requires production of coherent planar wavefronts at the transmitter aperture. If this can be done, the properties of the resulting beam are suitable for efficient energy transfer. The field produced by such a transmitter includes a near-field region where no appreciable beam divergence occurs, and a far-field region with beam divergence. For SPS transmitters of practical interest, the beam will have far-field characteristics at Earth. The applicable aperture theory shows that for an ideal antenna (no errors in producing the desired wavefront), the product of areas of the transmitting and receiving apertures is a constant:

$$A_T A_R = \left(\frac{\pi H K \lambda}{2} \right)^2$$

(See Figure 3.2.1-1.)

H is range, i.e., 37×10^6 m

λ is wavelength, i.e., 0.1224 m at 2450 Mhz

K is a constant depending on the transmitter illumination pattern as discussed below: it varies from 1.2 to 1.8 for typical SPS transmitters. With $K = 1.5$, and a transmitter area of 10^6 m^2 (1 km^2), the expression above yields $A_R = 114 \times 10^6 \text{ m}^2$. Thus the sizes of transmitter and receiver required to effect an efficient energy transfer from geosynchronous orbit to Earth are large, but not beyond engineering techniques now realizable. One can, of course, consider making the transmitter larger and the receiver smaller or vice versa. The correct sizing is a constrained cost optimization problem as discussed below in Section 3.2.1.5.

The simplest illumination pattern for a transmitter is constant RF power density across the entire aperture. One might imagine this also to be the best, but it is not. Some of the energy transmitted does not fall within the main beam, but is scattered into rings of "sidelobes." The intensity of these sidelobes and the total energy so lost is a function of the illumination pattern. For a constant illumination pattern, 16% of the energy is lost and the first sidelobe (the ring nearest the main beam) has a peak intensity 1/50 of the maximum beam intensity at the center of the beam.

3.2.1.2 Characteristics of Power Transmission Beams

This discussion of beam patterns requires familiarity with the term "decibel." The decibel is a relative logarithmic measure such that 0 db is a unit factor, 10 db is a factor of 1, 20 db is a factor of 100, 30 db is a factor of 1000, and so forth. Thus, a statement that a sidelobe is "34 db down"

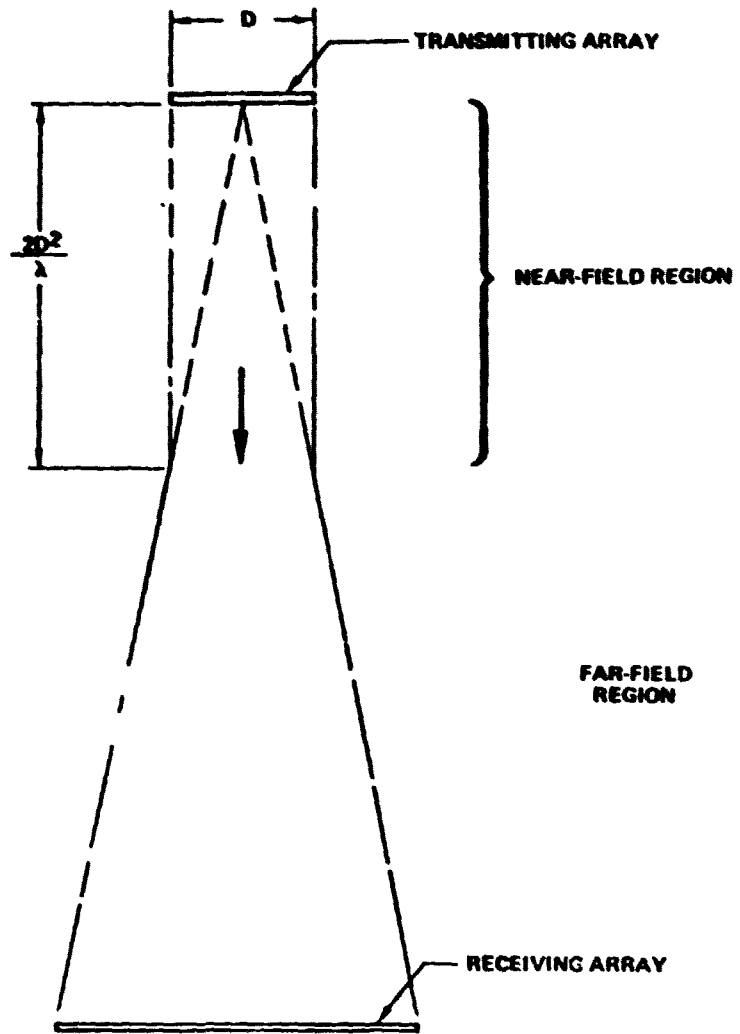


Figure 3.2.1-1 Transmitter Beam Spatial Distribution

means the sidelobe intensity is $10^{-34/10} = 10^{-3.4} = 1/2512$ of the main beam maximum intensity. A "10 db taper" means that the transmitter RF intensity at the edge of the transmitter is 1/10 that at the center.

As noted, the uniform illumination pattern is not the best. Illumination patterns which maximize intensity at the center of the antenna, tapering off to lower intensities at the outside, reduce scattered energy and reduce sidelobe intensity levels. (Taper patterns varying both intensity and phase are possible.) The investigations in this study considered mainly intensity (amplitude) variation. Many pattern and shapes have been investigated and proposed for illumination tapers. Within the design constraints that exist for the SPS power transmission system, a truncated gaussian taper is about as good as any of the alternatives. The taper is ordinarily described by expressing the ratio of power intensity at the center of the antenna to that at the edge, in terms of decibels. Figure 3.2.1-2 illustrates several power intensity tapers with all cases adjusted for constant beam diameter on the ground. The ideal beam efficiencies for these tapers are also shown. This is the fraction of total radiated power in the central beam. Figure 3.2.1-3 shows the degree of sidelobe intensity suppression as a function of transmitter intensity taper.

For gaussian illumination patterns the power beam intensity distribution at the receiving point is also approximately gaussian in shape. Intensity is maximum at the center of the beam and tapers off rapidly to the first null with successively lower sidelobe levels as distance from the beam center increases. Note that the scale used in Figure 3.2.1-3 was logarithmic and that most of the main beam is at relatively low intensities. This is better illustrated in Figure 3.2.1-4, using a linear scale, linear scale.

Patterns which vary both in intensity and phase at the transmitting antenna can provide beam patterns at the ground that have a more constant intensity distribution in the main beam while retaining desirable levels of sidelobe suppression. The simplest such pattern is one that provides a reversed phase ring around the main part of the antenna. This and the related techniques require that the transmitting antenna be considerably larger for a given beam diameter at the receiving point. Figure 3.2.1-5 shows a typical pattern achievable with a reverse phase ring around the antenna. Further slight improvements in beam characteristics can be provided by using a continuous phase distribution, rather than a simple phase reversal.

The issue of which pattern to use, or how much taper, may be a cost optimization or it may be dictated by design constraints, as discussed below in section 3.2.1.5.

SPS 068

- RECTENNA RADIUS TO FIRST NULL = 6,485 METERS
- DELIVERED GROUND POWER = 5GW
- ASSUMED RECTENNA EFFICIENCY = 88%

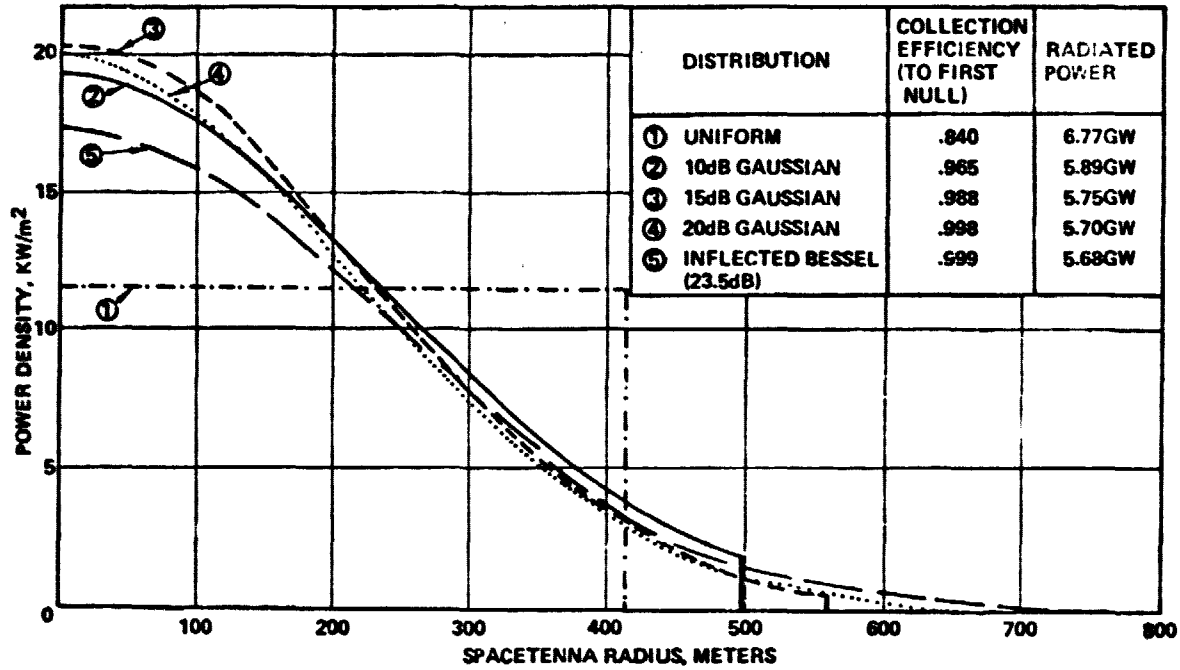


Figure 3.2.1-2 Spacenna Size and Power Density Required for Fixed Rectenna Size and Power Output

SPS 068

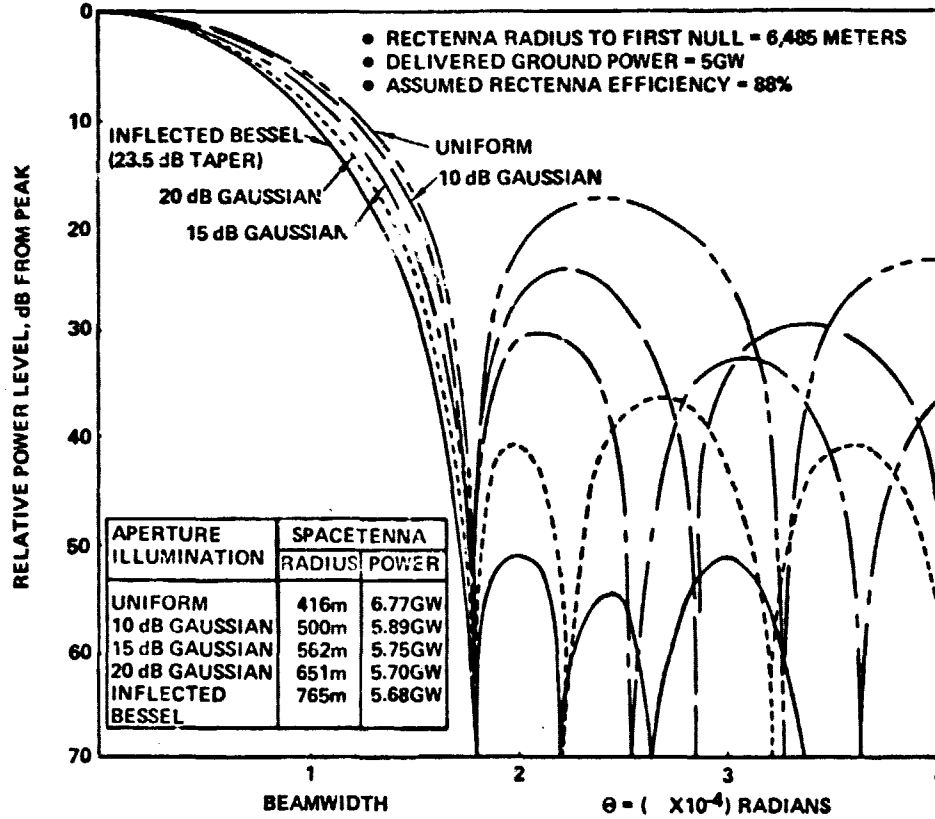


Figure 3.2.1-3 Sidelobe Distributions for Fixed Rectenna Constraints

D180-22876-2

(A CROSS-SECTION THROUGH THE BEAM)

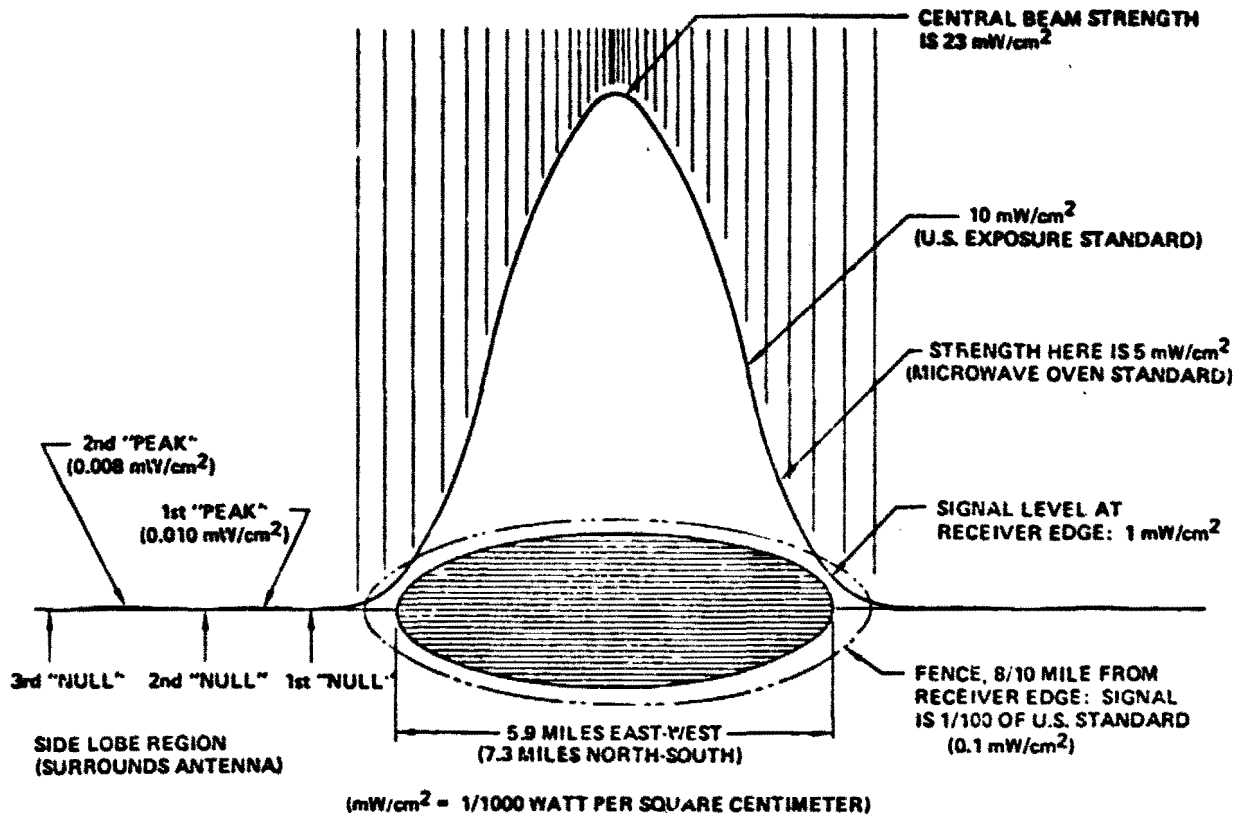
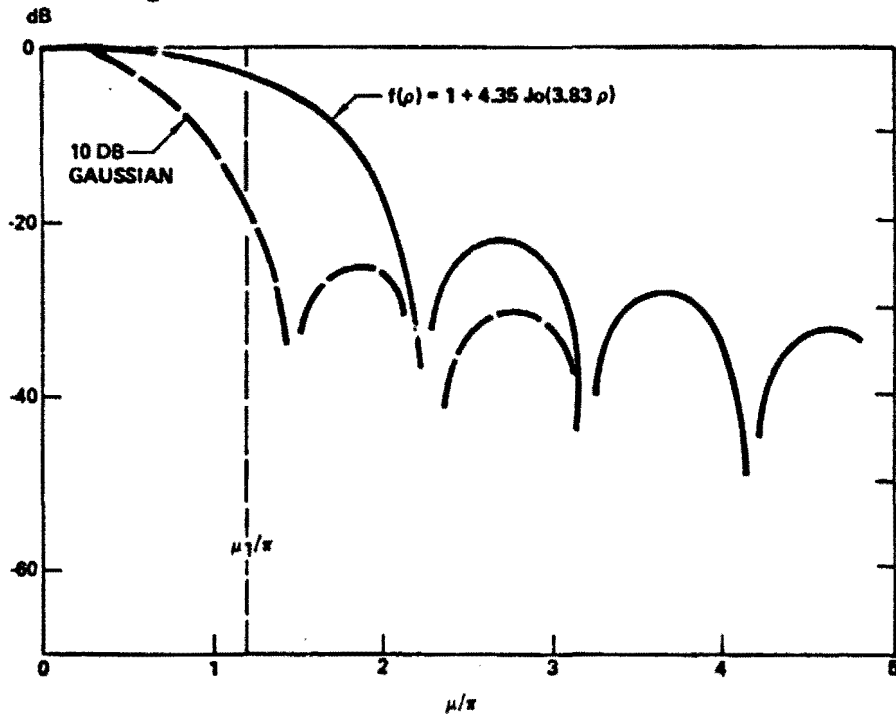


Figure 3.2.1-4 The Microwave Beam: A Safe Power Carrier



3.2.1-5 Spacetenna Pattern

3.2.1.3 Transmitter Design Concept

Overview

The main features of the power transmitter design are illustrated in Figure 3.2.1-6. The basic power amplifier element is a 70 kw heat-pipe-cooled klystron. Each transmitter element includes one klystron, its control and support circuitry, its thermal control equipment, its distribution waveguides and its section of radiating waveguide. The subarray is the basic Earth-manufactured unit. It is approximately 10 meters square and will contain from 4 to 36 klystron elements. The subarrays, in turn, are integrated into the overall transmitter. Each transmitter includes 6,932 subarrays supported on a two-tier structure. At the back of the structural assembly are the power processors that provide the necessary voltage changes and voltage regulation required by the RF systems. Approximately 15% of the total power is processed, the other 85% being used directly by the klystrons without processing or regulation. Power interrupters and switch gear are provided for all power supplied to the transmitter, so that the sector supplied by any power processor assembly can be isolated or shut off in the event of failures or malfunctions.

The power transmitter design illustrated is an integrated design meeting the structural, thermal, electrical, and RF requirements of the SPS power transmission system.

The principal features of the power transmission system are indicated in Table 3.2.1-1. The reference system employs a 10 dB taper in ten steps with an option being a fourteen-step, 17-dB taper providing an additional 10 dB of sidelobe suppression.

Klystron RF Generators

The klystron design was selected using the following criteria:

- Power level of 70 kw compatible with a maximum voltage of 42 kv and a perveance ($I_0/V_0^{3/2}$) of 0.25×10^{-6} , resulting in high efficiency.
- RF Design: Single second harmonic bunching cavity resulting in short interaction length; 6 cavity design to give 40 db gain i.e., feasibility of solid state driver.
- Focusing: Body-wound lightweight solenoid for low risk and high efficiency.
- Cathode: Coated powder or metal matrix, medium convergence cathode to obtain an emission of $\approx 200 \text{ ma/cm}^2$ for 30 year life to emission wearout.;

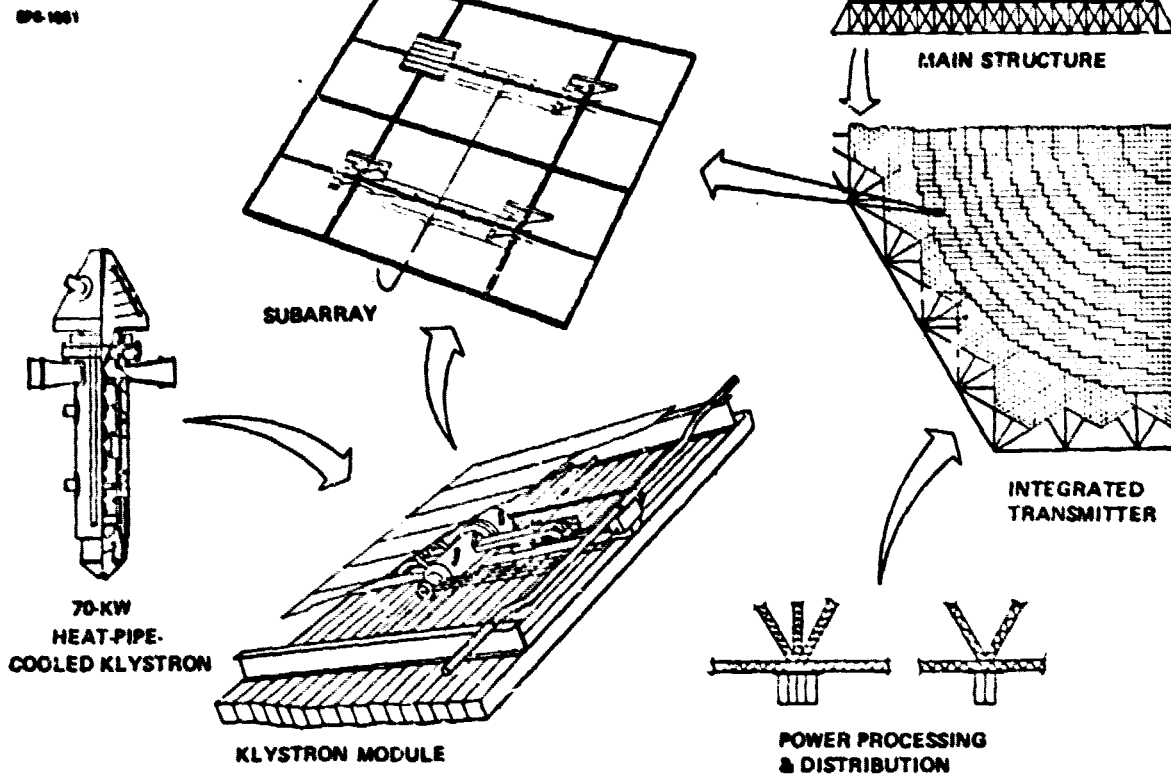


Figure 3.2.1-6 Microwave Power Transmitter Design Concept

Table 3.2.1-1 Power Transmission System Highlights

SPC-1682	JSC GREEN BOOK	CURRENT REFERENCE	REASON FOR CHANGE
OUTPUT POWER TO GRID FROM EACH RECTENNA	5GW	4.65GW	EFFICIENCY CHAIN VARIANCE
ARRAY APERTURE ILLUMINATION (ALTERNATE ILLUMINATION)	10-STEP TRUNCATED 10db GAUSSIAN	SAME (14-STEP) (17db)	PROVIDES ADDITIONAL 10db OF SIDELobe SUPPRESSION
SUBARRAY SIZE	100m ²	113.8m ²	GEOMETRIC CONSTRAINTS
NUMBER OF SUBARRAYS	7850	6932	LARGER AREA PER SUBARRAY
ERROR BUDGET - PHASE CONTROL AMPLITUDE SUBARRAY MECHANICAL RF DISTRIBUTION	±10° ±1db ±3 ARC MIN NONE	SAME SAME ±1 ARC MIN 2% TOTAL LOSS	REDUCE LOSSES DETAILED SUBARRAY ANALYSIS
PHASE CONTROL	ACTIVE RETRO-DIRECTIVE	SAME	
RECTENNA SIZE	10 x 14km	9.4 x 13 km	HIGHER RECTENNA UNIT COSTS YIELD SMALLER OPTIMUM SIZE
MAXIMUM BEAM POWER DENSITY	23 mw/m ²	SAME	

- **Thermal Design:** Heat pipe with passive radiators to obtain the desired CW level with conservative heat dissipation ratings.
- **Auxiliary Protection:** Modulating anode to provide rapid protection shut off capability at the individual tube level, expected to obviate the need for crow-bar type of turn-off.

The tube design concept is shown in Figure 3.2.1-7.

The use of a klystron appears to require a heated thermionic cathode. Assurance of 30 year r.f. transmitter life will require continued testing and assessment to provide a credible data base from which to select either a cold cathode or a thermionic cathode operation. High secondary emission cold cathodes (Beryllium Oxide) have best known life of 18,000 hours and require oxygen replenishment. Best platinum cathode data is currently 10,000 hours at 5 GHz. Best thermionic cathode life data, for the Intelsat transmitter TWTs and BMEWS, is over 50,000 hours and cathode wearout due to emission can be designed to be 30 years with conservative current density as shown in Figure 3.2.1-8. The candidate thermionic cathodes are a proven oxide cathode operating below 900°C and a tungsten matrix cathodes at slightly over 1000°C. Actual cathode testing should be conducted in a realistic cathode-tube environment, not just a test diode. The SPS tube parameters are compatible with conservative cathode ratings with a cathode-to-beam convergence of less than 50.

To avoid excessive infant mortality, a burn-in period is recommended, which may be possible in space. The question of open envelope operation requires further assessment of space contaminants and can offer significant cost reduction if realizable.

Design Integration

An actual antenna design for SPS requires that the selected taper pattern be quantized in intensity level steps. Each step represents a specific subarray configuration in terms of numbers of klystrons on the subarray and arrangement of RF power distribution to the radiating waveguide "sticks." It is clear that each subarray must have an integral number of radiating waveguide sticks, and an integral number of klystrons.

Also each radiating waveguide must be an integral number of wavelengths long in order for the standing wave configuration to function at maximum efficiency. Thus, there are only certain permitted solutions to subarray size, numbers of klystrons per subarray, and waveguide stick arrangements. Fortunately, some of the permitted solutions fall closely within the bounds of our earlier notions as to what a subarray size should be and what a typical klystron power level should be.

SPC-1004

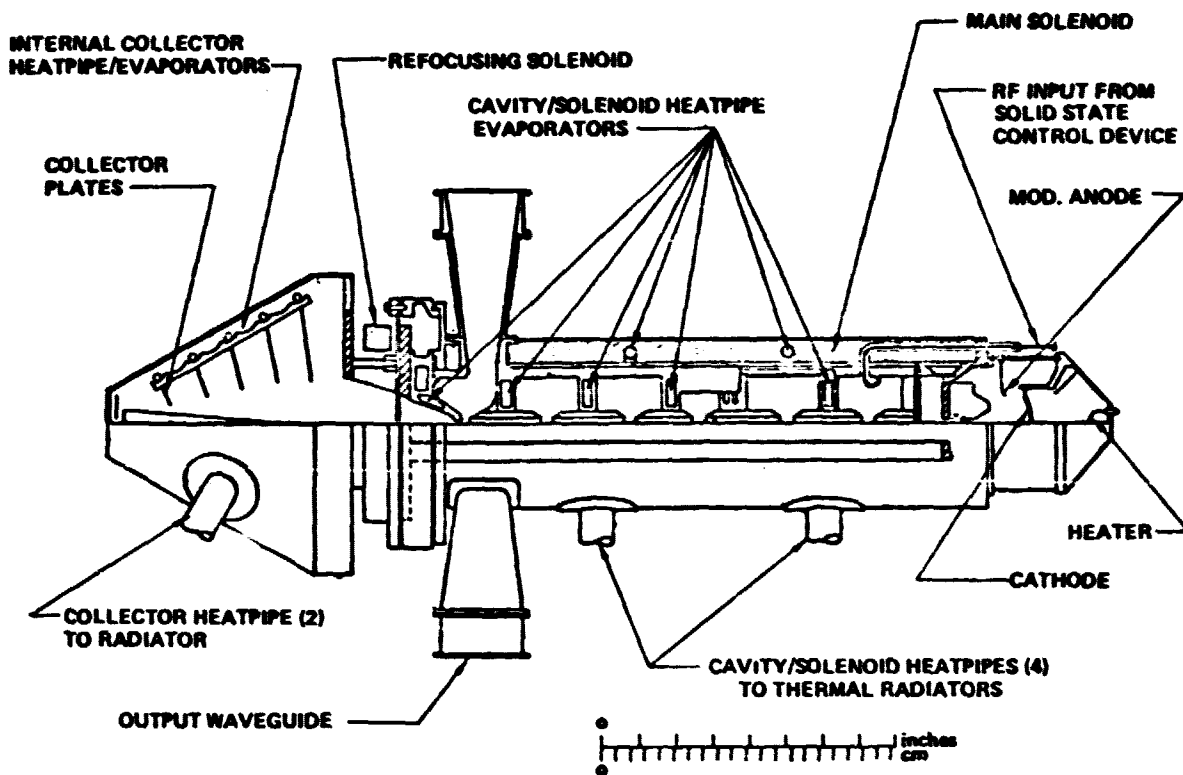


Figure 3.2.1-7 70 Kw Klystron

SPC-1006

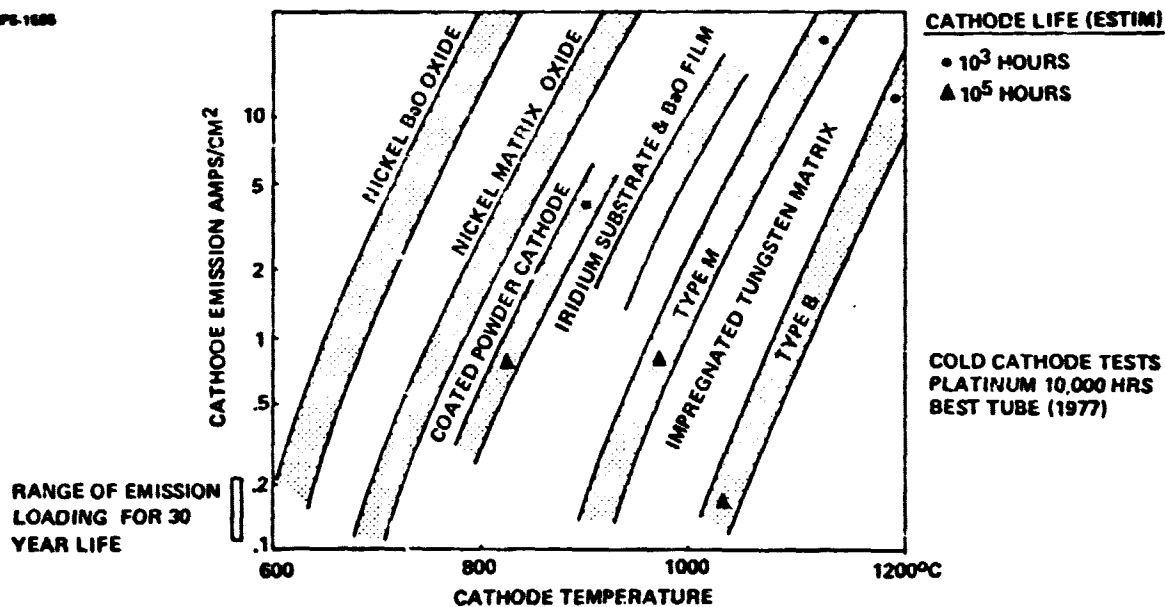


Figure 3.2.1-8 Cathode Emission Data

A subarray consisting of 120 radiating waveguide sticks, each 60 wavelengths long, is approximately 10 meters square, and can be divided into N by M elements, each fed by one klystron, where N and M can each be any integer from 1 to 6. Therefore, a maximum power density subarray would be 6 x 6 elements with 36 klystrons and a minimum power subarray would be one large element fed by one klystron. With the 70 kilowatt klystron, selected for its compatibility with the desired bus voltage of 40 kilovolts, the maximum power density subarray has the power density needed at the center of the antenna with 10 dB taper, and its thermal dissipation at the heat rejection temperatures selected is just within the limitations of thermal radiating area available. A minimum power density subarray with 4 klystrons then provides approximately 10 dB of taper and this was adopted as the reference design.

The waveguide configuration is shown in cross-section in Figure 3.2.1-9. This configuration was selected on the premise that waveguides would be assembled in orbit; it provides high packaging densities. Ground-based assembly has since been selected. This and the tolerances required to minimize losses indicate that a rectangular stick configuration should be used.

The actual configuration of power density rings is illustrated in Figure 3.2.1-10, a view of one-fourth of the radiating face of the antenna. Listed for each step are the number of modules per subarray, the number of subarrays of that type and the number of klystrons in that step for one antenna.

To meet all of the design constraints shown previously, a power taper was achieved using the ten quantized steps available that would provide a ground output of 5.0 GW for a 1.00 kilometer diameter transmitter antenna with a 9.5 dB power density taper.

The MPTS power distribution system shown in Figure 3.2.1-11 provides power transmission, conditioning, control, and storage for all MPTS elements. The antenna is divided into 228 power control sectors, each sector providing power to approximately 420 klystrons. The two klystron depressed collectors which require the majority of supplied power are provided with power directly from the power generation system to avoid the dc/dc conversion losses. All other klystron element power requirements are provided by the DC-DC converter. System disconnects are provided for isolation of equipment for repair and maintenance.

Promising alternate candidates for the radiating elements of the spaceborne transmitter are shown in Figure 3.2.1-12.

- Cylindrical Lens Horn Array
- Traveling Wave End Fire Array
- Enhanced Slot Element

The lensed horn exhibits extremely high efficiency as a result of the lens in the horn aperture.

The traveling wave end fire array provides an open structure which is thermally transparent.

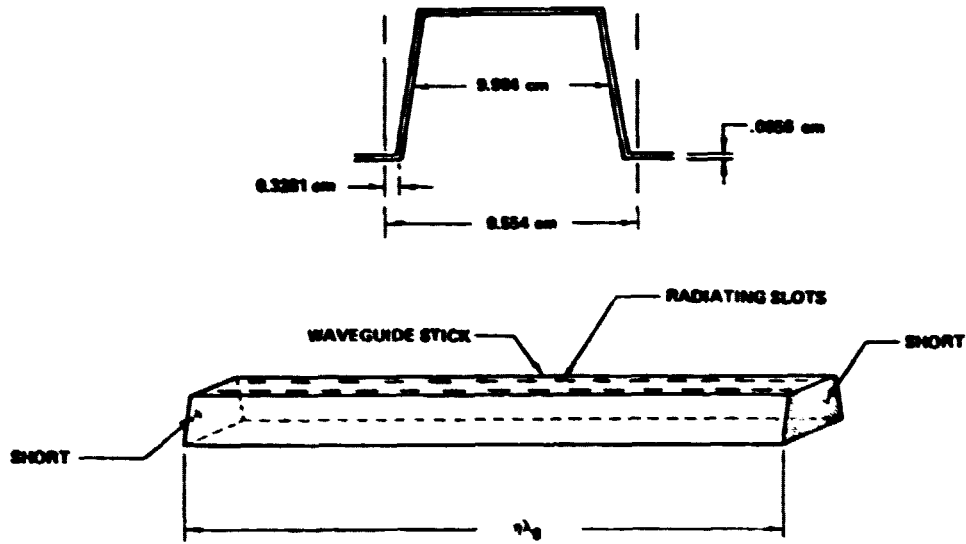


Figure 3.2.1-9 Waveguide

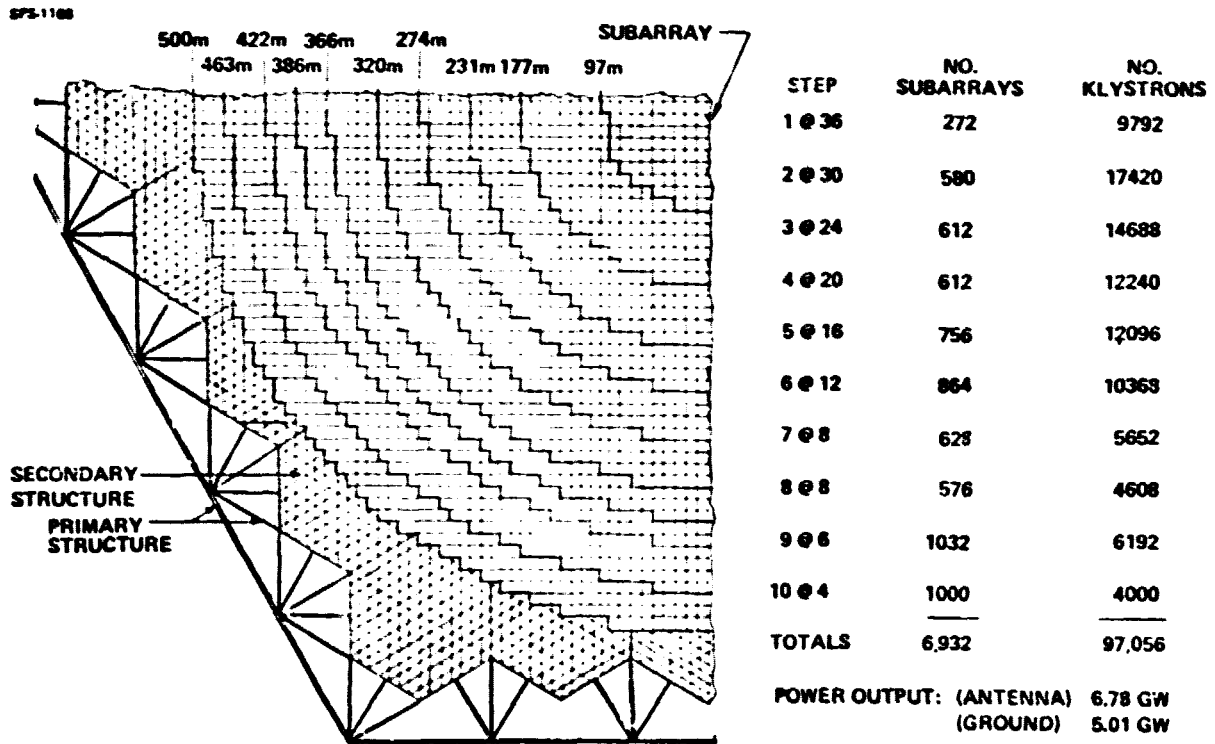


Figure 3.2.1-10 Power Taper Integration

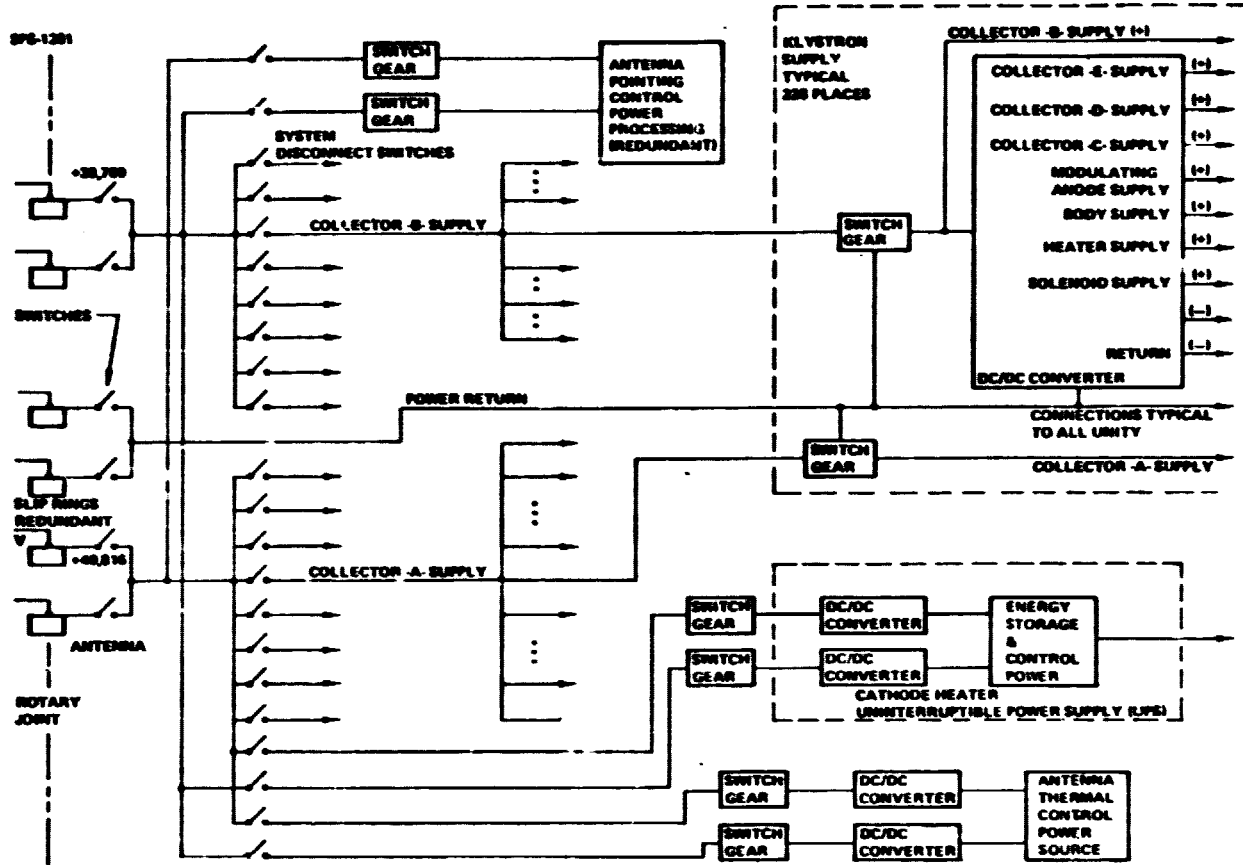


Figure 3.2.1-11 MPTS Power Distribution System Block Diagram

SPS-1645

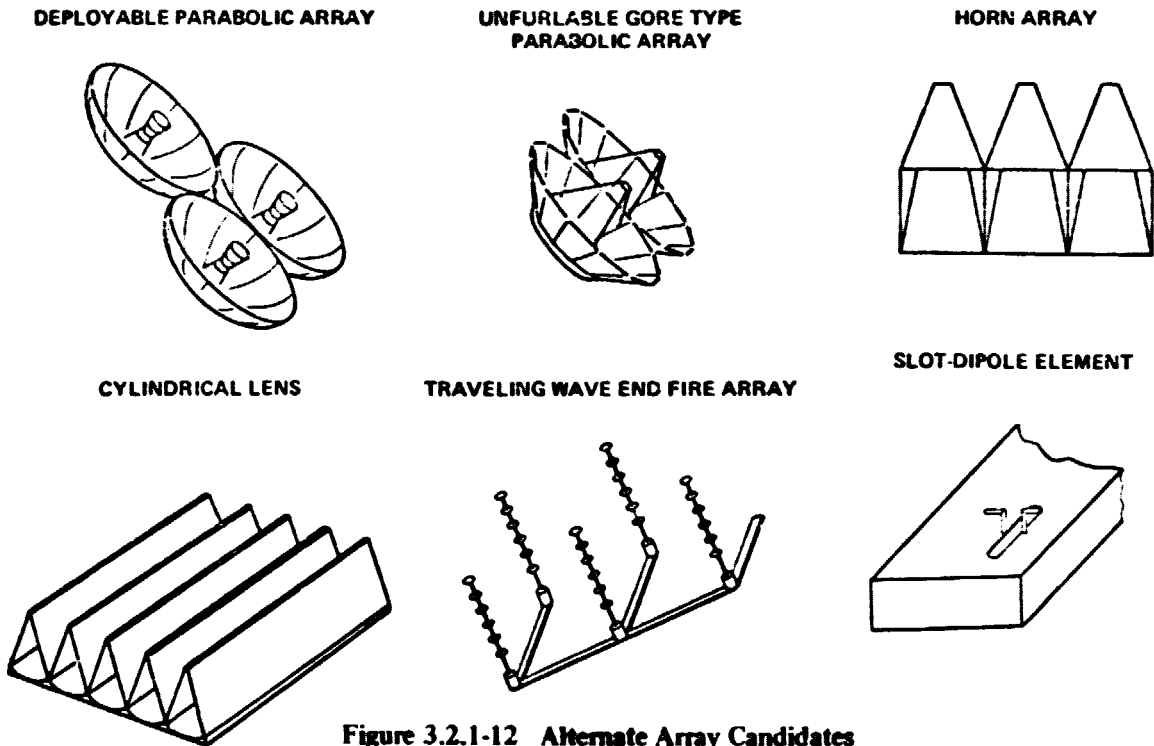


Figure 3.2.1-12 Alternate Array Candidates

Using enhancing elements on each of the radiating slots in a planar array reduces mutual coupling, and consequently losses due to edge effects. Although some of the other options are promising, structural complexity or increased mass have reinforced the selection of the slotted waveguide for the reference design for this phase of the study.

Actual Transmitted Beam Patterns

The left-hand plot in Figure 3.2.1-13 illustrates the 10 step, 9.5 dB taper for the reference system. The right-hand plot shows the actual power density delivered to the ground by this taper pattern including the first 4 sidelobes. The reference taper is shown in solid lines and optional ways of providing the same amount of taper are shown as dotted lines. As can be seen, differences between the reference and the options are slight. The performance closely approaches the ideal continuous taper.

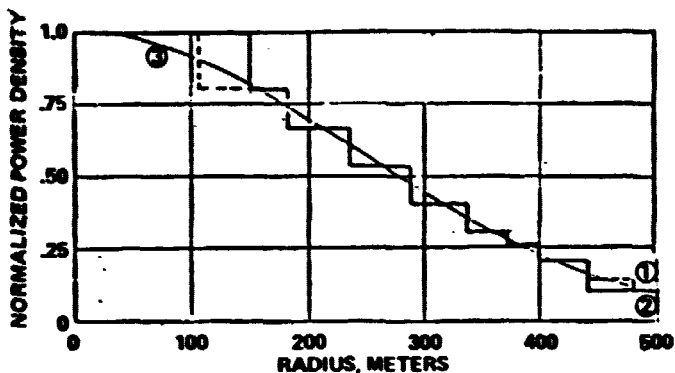
The sidelobe suppression provided by the reference system is 24 dB resulting in a first sidelobe at 0.1 MW/cm^2 . The ideal beam efficiency is 96.5%. (If there are no errors in the production of the beam, 96.5% of the energy is in the main lobe with the remainder in the sidelobes.)

It may be desirable to provide additional sidelobe suppression. The pattern shown in Figure 3.2.1-14 provides an additional 10 dB of sidelobe suppression resulting in a first sidelobe level of $.01 \text{ MW/cm}^2$. The 17 dB power taper is quantized in 14 steps and a slightly larger antenna is required to accommodate the additional power taper without excessive thermal power dissipation at the center of the array.

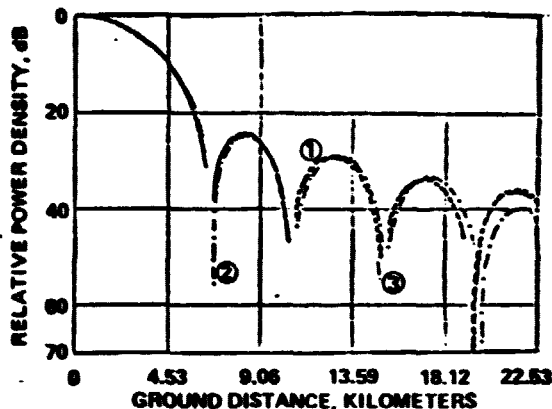
A numerical integration technique was used to calculate the radiation patterns. It was established that the sidelobes for the quantized 10 dB Gaussian tapered distribution rolled off at a 30 dB/decade of angle rate. Figure 3.2.1-15 shows the first five sidelobes and the average power line 3 dB below the peaks. The error plateaus were computed from the assumed error magnitudes and the number of subarrays associated with three different subarray sizes. The aperture efficiency was also obtained by numerical integration. The subarray roll-off characteristics were obtained by numerically integrating the square aperture distribution for each of 19 different cuts over a 45 degree sector. These cuts were then averaged to give the pattern shown. The resultant subarray sidelobes also roll off at a 30 dB/decade of angle.

Failures have an influence on transmitter performance. Individual klystron failures will result in a random thinning of the array and have little effect on the beam pattern if the number of klystron failures is acceptable from the power loss standpoint. Failure of a dc/dc converter, however, would shut down 420 klystrons all in one location. Consequences of a dc/dc converter failure are shown in Figure 3.2.1-16.

SP-1211



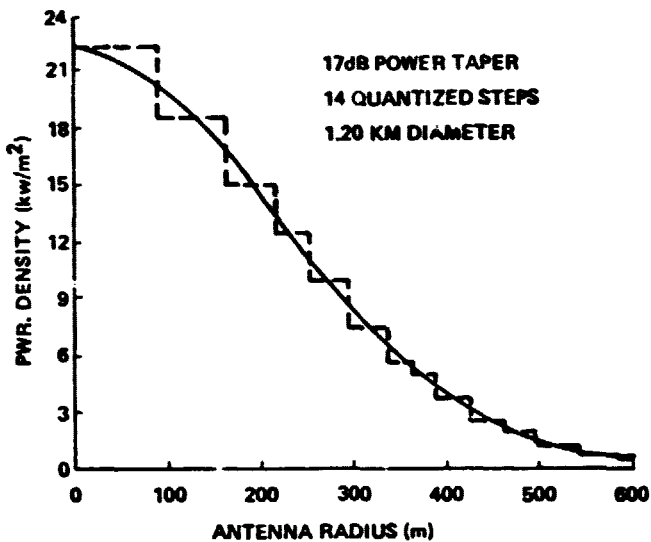
(A) TRANSMITTER DISTRIBUTION FUNCTIONS



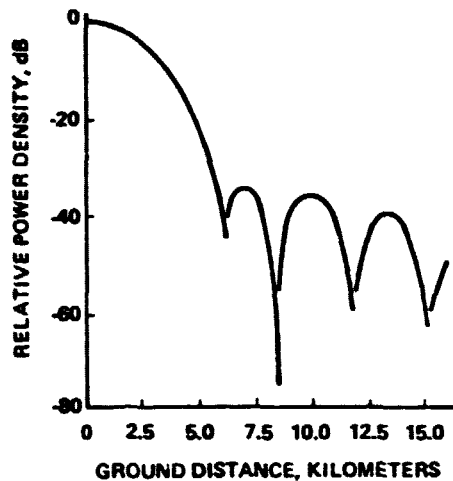
(B) FAR FIELD GROUND DISTRIBUTION

Figure 3.2.1-13 MPTS - Reference 10 dB Taper

SP-1203



(A) ANTENNA POWER TAPER



(B) FAR FIELD GROUND DISTRIBUTION

Figure 3.2.1-14 MPTS 17 dB Power Density Taper

D180-22876-2

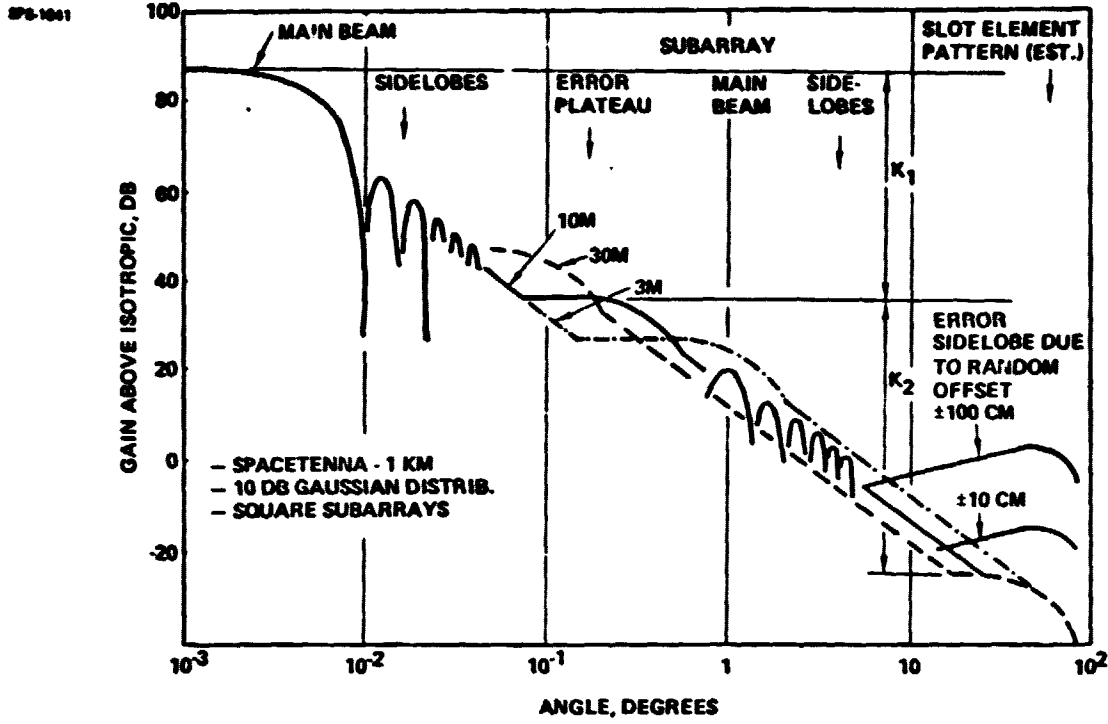


Figure 3.2.1-15 Array Pattern Roll-Off Characteristics

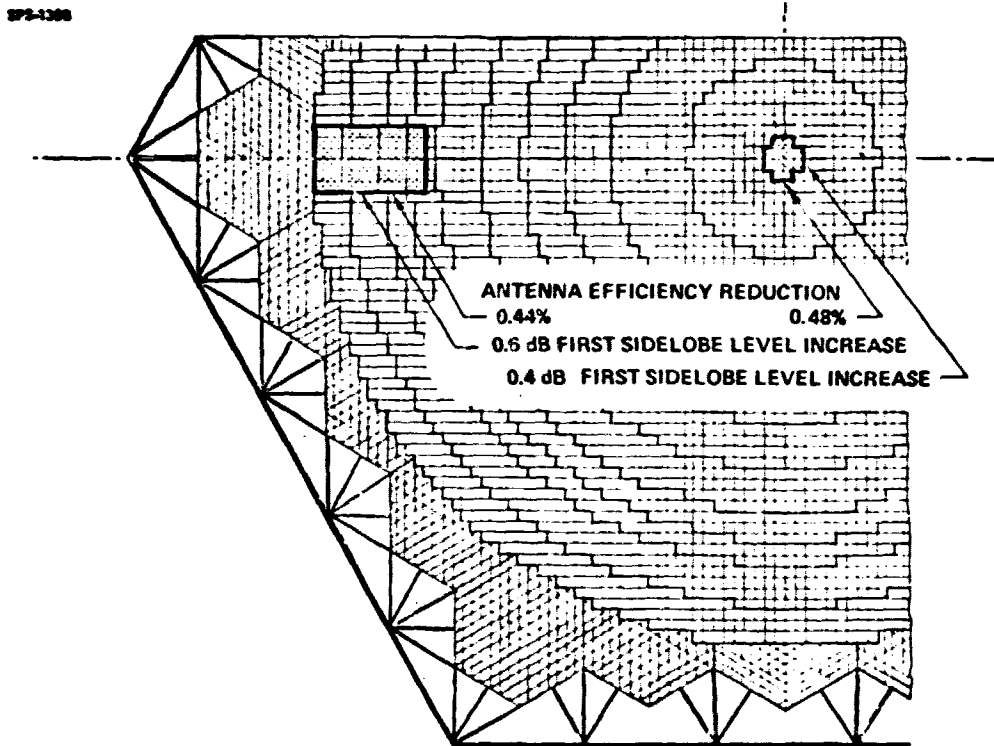


Figure 3.2.1-16 Spacotenenna Section With One DC - DC Converter Failure

The "Bigmain" computer program (obtained from JSC) was exercised to provide estimates of performance degradation due to the failure of one DC/DC converter which supplies processed power to 420 klystrons. The results indicate an antenna efficiency degradation of roughly 0.4 to 0.5 percent and an increase in first sidelobe level of about 0.1 to 0.3 dB depending on the location of the disabled converter. The total power loss thus approaches 0.9 percent, since the loss due to disconnected RF power is added to the reduced array efficiency.

3.2.1.4 Power Transmission Link Efficiency

The end-to-end efficiency of the power transmissions system is a critical parameter in the overall feasibility and cost-effectiveness of the SPS. In the present study, priority was given to a careful evaluation of transmission efficiency. The resulting end-to-end figures (including power conversion) are summarized in Table 3.2.1-2, and compared to estimates given in the JSC "green book" (JSC-11568). JSC-11568 was the point of departure for the study.

Transmitter power distribution losses were determined from a mass and efficiency optimization of conductors and processors, and included consideration of the transmitter self-induced thermal environment.

Klystron conversion efficiency estimates from various sources have ranged from 80% to 87%. Optimization of efficiency requires a joint optimization of electronic efficiency, circuit efficiency, and collector energy recovery. Although it is relatively easy to increase the overall efficiency from 50 to 65% using a 3-stage depressed collector with a collector energy recovery of about 70%, the task of obtaining an 85% efficient klystron will likely require the use of a 5-stage collector. With an undepressed efficiency of 74% and collector recovery of 50%, a net efficiency of 85% would be realized. The design parameters for the 70 kw klystron support this estimate.

Waveguide I²R losses were computed on the basis of an "average" waveguide length and power level. Ideal beam efficiencies and inter-subarray effects, including phase errors, amplitude errors, and klystron failures, were evaluated using the JSC "Bigmain" computer program. This program numerically integrates contributions from all subarrays to get beam patterns, total power, and efficiencies.

The principal new area of analysis was intra-subarray effects: mechanical errors within the subarrays that produce losses.

Because of manufacturing tolerances and thermal distortions, waveguide size as well as slot shape and position will be displaced from the ideal. These dimensional changes will produce unwanted scattering and impedance mismatch resulting in a reduction in efficiency. Factors affecting the losses in the subarrays were studied for a set of given manufacturing and control tolerances. These were found to produce non-dissipative power losses of 1.87% and dissipative power losses of 1.5% for aluminum plated waveguide 9.09 x 6 cm I.D. (The dissipative loss is carried in the efficiency chain as "waveguide I²R"). Thermal effects were found to be negligible if a composite waveguide was used. A number of factors including tolerance in the feeder guide from the klystrons and beam squint due to stick errors were found to produce negligible power losses.

ORIGINAL PAGE IS
OF POOR QUALITY

Table 3.2.1-2 Nominal Efficiency Chains Photovoltaic SPS

SPS-1053

ITEM	JSC GREEN BOOK	CURRENT NOMINAL	REASON FOR DIFFERENCE
SUMMER SOLSTICE FACTOR	NOT INCLUDED	.9765	} THESE WERE INCLUDED IN ENERGY INTENSITY ON SPS
COSINE LOSS (POP)	NOT INCLUDED	.919	
SOLAR CELL EFFICIENCY		.173	
RADIATION DEGRADATION		.97	
TEMPERATURE DEGRADATION	0.103	.954	} 0.151 SLIGHTLY BETTER CELL; CR = 1
COVER UV DEGRADATION		.956	} DISTRIBUTION OPTIMIZATION
CELL-TO-CELL MISMATCH		.99	
PANEL LOST AREA	NOT INCLUDED	.961	
STRING I ² R	.92	.998	
BUS I ² R		.934	
ROTARY JOINT	1.0	1.0	} PROCESSING & TEMPERATURE VARIAN ESTIMATE
ANTENNA POWER DISTR	.98	.97	
DC-RF CONVERSION	.87	.85	
WAVEGUIDE I ² R	.98		
IDEAL BEAM		.965	
INTER-SUBARRAY ERRORS	.88	.956	} .86
INTRA-SUBARRAY ERRORS		.981	
ATMOSPHERE ABSORP.	.98	.98	} INTRA-SUBARRAY EFFECTS NOT INCLUDED IN GREEN BOOK
INTERCEPT EFFICIENCY		.95	
RECTENNA RF-DC	.90	.848	
GRID INTERFACING	.99	.97	} NUMERICAL INTEGRATION INCLUDES DC-DC PROCESSORS
PRODUCTS/SUMS SIZES (Km ²)	.0608	.0679	
		108.8	

Atmosphere losses were unchanged from the JSC estimate. The efficiency chain up to this point includes all power in the main beam. The cost-optional receiver intercepts only about 95% of the main beam power, as discussed in Section 3.2.6.3.2 of this report.

RF-to-DC conversion efficiency at the receiver was derived by numerical integration averaging with receiver element efficiency varying as a function of incident intensity. The current reference value is probably slightly pessimistic for two reasons: (1) the average was based on a receiver filling the entire main beam. The cost-optimized receiver does not intercept the low-intensity outer part of the beam and its average intensity should be slightly greater; (2) recent data received from Raytheon and JPL indicate slightly higher element efficiencies.

DC-to-grid conversion efficiencies were adjusted to include an allowance for power processing.

3.2.1.5 Power Transmission System Sizing

System sizing was investigated by use of a parametric model constructed for the purpose. The parametric model examined characteristics of the system over a range of transmitter sizes and total input electric power with specific constraints applied to the energy density in sidelobes. Incorporation of the sidelobe limitations necessitated an iteration loop within the model to select the transmitter antenna power illumination taper. The loop is diagrammed in Figure 3.2.1-17. It may be seen that this iteration loop includes two other parameters that may be limiting factors: power beam maximum intensity at the center of the beam and the maximum thermal power that must be dissipated on the transmitter antenna.

Operation of this iteration loop is illustrated by Figs. 3.2.1-18 thru 3.2.1-23. Figs. 3.2.1-18A and -18B show transmitter and receiver average-to-peak power intensity ratios. These were determined by numerical integration of antenna patterns for a range of power tapers. Average beam intensity can be determined from total power in the beam and beam diameter and the peak values then determined from these curves. Figure 3.2.1-19 shows the variation in beam spread factor with power taper. The beam spread factor, in turn, affects the beam diameter at the receiver and therefore the peak beam strength. Figures 3.2.1-20 and 3.2.1-21 show thermal power dissipation and beam intensity at the receiver over the range of antenna diameters and beam intensity at the receiver over the range of antenna diameters and input power considered. These curves are used to cross plot the design constraint line on final results such as the cost results shown in Figure 3.2.1-22. It may be seen from Figure 3.2.1-22 that the minimum cost SPS design is essentially bounded by constraints. As would be expected, the minimum unit cost system is the highest power system that can be designed within the constraints. The power level is set by the thermal dissipation and ionosphere beam intensity limits. Sidelobe suppression limits exert considerable influence on the design point selection. Reducing the sidelobe limits results in a greater degree of power taper and, therefore, a peakier antenna pattern. This, in turn, causes the thermal dissipation limit and peak beam strength limit to converge at a larger transmitter diameter and lower power as shown in Figure 3.2.1-23.

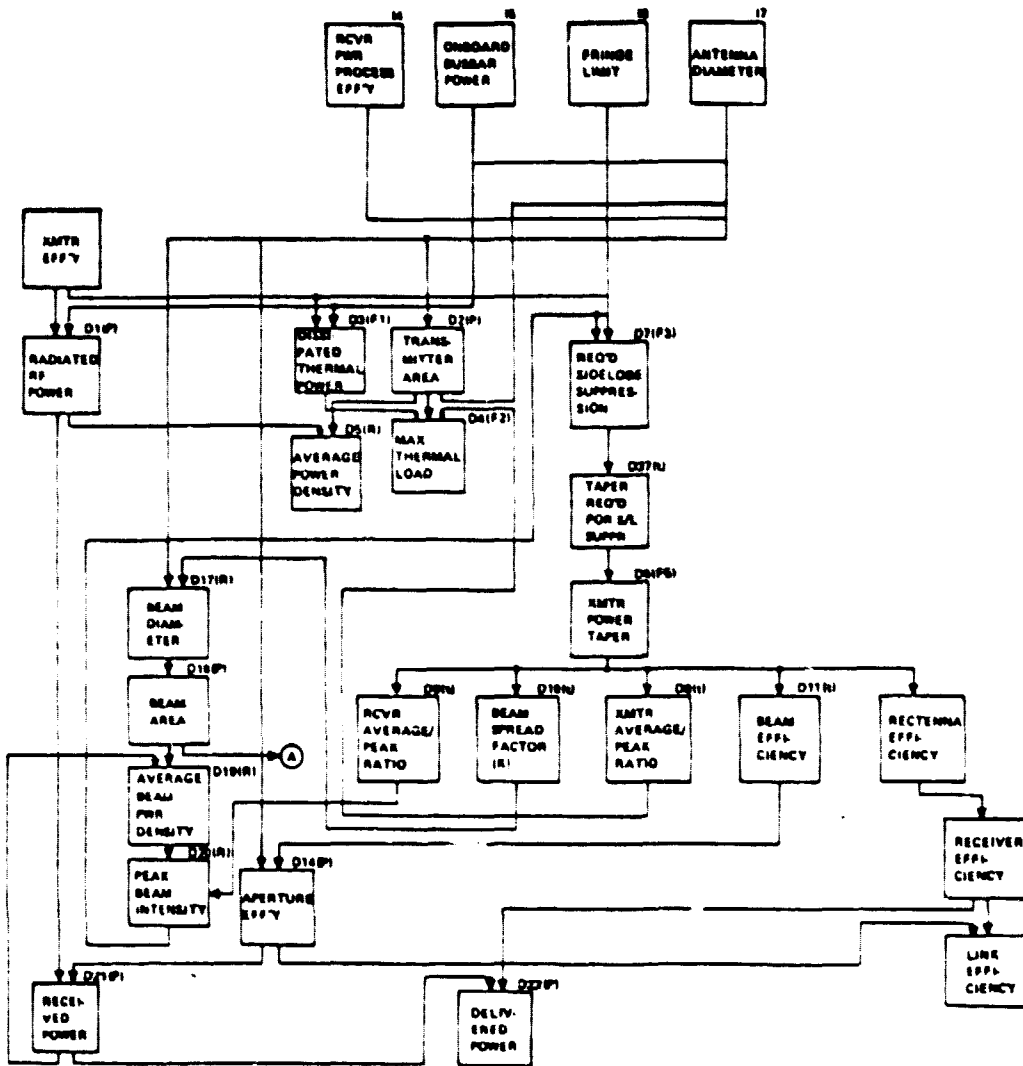


Figure 3.2.1-17 SPS High Level Systems Model ISAIH Implementation Diagram

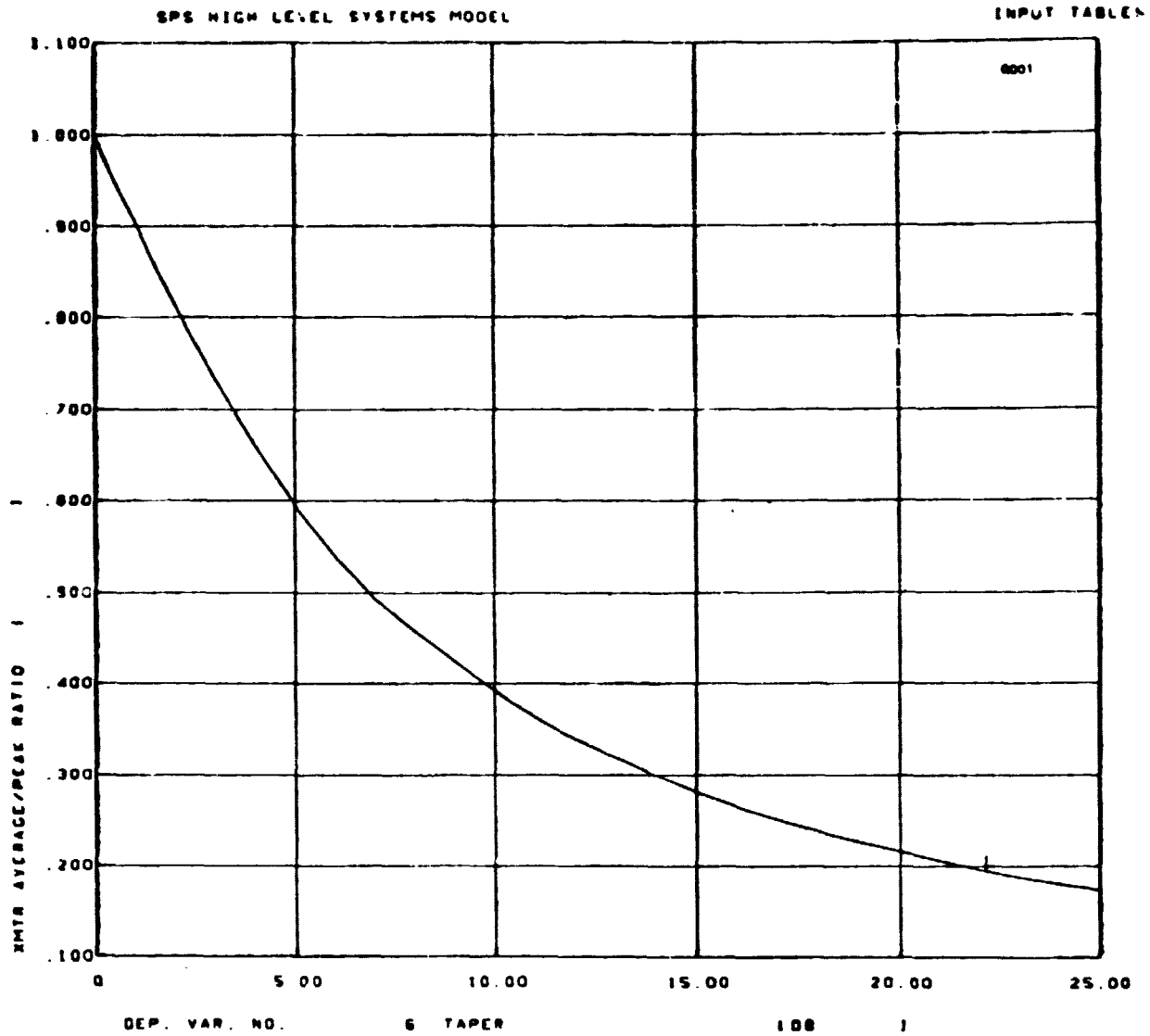


Figure 3.2.1-18A Transmitter Average-to-Peak Power Ratio

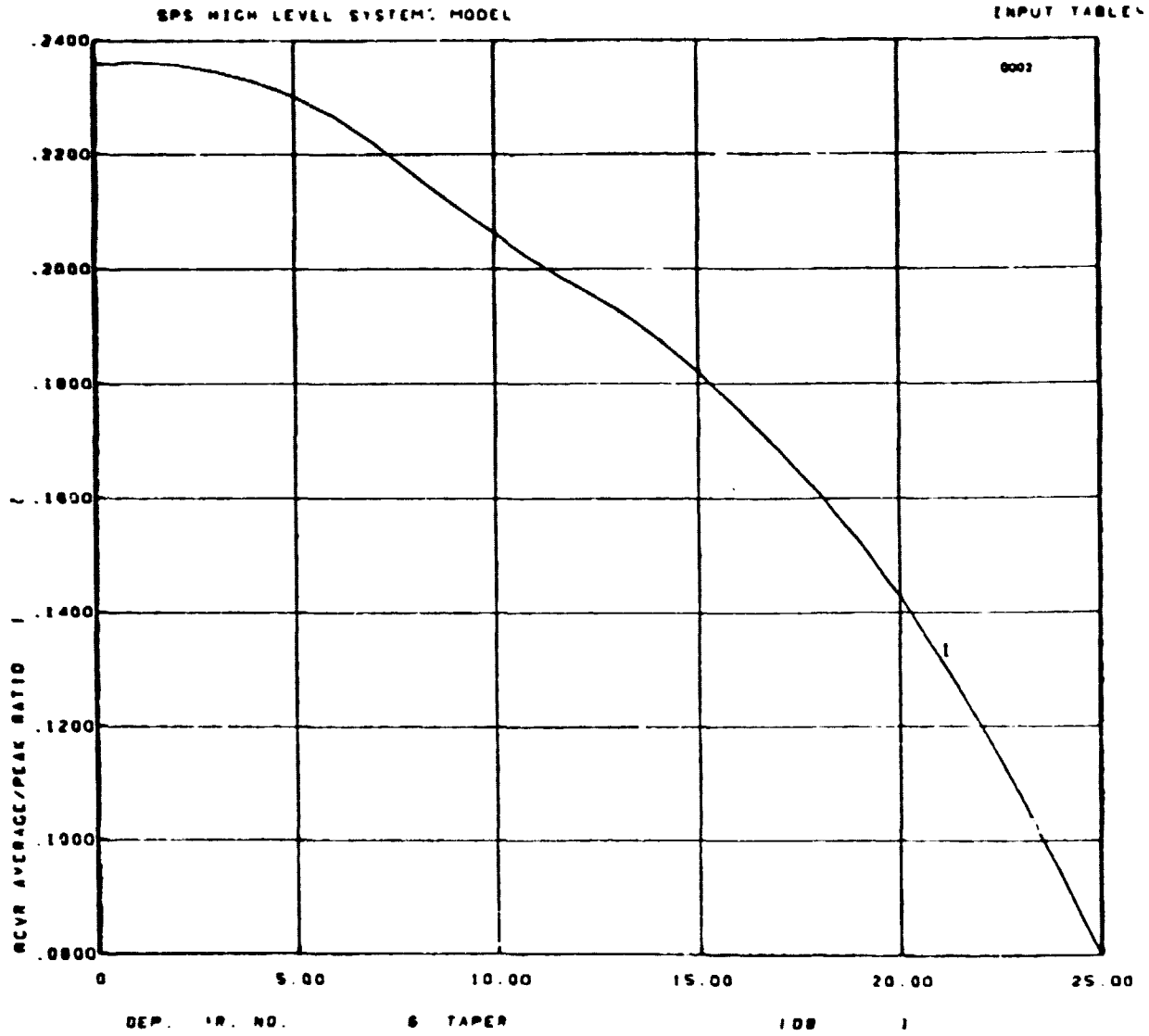


Figure 3.2.1-18B Receiver Average-to-peak Ratio

ORIGINAL PAGE IS
OF POOR QUALITY

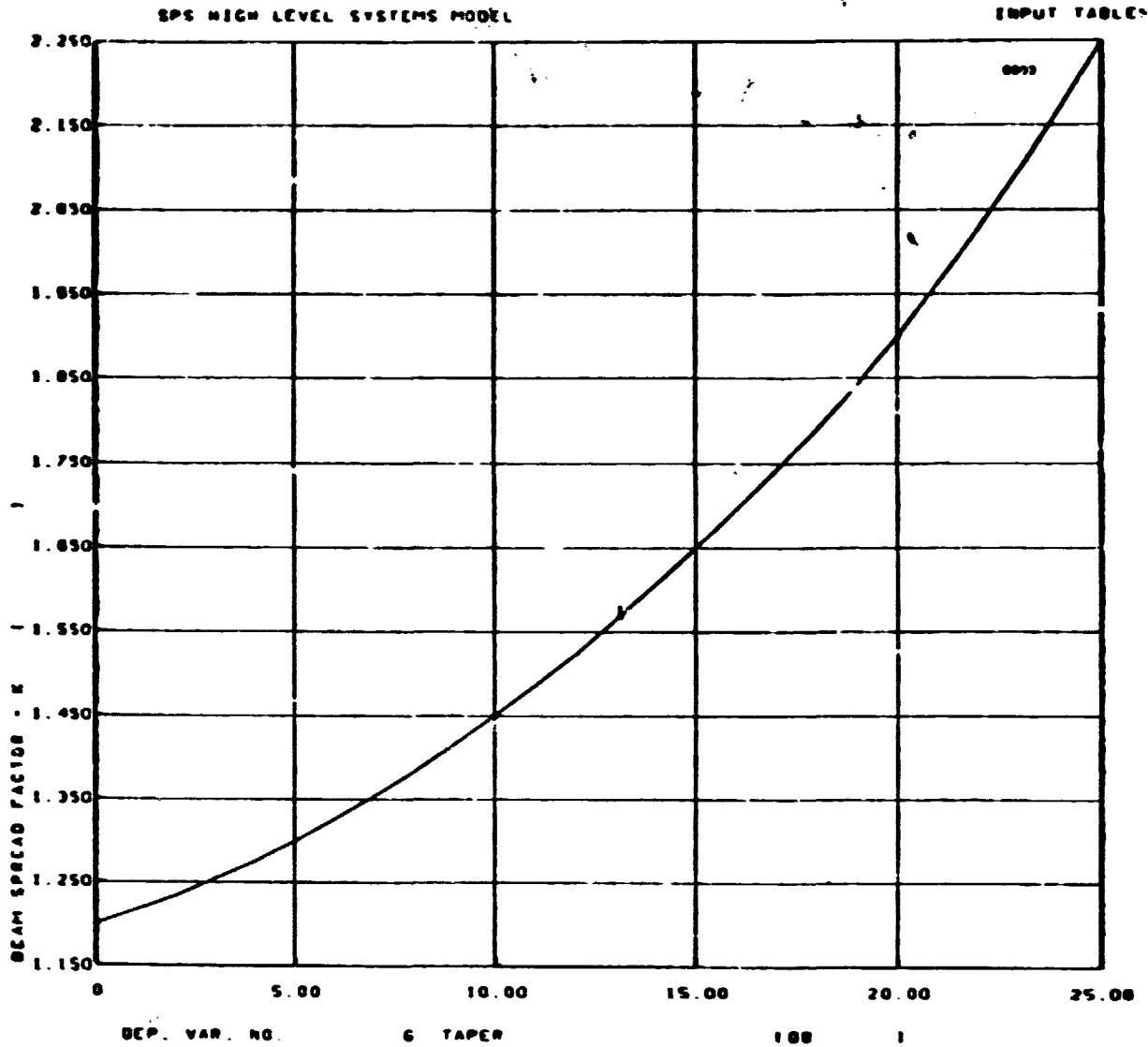


Figure 3.2.1-19 Beam Spread Factor

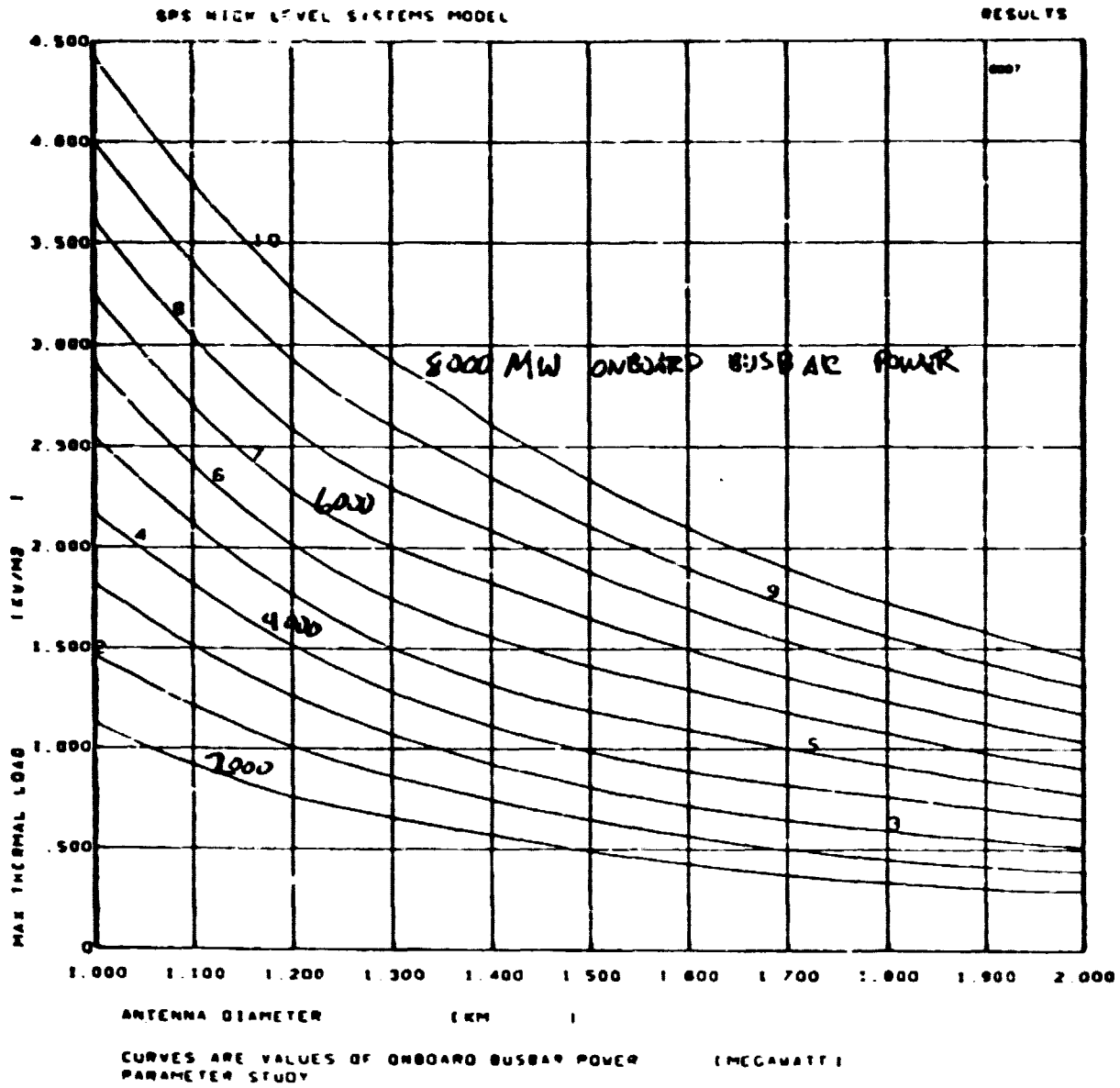


Figure 3.2.1-20 Max Thermal Load

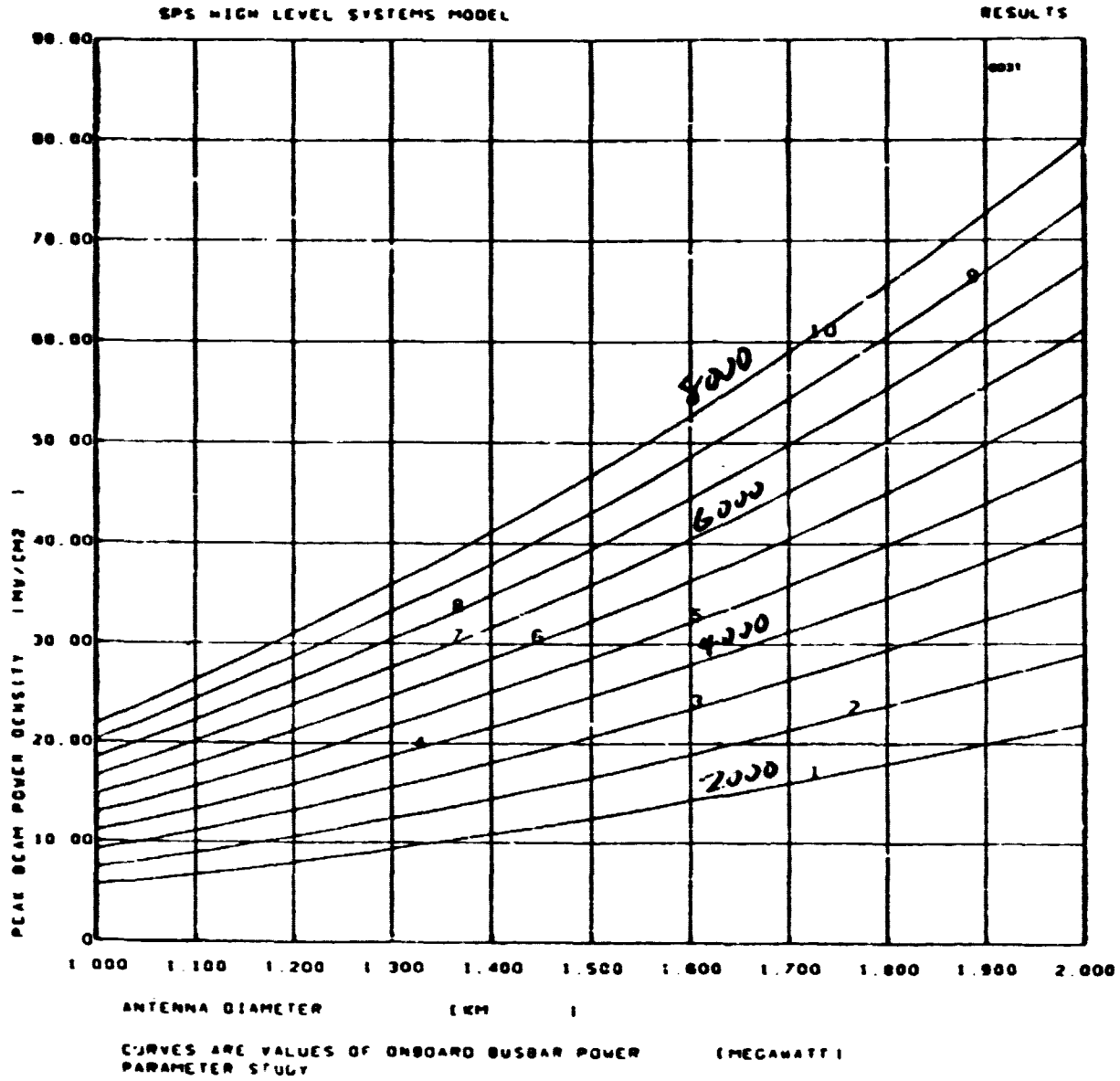


Figure 3.2.1-21 Peak Beam Power Density

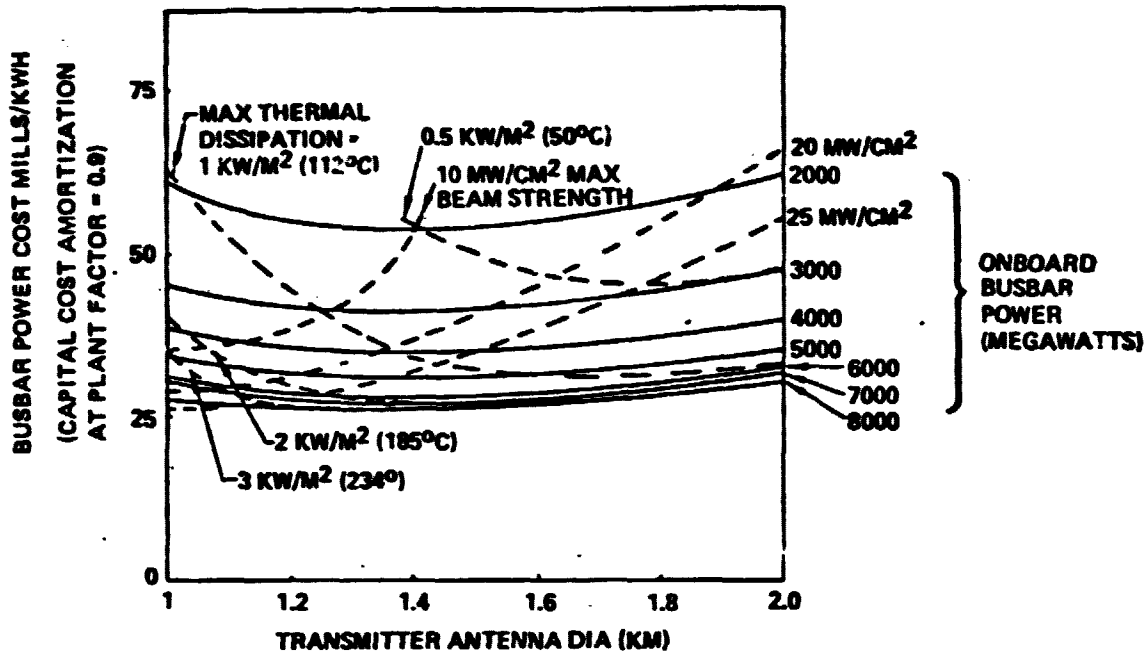


Figure 3.2.1-22 SPS System Performance With Sidelobe Limits $100 \mu\text{w}/\text{cm}^2$

SPS-1671

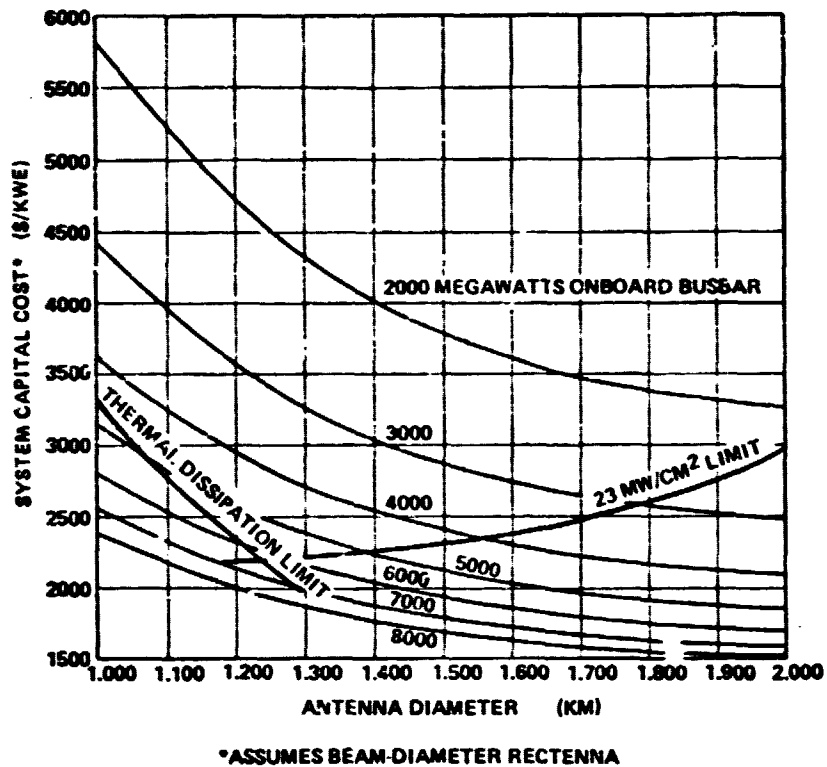


Figure 3.2.1-23 Transmitter Constraints Determine Minimum Cost Design Point (sidelobe limits set at $10 \mu\text{w}/\text{cm}^2$)

The system design point selection also has a significant influence on transportation and construction operations. For the reference design (photovoltaic SPS and 1 kilometer transmitter) and for the reference launch vehicle with its available payload volume, it was just possible to package the entire SPS and its transmitter with the subarrays preassembled on the ground. The packaging density of assembled subarrays is quite low, on the order of 25 kg/m³ average. However, the packaging density of the photovoltaic blankets is very high, about 1200 kg/m³. Detailed packaging studies show that mixing subarrays with high density components allows all of the flights to low Earth orbit to be mass limited. However, if a) transmitter diameter is increased relative to busbar power, or b) the thermal engine energy conversion system is selected, or c) an alternate vehicle with a less voluminous shroud is selected, it will be necessary to perform final subarray assembly on orbit in order to avoid high transportation costs associated with volume limited launches. This in turn increases the on-orbit assembly crew and requires a subarray assembly facility. These items are discussed under construction.

Although it is quite possible that early SPS's will be considerably smaller than the 10,000 megawatt reference design, we are left with the uncomfortable result that one of the penalties associated with selection of a smaller SPS may be the need for final assembly of subarrays in the orbital construction facility.

3.2.2 Photovoltaic SPS Designs

3.2.2.1 Technical Factors Influencing System Design

Insolation

The power output of a solar array depends on the intensity of illumination at the cells and the temperature of the cells, the maximum-power point of cells diminishing as the cells become hotter. The temperature of the solar cell is related to the intensity of sunlight for any given panel configuration.

Sunlight is most intense when Earth is at perihelion, which occurs around winter solstice when the orientation of the array is such that the sun's rays arrive at 23.5 degrees off normal incidence. The worst-case illumination is at summer solstice where the 23.5-degree misorientation occurs at aphelion where the intensity of sunlight is 0.967 of average. However, the solar array temperature is also down, being 36.5°C rather than 46.0°C as at the spring and autumn equinoxes. Net seasonal output variations are shown in Figure 3.2.2-1.

Solar Cell Performance

Solar cell improvements occurred in 1977 in the areas of cell efficiencies and in large grain growth on thin polycrystalline gallium arsenide films.

SP-1637

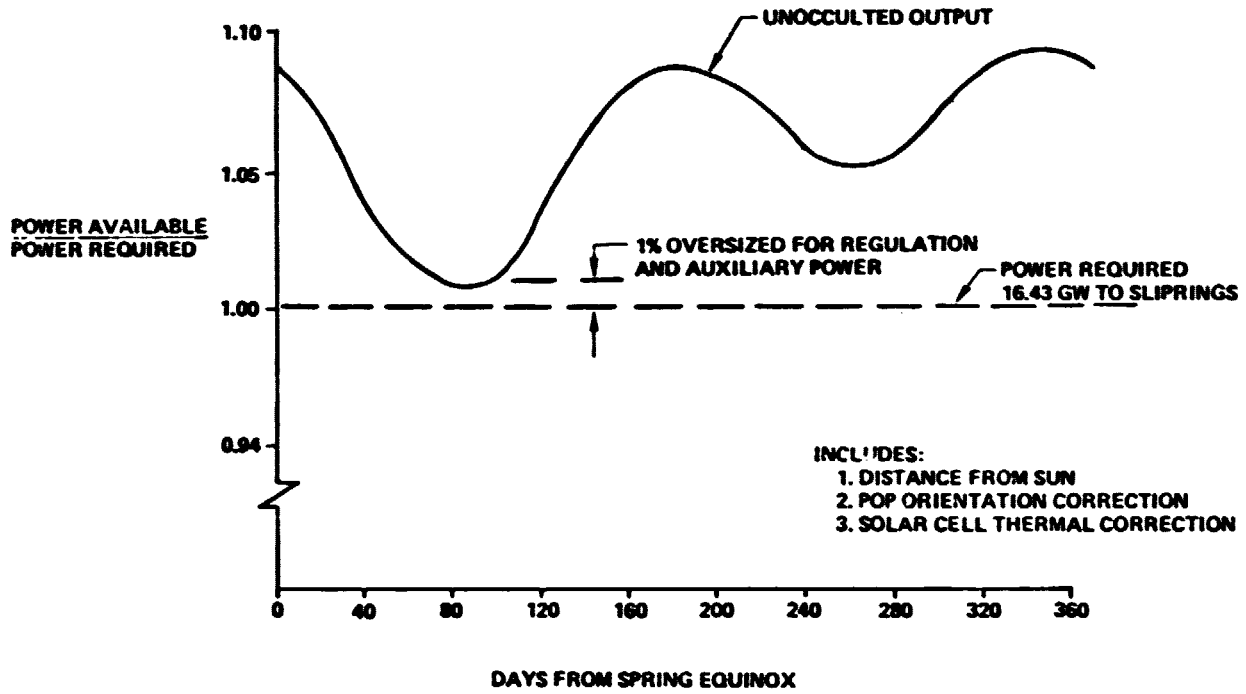


Figure 3.2.2-1 Annual Power Variation

For silicon solar cells, a significant item was the achievement of 12.5 percent efficiency in 50 μm (2 mil) cells. Even though in our reference system, we used a 2 mil cell with 15.75 percent efficiency, an efficiency of 18 percent is quite possible by 1985 for this solar cell.

In gallium arsenide solar cells, John C. Fan of MIL's Lincoln Labs has achieved a 20.5 percent efficient homojunction solar cell in AM1 sunlight. He projects a 22 percent efficiency by optimizing the cell contacts.

A 16.2 percent efficiency has been reported in JPL's gallium arsenide AMOS (polycrystalline) solar cell by Stim and Yeh. Lincoln Labs has also grown 25 μm thick by heating with a laser beam.

Solar Cell Degradation

Solar cells are degraded by the ionizing radiations in space. Radiation damage results from defects produced in the cell material by the passage of the ionizing particles. Solar cells in space applications are protected by a thin cover glass of fused silica or borosilicate glass from 50 to 300 μm thick. This glass greatly reduces the radiation absorbed by the cell by stopping the low-energy particles.

Using Prof. Webber's solar activity predictions, we calculated that in 30 years in geosynchronous orbit a silicon solar cell under a 150 μm (6 mil) fused silica cover will be exposed to the equivalent of 2.25×10^{11} protons per cm^2 having greater than 10 MeV energy. The spectrum of the protons is plotted in Figure 3.2.2-2 with fluence as a function of proton energy. Note how copious are the low energy protons, when compared with the high-energy ones.

A trade-off exists for coverglass thickness. Thinner covers admit more radiation but are less massive, as illustrated in Figure 3.2.2-3.

The optimum turns out to be relatively flat as shown in Figure 3.2.2-4. Any cover thickness in the 50 μm to 100 μm (2 to 4 mil) range is desirable. At least 75 μm is required to use the diffractive sawtooth cover treatment described below.

A significant new development occurred in radiation degradation of silicon solar cells. Since the reference design was changed to thinner solar cells (50 μm) to reduce system mass, it became necessary to reinvestigate the area of solar cell radiation degradation. A plot was made of radiation degradation at various fluences as a function of solar cell thickness. Data were obtained from JPL's "Solar Array Design Handbook." The curves that were developed, when extrapolated to a 50 μm (2 mil) cell thickness, showed a significant reduction in radiative degradation. Information was also published by Solarex on the radiation degradation characteristics of 50 μm cells, also shown in Figure 3.2.2-5.

896-326

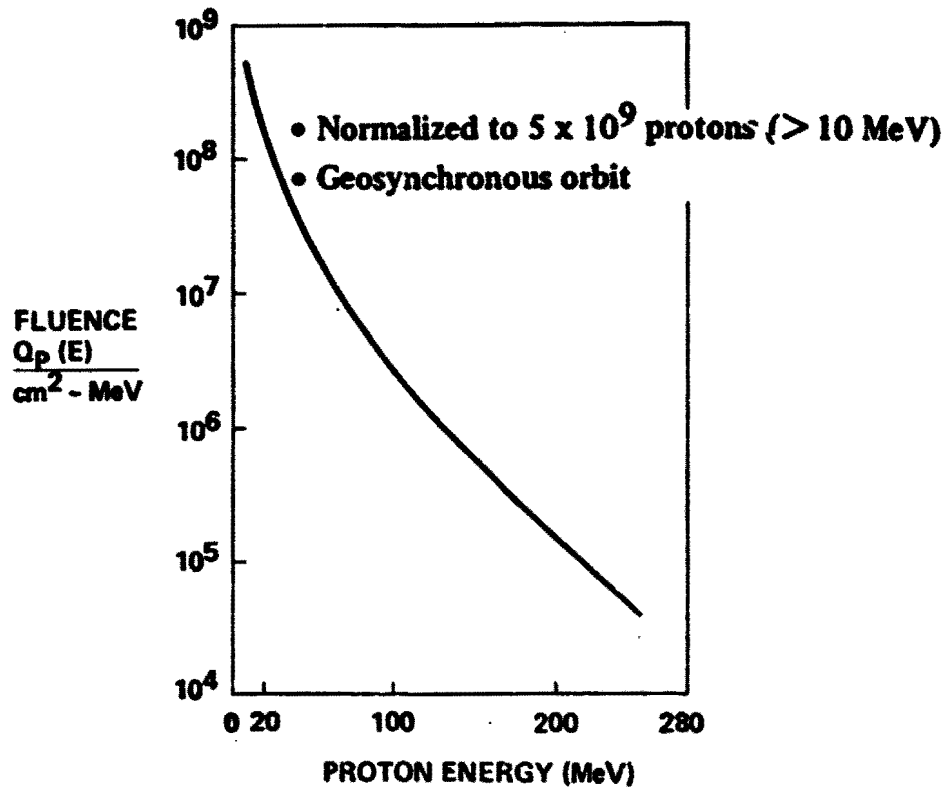


Figure 3.2.2-2 Spectrum of Protons Incident on Solar Cells

896-327

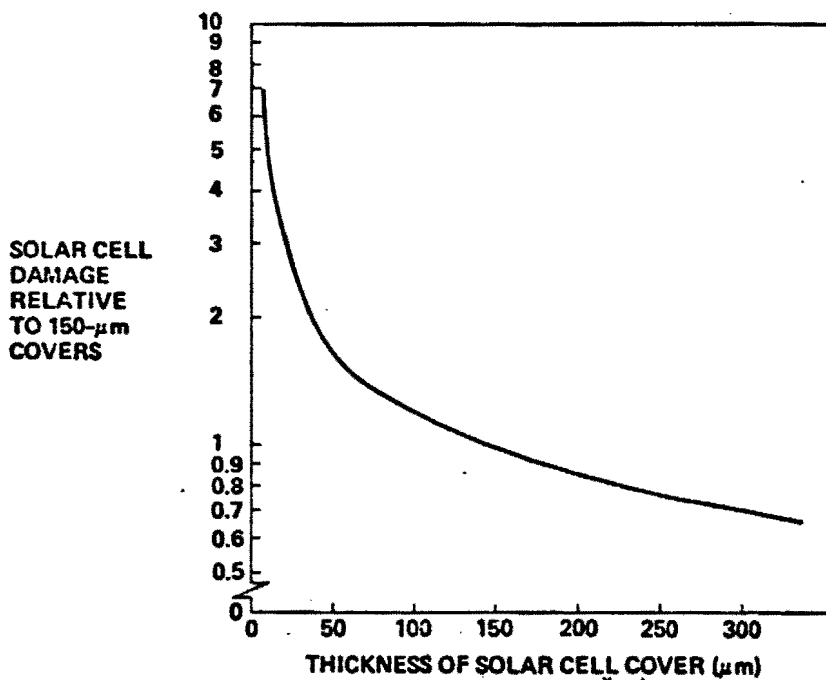


Figure 3.2.2-3 Reducing Cover Thickness Increases Damage

SPS-002

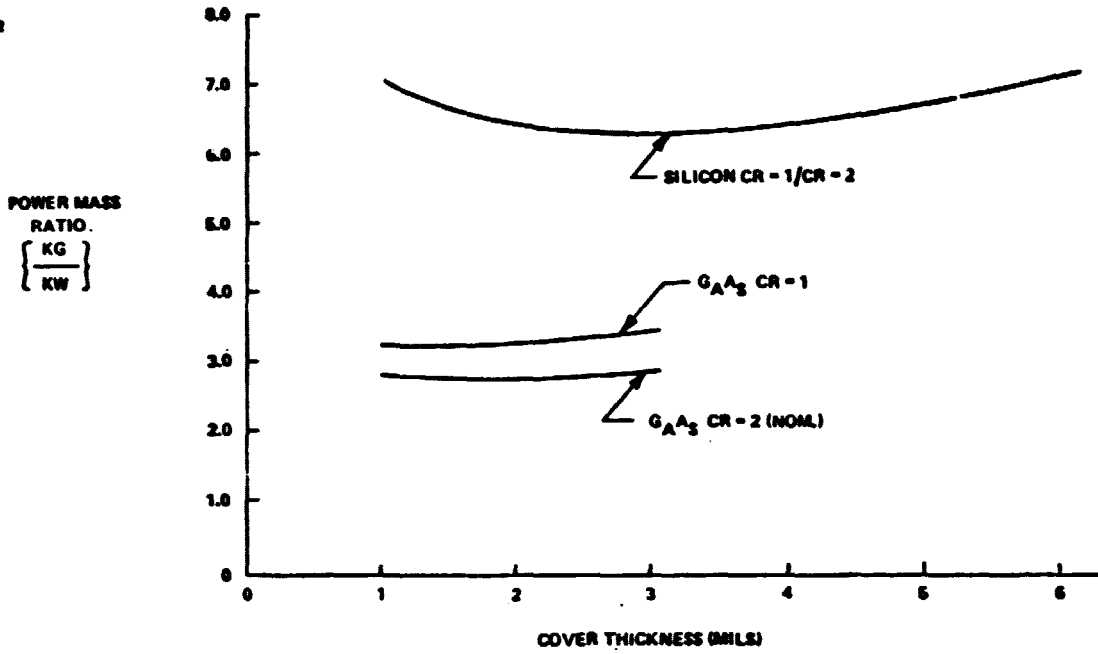


Figure 3.2.2-4 Effect of Cover Thickness On Power Mass Ratio
30 Year Degradation

SPS-1633

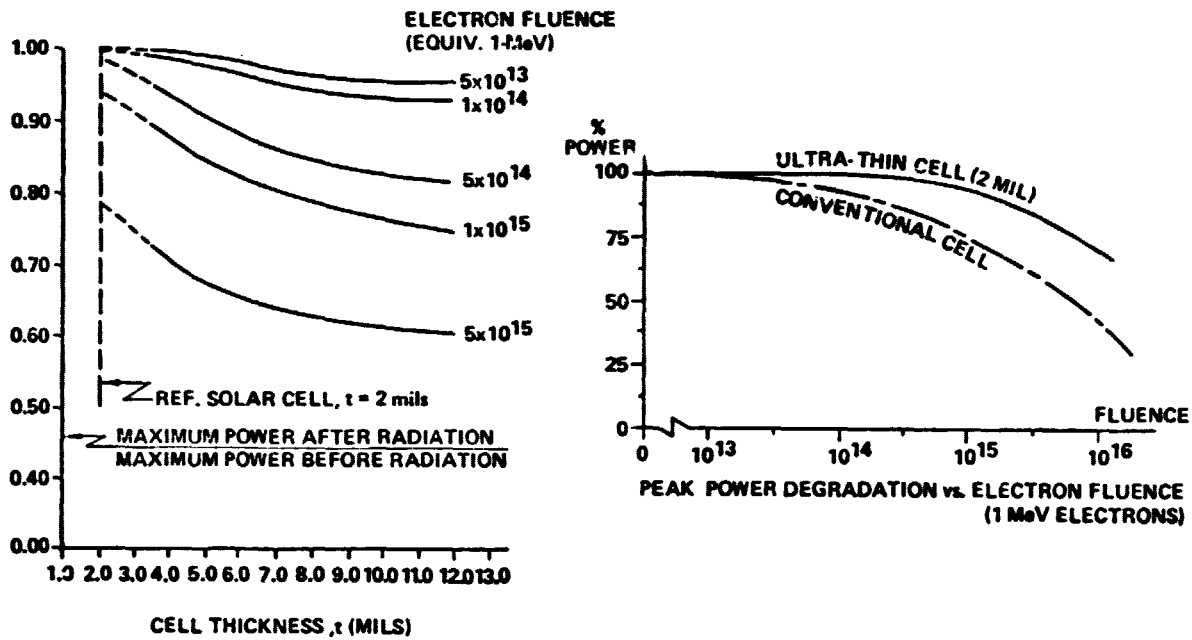


Figure 3.2.2-5 Thin Cells Exhibit Lower Radiation Degradation

The effect of this is that annealing, although still very advantageous, is not as critical an issue as previously reported.

Annealability of Solar Cells

During the part I study effort, a subcontract activity with SPIRE Incorporated investigated annealing of radiation-damaged solar cells by the use of directed energy. Laser and electron beam methods were tried. Both methods yielded about 50 per cent recovery of radiation damage which has been induced by proton irradiation in the Boeing test facility. The cells tested at that time were annealed without cover glasses. The results were reported in detail in Volume II of the part I report.

A continuation of the effort was accomplished during part II. Principal objectives were to extend the previous exploratory results to cells with covers and to test the thinner (50 micron) cells now available in experimental quantities. Final results were not available for inclusion in this report. The following is a status report.

Conventional adhesive-bonded covers cannot be used on cells which are to be annealed because the annealing temperature can be over 500°C.

SPIRE attempted to fasten cover glasses to Solarex 50 μm cells by adhesiveless electrostatic bonding. However, the cell surface was not smooth, apparently as a result of the potassium hydroxide etch which had been used to reduce the cell thickness to 50 μm. As a result, the 50 μm cells broke when electrostatic-bonding pressure was applied.

SPIRE sent to Boeing four thicker cells with electrostatic-bonded covers for irradiation with one MeV electrons. Attempts to anneal the radiation damage with a neodymium -YAG laser were not particularly successful, probably because the covers absorbed the laser light and heated excessively during the laser pulse. Better annealing was obtained with a longer laser pulse (about 1 second) from a CO₂ laser. Four more cells have been irradiated with one-MeV electrons and a refined CO₂ laser irradiating technique will be used in annealing them.

Covered cells cannot be effectively irradiated with protons having 1.9 MeV, the limiting energy of the Boeing Dynamitron. Therefore, four uncovered 50 μm Solarex cells were irradiated with 1.9 MeV protons, degrading in their maximum power output as follows:

Cell Number	Before Irradiation		Fluence of 1.9 MeV Protons	After Irradiation	
	Max. Power, Milliwatts	Efficiency, Percent		Max. Power, Milliwatts	Efficiency, Percent
8	51.9	9.59	1×10^{11}	48	8.87
9	53.3	9.85	1×10^{11}	47.4	8.76
10A	52.2	9.65	1×10^{12}	38.5	7.41
10B	52.2	9.65	1×10^{12}	40.0	7.39

Figure 3.2.2-6 compares the radiation degradation of these thin cells with that of conventional cells.

A proton having an energy of 1.9 MeV is equivalent to about 3×10^4 one-MeV electrons.

These four irradiated 50 μm cells will be sent to SPIRE Corporation for annealing out the radiation damage.

Array Sizing

Factors used in calculating the solar array power output are summarized in Table 3.2.2-1 with solar cells having 15.75 percent efficiency. To this we add a 10 percent improvement, which could be achieved by any one of several means. For example, A. Meulenberg of COMSAT Laboratories estimates that his sawtooth cover will improve the efficiency of solar cells by 8 to 12 percent.

The blanket factors of 0.9453 account for the power losses shown in the table. The individual elements of the blanket factors will change, but the product will probably remain around 0.9453.

The summer solstice loss accounts for the 23.5 degrees misorientation with respect to the Sun's rays. This loss could be avoided by having the satellite oriented perpendicular to the ecliptic plane, but the cost in thrusters and propellants required for attitude control in that mode results in no real advantage.

The aphelion intensity factor accounts for the reduced solar intensity when the Earth is at its aphelion, around the first part of July.

The temperature losses result from the solar cells operating between 36.5°C and 46°C, rather than at the 25°C at which cell efficiency is commonly expressed.

The output is further reduced by 3 percent to account for radiation damage that cannot be removed by thermal annealing. In past tests, 95 percent of the radiation damage in solar cells has been annealed out, even though the cells had not been designed for thermal annealing. There is no theoretical reason why all of the radiation damage in solar cells cannot be annealed out, annealing temperatures of around 500°C being well below the 800°C region where diffusion of impurities starts. On the other hand, the operating plan for the solar power satellite involves repeated annealing, which has not been attempted by anyone, as far as we know.

The power requirement of 17.55×10^9 watts was based on supplying 16.43×10^9 watts to the slip rings and compensating for bus I²R losses. Another one percent was added to this power in the calculation of solar cell area to provide power regulation, auxiliary power, attitude control and energy storage.

The other items include the lost area factors considered for each case. This information was used in the formulation of final reference system sizing.

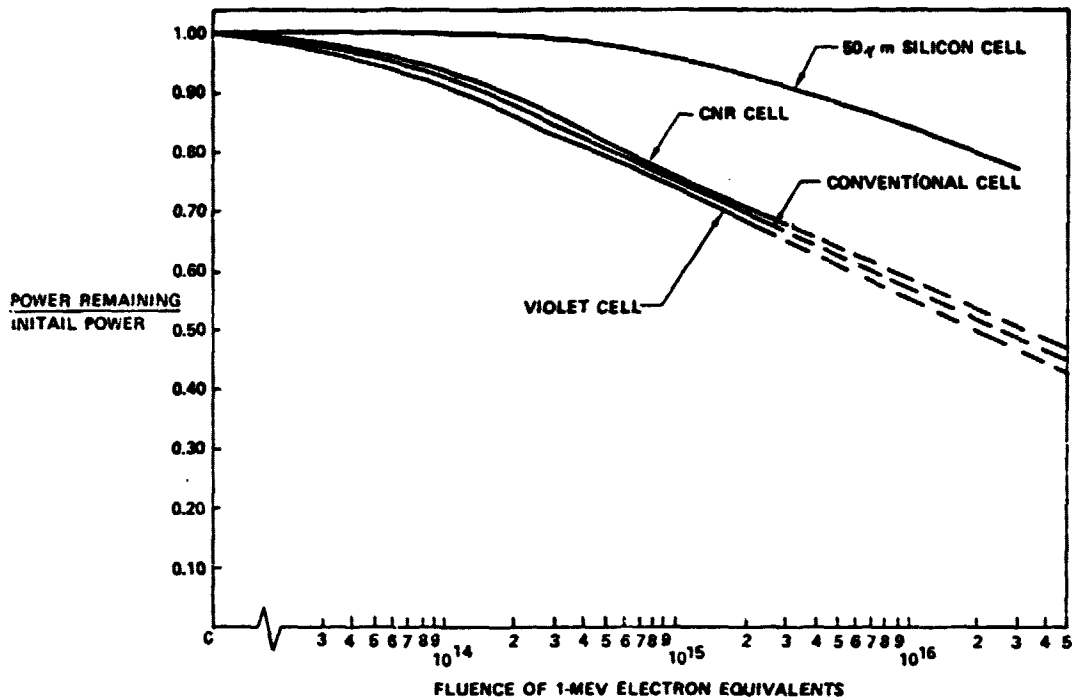


Figure 3.2.2-6 Comparative Radiation Characteristics

Table 3.2.2-1 Part II Reference System Energy Conversion/Sizing

SPS-1536

	OUTPUT - W/M ²
● BASIC CELL PERFORMANCE @ AMO-25°C (.1575)	213.1
● 10% IMPROVED PERFORMANCE DUE TO TEXTURED COVERS (.1733)	234.4
● BLANKET FACTORS (.9453) (STRING I ² R, UV LOSSES, & MISMATCH)	221.6
● SUMMER SOLSTICE COSINE LOSS (.9190)	203.6
● APHELION INTENSITY FACTOR (.9675)	197.0
● TEMPERATURE LOSSES (36.5°C @ SUMMER SOLSTICE = 0.9540)	198.0
● 30 YEAR NON-ANNEALABLE RADIATION DEGRADATION (0.970)	182.3
● POWER REQUIRED TO BUS (INCLUDES I ² R LOSS)	17.55 (10) ⁹ WATTS
● SOLAR CELL AREA (1% OVERSIZE FOR ENERGY STORAGE, ATTITUDE CONTROL REGULATION, AUX. PWR & ANNEALING CAPABILITY)	97.3 km ²
● ARRAY AREA (CELL, PANEL, STRING AND SEGMENT LOST AREAS)	102.5 km ²
● SATELLITE AREA (BEAM, CATENARY & ATTACHMENT LOST AREA FACTOR)	112.8 km ²

Control Requirements

Attitude control requirements are at GEO dominated by gravity gradient effects. Orbit trim requirements are dominated by solar pressure. A good flight control strategy combines the corrections, using unbalanced couples to provide translation corrections for solar pressure while applying torque to counter gravity gradients.

Solar pressure for an absorptive surface is readily calculated as:

$$F = \frac{P}{C} = \frac{1353 \text{ watts/m}^2}{3 \times 10^8 \text{ m/sec}} = 4.51 \times 10^{-6} \text{ n/m}^2$$

The reference photovoltaic system has a projected area of 112 km^2 ; the solar pressure is $4.51 \times 10^{-6} \times 119 \times 10^6 = 505\text{N}$.

Gravity gradient torques can occur around all three SPS axes as a result of the sun-facing attitude requirement.

Significant torques occur only about the y axis when flying perpendicular to the orbit plane (POP). The peak thrust required is 390n. (100n. each 4 places). The duty cycle is that for a sinusoid, 0.64.

The mass penalty for gravity gradient control includes: 1) thrust production hardware: thrusters plus power processing; 2) generating capacity required to power the thrusters; 3) propellant required. The correct propellant quantity penalty reflects the time value of the cost of propellant resupply; the penalty should be the *net present value* (in economic terms) of the lifetime propellant requirement. The penalty value ranges from 10 years' annual supply (10% discount for 30 years) to 14 years' annual supply (7½% discount, infinite life).

Propulsion system Isp is a variable, assuming electric propulsion. As Isp is increased, propellant mass penalty decreases but hardware penalty increases. Accordingly, an optimum occurs as shown in Figure 3.2.2-7. 20,000 seconds Isp is selected as a representative value. For POP operation, assuming perfect control laws (no control authority margin, no wasted propellant) about 250 tons of hardware, including generating capacity, and 41 tons/year argon propellant is required. Electric propulsion characteristics were taken from the Part I technical report, Volume 5. About 50 megawatts peak, 32 megawatts average, power is required to drive the thruster system. Chemical propulsion will be needed to provide control during equinoctal occultations. Despite the low Isp (400 sec), only 1 to 1½ tons of propellant is needed annually due to the small duty cycle. Complete reliance on chemical propulsion would result in a propellant requirement of about 2100 tons per year. Thus electric propulsion is nearly mandatory for flight control at GEO.

All 3 torque terms are operative when flying perpendicular to the ecliptic plane (POP). ϕ varies $\pm 23\frac{1}{2}^\circ$, θ varies from 0 to 360° . An approximate numerical integration gives peak thrust (total 4

SPS-1288

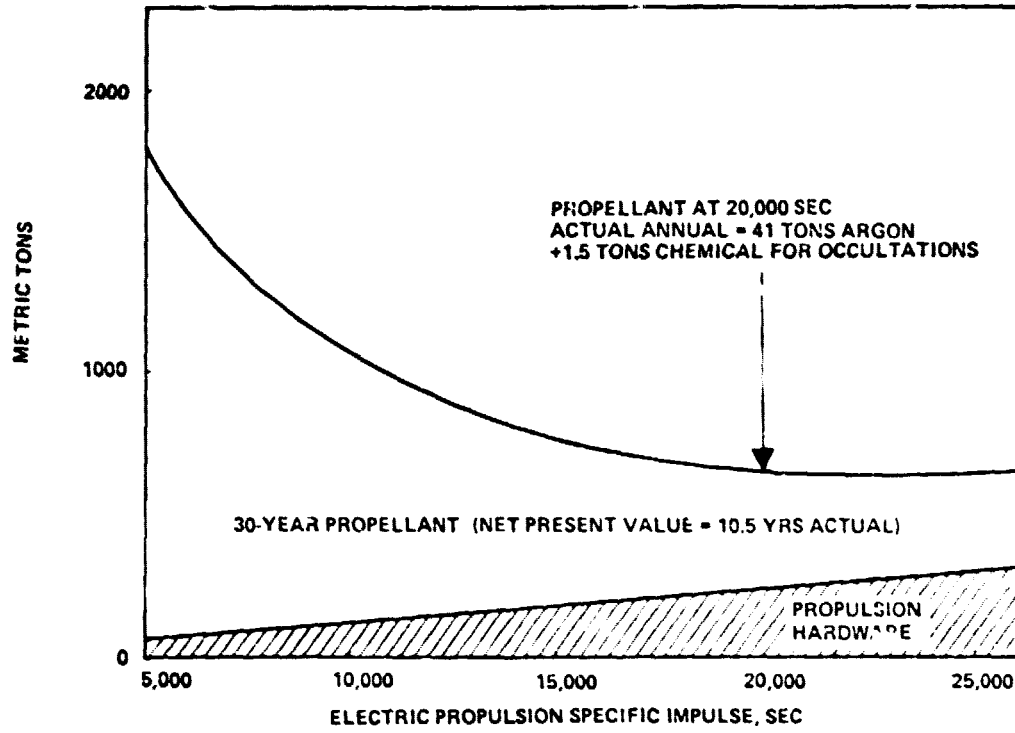


Figure 3.2.2-7 Attitude Control Propellant – Photovoltaic POP

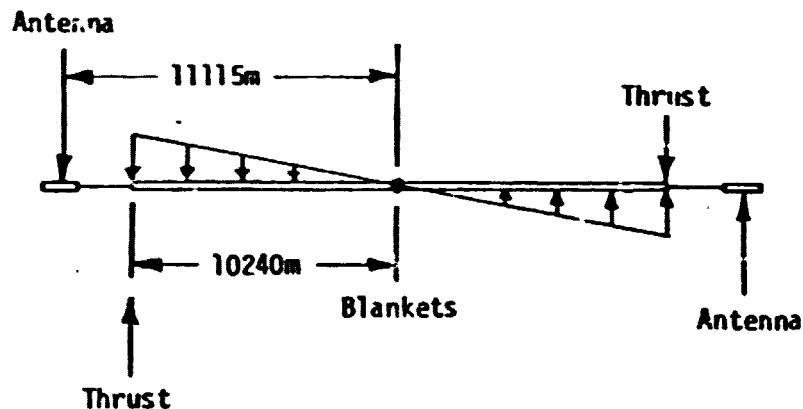
corner is 2230 newtons with an average duty cycle of 0.4. Therefore, the hardware penalty is 5.6 x that for flying POP (1390 tons) and the propellant penalty is 3.5 x that for flying POP (144 tons/yr). This is a 1.4% hardware mass penalty (for a ~3% gain in output due to sun orientation) and a propellant penalty roughly equivalent to one chemical OTV flight to GEO every 2.75 years. The hardware plus net present value propellant penalty is about 3% compared to output gain of also about 3%. Thus flying PEP is about a break-even and should be adopted only if it provides design advantages (as it does for the thermal engine).

If the orbit were to remain precisely trimmed with respect to solar pressure perturbations, a continuous solar pressure balancing thrust of 505N would be required. If the orbit is allowed to become perturbed, less impulse is required. It is likely that the gravity gradient control impulse will be sufficient for orbit maintenance.

Loads Arising from Gravity Gradient Control Authority

A requirement has been identified that an operational SPS should be able to recover from any attitude to the normal operational attitude. If the SPS is in an anomalous attitude as a result of some sort of accident or problem, it may not be able to generate power. Accordingly, chemical thrust will be used to recover to normal attitude. The worst case is presumably a gravity gradient stable attitude (90° around Y-axis from POP).

An example case was examined with $\theta = 0$ and $\phi = 45^\circ$ (worst case gravity gradient torque about the X-axis). The force diagram (1-dimensional approximation) is shown below:



Sufficient thrust was assumed to balance the gravity gradient torques. For example calculations, antenna mass was taken as 7686×10^3 kg each (the green book value). The blanket mass was taken as 0.55 kg/M^2 .

The thrust force required to balance the gravity gradient is 1525 newtons. The shear and moment diagrams are shown below:



The moment from point 1 to 2 is $681l$ and is equal to 555.875 n-m at point 2. The moment from 2 to X peaks at 1.25×10^6 n-m at $y = 5000$ (halfway between the center and end of the blanket).

Under a gravity gradient upset condition, the SPS would probably not be generating power. Therefore, chemical thrust would be needed to reestablish attitude control. Propellant consumption would be minimized by using high thrust to impart an angular momentum just sufficient to cause the SPS to coast to the desired attitude. In practice, a thrust about 4 times the maximum gravity gradient torque equivalent calculated above should be sufficient. The angular work done by gravity gradient in rotating the satellite is 15.61×10^7 n-m radians.

If a thrust level of 6000 n. is used, this amount of work is done in 0.254 radians rotation. The acceleration is 3.14×10^{-8} rad/sec². At this angular acceleration, 4000 sec are required to rotate through 0.254 radians. The total propellant required is 12,000 kg for the total SPS at an lsp of 400 sec ($\mu \approx 4000$). Moments due to this thrust level will be 4X the values quoted above, 2.2×10^6 at the rotary joint and 5×10^6 n-m, maximum at the blanket structure mid point. With a structural depth of 500 m., the top and bottom loads are $\approx 10^4$ n (≈ 2200 lb) divided more or less evenly among all the beams. This load is considerably less than the blanket stretching internal loads.

Structural Criteria and Structural Sizing

System structural criteria have been updated as indicated in Table 3.2.2-2. The solar blanket stretching load is the primary design load on the structure.

3.2.2.2 Reference Photovoltaic System Design

The reference design that resulted from the Part II activity is shown in Figure 3.2.2-8. It consists of eight modules each containing 32 bays for a total of 256 bays, plus the two power transmitters. The modularization was to facilitate low Earth orbit (LEO) construction and the bay size was selected somewhat arbitrarily. Subsequent parametric analyses indicated that structural mass was insensitive to bay size.

The final result for the LEO construction case indicated that a slightly larger array area was needed, resulting in a 680-meter bay size requirement. This occurred when solar cell mismatch effects were included in transfer degradation considerations.

Each bay supports a solar blanket in trampoline fashion. Blankets are made up of individual panels about 1 meter square. The blanket and panel design are compatible with periodic array annealing.

Table 3.2.2-2 Structural Design Criteria

ITEM	LEO OR GEO	REPRESENTATIVE VALUE (PHOTOVOLTAIC)
RECOVERY FROM LOSS OF ATTITUDE CONTROL	GEO	3000N THRUST AT EACH OF 4 CORNERS
NORMAL ATTITUDE CONTROL	GEO	100 TO 200N THRUST AT EACH OF 4 CORNERS
CONSTRUCTION LOADS: FRAGILITY	BOTH	??
THERMAL DUE TO OCCULTATIONS	BOTH	300K TEMP. CHANGE = 3000 psi FOR GRAPHITE } = 60 ksi FOR ALUMINUM } FIXED
LAUNCH	BOTH	5 g's AS PACKAGED FOR LAUNCH
DYNAMIC	BOTH	CONTROL < STRUT < BLANKET SUSPENSION FREQ. < FREQ. < FREQ. (0.8 C/H) (3.5 C/H) (-10 C/H)
BLANKET STRETCHING	BOTH	4.5N/M BIAxIAL
INTERNAL PRESSURE	GEO	30-YEAR CREEP RUPTURE/50% MARGIN
ORBIT TRANSFER	LEO	MAX INSTALLED THRUST = 10^{-4} g's =

SPB-1000

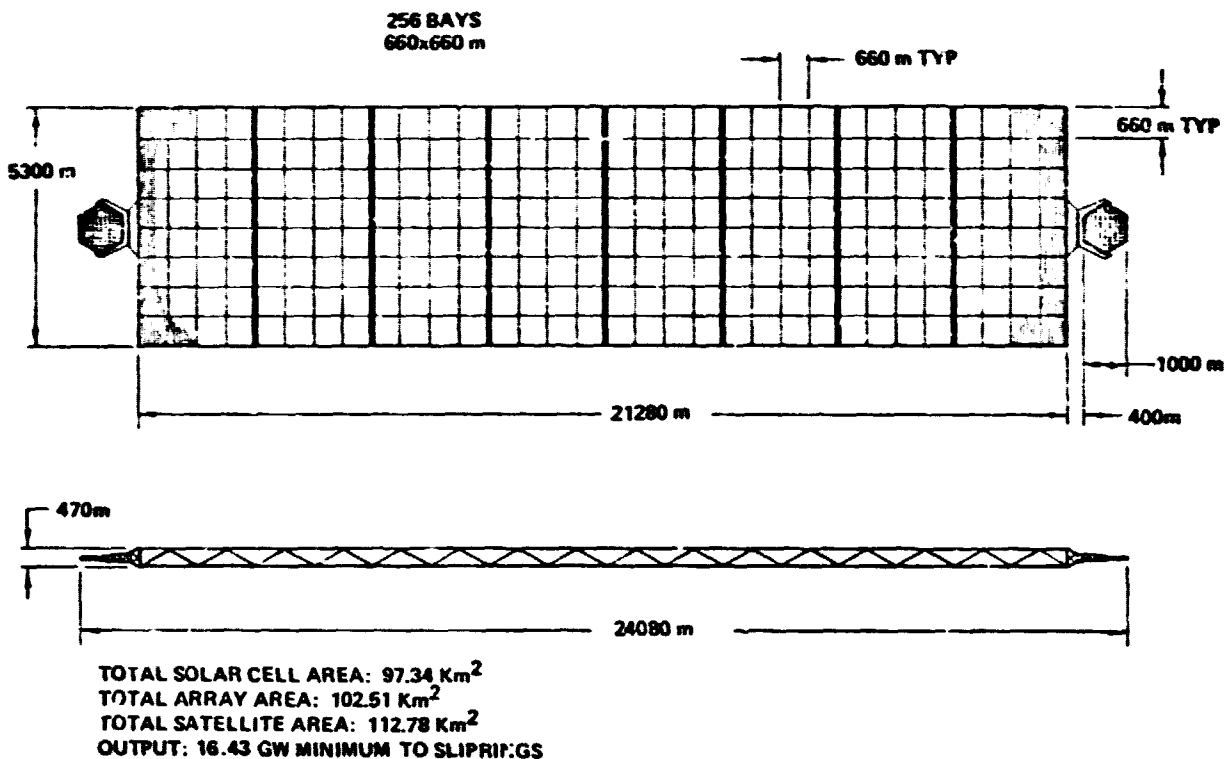


Figure 3.2.2-8 Photovoltaic Reference Configuration

Blanket Design

A silicon solar cell must be provided with a cover to increase front-surface emittance from around 0.25 to around 0.85, and to protect the cell from low-energy proton irradiation. Cerium-doped borosilicate glass is a good cover material because it costs only a fraction of the best alternate (7940 fused silica), matches the coefficient of thermal expansion of silicon, and yet resists darkening by ultraviolet light. Borosilicate glass can be electrostatically bonded to silicon to form a strong and permanent adhesiveless joint. In ATS-6 flight tests the cells having integral 7070 borosilicate glass covers lost only 0.8 ± 1.1 percent of their output because of ultraviolet degradation. These cells had no cover adhesive. Other cells having cell-to-cover adhesives degraded twice as much. Jena Glaswerk Schott & Gen Inc., in West Germany expects to be able to manufacture $75 \mu\text{m}$ borosilicate glass sheets one meter wide by several meters long.

The cell cover is embossed during bonding with grooves which refract sunlight away from the grid lines and buses on the cell surface. COMSAT Labs expects an 8 to 12 percent increase in cell output from this feature in cell covers.

Solar cells only $50 \mu\text{m}$ thick recently made by Solarex had an air mass-zero efficiency of 12.5 percent without a back-surface field or anti-reflection treatment. Texturing the sun-facing surface makes the incoming light arrive at the back surface of the cell at an angle of over 31° , so the light rays that have not been absorbed are reflected off the back surface with virtually no loss, the critical angle in a silicon-air junction being 15.3 degrees. This feature not only improves photon collection efficiency, when compared with thicker cells, by lengthening the light path in silicon for infrared photons, but also improves radiation resistance. Since all charge carriers are generated within $50 \mu\text{m}$ of the P-N junction which is $0.2 \mu\text{m}$ under the sun-facing surface, the cell can absorb radiation damage until the diffusion length in the bulk silicon is reduced to $50 \mu\text{m}$ by radiation-generated recombination centers.

The cells are designed with bot. P and N terminals brought to the backs of the cells. This feature makes it possible to use simple $50 \mu\text{m}$ silver-plated copper interconnections which are formed on the substrate glass. Complete panels are assembled electrically by welding together the module-to-module interconnections. The solar cell/cover combination is shown in Figure 3.2.2-9.

Glass was chosen for the substrate because it enables annealing of radiation damage by heating. With all glass-to-silicon bonds made by the electrostatic process there are no elements in the blanket which cannot withstand the 500°C annealing temperature which at present seems to be required. One researcher suggests that 500°C may not be needed for annealing out the radiation damage from solar-flare protons. However, his theory has not yet been confirmed by experiment.

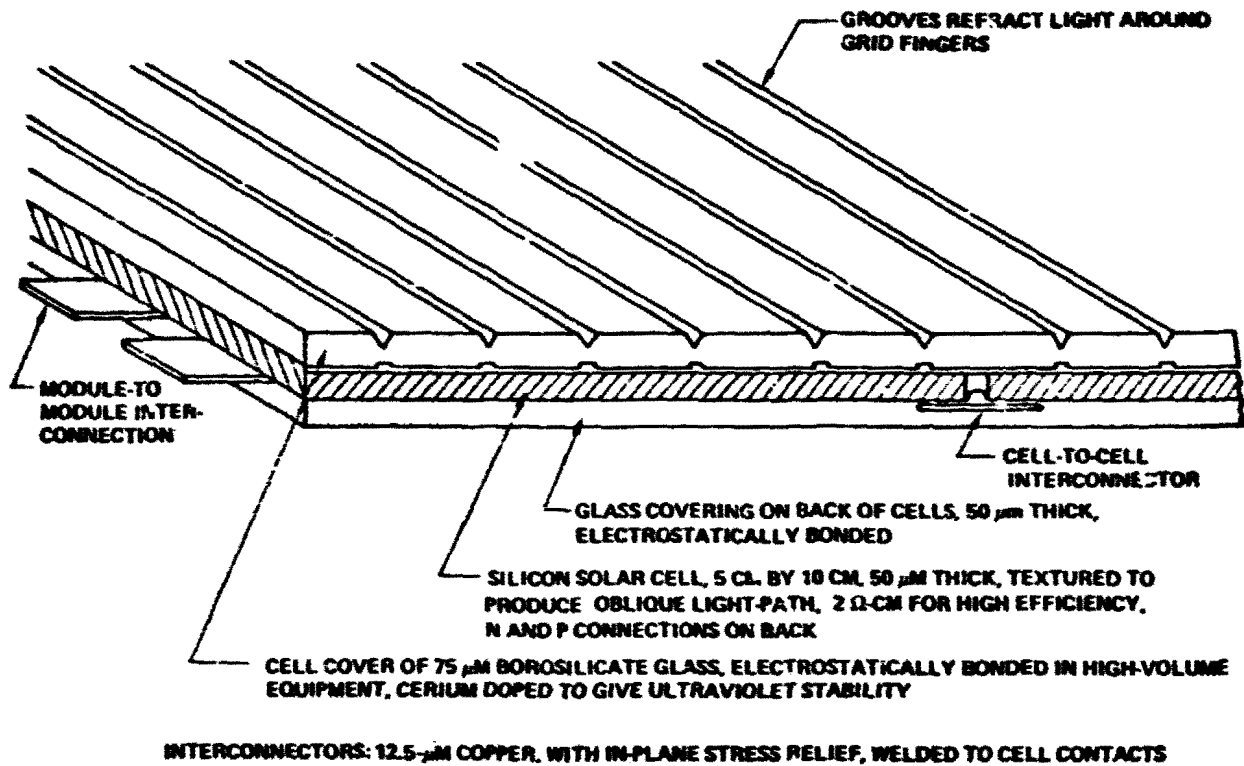


Figure 3.2.2-9 Low Cost Annealable Blanket Structure

Figure 3.2.2-10 shows the basic panel adopted for design studies. It has a matrix of 252 solar cells, each 6.4 by 7.7 cm in size, connected in groups of 14 cells in parallel by 18 cells in series. The cells are electrostatically bonded between two sheets of borosilicate glass. Spacing between cell and edge spacings are as shown. Tabs are brought out at two edges of the panel for electrically connecting panels in series. Cells within the panel are interconnected by conducting elements printed on the glass substrate.

Important panel requirements were these:

- The panel components and processes should be compatible with thermal annealing at 500°C.
- Presence of charge-exchange plasma during ion-engine operation may necessitate insulating the electrical conductors on the panel.
- The panel design should be appropriate for the high-speed automatic assembly required for making the some 78 million panels required for each satellite.
- Low weight and low cost are important.

SPS-1300

- 14 CELLS IN PARALLEL WILL TOLERATE 4 CELL FAILURES IN ANY ROW

CELLS/PANEL : 252
 WGT/PANEL : 426 GRAMS
 PANELS/BAY : 306,206
 PANELS/SATELLITE : 78,388,736

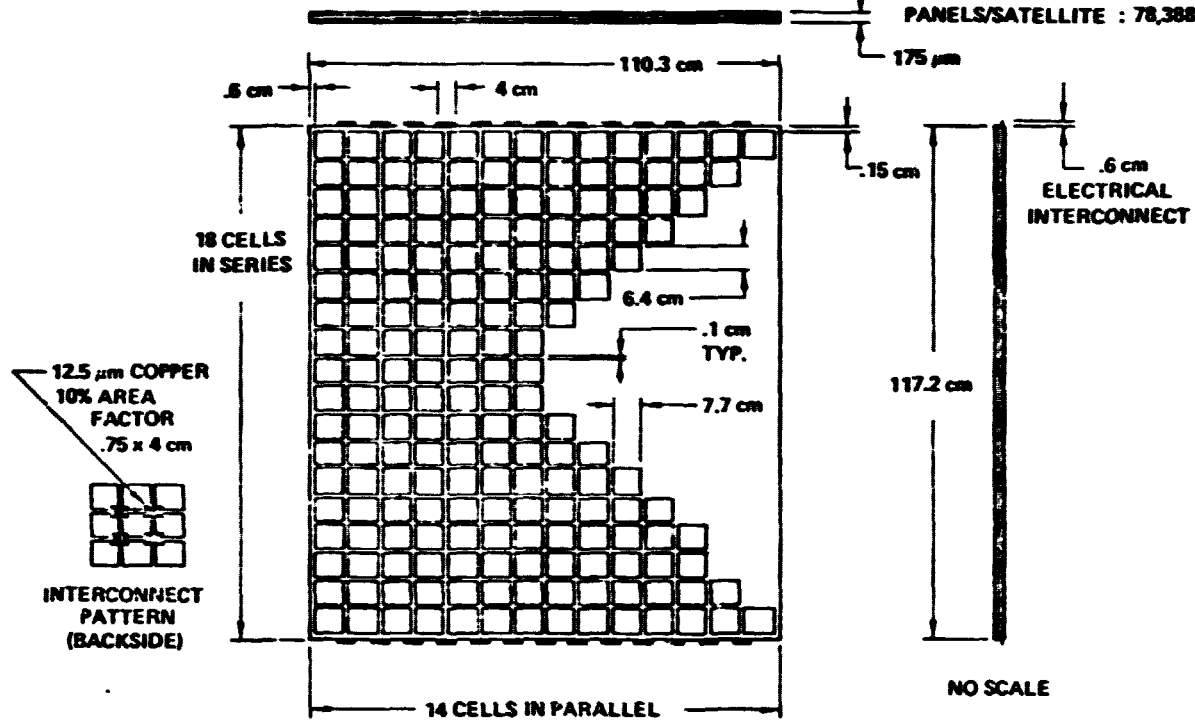


Figure 3.2.2-10 Photovoltaic Reference Configuration
 Solar Array Fundamental Element
 "Blanket Panel"

The glass-encapsulation technology, while not in use today, seems to be achievable by 1985. Simulation Physics has made excellent electrostatic bonds of covers to cells. Schott in West Germany is making thin microscope slides from borosilicate glass. The alternate panel design, using adhesives for bonding cells, covers and substrate, may also be feasible by 1985. Today polyphenylene sulfide adhesives can operate at 320°C, and polyphenyl quinoxaline adhesives are good for 370°C. Also, some of our research suggests that a temperature of 500°C may not be needed for annealing out the cluster defects, produced in solar cells by solar-flare protons.

Shown in Figure 3.2.2-11 is the way panels would be assembled to form larger elements of the solar array. The interconnecting tabs of one panel are welded to the tabs of the next panel in the string and then the interconnections are covered with a tape that also carries structural tension between panels.

Blanket Installation

Figure 3.2.2-12 shows a typical 660 meter bay and the method by which the solar cell blankets are supported within the bay.

The solar array panels are supported by a main web support system which attaches to the satellite structure at 20 meter intervals around the perimeter of the 660 meter bay. Further web support is provided by the catenary.

Thermal expansion and contraction are accommodated by use of a spring-loaded piston cylinder that provides a constant force to the solar array support system. This arrangement also provides for a movement of up to 2 meters, in both x and y directions, which may occur due to LEO-GEO transfer acceleration of 10^{-4} g.

Blanket Mass

The top of Table 3.2.2-3 shows the masses for the solar array blanket as reported at the time of the Part I final presentation. These were based on a blanket having Kapton as a substrate.

The current blanket design is compatible with thermal annealing of radiation damage, resulting in a significant reduction in array area and consequently array weight and cost. The annealable blanket has a 50 μ m glass substrate, electrostatically bonded to the solar cells to avoid adhesives and plastics that can be degraded by thermal annealing. The silicon solar cells are 50 μ m thick, and the cell covers are 75 μ m thick borosilicate glass, electrostatically bonded to the cells. Interconnections are printed on the substrate glass prior to bonding. The current blanket mass buildup is shown in the lower half of the table.

Power Collection and Distribution

Long solar cell strings were adopted for the reference configuration to permit generating the required voltage, around 40kV, directly from the solar array without intervening power electronics. The string length is around 5.1 km.

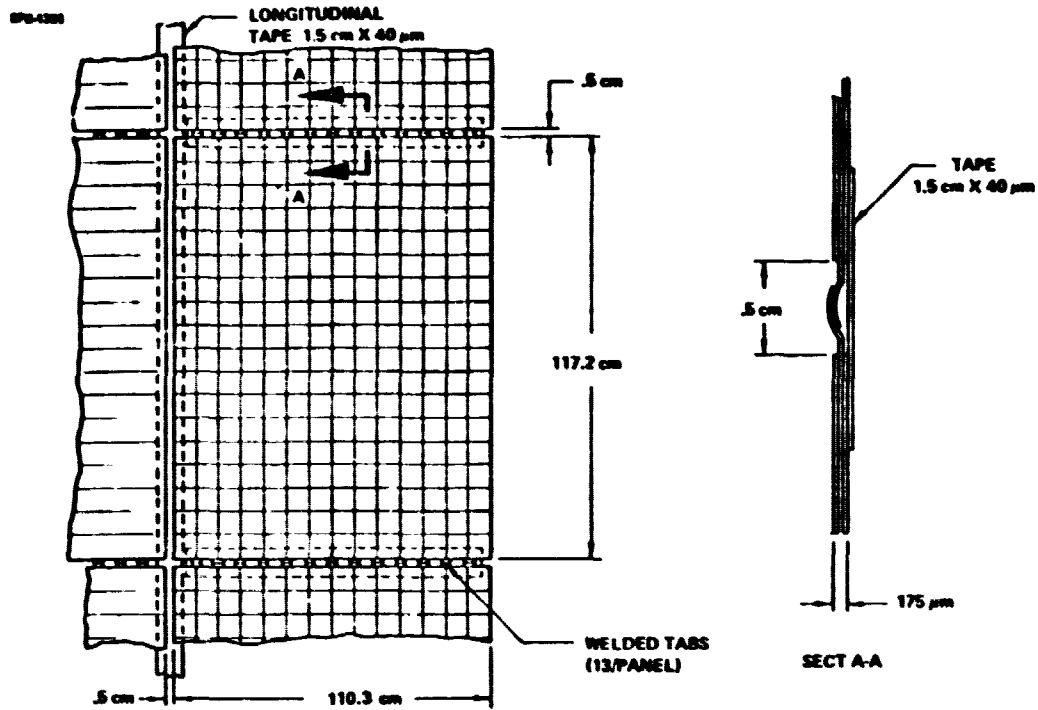


Figure 3.2.2-11 Photovoltaic Reference Panel to Array Assembly

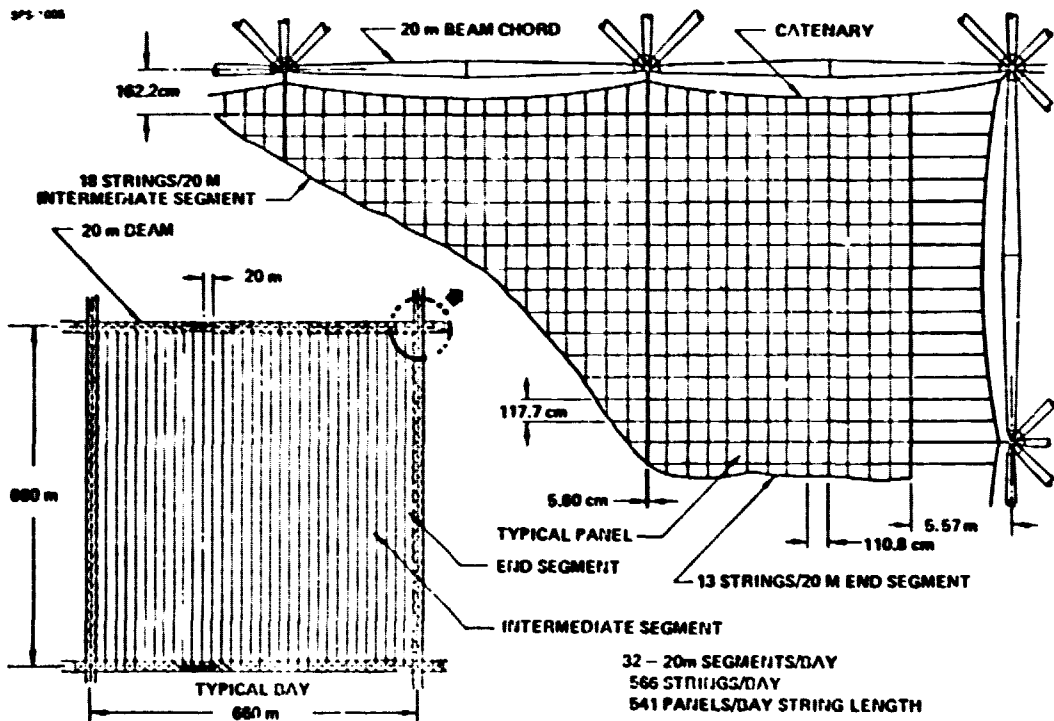


Figure 3.2.2-12 Photovoltaic Reference Solar Array Arrangement and Attachment

Table 3.2.2-3 Photovoltaic Blanket Weight Buildups

SP8-1012

SILICON SOLAR CELL BLANKET WEIGHT @ PART I FINAL

ITEM	DENSITY (S.G.) (g/m ² /MIL)		THICKNESS (MILS)	AREA FACTOR	WEIGHT (g/m ²)
COVERS-FUSED SILICA	2.20	55.88	2.00/3.00	0.986	107.96/161.84
CELLS-SILICON	2.36	59.94	4.00	0.988	231.61
INTERCONNECTS-COPPER	8.94	227.08	0.50	0.200	22.71
SUPPORTING FILM-KAPTON*	1.42	36.07	2.00	0.900	32.46
ADHESIVE, CELLS TO FILM	1.40	35.56	0.50	0.900	16.00
ADHESIVE, KAPTON TO KAPTON	1.40	35.56	0.50	0.800	14.22

} 62.68

8 MILS	2 MILS COVER	2 MILS BLANKET & INTERCONNECT	THEORETICAL WEIGHT	424.96/478.84
	4 MILS CELL		TOLERANCES & INSTALLATION (15 %)	63.74 / 71.86
			ESTIMATED ACTUAL WEIGHT	488.7/550.8

AVAILABLE BLANKET @ PART II MIDTERM

COVERS-FUSED SILICA	2.20	55.88	3.0	1.0	167.64
CELLS-SILICON	2.36	59.94	2.0	0.9607	115.17
INTERCONNECTS-COPPER	8.94	227.08	.5	0.100	11.35
SUBSTRATE-FUSED SILICA	2.20	55.88	2.0	1.0	111.76

7 MILS	3 MILS COVER	THEORETICAL PANEL WEIGHT	405.92
	2 MILS CELL	TOLERANCES ALLOWANCE (5%)	20.30
	2 MILS SUBSTRATE & INTERCONNECTS	ESTIMATED PANEL WEIGHT	426.22
		PANEL AREA FACTOR (.9913)	422.51
		SEGMENTS AREA FACTOR (.9972)	421.33
		JOINT/SUPPORT TAPES	2.93
		CATENARY SYSTEM	2.52
		ESTIMATED ARRAY WEIGHT	426.78

CELL AREA = 380,264 m²/BAY
 PANEL AREA = 386,843 m²/BAY
 ARRAY AREA = 480,454 m²/BAY
 NO. OF BAYS = 256

Current generated by the solar cells can be carried by conductors or by the solar cells themselves. The configuration shown in Figure 3.2.2-13 uses the solar cells to the maximum possible extent for carrying the current. It will be noted that no conductors are needed for bringing in the current from the edges of the array, the solar-cell strings being arranged in loops which start from one center bus, loop around the edge of the array, and return to the other bus at the center of the array.

Solar array power is controlled by vacuum circuit breakers near the buses. Voltage is controlled by turning groups of strings on or off, depending on load requirements.

Two sections of the array provide the required voltage at the slip-rings using the sheet conductor voltage drop to achieve the required voltage at the slip-rings. All solar cell strings are of the same design.

Power source 'A' provides power directly to the fifth stage of the Klystron depressed collector. Power source 'B' provides power directly to the fourth stage of the Klystron depressed collector and to the MPTS dc/dc converters which supply all other Klystron element power requirements.

SPS Structures

The SPS structure must support a very large solar array and should be as light as possible. Only open trusswork structures can fulfill this requirement. The study began with a three-tier structure. Basic members on the order of 10 cm in width made up beams 1 to 2 meters in section; these beams in turn made up 20-meter beams that formed the satellite trusswork. The number of piece parts in this structure was enormous, but the estimated mass was attractive: 2500 metric tons. Early in the effort a simplification was introduced by replacing the built-up 1-meter beams with structural elements. The 20-meter beam was a triangular design using thermally-formed cap sections quasi-triangular in section with hat section cross members and tension straps for diagonals. The primary loading condition at this time was tensioning of the plastic film reflectors in the (then) concentration ratio 2 configuration. A structural sizing analysis was conducted and led to a structural mass of about 15,000 metric tons for the energy conversion system. Significant in this mass increase was the relatively poor capability of the cap section to carry the compression loads that resulted from reflector stretching.

A strong motivation was present to employ an ideal member section: i.e., a tube. This afforded a mass reduction to about 8000 tons. An effort was made to develop design details for the tubular-section beam. Great difficulty was encountered in finding a way to introduce loads into the continuous thin-walled tubes; no satisfactory design solution was found. An approach employing segmented tubes to form the 20-meter beams was developed as illustrated in Figure 3.2.2-14. The tapered tube sections could be nested for shipment to orbit to achieve a satisfactory packaging density. Concurrent with the development of this approach, the decision was made to change the satellite design to one with no sunlight concentrators. The major loading condition therefore was eliminated. The remaining loading condition was stretching of the solar blankets as discussed above, but

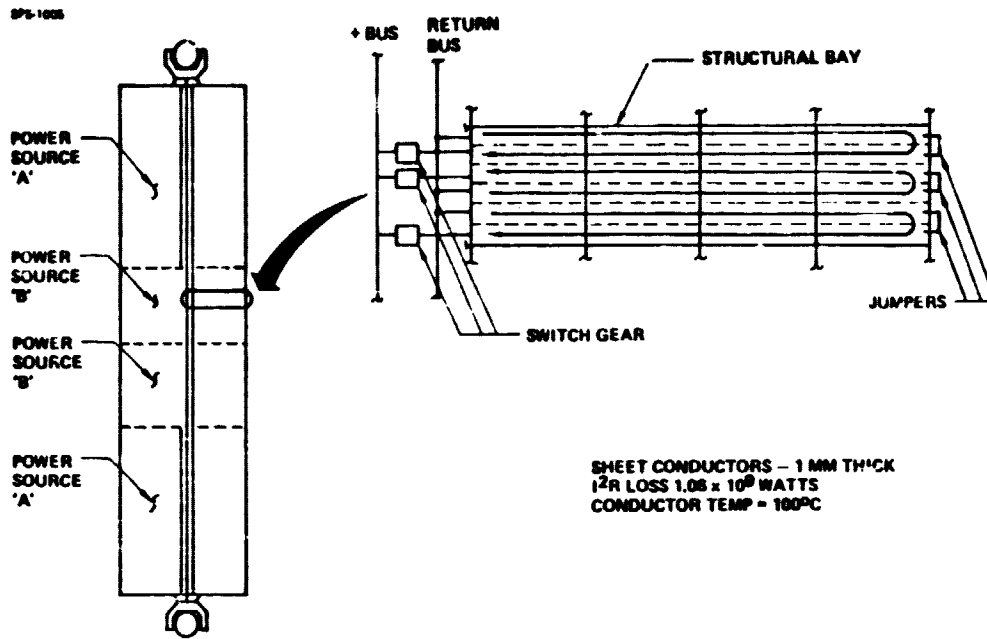


Figure 3.2.2-13 Photovoltaic Reference Power Collection

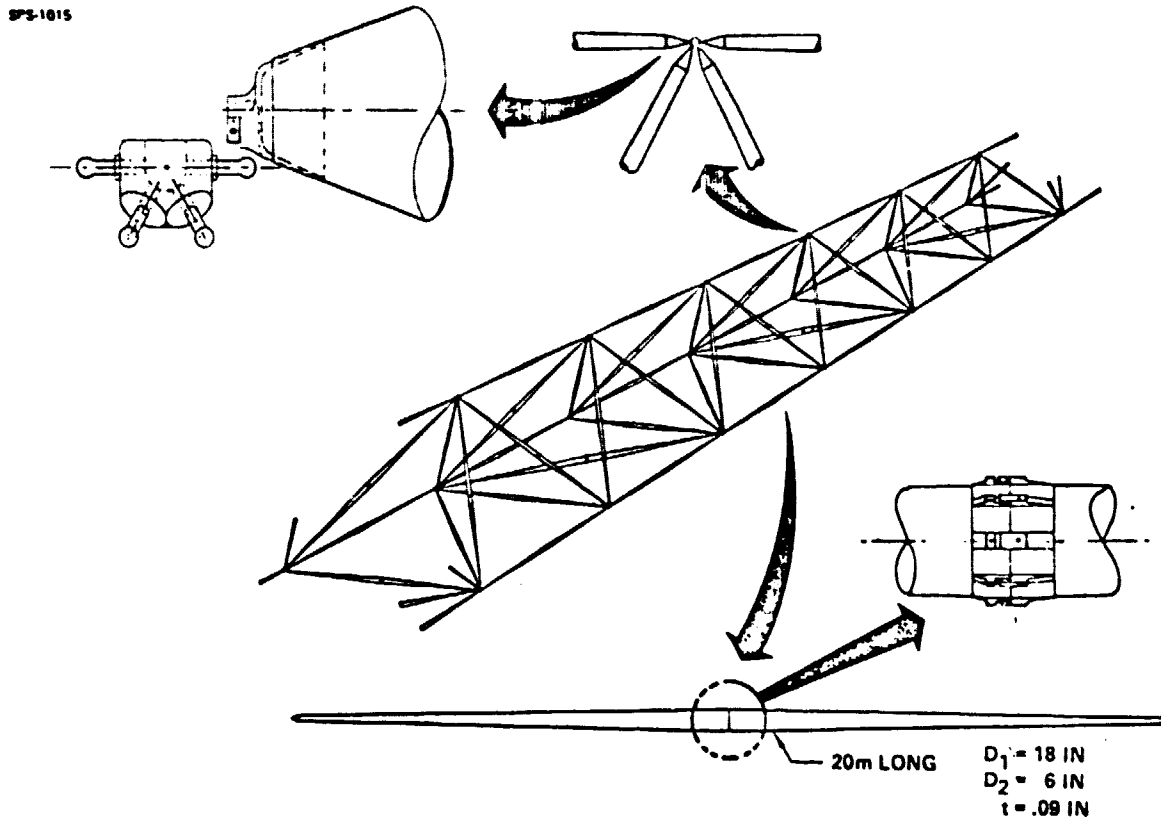


Figure 3.2.2-14 Photovoltaic Reference 20 Meter Beam Structure

the load was much smaller, about 4.5 newtons per meter of beam length. Only the upper plane of the two-tier structure was so loaded; in terms of actual loaded members only about 10% of the total structure was loaded enough to be greater than minimum-gage member thickness. The mass advantage of employing the ideal tubular section was no longer a decisive factor and the continuously-formed beam could again be brought into consideration.

Both structure types have their advantages and disadvantages as summarized in Table 3.2.2-4. Probably the most important consideration is the relative practicality of the beam machine types. This question can only be answered by constructing prototypes of each and conducting comparative tests. The primary issues are the problem of beam straightness for the thermal forming machine and the problem of maintaining adequate alignment with the assembler machine to avoid jamming. The latter problem arises because joint assembly will require alignment to within a few millimeters in handling the 20-meter long struts. The thermally-formed beam configuration is shown in Figure 3.2.2-15. Open and closed section beams were analyzed. The closed section beam performed better than the open section, but not by as much as was expected. Table 3.2.2-5 compares results for these two sections with the tapered-tube structure. The differences in mass for equal load carrying capability are not sufficient to be a primary decision factor in final selection of the SPS structural design. Details of joining the continuous-chord beam designs were not developed. A thorough development of this detail will be necessary before final selection can be made.

Antenna Support and Mechanical Turntable

The antenna support structure and mechanical turntable are the structural interfaces between the basic satellite structure and the antenna yoke structure, and provide for the 360° rotation of the antenna.

The electrical slip rings are mounted at the center of the mechanical turntable and provide for energy transfer across the rotating connection. Flexible conductors provide for energy transfer across the elevation joint on the antenna yoke. Figure 3.2.2-16 illustrates the yoke and its attachment to the SPS.

Electrical Rotary Joint

The electrical rotary joint is small enough to be completely fabricated and checked out on the ground. As illustrated in Figure 3.2.2-17 it includes three concentric slip rings for the "A" and "B" busses and their returns. A total of 832 brushes contact the three rings. The current density at the brush contacts is 10 amps/cm², representative of today's state of the art.

Instrumentation and Control

A preliminary instrumentation and control list was compiled for the power generation, distribution, and transmission systems. A summary of the number of items in each major category for the power generation and distribution systems is shown in Table 3.2.2-6.

Table 3.2.2-4 Qualitative Comparison of Structural Options

SP8-1728

	<u>TAPERED TUBE</u>	vs	<u>CONTINUOUS CHORD</u>
• MASS PER SPS	✓		(DIFFERENCE PROBABLY <1000 TONS ~ 1%)
• COST			NO DIFFERENCE IDENTIFIED
• PACKAGING DENSITY			(EITHER OPTION IS ADEQUATE) ✓
• CONSTRUCTION OPERATIONS			NO SIGNIFICANT DIFFERENCES IDENTIFIED
• NUMBER OF PARTS			NO SIGNIFICANT DIFFERENCE
• JOINT SLOP			(ANALYSIS INDICATES NOT A PROBLEM) ✓
• BEAM MACHINE	• ALIGNMENT PRECISION MAY BE A PROBLEM		• STRAIGHTNESS OF BEAMS MAY BE A PROBLEM
• MACHINE COMPLEXITY			✓
• MACHINE RATE	✓		
• STRUCTURAL INTEGRITY VERIFICATION	✓		
• STRUCTURE DESIGN FLEXIBILITY	✓		(NOT A DECIDING FACTOR)
• AVAILABILITY OF HARDPOINTS ON STRUCTURE	✓		

**CONCLUSION: EITHER OPTION WILL WORK.
TECHNOLOGY VERIFICATION NEEDED FOR SELECTION.**

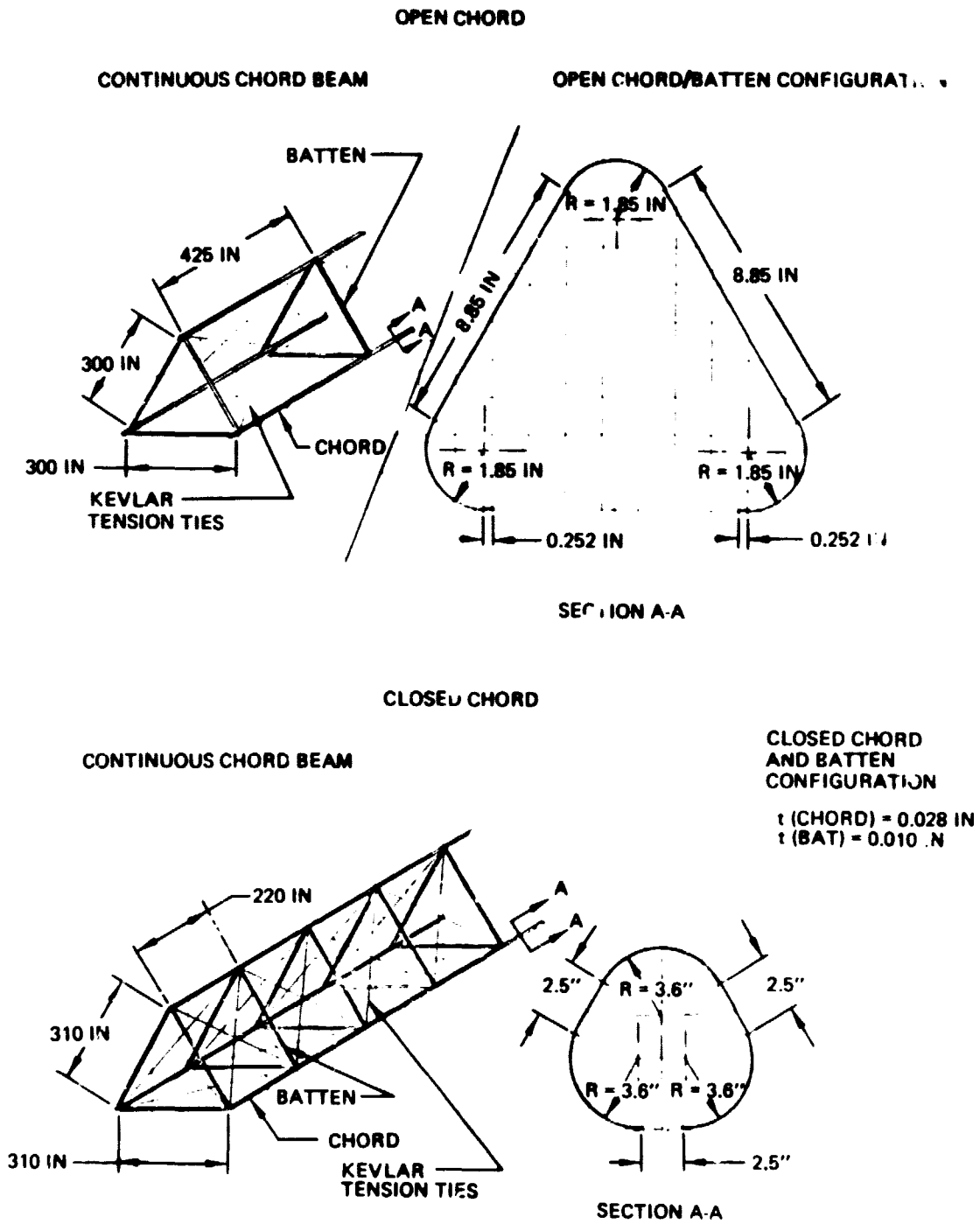


Figure 3.2.2-15 Continuous Beam Configurations

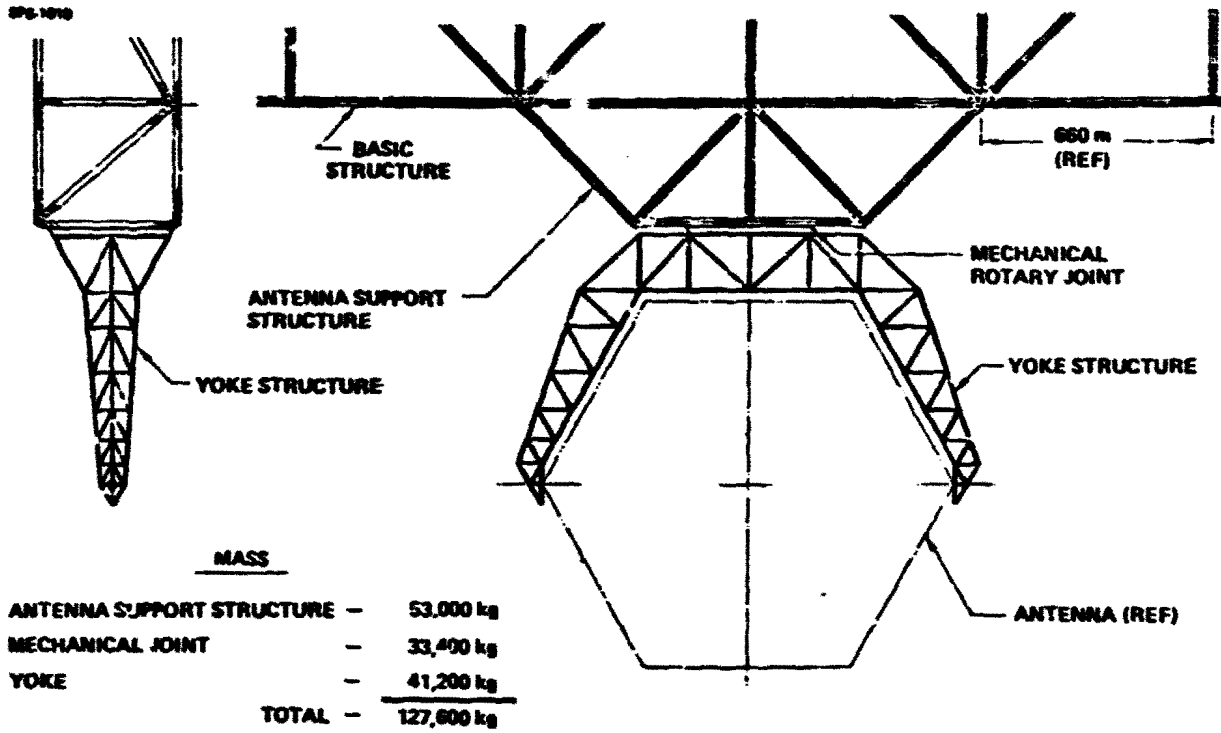


Figure 3.2.2-16 Antenna Support and Mechanical Joint Weights

D180-22876-2

SPS-1022

ELECTRICAL ROTARY JOINT MASS SUMMARY

SLIP RINGS	- 11,810 kg
BRUSH ASSEMBLY	- 1,970 kg
FEEDERS	- 3,340 kg
STRUCTURAL SUPPORT	- 900 kg
ASSY. & INSTL. HARDWARE	- 200 kg
CONTINGENCY ALLOWANCE	- 900 kg
TOTAL	- 19,600 kg

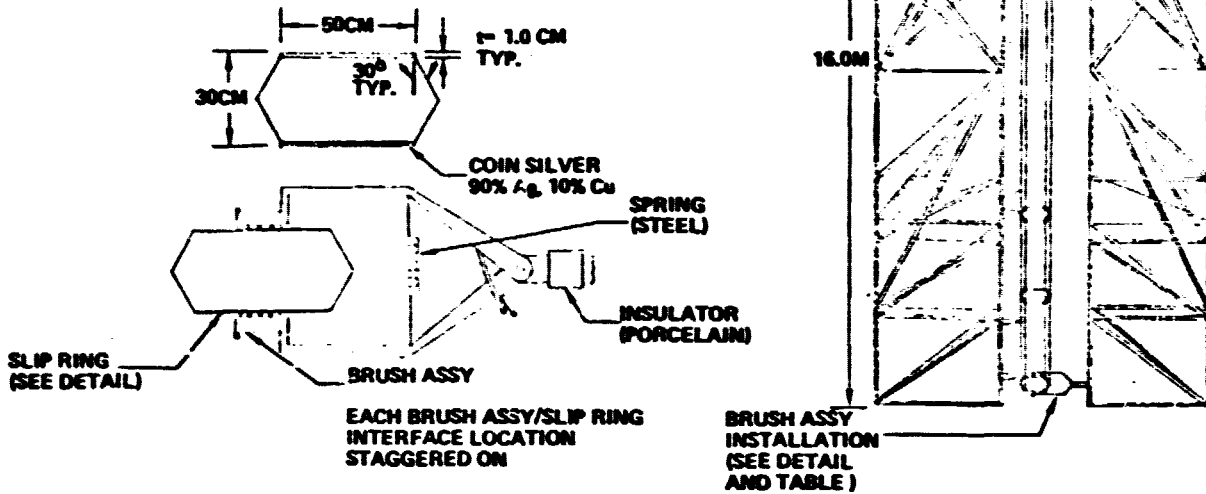


Figure 3.2.2-17 Electrical Rotary Joint and Mass

Table 3.2.2-6 Reference Photovoltaic Instrumentation and Controls

SPS-1022

	CONTROLS	INSTRUMENTATION
POWER GENERATION		
POWER SECTORS		1,152
SOLAR ARRAY STRINGS		36,224
POWER DISTRIBUTION		
SWITCH GEAR	420	1,680
MAIN BUS		4
ROTARY JOINT	104	149
DC-DC CONVERTERS		70
TOTALS*	524	39,279

*DOES NOT INCLUDE STATIONKEEPING, HOUSEKEEPING, OR ENVIRONMENTAL CONTROL AND MONITORING SYSTEMS.

Flight Control Stability

This analysis considered various sensor and control actuator locations to see if there were any substantial differences in the controllability of the SPS.

In summary, all the single sensor configurations analyzed were stable. In each case gain stabilization was achieved (see Table 3.2.2-7) with a simple, low cost attitude control design for roughly the same range of SPS structure flexible mode frequencies. The results shows that the first bending mode frequency of the SPS must be above 0.2 cycles per hour to ensure stable operation of the attitude control system. Results for multiple control loops were inconclusive.

Four different control station configurations were evaluated. Three single sensor configurations with different controller locations and one multiple station case with 8 sensors and controllers were modeled to determine the controllability of each configuration and to find a rough estimate of the stable range of SPS structural frequencies. The three single-station models were (1) sensor and controller at one end, (2) single sensor at the center and a thruster at each end, (3) single sensor at the end and a thruster at each end. The eight station case had each sensor and controller located together, with each spread evenly in the center, along the length of the satellite.

With the different configurations thus defined the control loop model was designed. Two different feedback systems were tried. The first was a position and rate feedback and the second a position feedback using a lead-lag compensation for stabilization. A damping ratio of .7 and an allowable SPS attitude offset angle (θ) of 4.4×10^{-3} radians were chosen. To find the control gain (KG) the identity:

$$T_{\text{dist}} = \theta \cdot KG \quad (1)$$

was used, where T_{dist} is the disturbance torque. Gravity-gradient torques were limited to torques about one axis.

The control loop natural frequency for this case was 1.43×10^{-3} rad/sec. The rate feedback gain, K_{gyro} , is found by manipulating the transfer function of the model (without the flexible modes) to give $K_{\text{gyro}} = 1 \times 10^3$ N-m/rad/sec.

The position gain was used in all the loop designs. Lead-lag compensation in the position feedback loop was designed to match these dynamic characteristics while eliminating rate feedback and therefore the need for continuous gyro operation.

Flexible modes were then added to the model. Flexible mode data were found using the NASTRAN program. The coefficients θ are the contribution from each mode to the angle of bending at different points on the satellite. ω_1 is the mode frequency. Values are given in the Table 3.2.2-8.

Table 3.2.2-7 Control Stability Analysis Results

<u>CONTROL LOOP DESIGN</u>	<u>STRUCTURAL MODE</u>	<u>RESULT</u>	<u>COMMENT</u>
1a Single end sensor gyro-rate feedback end control	1st Mode $w = 6.06 \times 10^{-3}$ rad/sec	Stable	Stable for $w > 1.5 \times 10^{-4}$
1b Single end sensor Lead-Lag position feedback end control	1st Mode $w = 6.06 \times 10^{-3}$ rad/sec	Stable	Stable for $w > 2.0 \times 10^{-4}$
2 Single end sensor rate-gyro feedback			
a) End thruster control	1st mode $w = 6.06 \times 10^{-3}$ rad/sec	Stable	Always stable (all modes stable)
b) End thruster control	2nd mode $w = 1.95 \times 10^{-2}$ rad/sec	Stable	Stable for $w > 1.5 \times 10^{-4}$
3 Single center control rate-gyro feedback			
a) End thruster control	1st mode $w = 6.06 \times 10^{-3}$ rad/sec	Stable	Always stable (all modes stable)
b) End thruster control	2nd mode $w = 6.06 \times 10^{-3}$ rad/sec	Stable	Stable for $w > 1.5 \times 10^{-4}$
4 Multiple loop	1st mode $w = 6.06 \times 10^{-3}$ rad/sec	Stable	Conditionally

ORIGINAL PAGE IS
OF POOR QUALITY

D180-22876-2

Table 3.2.2-8. Control Stability Analysis Results

1st Bending Mode
W1 = 6.06×10^{-3}

GM = 3.454×10^7 Kg
 θ (rad/m)

Position		Position
1	2.353×10^{-4}	11
2	2.306×10^{-4}	10
3	1.965×10^{-4}	9
4	1.325×10^{-4}	8
5	4.685×10^{-5}	7
6	0	6

2nd Bending Mode
W1 = 1.95×10^{-2}

GM = 1.718×10^7 Kg
 θ (rad/m)

Position		Position
1	2.152×10^{-4}	11
2	1.979×10^{-4}	10
3	9.030×10^{-5}	9
4	-5.550×10^{-5}	8
5	-1.572×10^{-4}	7
6	-1.715×10^{-4}	6

For 1st bending mode the satellite is bent symmetrically, and for the 2nd bending mode the satellite is bent antisymmetrically. W1 gets larger for the higher modes. Only the first bending mode was considered in most cases.

In the single-station cases, all the configurations were stable. In general, the addition of a flexible mode adds a loop into the gain-phase plot. Without flexible modes, all single mode models are stable. For different mode frequencies, the loop shape remains relatively constant with the loop itself shifting up and down the curve. Thus for lower frequencies the loop is higher in the curve and there is a possibility of the system going unstable.

Putting thrusters at each end and varying the sensor from end to center does little to change the controllability of the satellite. The lower limit on frequency for stable operation is 2.0×10^{-4} rad/sec. Applying a factor of 2 for a stability margin on mode frequency gives the lower limit of 0.2 cycles per hour for any single control loop configuration. All frequency ranges stated above are frequencies where the system is stable. The lower limit is not necessarily the point where the system is marginally stable, but is just a rough estimate of the stable system.

The multiple station case (case 4) was inconclusive. At this point it seems conditionally stable for the first bending mode. Future work should be directed towards the multiple station case. Also stability criteria should be developed for thermal engine satellite designs to complement the photovoltaic satellite data presented here.

Mass Summary

The structural mass difference from previous results is summarized in Table 3.2.2-9 and reflects integration of the new sizing criteria for the photovoltaic reference SPS. The secondary structure has been incorporated into the primary structure. The bay size and member dimensions have been changed to be compatible with the new reference system.

The mechanical systems mass is the mechanical rotary joint.

Investigation of the gravity-gradient torques and optimization and thrust I_{sp} led to a decrease in control system mass.

The mass of the solar cell blankets decreased due to a new blanket design consisting of 75 μm cover-glass, 50 μm silicon solar cells, and 50 μm silica substrate. Solar cell blanket decrease also resulted from lower radiation degradation of the 50 mm silicon solar cells.

The increase in power distribution system mass reflects a change from the no longitudinal bus bar configuration to no lateral bus bars and includes energy storage equipment.

The increase in MPTS mass reflects the inclusion of energy storage for antenna systems.

The growth used was 26.6% on the final configuration. This growth was the result of the uncertainty analysis discussed in Section 3.2.5.

3.2.2.3 LEO-GEO Differences

The most important cost differences between LEO and GEO construction occur in operational factors. There are, however, significant differences in the satellite design. The reference point design was intended to be the reference LEO case. It was originally believed that the ability to anneal radiation damage experienced during the slow transfer would result in essentially no oversizing required. This is true if one makes only a parametric power loss analysis. An additional effect must be included - this is the solar cell mismatch correction. The configuration finally selected for orbit transfer has the solar cells closest to the thruster installations deployed for orbit transfer power. These are at the outer bays of the modules as shown in Figure 3.2.4-31 in Section 3.2.4. The power distribution configuration of the satellite is such that these cells are in series with cells not exposed for the transfer. All must carry the same current. Therefore, the residual radiation damage in the cells used for transfer requires that all cells be operated slightly off their optimum power point. When this was taken into account, a 5% oversizing requirement was found. Therefore the LEO configuration must be resized to have 680-meter bays and correspondingly larger array blankets.

The GEO configuration is the same size as the reference point design but does not require the duplicate structure that enables modularization of the satellite. Table 3.2.2-10 summarizes the LEO-GEO

Table 3.2.2-9 Photovoltaic Reference Configuration Nominal Mass Summary Weight in Metric Tons

SPS-1547

CR-2 (10 GW B.O.L.)

CR-1 (10 GW MINIMUM/30 YRS)

COMPONENT	ORIENTATION	CR-2 (10 GW B.O.L.)		CR-1 (10 GW MINIMUM/30 YRS)		
		MIDTERM	PART I FINAL	PART I FINAL	PART II MIDTERM	PART II FINAL
1.0 SOLAR ENERGY COLLECTION SYSTEM	(36,616)	(58,313)	(49,512)	(56,357)	(56,184)	51,782
1.1 PRIMARY STRUCTURE	2,483	14,970	8,600	2,334	6193	6385
1.2 SECONDARY STRUCTURE	189	200	200	200	-	-
1.3 MECHANICAL SYSTEMS	40	40	40	40	67	67
1.4 MAINTENANCE STATION	85	-	-	-	-	-
1.5 CONTROL	340	340	340	340	150	178
1.6 INSTRUMENTATION/ COMMUNICATIONS	4	4	4	4	4	4
1.7 SOLAR-CELL BLANKETS	25,746	37,592	34,111	61,897	47,319	43,750
1.8 SOLAR CONCENTRATORS	5,149	2,978	3,276	-	-	-
1.9 POWER DISTRIBUTION	2,570	3,180	3,532	1,588	2451	2398
2.0 MPTS	15,371	15,371	15,371	15,371	(24,384)	25,212
SUBTOTAL	51,987	74,644	64,883	71,728	80,568	76,994
GROWTH	25,984	37,342	32,442	35,984	20,142	20,480.1
TOTAL	77,981	112,026	97,325	107,692	100,710	97,474

1 26.6% GROWTH FROM UNCERTAINTY ANALYSIS

ORIGINAL PAGE
OF POOR QUALITY

Table 3.2.2-10 Satellite Weight Delta GEO vs. LEO Construction

STRUCTURE WEIGHT - LEO (UNADJUSTED)	5,325,000	REF. CONFIG.
ARRAY WEIGHT - LEO (UNADJUSTED)	43,750,000	
POWER DISTRIBUTION - LEO (UNADJUSTED)	2,398,000	
STRUCTURE WEIGHT - LEO (ADJUSTED, + 5%)	5,655,000	
ARRAY WEIGHT - LEO (ADJUSTED, + 5%)	45,938,000	
POWER DISTRIBUTION - LEO (ADJUSTED, + 5%)	2,457,000	
STRUCTURE WEIGHT - GEO	4,530,700	
ARRAY WEIGHT - GEO	43,750,000	
POWER DISTRIBUTION - GEO	2,398,000	
STRUCTURE WEIGHT LEO-TO-GEO	-1,124,300	▷
ARRAY WEIGHT LEO-TO-GEO	-2,188,000	
POWER DISTR. LEO-TO-GEO	-58,700	
<hr/>		
TOTAL - LESS GROWTH	-3,371,000	
GROWTH ADJUSTMENT	-899,000	
<hr/>		
TOTAL - INCL. GROWTH	-4,270,000 kg	
<hr/>		
TOTAL BEAM LENGTH	<u>GEO</u> <u>LEO</u>	
10 ⁶ m	1.180 1.340	

▷	{	MODULARIZATION	+649,200
		SELF TRANSPORT	+53,500
		ANTENNA TRANSPORT	+151,600
		OVERSIZING	+270,000

differences in the satellite mass statements. The GEO configuration is 4270 metric tons less in mass. These differences have been taken into account for the final cost comparisons and cost figures.

3.2.3 Thermal Engine SPS's

3.2.3.1 Summary

Of the thermal engine systems studies, the potassium Rankine is the lightest near-term technology SPS option. Our study results show it to be lighter than steam Rankine, helium Brayton or thermionic SPS systems. In the area of solar concentrators, we had previously anticipated approximately 30% degradation in the 30 year life of the SPS. More recent data has however, indicated that little or no degradation should be expected. Therefore, none has been assumed. An investigation of potential materials for thermal engine SPS usage has indicated that some of the best materials are in short supply. However, suitable options exist and these have been selected. We have selected a turbine sizing of 32 megawatts. At this size, 576 turbines are required for a 10 GW output SPS. This turbine size is approximately that of the SST engine partially developed by General Electric for the American SST program, and is appropriate to the national fabrication capability. By the use of relatively small heat pipes it has been possible to configure a radiator system which is sufficiently immune to meteoroid penetration. At the end of this study phase we indicate that the mass of the thermal engine SPS is approximately 80,000 metric tons (without growth) and that the average cost for one SPS at a rate of four per year is approximately 18 billion dollars or 1,800 dollars per kilowatt produced on the ground.

3.2.3.2 Recap of Options

The steam Rankine SPS would be an extremely heavy option. This is primarily because the maximum turbine inlet temperature is in the neighborhood of 1,000 to 1,100 degrees Fahrenheit and the heat rejection temperature is near the condensation point of water. Consequently, the Carnot efficiency is low and the realizable efficiency is even lower. Thermionic systems are also very heavy. This is because thermionic diodes and the interelectrode busbars required to connect them are heavy and the radiator system required for heat rejection from the thermionic diodes is also quite heavy. The Brayton SPS i.e. a helium closed cycle system, is a near competitor to the potassium Rankine system. However, it is only competitive in mass with very high turbine inlet temperatures, in the vicinity of 1,600 K (2,500°F). This turbine inlet temperature is only achievable with ceramic materials such as silicon carbide. This material is now in development but is not considered to be appropriate for baseline SPS use. We have emphasized the potassium Rankine SPS in Part II of this study and details of the results are concluded in the remainder of this section.

3.2.3.3 Reference Design Description

A plan view of the thermal engine SPS is shown in Figure 3.2.3-1. This satellite has two 5 GW output rectennas located on the north-south axis of the satellite. The satellite is divided into 16 modules each of which has 36 turbogenerators, for a total of 576 per SPS. The satellite flies in a perpendicular-to-ecliptic plane orientation at all times.

Cycle

The working fluid in the potassium Rankine loop is potassium vapor in a portion of the loop and liquid potassium in the remainder. Figure 3.2.2-2 shows the cycle schematic. Liquid potassium is introduced into the heat absorber tubes of the boiler located within the high temperature cavity absorber. Boiling produces potassium vapor which passes through the turbine and does the work of turning the generator which produces the useful power required for the SPS microwave transmitter and the power required to drive the electromagnetic pump. Potassium vapor leaving the turbine is cooled by the expansion in the turbine. It is introduced into the radiator system where it flows through the vapor manifold into potassium throughpipes which are cooled by sodium heat pipes. Condensation occurs in the throughpipes so that liquid potassium is collected in the radiator outlet manifold and flows to the electromagnetic pump.

The General Electric Corporation, our subcontractor for Rankine turbines, produced the data shown in Table 3.2.3-1. We have used a turbine efficiency of 80%. This was demonstrated in tests in the late 1960's at the Lewis Research Center. The 80% figure is probably quite conservative for large potassium turbines. In the area of erosion control three promising methods were demonstrated in the Lewis tests. A total of nearly 800,000 hours of testing was accumulated relative to potassium systems. Note that this includes a total of more than 10,000 hours of running tests on turbines and more than 10,000 hours of electromagnetic feed pump testing.

Materials

The abundance data given in Table 3.2.3-2 were drawn from Department of Interior publications for 1973. The first of the general rules shown states that since solar power satellites will not be available in large quantities until after the year 2000, it is appropriate that we select materials sufficiently abundant in that time period. Our baseline SPS quantity for this study was 112 units, probably sufficient for U.S. electrical needs in the early part of the 21st century. However, more units may ultimately be required for the United States; up to 1000 units or more for the world. Therefore, it is probably appropriate that we do not use a material such that 112 satellites would use over 5% of any world material source. Rule 3 tends to minimize the impact of SPS incorporation and the concomitant industrialization required. Turbine wheels and blades for potassium Rankin turbines are baselined as using molybdenum, a wrought material. Silicon carbide could also be used, however, this material is in its very early development stage and it's probably too advanced to baseline. Turbine housing materials must be ductile and weldable. Tantalum alloys would be ideal, however world resources are not adequate. Therefore, we have selected niobium, also called colum-

bium, for the baseline material. Cesium would be an ideal Rankine cycle working fluid. It would result in the turbines having fewer stages and a smaller disc diameter. However, the supplies of cesium are clearly not adequate for large scale SPS usage. Potassium, an abundant material, has been selected.

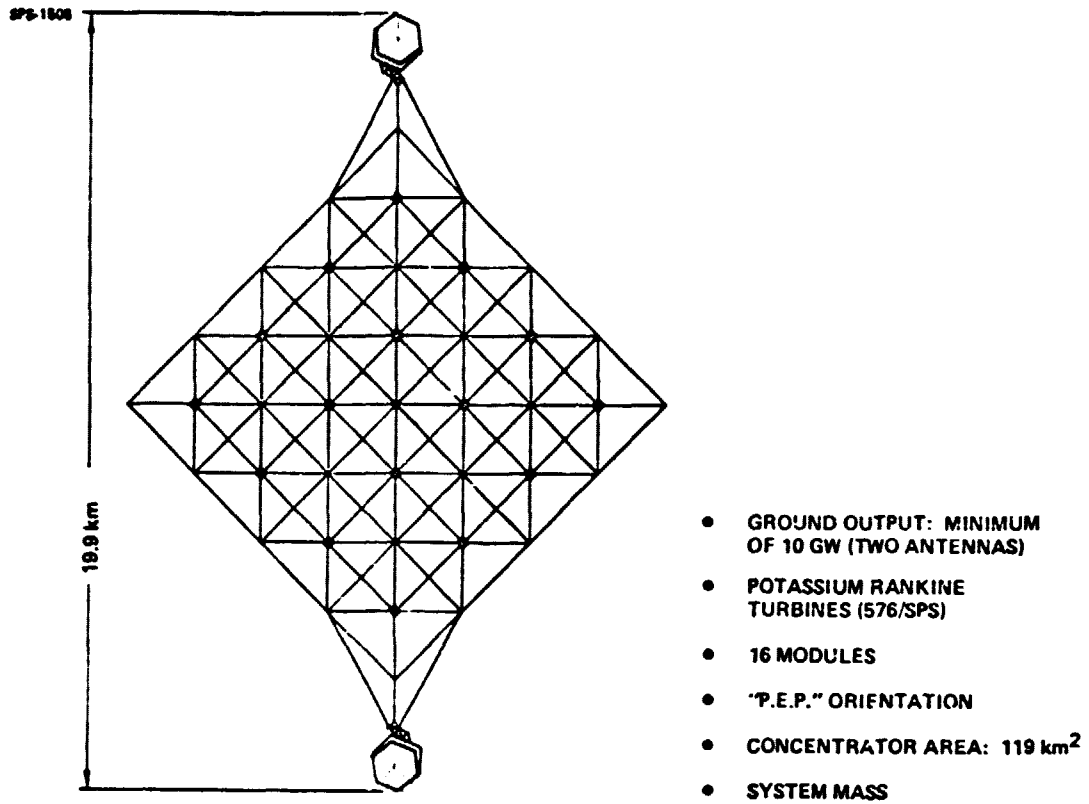


Figure 3.2.3-1 Reference Rankine SPS Design

SPS-1504

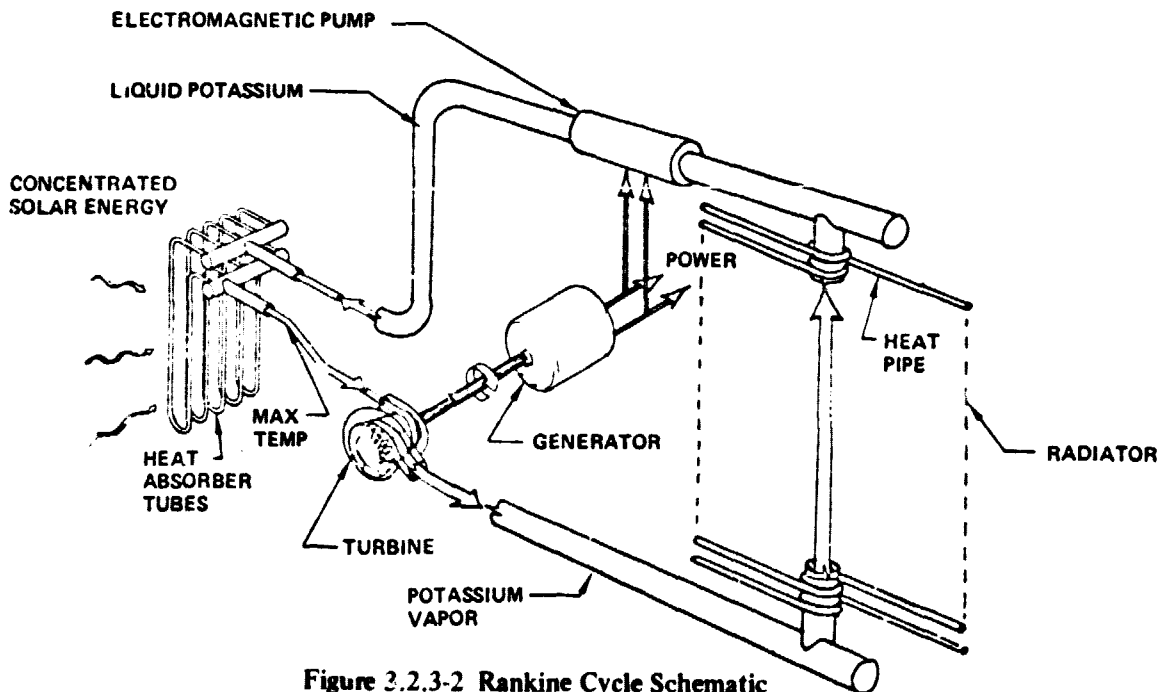
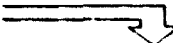


Figure 3.2.3-2 Rankine Cycle Schematic

ORIGINAL PAGE IS
OF POOR QUALITY

Table 3.2.3-1 Data Base Draws Heavily on Demonstrated Technology (General Electric Data)

SPS-1808

TURBINE EFFICIENCY: 80%; LeRe TESTS
 EROSION CONTROL: THREE METHODS DEMONSTRATED
 POTASSIUM HARDWARE: 

	Potassium (800,000 hours testing)							Cesium (>23,000 hours testing) (b)
	AIResearch	GE	JPL	NASA-Lewis	ORNL	P&W	Other ^a	
	Testing hours accumulated							
Corrosion test systems:								
Boiling	1300	25 500	-----	-----	62 800	12 000	-----	3500
All-liquid	-----	-----	-----	-----	-----	-----	156 000	-----
Component test systems, boiling	5900	19 600	-----	1000	2 800	4 900	300	2400
Simulated powerplant systems	-----	-----	~1000	-----	10 200	-----	-----	-----
Boilers	7200	40 100	1000	1000	75 800	16 900	300	6000
Turbines	3050	10 100	-----	-----	5 000	-----	100	-----
Boiler feed pumps:								
Electromagnetic	7200	34 600	3600	1000	26 900	4 900	3 300	5600
Turbine driven	-----	-----	-----	-----	5 000	-----	-----	-----
Other pumps	5900	18 600	3600	1600	6 100	1 300	57 600	-----
Condensers	7200	40 100	~1000	1600	75 800	16 900	300	5600
Scals	3050	10 100	-----	-----	-----	-----	-----	-----
Bearing tests	3000	-----	-----	-----	4 500	-----	1 600	-----

^aIncludes testing hours of Aerojet Nucleonics, Allison, Rocketdyne, United Nuclear.

^bIncludes testing hours of Brookhaven, Aerojet Nucleonics, Westinghouse Astronuclear.

Table 3.2.3-2 Material Availability

SPS-1146

- GENERAL RULES: 1) MATERIAL TO BE PREDICTED TO BE "SUFFICIENTLY ABUNDANT" IN 2020.
- 2) SPS TO NOT USE OVER 5% OF WORLD RESOURCES OF ANY MATERIAL
- 3) CURRENT WORLD PRODUCTION RATE ADEQUATE FOR ONE SPS/YEAR

- TURBINE WHEEL/BLADE MATERIAL (NEED ≈ 6000 MT/SPS)
(WROUGHT MATERIAL)

MATERIAL	STATE OF ART	WORLD RESOURCES (MT)	PRODUCTION RATE (MT/YR)
MOLYBDENUM (TZM)	DEVELOPED	29,000,000	91,000
SILICON CARBIDE	EARLY TEST	VERY ABUNDANT	VERY SMALL

- TURBINE HOUSING MATERIAL/BOILER TUBES (NEED 4000 TO 7000 MT/SPS)
(WELDABLE DUCTILE MATERIAL)

MATERIAL	STATE OF ART	WORLD RESOURCES (MT)	PRODUCTION RATE (MT/YR)
TANTALLUM (T111)	DEVELOPED	100,000	PERHAPS 1,000
NIوبيUM (C103)	DEVELOPED	17,000,000	ABOUT 20,000
SILICON CARBIDE	EARLY TEST	VERY ABUNDANT	VERY SMALL

- RANKINE CYCLE WORKING FLUID

MATERIAL	STATE OF ART	WORLD RESOURCES (MT)	PRODUCTION RATE (MT/YR)
CESIUM	DEVELOPED	100,000	≈8
POTASSIUM	DEVELOPED	> 10 ⁹	10,000,000

*MT = METRIC TON/SPS

Concentrator

The solar concentrator is made up of a structural system supporting a large number of plastic film reflector facets and is a segment of a sphere. The reflected light is concentrated into the focal point assembly which mounts to the concentrator by four cavity support arms. These arms are made up of graphite epoxy tube sections forming a 20 meter beam. The thruster systems required for self power transport to geosynchronous orbit in the LEO construction option are located at the 3 points shown in Figure 3.2.3-3.

The concentrator structure which supports the reflector facets is made up of a large number of tetrahedral elements which are in turn composed of a number of tapered graphite epoxy tubes, jointed as shown in Figure 3.2.3-4. The graphite epoxy tubes can be nested to provide a high density payload for transportation.

Figure 3.2.3-5 is a photo of a "Toothpick Model" of a portion of the concentrator frame. It is seen that this structure is composed of repetitive tetrahedrons. A curved surface is required. This is formed by having the lower members of any tetrahedron larger than the upper members of the adjacent tetrahedron so that a bidirectional curvature is produced.

The reflector facets shown in Figure 3.2.3-6 are hexagons of thin aluminized Kapton. The Kapton is 3 micrometers thick. It is tensioned by 3 rigid end members, pulled outward by bridles. This tensioning system causes the three edge members to be coplanar, so that a flat reflector is produced. The rocker arm and spring canister systems which pull outward on the bridle are mounted to the concentrator frame. A "scallop" at the three free edges of the facet controls wrinkling at the facet edges.

The three bridles of the reflector facet are attached to the rocker arms which mount to the midpoint of the concentrator tube structural elements, as shown in Figure 3.2.3-7. The springs, contained in canisters, provide the pull that causes the rocker arm to tension the plastic film. Note then that the facet is mounted directly to the concentrator support structure and does not include the radial arm and hub system used in Part I of this study.

The plastic film material is aluminized Kapton. DuPont Corporation, the manufacturer of Kapton, believes that a thickness of 3 micrometers is producible by nearly standard roll methods and will demonstrate this in tests in late 1977. Data from project ABLE has shown a potential degradation of reflector film specular performance of approximately 30% due to the radiation encountered, first in a self-power transfer from low orbit to high orbit, and then 30 years of operation in geosynchronous orbit. Tests performed for the solar sail program at the Jet Propulsion Laboratory have indicated, however, that this degradation mode will probably not occur, and that the degradation previously seen is an artifact of the test method itself. We consequently do not forecast radiation degradation. We do anticipate approximately 2.25% degradation due to meteoroid impacts in 30 years of reflector film operation. Our reflectivity estimate is .90 for a reflector cone angle of .22 degrees. This is relatively conservative since even higher reflectivities are probably achievable.

D180-22876-2

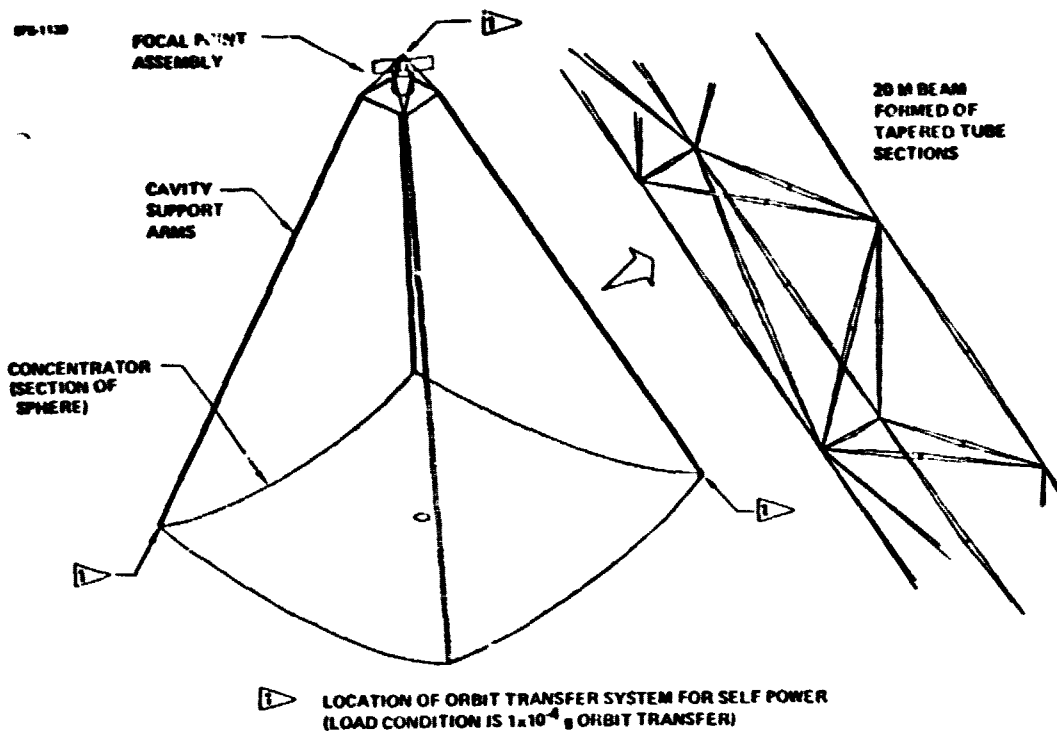


Figure 3.2.3-3 Modules Consist of Concentrator & Focal Point Assemblies

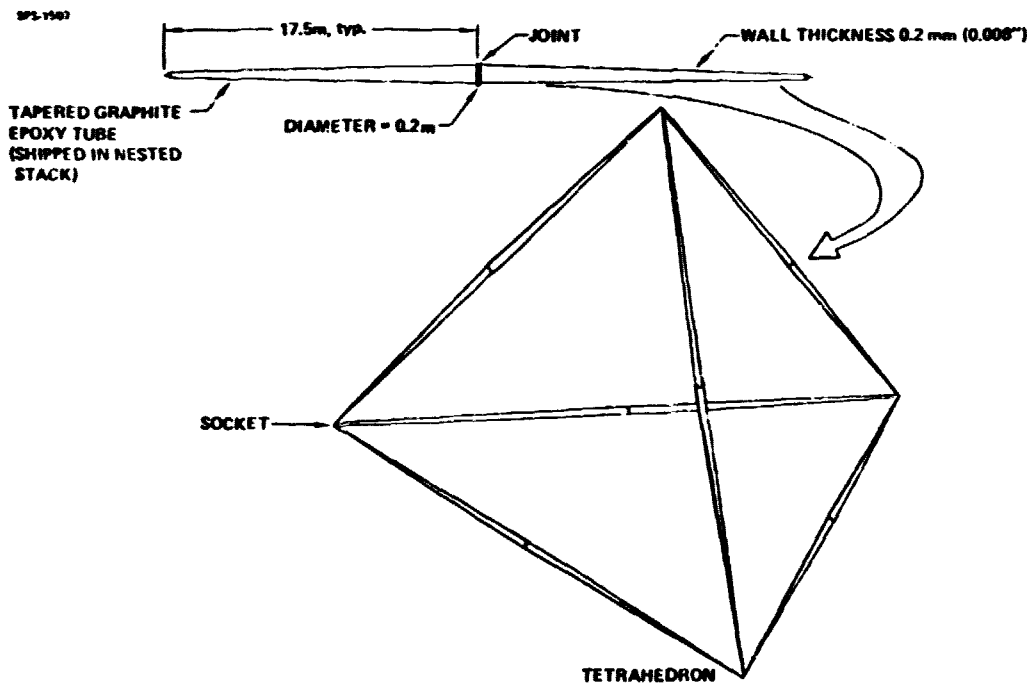


Figure 3.2.3-4 Concentrator Frame Element

D180-22876-2

SPS-1286

(TOOTHPICK MODEL)

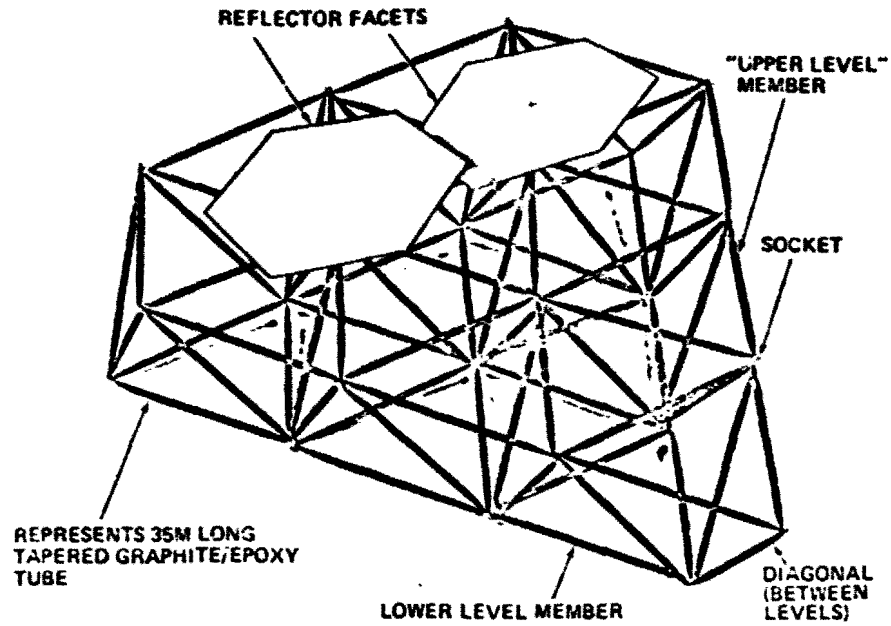


Figure 3.2.3-5 Facet Support Structure

SPS-1184

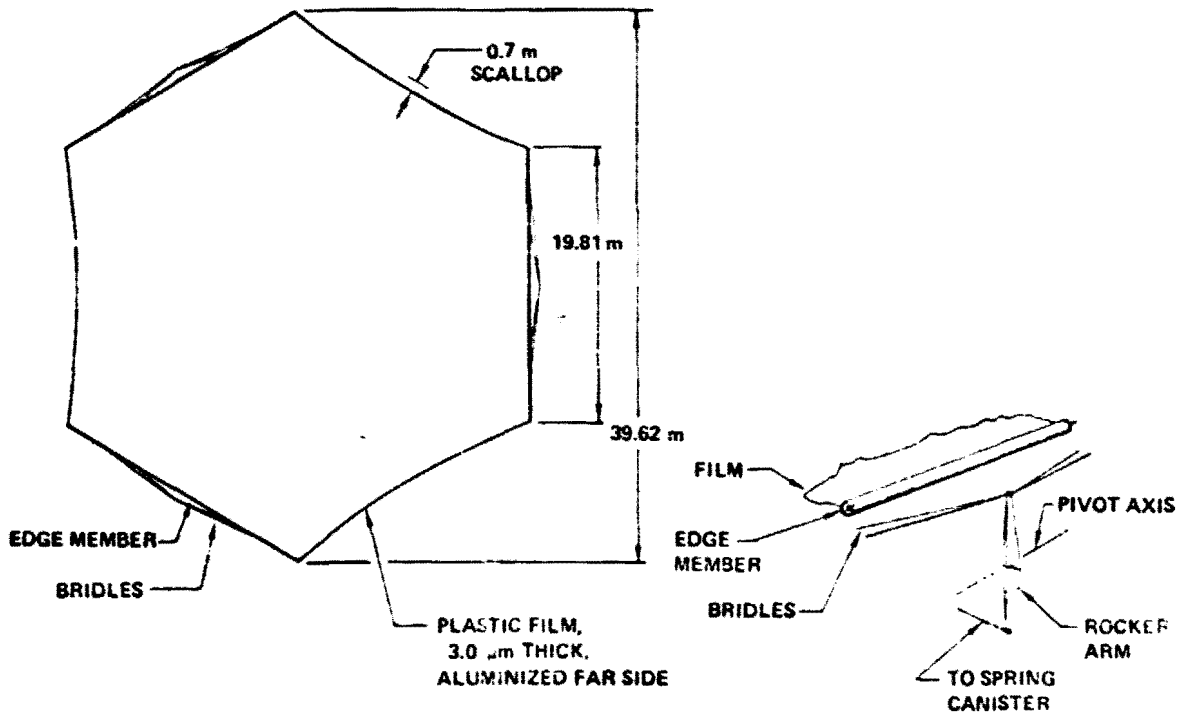


Figure 3.2.3-6 Reflector Facet 1000 M² of Reflecting Area

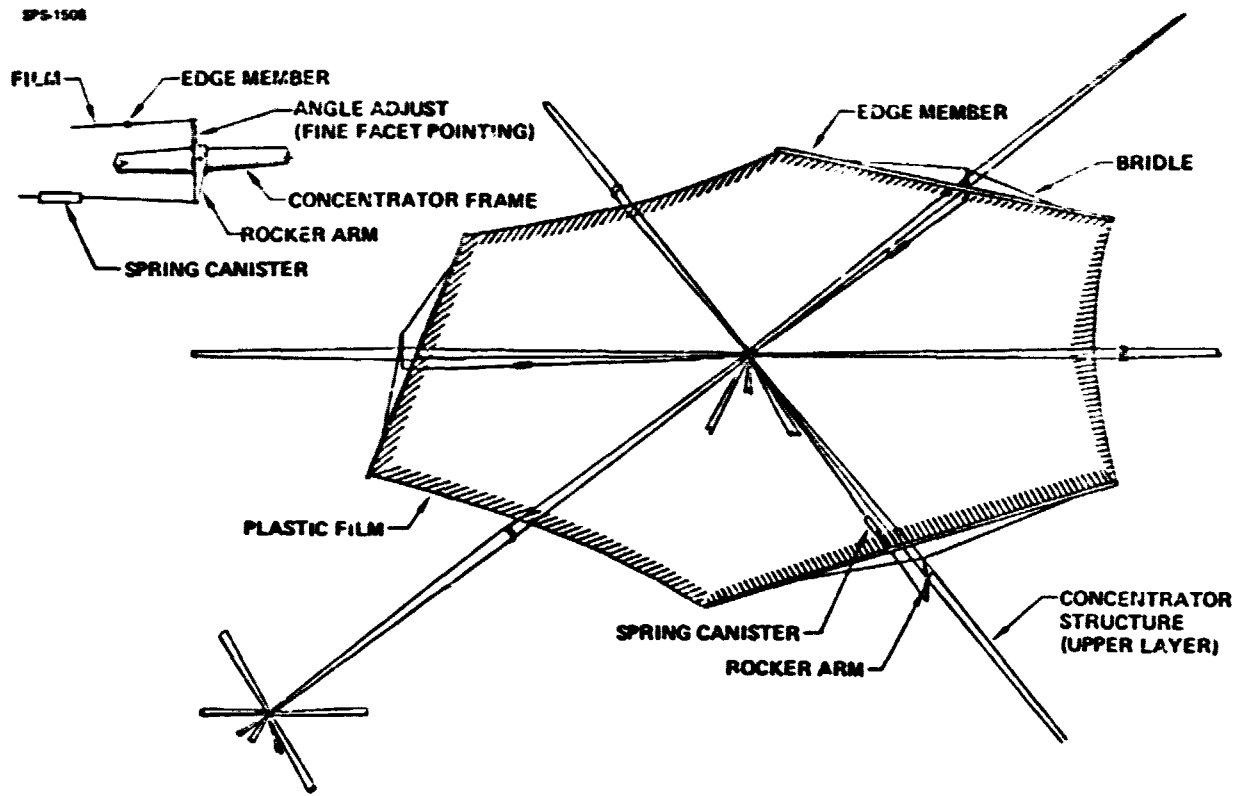


Figure 3.2.3-7 Reflector Facet Mounting

Focal Point Assembly

Each of the 16 modules of the thermal engine SPS is equipped with the assembly shown in Figure 3.2.3-8 at its focal point. Reflected sunlight from the reflector facets enters the CPC at its aperture and by reflections reaches the cavity absorber which contains the boiler tubes for the thermal engine. The CPC is made up of a framework supporting a single layer of molybdenum foil. A reflectivity of .8 is estimated for this foil with the use of a rhenium reflective coating. The walls of the cavity absorber are composed of a framework system supporting 5 layers of molybdenum multifoil. Selection of the number of layers was based on a mass optimization trade. Heavy cavity walls leak relatively little energy to space and therefore require somewhat smaller concentrators. Thin walls are lighter but require larger solar concentrators. Five layers are approximately optimum. The purpose of the CPC is to allow a relatively large reflector facet image to fit within the aperture; also the large aperture of the CPC accommodates satellite pointing errors and some distortion in the framework in the solar concentrator.

The aperture door assembly shown in Figure 3.2.3-9 allows a variation in turbine output power while maintaining a constant orientation with respect to the sun. The door is composed of molybdenum foil panels mounted on cables driven by pulley assemblies attached to the cavity support arm frame. The doors are shown in the open position. The rhenium reflective coating on the doors is used to maintain a low temperature for the door panels when they are fully closed and exposed to the full output of the solar concentrator assembly.

The primary equipment of the focal point assembly is shown in Figure 3.2.3-10. The cavity absorber assembly and CPC are supported by a vertical steel tubing framework system. A framework member on each side of the cavity supports the turbogenerator assemblies. 18 turbogenerators are mounted on each side of the cavity. One radiator assembly is provided per turbogenerator and extends directly outward, either to left or right, from the turbogenerator. The radiator assembly which cools the generator is mounted above the cavity.

System flow and state point data are shown in Figure 3.2.3-11. Liquid potassium from the electromagnetic pump enters the boiler tubes which are located within the high temperature cavity assembly. Vapor from the boiler enters the double ended turbine and is exhausted into a single tapering radiator vapor duct. Pertinent state point parameters for various points around the flow loop are given at the bottom of the figure. Note that while the vapor duct is relatively large in diameter, the pressures are quite low.

While there are certain advantages to recirculation type boilers operating under gravity conditions, zero gravity conditions favor the use of once-through boiling and delivery of dry, slightly superheated vapor.

The condensation of liquid in the turbine during extraction of heat from the vapor is a special case involving need for liquid extraction devices to control droplet erosion damage.

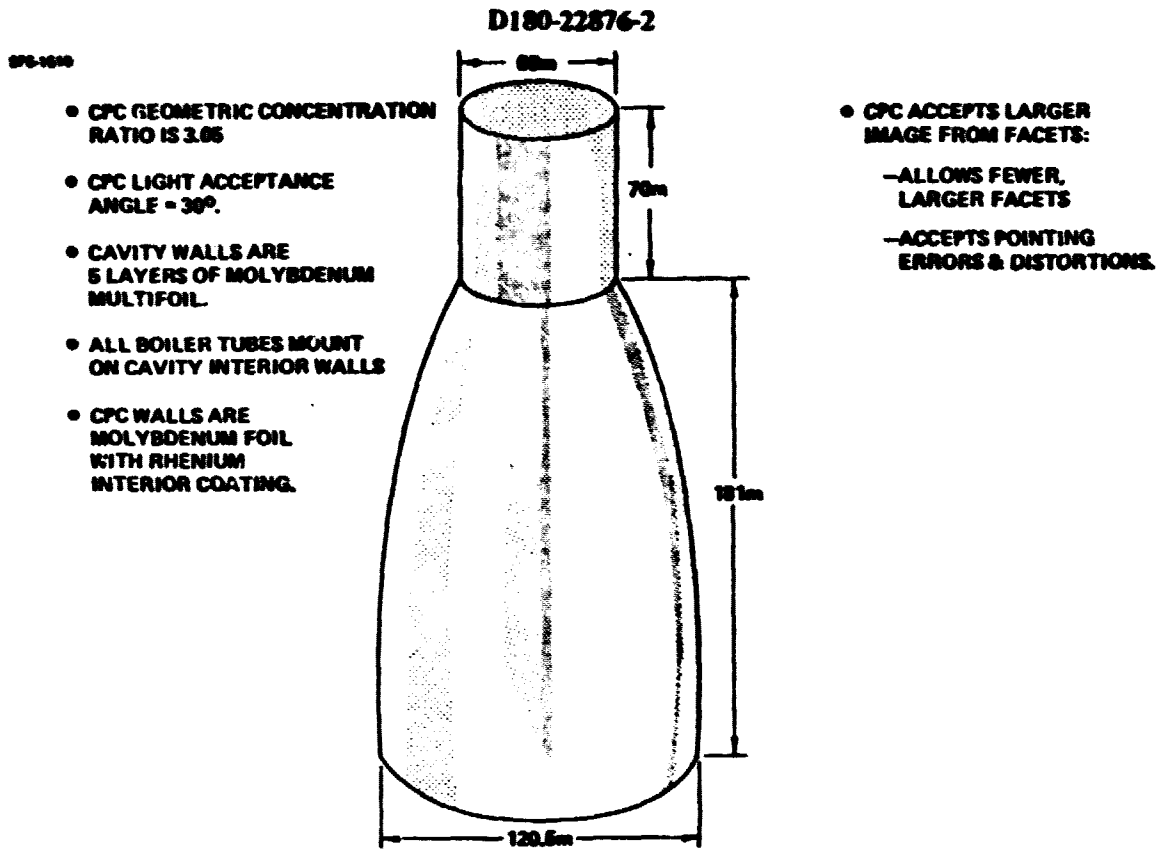


Figure 3.2.3-8 Cavity and Compound Parabolic Concentrator (CPC)

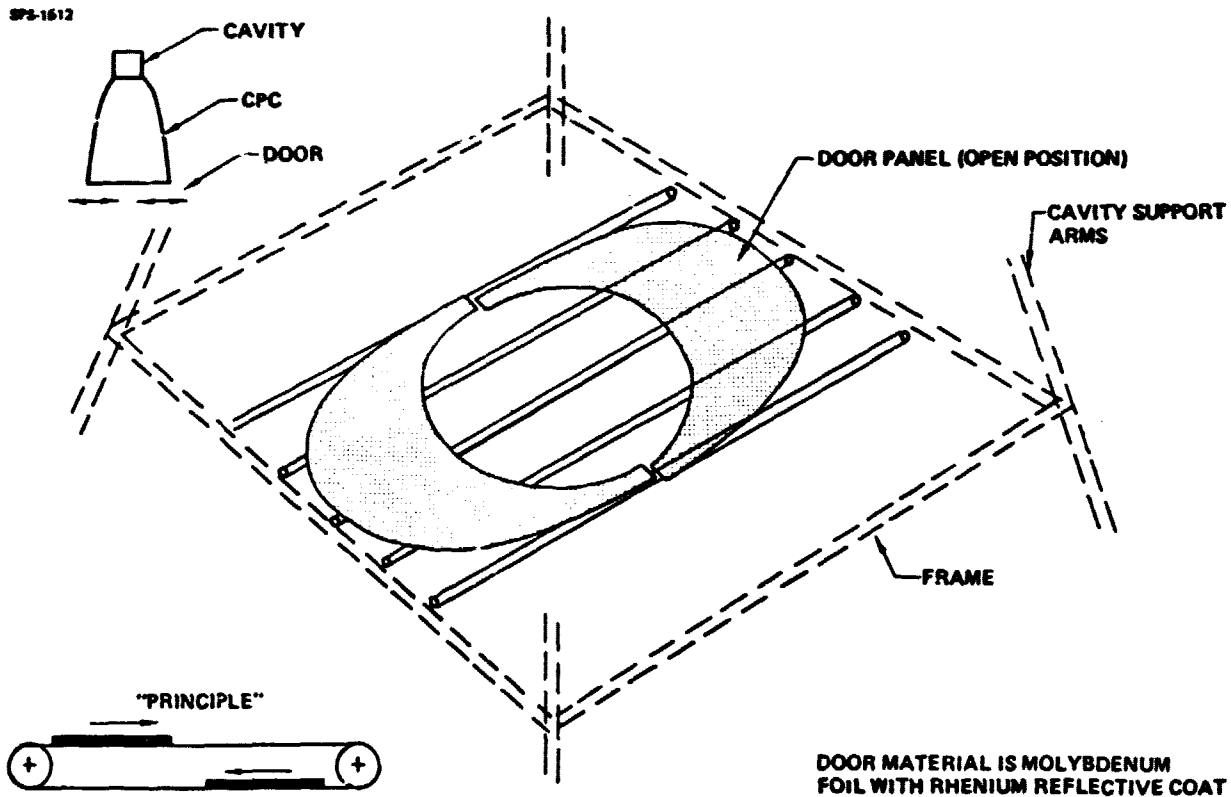


Figure 3.2.3-9 CPC Aperture "Door" Maintains Correct Cavity Temperature Despite Varying Power Output

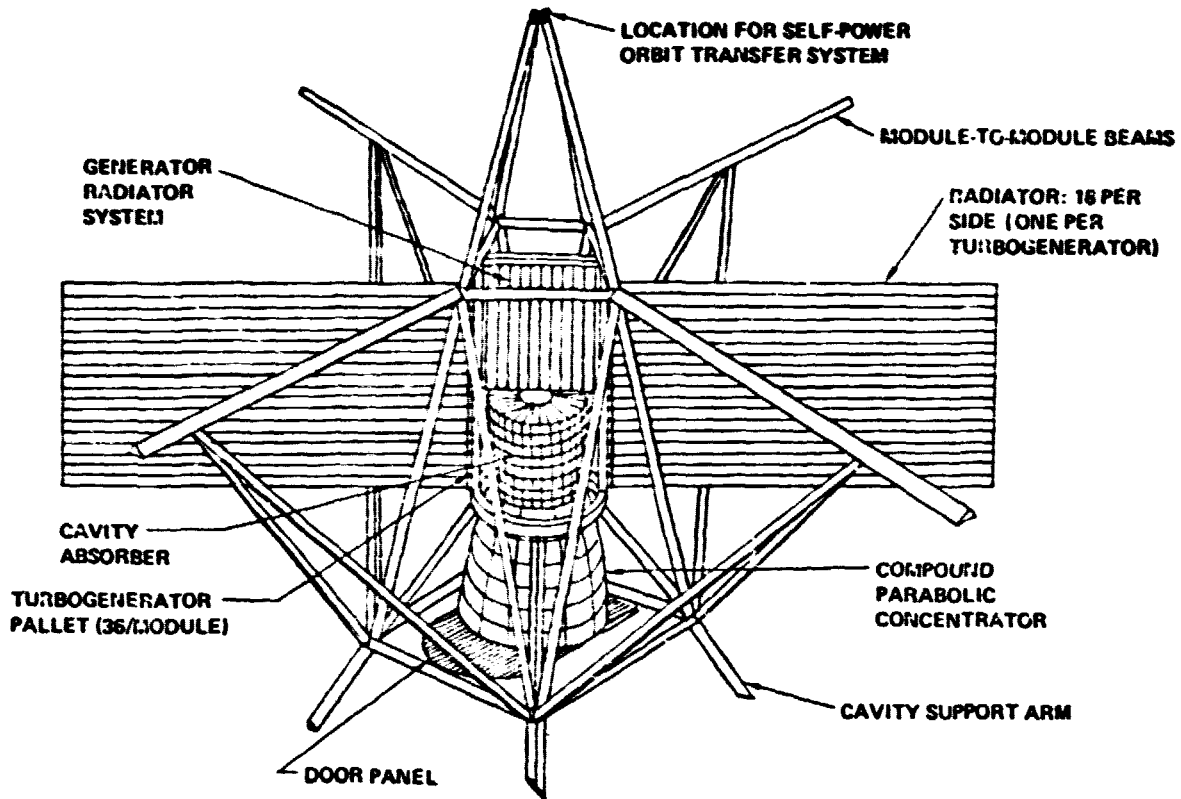
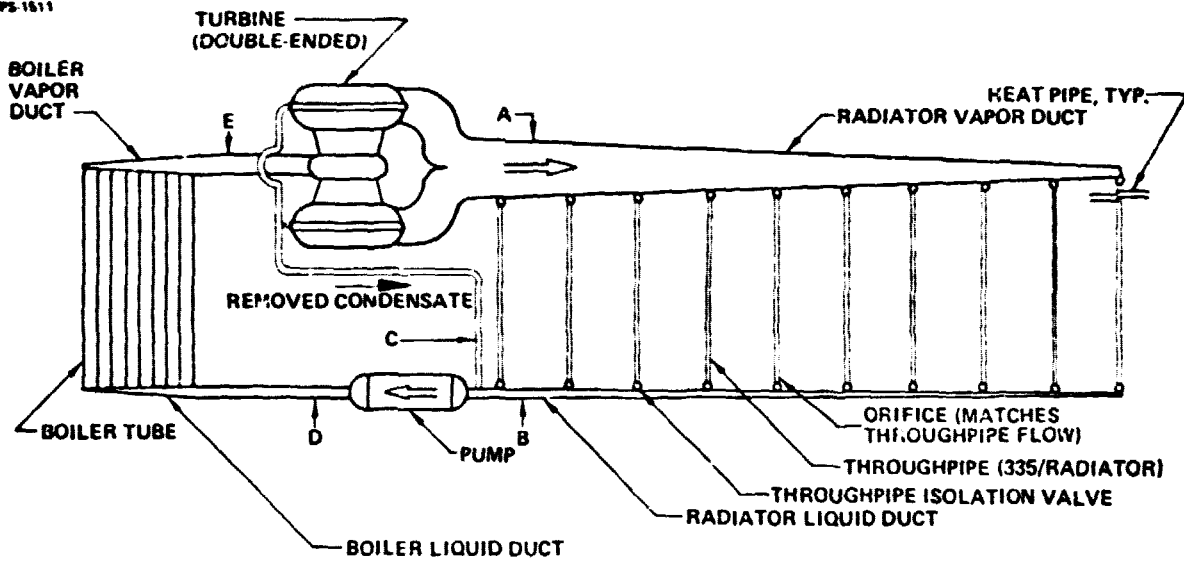


Figure 3.2.3-10 Focal Point Assembly



LOCATION	PRESSURE		FLOW RATE		TEMPERATURE		DUCT DIA
	kPa	PSI	kg/s	lbm/s	K	°F	
A	37.9	5.50	74.67	164.6	932	1218	1.60 5.25
B	16.8	2.43	74.67	164.6	932	1218	0.28 0.92
C	37.9	5.50	9.23	20.3	928	1210	0.10 0.33
D	676	98.0	83.90	185.0	929	1212	0.145 0.48
E	531	77.0	83.90	185.0	1242	1776	0.55 1.80

Figure 3.2.3-11 System Flow Schematic (Not to Scale)

D180-22876-2

In the condenser, liquid is swept along the inside length of the tubes by the much higher velocity of the vapor. The tube might be tapered along its length to maintain high vapor velocity, but this is not necessary. S. Sawochka, near the 1965 time period, conducted experiments on upward flow condensation of potassium in vertical, constant diameter tubes; the performance of these condenser tubes was not adversely affected by a 1 "G" force acting to restrict sweeping of liquid condensate by the high velocity vapor.

Possible thermal fatigue cracking in condensers under 2-phase flow has been considered. In air-cooled metal vapor condensers for land based applications, the poor air-side heat transfer coefficients controlled heat transfer; thus the alternate presence of either a liquid or a vapor phase at a given point on the condenser tended to cause thermal fluctuations and possible thermal fatigue. This possibility occurred since the hot side heat transfer film coefficients varied appreciably in the presence of a liquid or a vapor phase. In the SPS a high heat transfer film coefficient on the cold side of the condenser tube will control the metal temperature and prevent such abrupt thermal fluctuations.

During prior Rankine cycle space power system studies, the problems of 2-phase flow were recognized and plausible solutions and reasonable approaches to these solutions were proposed.

Turbogenerators

Electromagnetic (EM) pumps have been used extensively in the pumping of liquid metals. They have the advantages of absence of seals and bearings, operating reliability and reduced maintenance requirements.

For the Rankine cycle space power program, a light weight 193 kg (425 lbs) electromagnetic boiler feed pump, capable of operating at a liquid metal temperature up to 1033K (1400°F), was designed, built and tested for 10,000 hours. It pumped 811K (1000°F) potassium at flow rates up to 1.47 Kg/sec (3.25 lbm/sec) at a developed head of 1654 kPa (240 psi), a NPSH of 48 kPa (7 psi) and an efficient of 16.5%. The pump featured a T-111 alloy helical pump duct and a high temperature stator with a 811K (1000°F) maximum operating temperature; the stator materials consisted of Hiperco 27 magnetic laminations, 99% alumina slot insulators, type "S" glass tape interwinding insulation and nickel-clad silver conductors joined by brazing in the end turns. Pump windings were cooled by liquid NaK at 700-756K (800-900°F).

Large size annular linear EM pumps are under development for the liquid metal fast breeder reactor. A 14,500 GPM (681 Kg/sec; 1502 lbm/sec) pump has been built and is awaiting test; pumps of larger sizes have been considered in the range of 30,000; 70,000; 80,000 and 130,000 GPM (1410, 3435, 3759 and 6110 Kg/sec; 3108; 7573; 8289 and 13,470 lbm/sec). Weight and cost estimates for commercial land based versions of these pumps have been initiated. While these pumps were designed for handling sodium at about 858°F, their development indicates pump scale-up experience well above that of the earlier higher temperature boiler feed pumps for Rankine space power systems.

D180-22876-2

Since the design technology for EM pumps is well-developed and relatively large pumps have been built, the design and production of pumps of the required size and operating characteristics for the SPS should be a straightforward engineering problem. The use of higher pump voltages and improved high temperature electrical insulation, magnetic and conductor materials will be required utilizing experience gained in the design and test of the 1033K (1400°F) boiler feed EM pump.

Pumping at low NPSH has been demonstrated and avoidance of cavitation in these pumps can be circumvented by (1) subcooling of the condensed potassium to minimize possibility of cavitation (only very low energy losses are involved), (2) minimizing condensate return line pressure losses and (3) reliance upon the dynamic pressure head of the high velocity condensing potassium vapor to help support the minimum NPSH required to prevent cavitation.

The conceptual design of the 31.7 MWe, five state, double flow alkali metal vapor turbine shown in Figure 3.2.3-12 is based on technology developed for smaller scale space power turbines.

It features hydrodynamic lubricated liquid metal pivoted pad journal and thrust bearings. In addition, the turbine shaft leading to the generator would feature an essentially zero leakage potassium seal of a type on which experimental testing has been accomplished; in smaller scale seal tests over 100 hours in duration, it was estimated that the leakage of potassium would not be of engineering significance in over 10,000 hours operation.

Liquid extraction devices, as shown in detail on other pages, can be incorporated in the design using vane trailing edge droplet extraction or trailing edge turbine rotor droplet extraction.

The selection of the suggested modular size provides a nominal point in the design production and test of the alkali metal vapor turbines needed for Rankine cycle solar power satellites.

Each potassium Rankin turbine turns a generator such as shown in Figure 3.2.3-13. These generators produce either 41,000 or 39,000 volts direct current as required by the microwave transmitters. The generators are oil cooled using coolant passages through both the rotor and stator. Although they are quite efficient the generators must dissipate waste heat at such a rate that their own surface area is not sufficient for this dissipation; external radiators are used. A high copper temperature is advantageous to reduce the area and mass of these radiators.

The complete turbogenerator assembly is palletized for shipment as shown in Figure 3.2.3-14. These pallets mount one turbine, one generator and electromagnetic pump, and associated auxiliaries. The structure of this pallet is designed to allow launching of the unit preassembled; at least a 5 g acceleration capability is required.

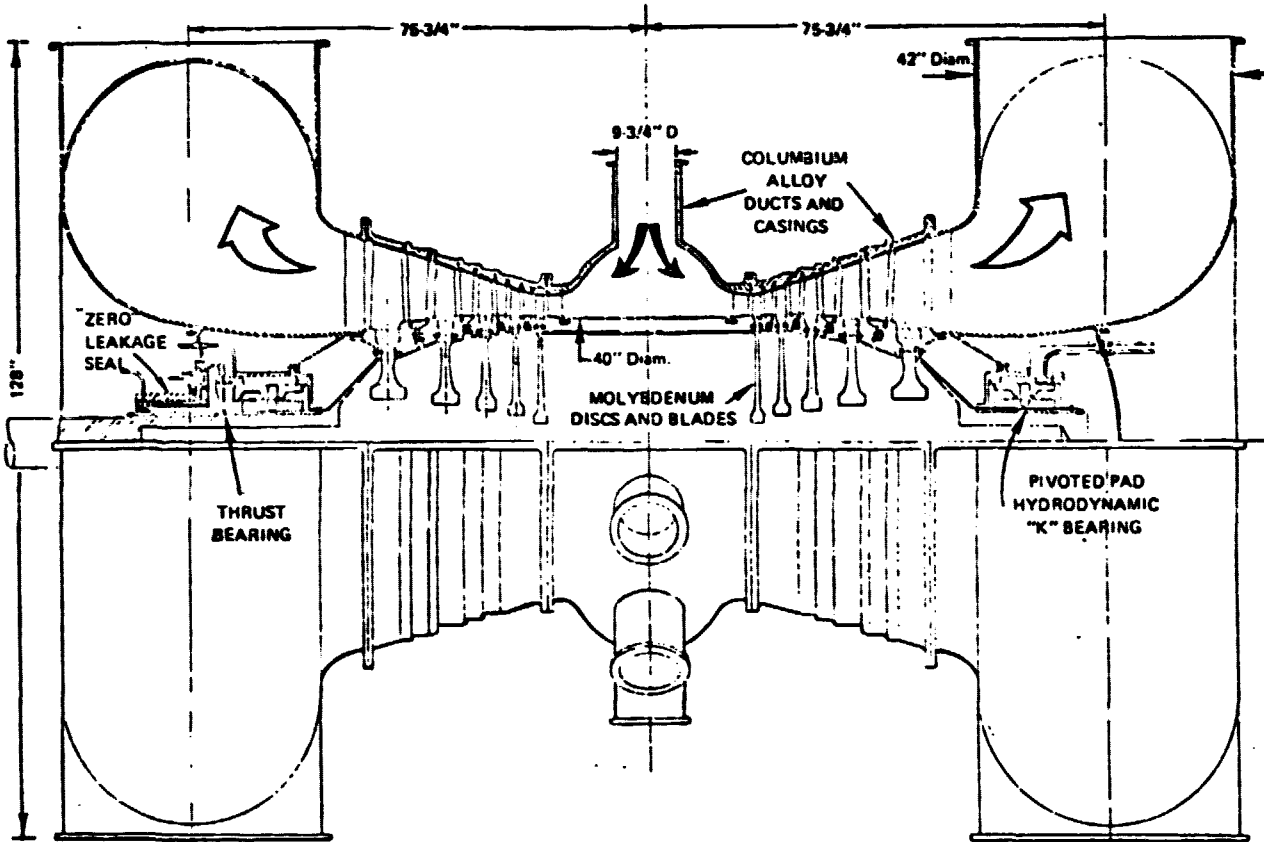


Figure 3.2.3-12 Alkali Metal Vapor Turbine

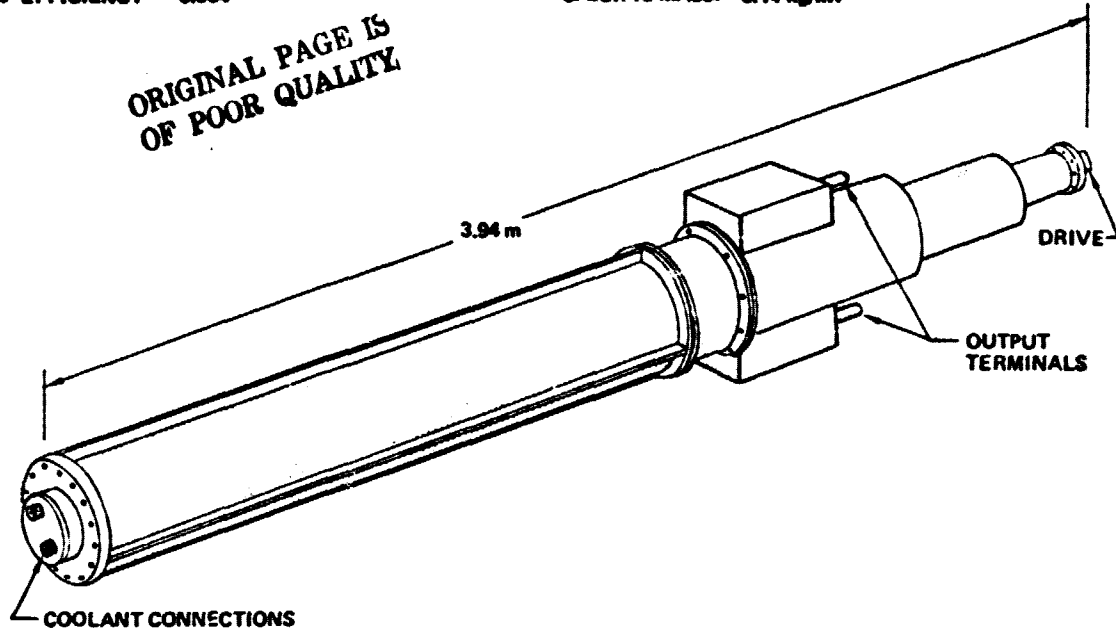
D180-22876-2

SPS-1513

- OUTPUT 31.43 MW
- ROTOR SPEED 7500 RPM
- COOLANT OIL (DC-200)
- EFFICIENCY 0.984

- VOLTAGES: EITHER 41000 OR 39000 VDC, NOMINAL
- COPPER TEMP: 478K (400°F)
- DUTY CYCLE: CONTINUOUS
- SPECIFIC MASS: 0.14 kg/kW

ORIGINAL PAGE IS
OF POOR QUALITY



PRIMARY DATA BASE: AIRESEARCH MFG. CO. OF CA. STUDY FOR AIR FORCE, CONTRACT F33615-75-C-2071

SPS-1636

Figure 3.2.3-13 Generators

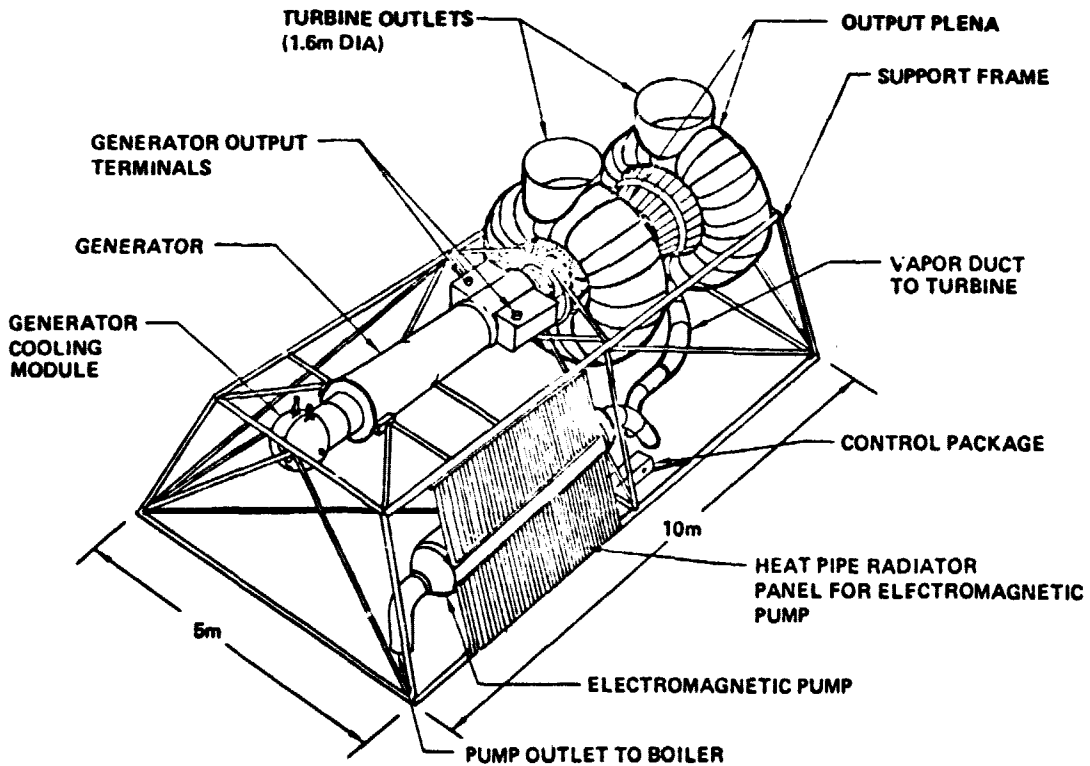


Figure 3.2.3-14 Turbogenerator Pallet

Radiators

Shown in Figure 3.2.2-15 is a segment of the radiator for one generator. A vapor duct is at the top and the liquid return duct is at the bottom. The heat pipe panels with their throughpipes pass between the ducts. Also shown are the triple layers of meteoroid bumper installed on the ducting. At the lower left is a detail of the throughpipes and the wraparound sodium heat pipes. These sodium heat pipes are spaced apart such that their centerlines are 1.6 diameters from each other. This spacing is an optimum compromise between greater spacing, which would improve heat radiation, and reduced spacing which would reduce manifold mass by requiring fewer throughpipes. On the right is a cross section through two adjacent radiator systems showing how the vapor ducts share common meteoroid protection systems for a reduction in bumper mass.

Antenna Mount

The additional, seasonal axis and dog-leg structure required for PEP operations is shown in Figure 3.2.3-16. Slip-rings need not be used at the seasonal axis pivot. Flat cables which are wound during one year of operation and unwound during an annual shutdown period are instead proposed.

A breakdown is given in Table 3.2.3-3 of the radiator mass elements per engine and for the entire SPS. Note that the heat pipes and the potassium for the fill of the radiator systems dominates this mass statement. The heat pipe sheet thickness is driven by meteoroid protection requirements and allows approximately 10% of the heat pipes to be penetrated and thereby made inoperable in 30 years of geosynchronous operation. Because the heat pipes wrap the throughpipes they provide significant throughpipe protection, however, approximately 3% of the throughpipes can be expected to be holed in 30 years of operation. The radiator is consequently oversized by 13 percent.

Performance and Mass

Table 3.2.3-4 is a breakdown of the system power requirements aboard the SPS. The generators require 16.43 GW. Additional utilizations within the system bring the busbar total to 17.913 GW. The power distribution losses are those associated with resistance effects within the distribution busbars. The pumping power is that required to operate the electromagnetic potassium pumps. The attitude control power is a maximum value and corresponds to the time period when maximum thrust is required to maintain the perpendicular-to-ecliptic plane orientation. The total output can be produced by 570 of the generators. 576 generators are installed allowing approximately a 1% margin. It is anticipated that the microwave transmitters will degrade in output and required power input by approximately 2% in the course of a year, consequently in one year about 3% of the turbo-generator systems could be automatically shut down by malfunction detection systems without impacting the power output of the microwave transmitter.

Systems efficiencies are summarized in Table 3.2.3-5. The 17.913 GW required for busbar power as indicated by the previous table is the beginning point for this system efficiency chain. The generators have an efficiency of 98.4%. This requires that the turbines have a shaft output of 18.204 GW.

D180-22876-2

SPS-1814

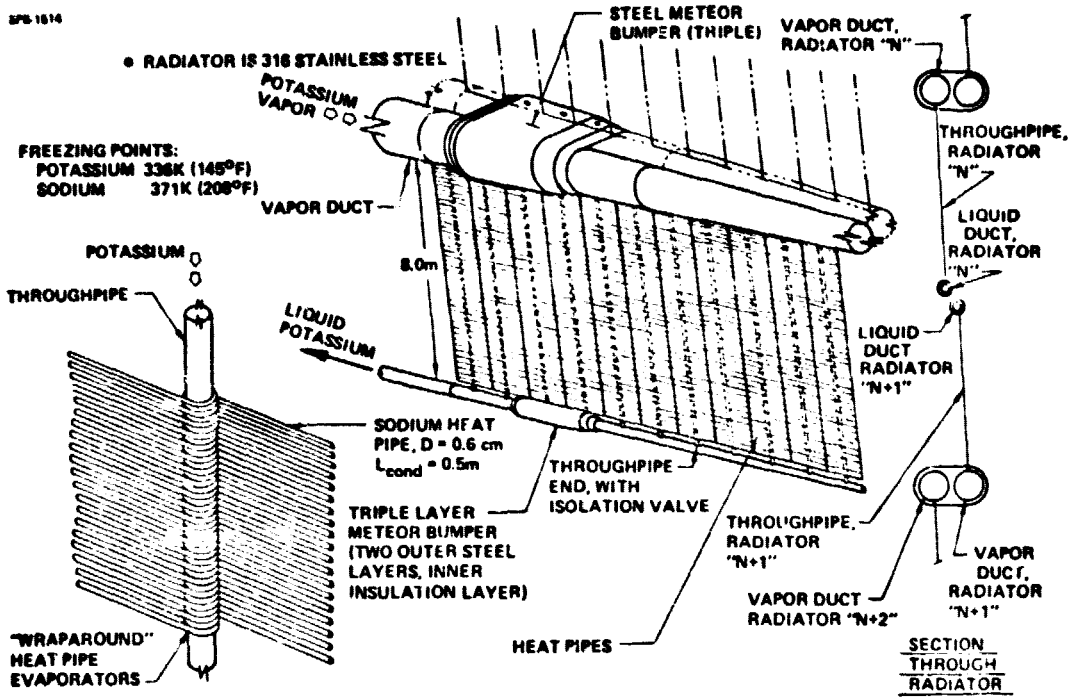


Figure 3.2.3-15 Primary Radiator System

SPS-1236

NOTE: TRANSMITTER C. G. REMAINS IN CONSTANT POSITION RELATIVE TO THE SPS

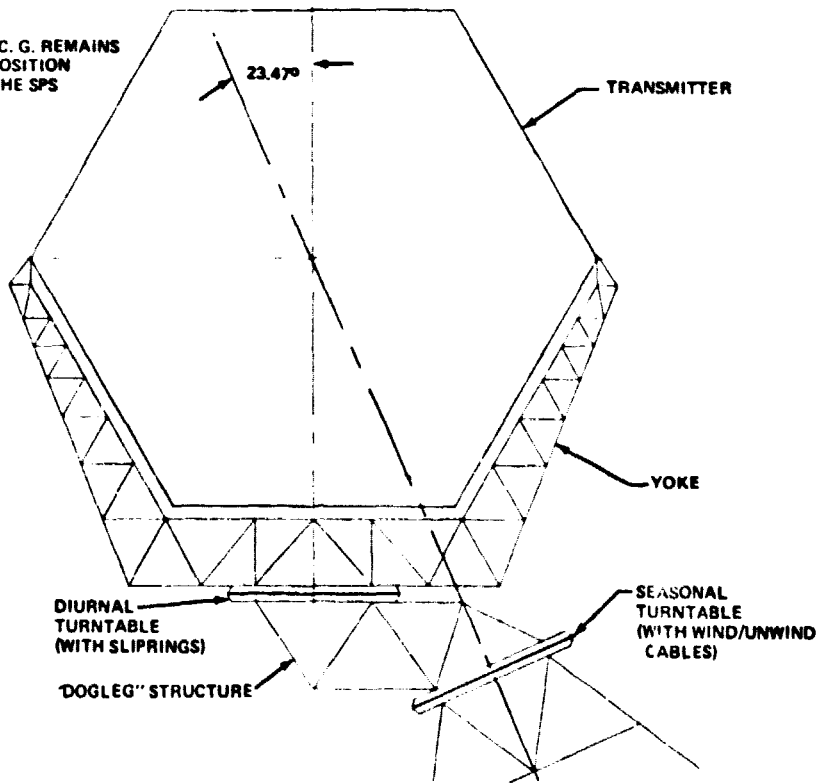


Figure 3.2.3-16 Antenna Joint for "P.E.P." SPS

D180-22876-2

Table 3.2.3-3 Radiator Mass

SPS-1834

	PER ENGINE KG	PER SPS 10 ⁶ KG
MANIFOLDS	3895	2.24
VAPOR DUCT	(1240)	(0.71)
LIQUID DUCT	(216)	(.12)
METEOROID PROTECTION	(2439)	(1.40)
THROUGHPIPES	1500	0.86
THROUGHPIPES (335/ENGINE)	(790)	(.46)
ISOLATION VALVES	(710)	(.41)
HEAT PIPES	13,299	7.66
SHELL	(10,838)	(6.24)
WICK	(1729)	(0.99)
SODIUM	(732)	(0.43)
<u>POTASSIUM</u>	<u>8046</u>	<u>4.63</u>
TOTAL	26,740	15.39

Table 3.2.3-4 Power Budget

SPS-1816

	10 ⁶ kW
TRANSMITTERS	<u>16.430</u>
POWER DISTRIBUTION	0.898
PUMPING	0.282
ATTITUDE CONT, MAX	0.300
MISC.	0.003
BUSBAR	17.913

570 GENERATORS AT 31.426 MW₀ EACH
(576 INSTALLED)

Table 3.2.3-5 System Efficiency Chain

SPS-1516

	10 ⁶ kW
BUSBAR (GENERATOR OUTPUT) (GEN. EFFICIENCY = 0.984)	<u>17.913</u>
TURBINE SHAFT OUTPUT (CYCLE EFFICIENCY = 0.99)	18.204
POWER ADDED TO POTASSIUM	96.317
SOLAR ENERGY INTO CAVITY	112.397
(REFLECTION LOSS, 5%)	(5.620)
(LOSS THROUGH INSULATION)	(0.500)
(RERADIATION THROUGH APERTURE)	(8.836)
(MISC, I.E., MANIFOLD HEAT LOSS)	(1.124)
INTO SECOND STAGE CONCENTRATOR (CPC REFLECTIVITY = 0.865)	129.939
IMPINGING UPON PLASTIC FILM (FILM END-OF-LIFE REFLECTIVITY = 0.877)	148.079

D180-22876-2

output of 18.204 GW. Since the turbines and the rest of the system have an overall cycle efficiency of 0.189 a power level of 96.317 GW must be added to the potassium flow within the boilers of the cavity absorber. A breakdown of the losses associated with the cavity absorber is also given. For example, 5% of the energy entering the cavity is reflected back out again. This is based on tests of "bench model" absorbers for ground solar power programs. The five layers of insulation making up the cavity walls allow a heat loss of approximately 1/2 GW. The hot walls of the cavity reradiate energy back out through the aperture. Some of this passes directly to space and some of it is reflected to space from the solar concentrator. Other losses, such as heat losses through the walls of the manifolds connecting the boilers to the turbines, amount to approximately 1.1 GW. The CPC also has losses due to energy absorbed rather than reflected by its walls. The end of life reflectivity of the plastic film facets is 0.877. This is the reflectivity after a reduction of 2.25% due to meteoroid scouring, in 30 years of operation.

The PEP orientation has been selected primarily because moving facets are not required. However, other benefits accrue as summarized in Table 3.2.3-6.

The disadvantages of the additional, seasonal antenna axis are somewhat offset by two advantages relative to microwave power transmission. The first of these is that rectennas can be switched without polarization loss even if the antennas are at different longitudes without moving the satellite along the geosynchronous path. Additionally, the seasonal antenna axis can be used to provide antenna tilt to compensate for Faraday rotation caused by the ionosphere.

Table 3.2.3-7 is a breakdown of the Part II final mass. Prominent elements in this mass are the transmitters, the turbines, the radiator systems, the structure (primarily the facet support structure), and the potassium inventory for the system. The turbine mass was estimated by General Electric and represents a value which is probably correct to within +20% and -40%.

Thermal Engine Conclusions

It was determined that the potassium Rankine cycle thermal engine is the lightest of the potential approaches investigated. At the beginning of this study the solar concentrators involved steerable facets with individual power supplies, sensors and servomechanisms. These have been eliminated by using a perpendicular-to-ecliptic orientation and a concentrator dish of the requisite curvature. Instead of electromechanical pumps, composed of an electric drive motor and a pump with the requisite seal between them (which could be subject to leakage), we now utilize electromagnetic pumps. Although somewhat heavy, the low pumping power associated with potassium Rankine makes these potentially low-failure-rate pumps practical. Although certain materials such as silicon carbide and tantalum may offer advantages for thermal engine SPS they are either too advanced or insufficiently abundant to allow them to be baselined. The materials selected are in common use and resource data indicates that there is enough to allow a significant thermal engine program to be accomplished. The perpendicular-to-ecliptic plane orientation is critical in allowing the fixed reflector facets. This requires somewhat more thruster power, but is a proper orientation for the

D180-22876-2

Table 3.2.3-6 "Perpendicular-to-Ecliptic Plane" Orientation

SPS-1212

<u>DISADVANTAGES</u>	<u>ADVANTAGES</u>
<ul style="list-style-type: none"> ● HIGHER PROPELLANT CONSUMPTION (UNLESS CONFIGURATION IS INERTIALLY SYMMETRIC, USES MAGNETIC TORQUEING OR SOLAR PRESSURE EFFECTS) ● BEST PERFORMANCE REQUIRES TIGHTER ATTITUDE CONTROL LIMITS (E.G., 0.1°, NOT 0.5°) ● REQUIRES ADDITIONAL (SEASONAL) AXIS ON ANTENNA ● 300 MW PEAK POWER REQUIRED TO OPERATE THRUSTERS 	<ul style="list-style-type: none"> ● FACETS NEED NOT FOLLOW SEASONAL SUN MOTION ● ELIMINATES COSINE EFFECT ON SIZING ● FACETS NEED NOT BE SPACED APART TO ALLOW MOTION ● LOWER METEOROID FLUX ON RADIATORS ● ADDITIONAL ANTENNA AXIS PERMITS TRANSMISSION TO VARIOUS RECTENNA LONGITUDES WITHOUT POLARIZATION LOSS (FROM GIVEN ORBIT LONGITUDE) ● ADDITIONAL ANTENNA AXIS PERMITS COMPENSATION FOR DIURNAL IONOSPHERIC FARADAY POLARIZATION ROTATION ● RADIATOR IS ALWAYS EDGE ON TO THE SUN ● CONSTANT THERMAL ENVIRONMENT FROM FIXED SOLAR ORIENTATION

SPS-1423

Table 3.2.3-7 Potassium Rankine SPS Mass Statement

STRUCTURE	<u>10⁶ kg</u>
	6.976
FACETS	1.837
RADIATOR (W/O POTASSIUM)	10.768
POV DIST	4.760
SW. GEAR	0.218
GENERATORS, ACCESSORY PACK	2.508
GENERATOR RADIATORS	1.140
TURBINES	13.755
PUMPS, PUMP RADIATORS	0.984
BOILERS & MANIFOLDS	3.296
CAVITY ASSYS	1.000
CPCS	0.299
LIGHT DOORS	0.025
MONITOR, COMMAND & CONTROL	0.100
ATTITUDE CONTROL	1.200
START LOOPS, CONTROLS	0.250
ANTENNA SUPPORT	0.286
MISC, INCLUDING STORAGE	0.200
POTASSIUM INVENTORY	6.058
<u>POWER GENERATION</u>	<u>55.660</u>
<u>ANTENNAS</u>	<u>24.384</u>
SPS	80.044

thermal engine SPS. The turbines themselves, at their size of approximately 32 megawatts, use forgings which can be produced by existing U.S. industry. Little new industrialization is therefore required for the thermal engine SPS. The nation's current production capability is probably adequate to produce one SPS per year.

3.2.4 Space Construction and Transportation Operations

The linear dimensions of an SPS are some three orders of magnitude larger than the linear dimensions of the payload bay of any plausible launch vehicle that might be used to deliver SPS hardware to orbit. The mass of an SPS is at least two orders of magnitude greater than the lift capability of any plausible launch system. These figures clearly indicate that some sort of construction operation in orbit will be required. The question of where (i.e., in what orbit) this should take place was summarized earlier. This section describes the evolution of design concepts for space construction systems and a more detailed comparison of the equipment and operations needed for construction of photovoltaic SPS's as compared to thermal engines and for LEO construction compared to GEO construction.

3.2.4.1 Integrated Operations

Production of SPS's will require a logistics and operations network stretching from raw materials on Earth to finished products in space. The operation of the Earth-based network appears to pose no unusual problems,* but the space operations are much more complex and on a much larger scale than anything yet achieved. This description of integrated operations concepts will provide a framework for further technical discussion.

The operation* concepts for low Earth orbit (LEO) construction and geosynchronous orbit (GEO) construction are similar with important differences. The LEO concept is shown in Figure 3.2.4-1. The figure illustrates the photovoltaic option. (Photovoltaic and thermal engine construction are compared in Section 3.2.4-5.) Space operations crews and all hardware and consumables required in space are delivered to low Earth orbit by launch vehicles. The crew vehicle was assumed to be an improved space shuttle with the solid rocket boosters replaced by a reusable liquid propellant booster. The cargo vehicle is a new two-stage vehicle capable of delivering approximately 400 tons of payload per flight. Crew flights occur weekly and about 3 cargo flights are required every 2 days, to each space operations complex. (One operations complex was somewhat arbitrarily sized to construct an SPS in one year. Construction of more than one SPS per year could employ multiple complexes or possibly larger ones.)

The largest element of the LEO construction complex is the construction base, nominally located in a 478 km circular orbit at 31° inclination. This facility houses a crew of 480 with overflow quarters for transients, e.g., those awaiting transportation to some other location. The primary function

*The hardware throughput to construct one SPS per year is about 15 tons per hour. The hardware throughput of the U.S. auto industry is roughly 100 times greater.

SP-4788

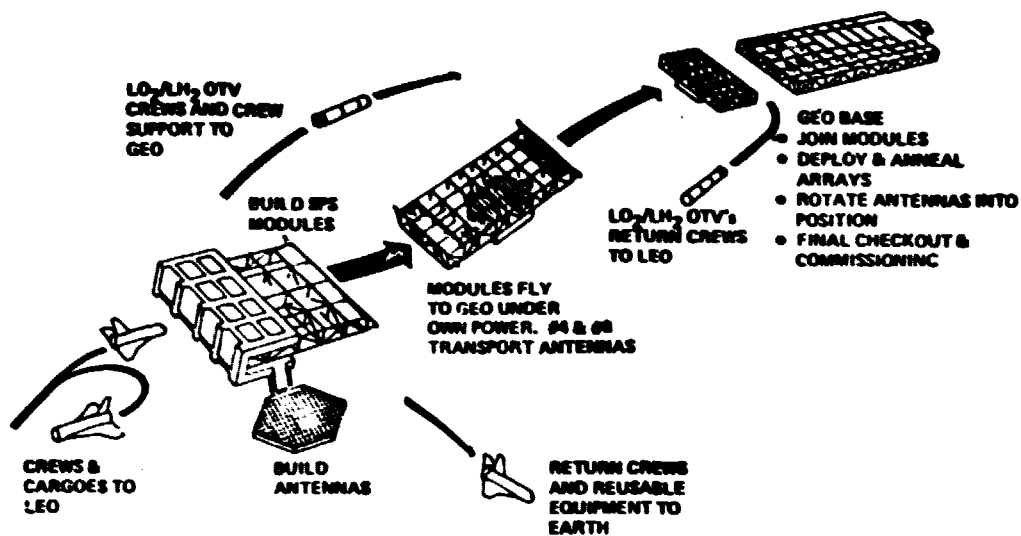


Figure 3.2.4-1 LEO Construction Integrated Operations

D180-22876-2

of the facility is construction of SPS power generation modules and antennas. It also serves as a staging base for orbit transfer vehicles used to carry crews and crew supplies to the GEO facility. A crew OTV flight to the GEO facility normally occurs once every three months.

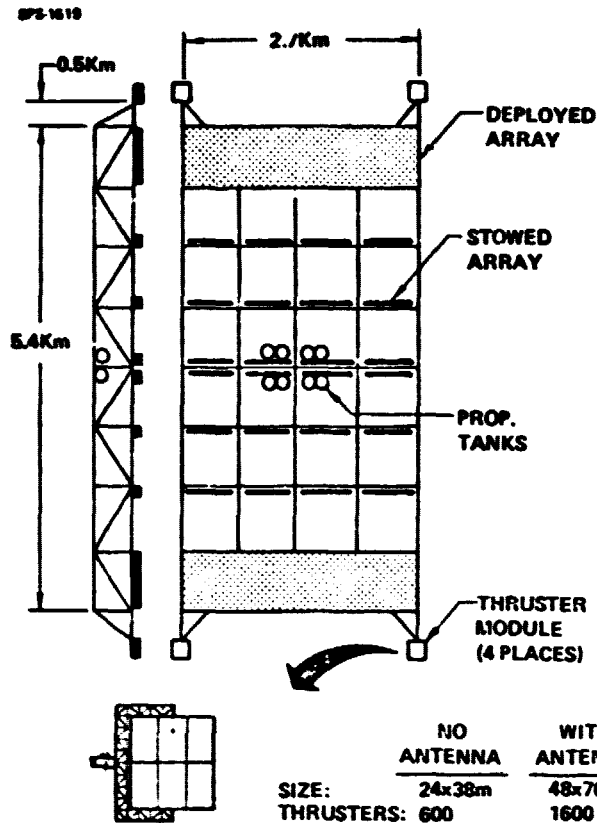
Satellite modules are equipped with electric propulsion systems and flight control systems for the solar-powered trip to GEO. Figure 3.2.4-2 shows a typical module arrangement as configured for the transfer. Thruster installations are located at the module corners for maximum control authority. Propellant tanks are located near the module centroid to minimize gravity gradients. Although the propulsion system is primarily solar-electric, some chemical (LO_2/LH_2) thrust capability is also provided so that control authority can be maintained while flying through the Earth's shadow. Because of the comparatively low chemical specific impulse (400 seconds versus 7500 seconds for the electric thrusters) and 1/3 of the onboard propellant is LO_2 and LH_2 . The remaining 2/3 is argon for the electric thrusters.

The GEO base controls module rendezvous and berthing, rotates the antennas into the operating position, deploys the remainder of the solar cells and anneals the solar cells used for orbit transfer to restore their performance after their exposure to van Allen belt radiation during the transfer. The GEO base is manned by a crew of 60.

In the case of GEO construction, most of the crew and the large base are located at GEO. All construction is carried out at this base. The integrated operations concept is shown in Figure 3.2.4-3. The base in low Earth orbit performs no construction tasks; it is a *transportation staging base* that facilitates transfer of propellants and payloads from the Earth launch vehicles to orbit transfer vehicles. The staging base receives about three flights from Earth each day. On the average, slightly more than two of each three flights will deliver hydrogen and oxygen propellants for the orbit transfer vehicles (OTV's) with the third flight bringing SPS hardware, or occasionally crew supplies or other support material. The staging base will also effect transfer of crews from the shuttle crew vehicle to a crew orbit transfer vehicle and provide sufficient transient or emergency crew quartering for crew operations. An orbit transfer flight must be dispatched to GEO every day, delivering SPS hardware, or (once every month) an exchange crew for the GEO base. Such in-space refurbishment of OTV's as is necessary and practical will be carried out at the staging base. Parking space for the OTV fleet is also provided by the staging base. (A ground-based versus space-based OTV trade study was conducted and showed the space-based OTV to have about a 15% performance and cost advantage.)

The GEO construction base is very similar to the LEO base, differing primarily in that (1) since the power generation portion of the SPS is built as a monolith rather than as modules, the 2 x 4-bay construction base must index the satellite in two directions to build an 8 x 32-bay satellite; (2) procedures for installing the completed antennas are different. The antenna portion of the facility must be able to separate and free-fly to the free end of the satellite then half complete, to install the first antenna. It then returns to the main facility; the second antenna and the power generation

D180-22876-2



GENERAL CHARACTERISTICS

- 5% OVERSIZING (RADIATION)
- TRIP TIME = 180 DAYS
- ISP = 7000 SEC

MODULE CHARACTERISTICS

	NO ANTENNA	WITH ANTENNA
• NO. MODULES	6	2
• MODULE MASS (10^6 KG)	8.7	23.7
• POWER REQ'D (10^6 Kw)	0.3	0.81
• ARRAY %	13	36
• OTS DRY (10^6 KG)	1.1	2.9
• ARGON (10^6 KG)	2.0	5.6
• LO_2/LH_2 (10^6 KG)	1.0	2.8
• ELEC THRUST (10^3 N)	4.5	12.2
• CHEM THRUST (10^3 N)	12.0	5.0

	NO ANTENNA	WITH ANTENNA
SIZE:	24x38m	48x76m
THRUSTERS:	600	1600

Figure 3.2.4-2 Self Power Configuration Photovoltaic Satellite

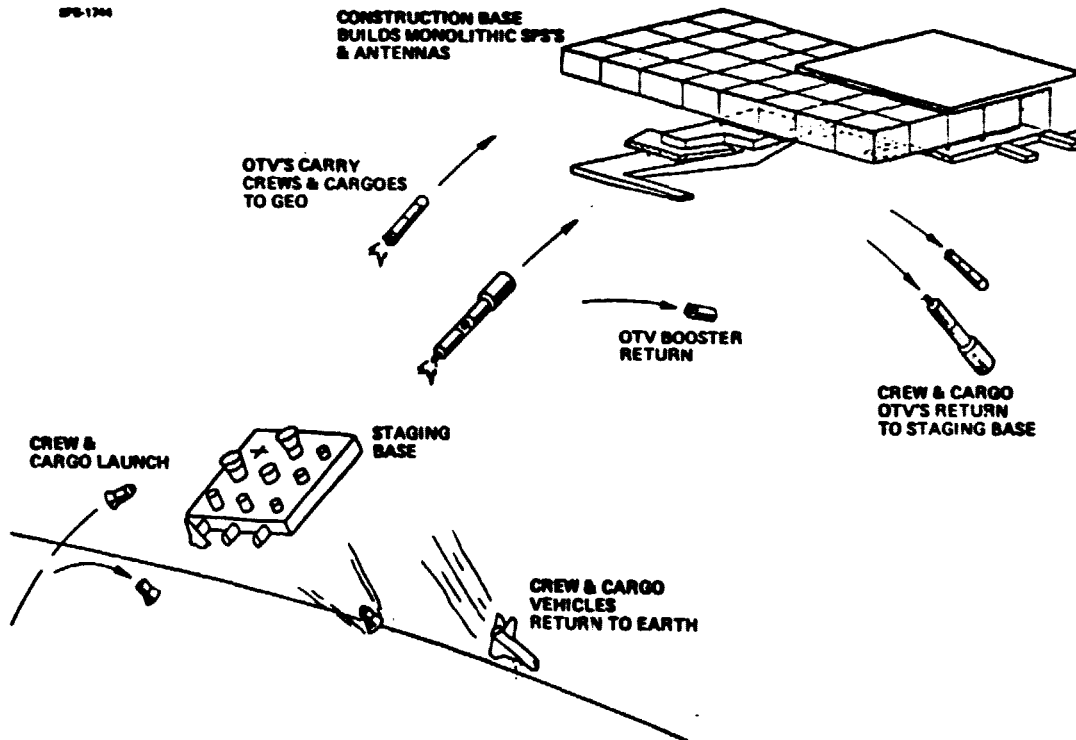


Figure 3.2.4-3 Integrated GEO Construction Operations Concept

D180-22876-2

section are completed concurrently and the free-flight mode is not required to install the second antenna. (Many alternatives to the free-flight mode were examined, but all involved operational complexities or problems judged to be more objectionable.)

The GEO construction option does not require electric-propelled low thrust orbit transfers. The electric propulsion installations on the SPS for operational flight control are a little more than 5% of the thrust level of those required for orbit transfer (125-150 newtons per installation vs. about 2000 newtons) but otherwise involve very similar hardware. As discussed under control requirements in Section 3.2.2.1, reliance on chemical propulsion for operational flight control would impose severe propellant resupply requirements.

3.2.4.2 Historical Synopsis

The initial studies of the SPS concept in the early 1970's gave primary emphasis to the issues that seemed most awesome to the investigators at that time:

- (1) The feasibility of a wireless energy transmission system requiring unprecedented antenna size, precision, directivity, and efficiency;
- (2) The design of a lightweight structure of unprecedented size;
- (3) The transportation of unprecedented masses of total payload into space at what had to be a much lower cost per unit mass than predicted for any system then under active study or development.

By 1973, favorable resolution of these issues began to seem possible and the construction problem began to receive much-deserved attention. Three options were quickly identified: *deploy*; *assemble*; *fabricate*. There was a natural desire to minimize the workload in space, so initial attention was focussed on deployables.

Figure 3.2.4-4 shows an early construction concept with a tubular truss structural element being deployed from its folded configuration. Calculation showed that the package density for folded structure of this nature was incredibly low, so low that mixing with high density components still presented a very difficult payload volume problem to the launch vehicle designer. In fact, any plausible tubular truss element, even if stacked like cordwood, presented a serious density problem. This led to a line of thought (pioneered by Grumman Aerospace) that developed concepts of fabricating structure in space from prepared flat stock. The latter could be rolled for shipment to attain high densities. Current concepts of SPS construction in space have developed around this and similar methods for producing the SPS structure.

ORIGINAL PAGE IS
OF POOR QUALITY

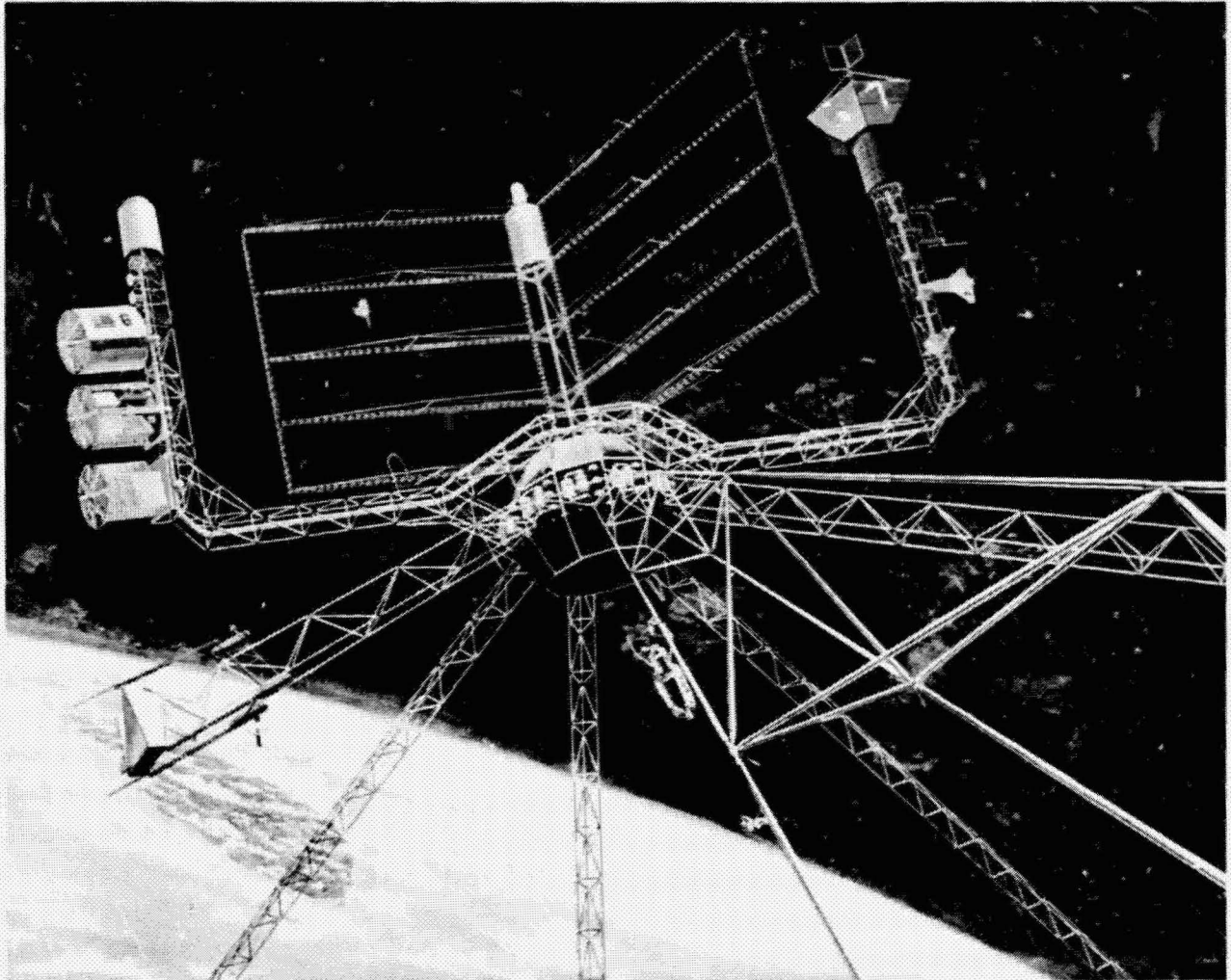


Figure 3.2.4-4 Thermal Engine SPS Construction Concept

3.2.4.3 Construction of Structure

Once the density issue had surfaced and been characterized, the emergence of concepts for on-orbit structure fabricators ("beam machines") was inevitable. The essential purpose of the beam machine is to make something with acceptable structural characteristics for SPS use out of something with acceptable packaging density for launch from Earth. Two approaches have evolved, the "assembler" machine and the "fabricator" machine. Figure 3.2.4-5 illustrates an "assembler" concept and Figure 3.2.4-6 illustrates a fabricator. The assembler makes structure from prefabricated nested parts and the fabricator makes structure by forming flat stock into suitable sections and assembling the beam from these sections. The former device uses mechanical joints; the latter uses bonded joints. A qualitative comparison of the resulting types of structure was presented earlier in Section 3.2.2.2. Considerable discussion has taken place over which approach is best. No clear cut advantage was found for either. A selection may require an operational suitability comparison of prototype machines.

Beam machines of either variety are predicted to produce 20-meter triangular-section beams at one to fifteen meters per minute. A rate anywhere in this range is acceptable and will allow relatively few machines to make enough structure for an entire SPS in one year. An important result of this study was how these and other kinds of machines could be effectively employed in an integrated construction system to build SPS's.

3.2.4.4 Construction Facilities

Earlier construction base concepts, such as the one illustrated above in Figure 3.2.4-4, included a minimum of facilities and equipment. At that time no comprehensive analyses of construction operations had been conducted. This study invested considerable effort in such analyses (see Volume 3 of the Part I report and Volume 5 of the Part II report). Out of these grew an awareness of the need of facilities. The construction operation must carry out several operations:

- (1) Receive payloads from Earth, unpack and sort them, and route the hardware to the right locations in a timely manner so that construction operations can proceed without logistics delays. Some warehousing is required to smoothly interface transportation and construction operations.
- (2) Build the SPS energy conversion, antenna and interfacing structures.
- (3) Install all equipment: solar arrays, power conductors, processing and switch gear, instrumentation, antenna subarrays, flight control systems and support systems.
- (4) Perform checkouts.
- (5) Route reusable payload packaging hardware to transportation operations stations for return to Earth by returning launch vehicles.

D180-22876-2

SPS-1246

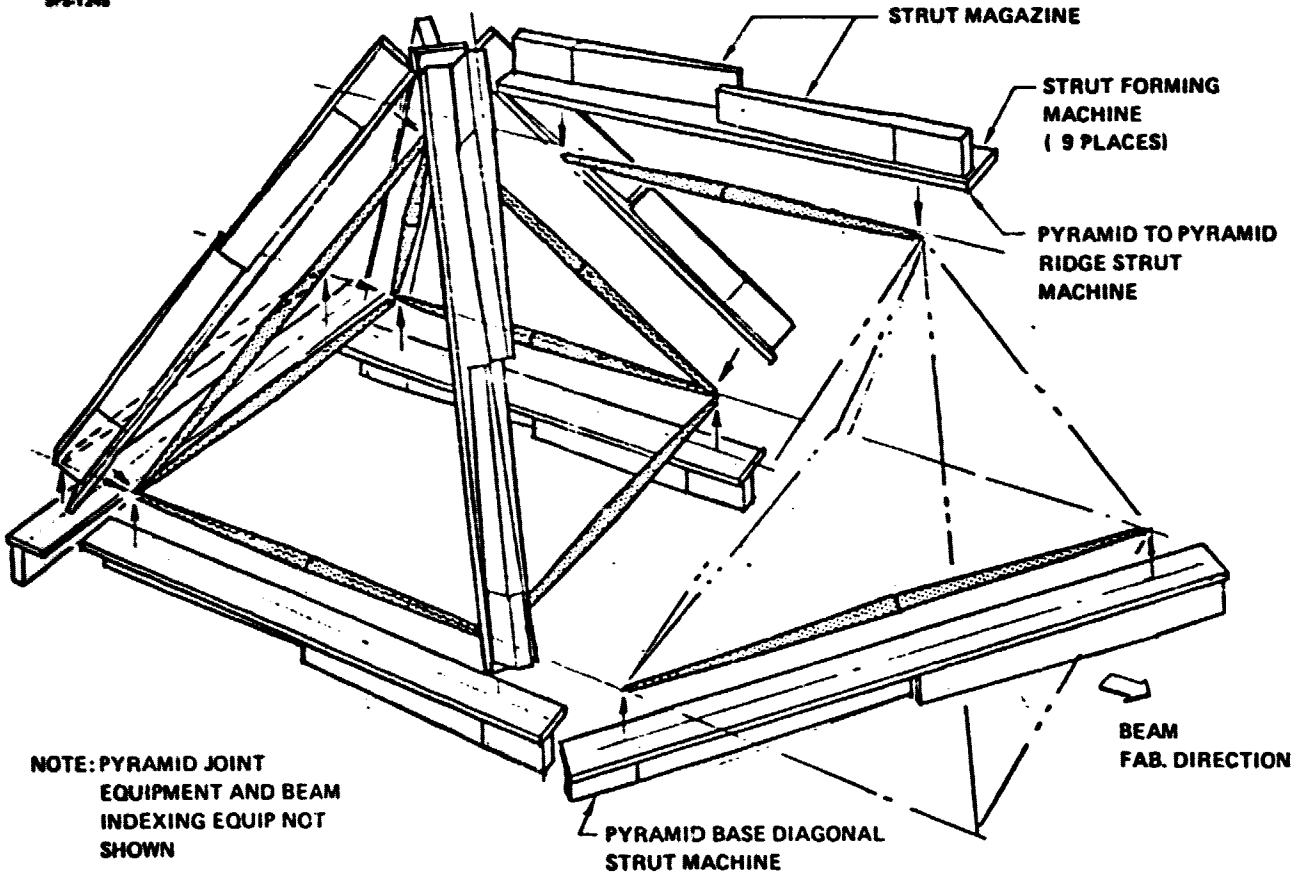


Figure 3.2.4-5 Beam Assembly Concept

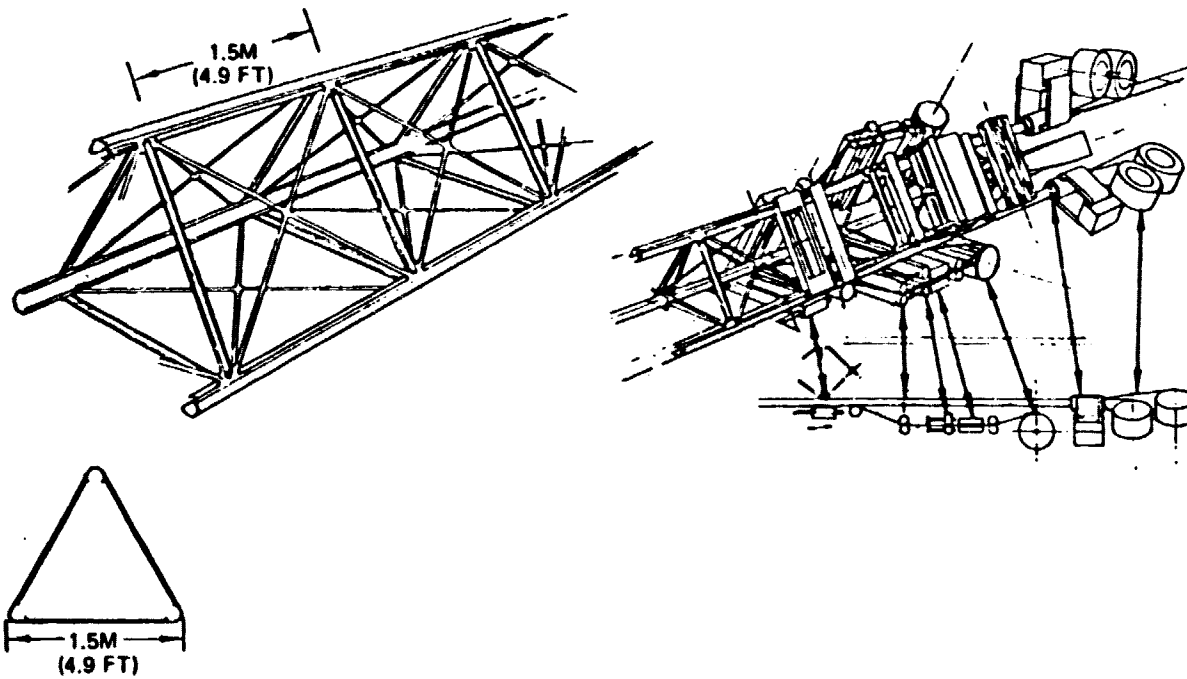


Figure 3.2.4.6 Beam Machine

D180-22876-2

A representative dimension of an SPS hardware element, e.g., a beam section or photovoltaic panel width, is 20 meters (66 feet). The zero-g environment greatly facilitates handling of these large elements; nonetheless, machinery and equipment of an appropriate scale is essential. Building the energy conversion portion of the photovoltaic SPS requires fabrication of structure, installation of solar arrays, installation of switchgear and power conductors, and installation of instrumentation, controls, propulsion and presumably many other items of secondary equipment not yet identified in the SPS designs. An analogous set of tasks has been identified for the thermal engine option: construction tasks are pictorially summarized in Figures 3.2.4-7 and 3.2.4-8.

One could imagine using the satellite structure itself, as it is built, supporting this construction equipment (early construction concepts, in fact, did). Structural and other design impacts on the SPS would presumably result. Also, serious questions are raised as to how the equipment is to be moved, serviced, supplied with power or controlled, and how personnel and SPS hardware are to be moved from receiving stations or crew quarters to work stations. The construction facility allows resolution of all these issues. It provides for conduct of major construction steps in parallel with a minimum of interdependence and interference. It provides support for the SPS while it is being worked on. It allows the various construction machines to operate independently so that a problem or breakdown at one machine need not interfere with the operation of others. Spare (backup) machines can be made available as necessary. The construction facility can be sized to provide enough parallel work areas to achieve the desired production rate, (one SPS per year in the subject studies). Equipped with crew habitats and work stations, transportation handling and bus-ing systems, and an onboard crew and cargo logistics network, the facility becomes an integrated construction base.

LEO Bases

The construction base for the photovoltaic satellite consists of two connecting facilities with one used to build the energy conversion modules and the other to build the antenna, as shown in Figure 3.2.4-9. The module construction facility is an open-ended structure which allows the four-bay-wide module to be constructed with only longitudinal indexing. There are two sets of internal working bays. The aft bays are used for structural assembly using beam machines and joint assembly machines attached to both the upper and lower surfaces of the facility. Solar array and power distribution are primarily installed from equipment attached to the upper facility surface in the forward bays. The satellite module is supported by movable towers located on the lower surface of the facility. These towers are also used to index the module as it is being fabricated.

The antenna facility is configured to enclose four antenna bays in width and four rows of bays in length. The minimum plan-view shape of the facility is obtained through use of a 60 degree parallelogram. This shape results because the basic unit of the primary structure is triangular in shape. The lower surface of the facility is used to support beam machines, joint assembly machines and a deployment platform that is used to deploy the secondary structures and antenna subarrays.

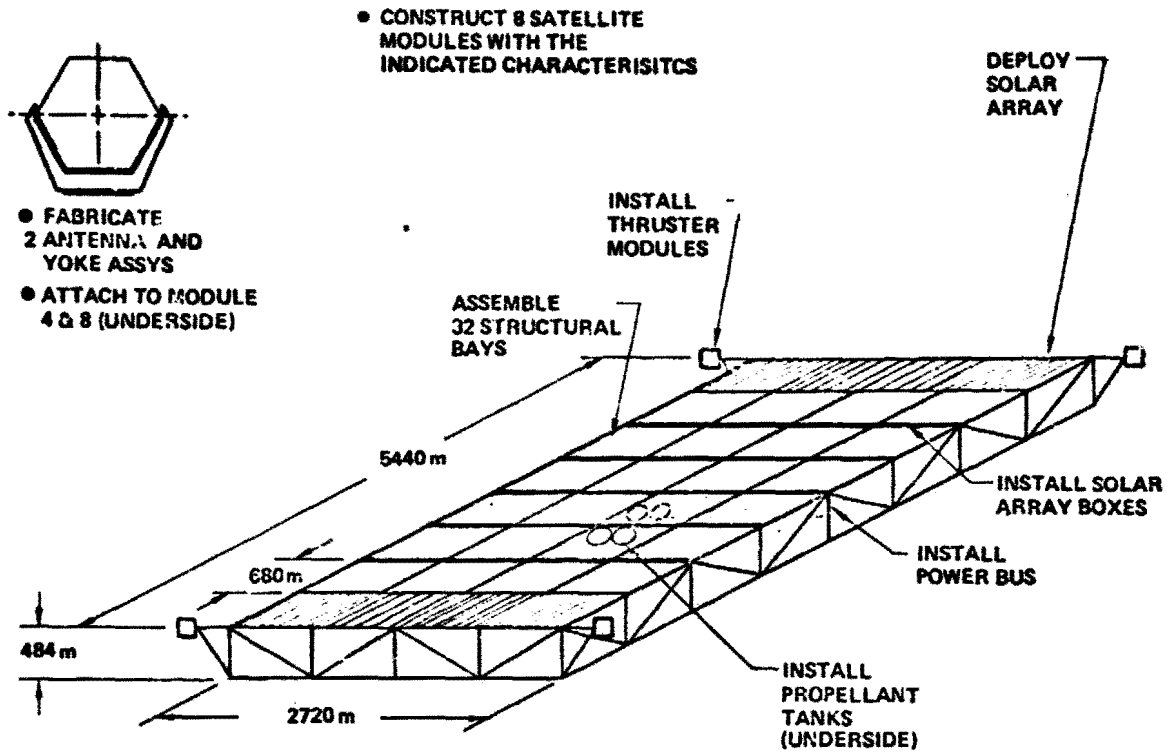


Figure 3.2.4.7 LEO Base Construction Tasks

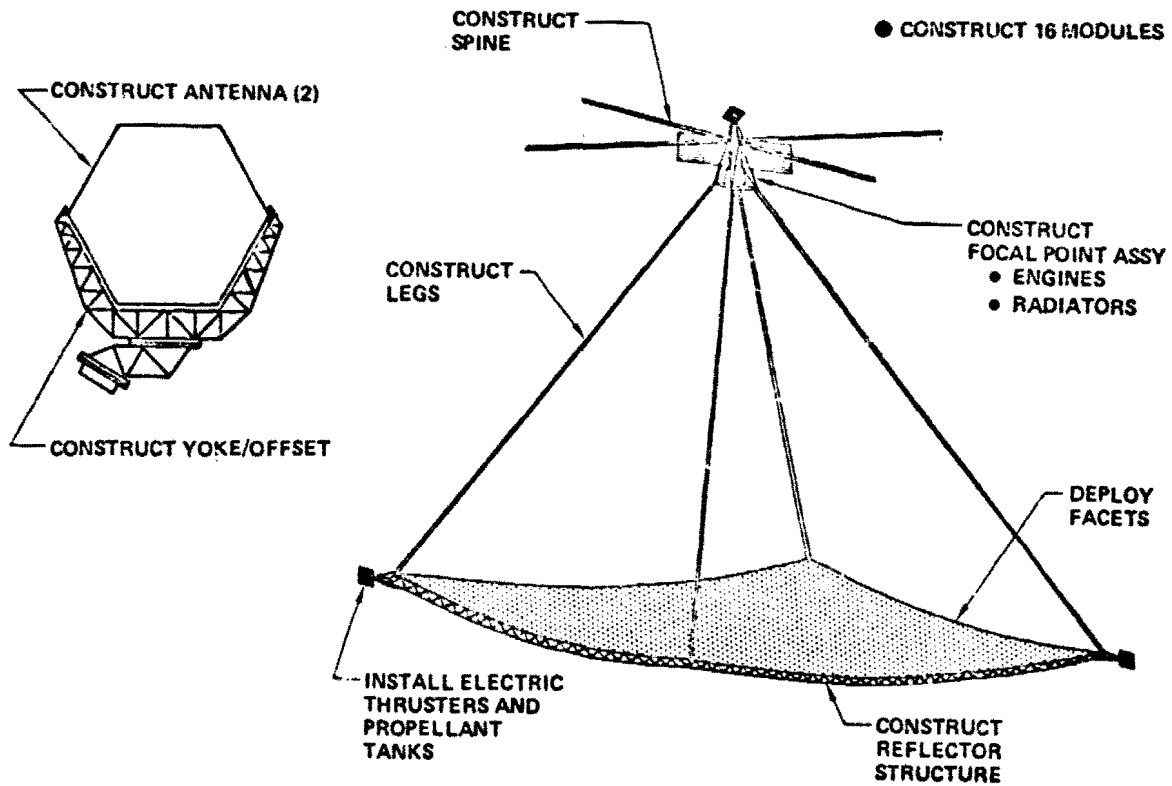


Figure 3.2.4-8 LEO Base Construction Tasks Thermal Engine Satellite

ORIGINAL PAGE IS
OF POOR QUALITY

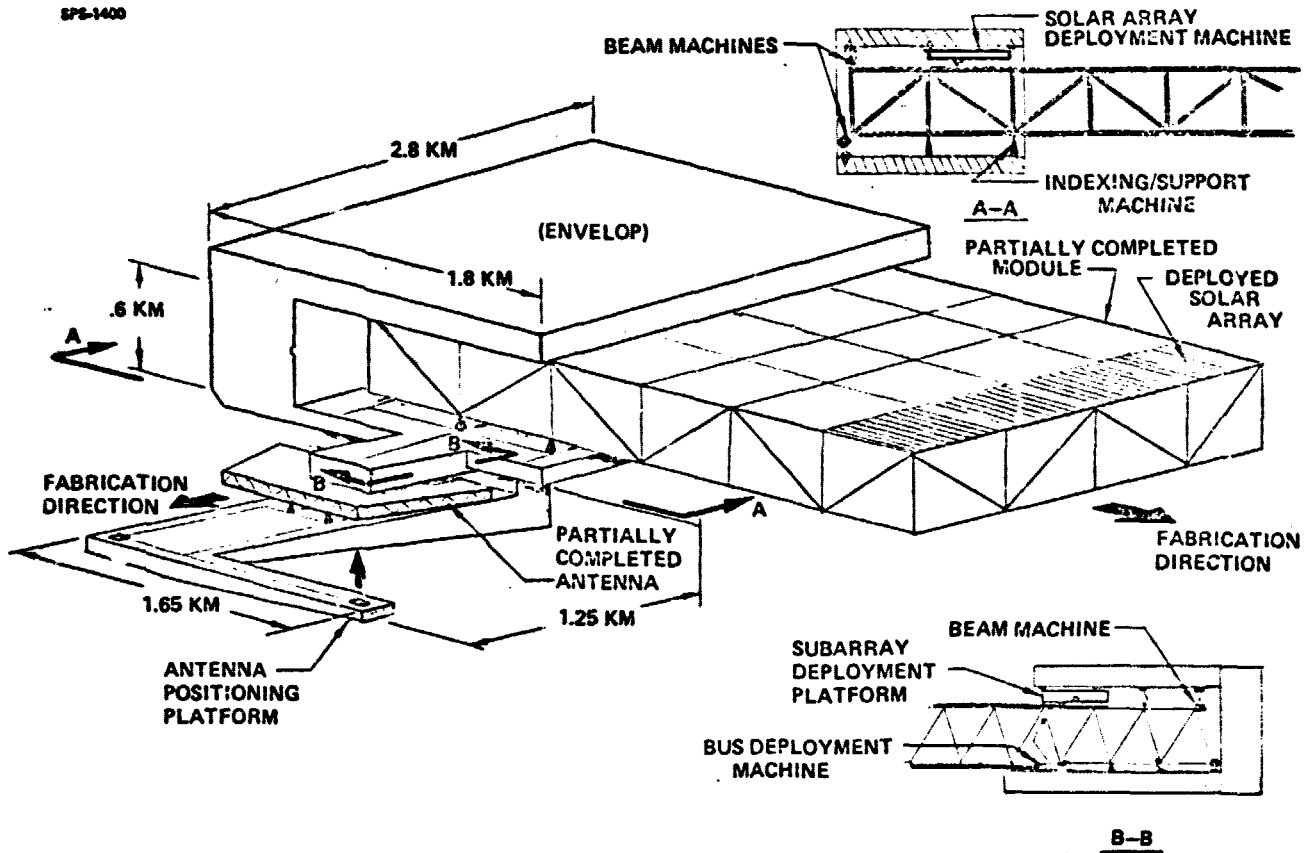


Figure 3.2.4-9. LEO Construction Base Photovoltaic Satellite

D180-22876-2

The thermal engine satellite construction base shown in Figure 3.2.4-10 has been designed to surround the thermal engine satellite module. As a result of the 3-dimensional nature of the thermal engine concentrator, the base exhibits some rather large dimensions. The construction operations are performed in three separate levels or areas of the base. The antenna construction facilities and those provisions necessary to construct the antenna yoke are at the lower level. Immediately above this area is the reflector construction factory which includes equipment necessary to construct reflector structure and install reflecting facets. Deployment of the constructed reflectors is accomplished using indexing devices moving down two side rails. These rails are also used to support beam machines used to construct the four supporting legs between the reflector surface and the focal point. At the upper level of the construction base is located the focal point factory which has the task of constructing the second stage concentrator, cavity, installing the thermal engines, constructing radiators and the spine which serves as the power distribution system. A fourth area, only used in the construction of two modules, is the assembly platform used to form the antenna structure support point for the antenna.

Because the satellites must be transferred from LEO to GEO in modules in order to have adequate attitude control authority, and because the solar cells not needed for transfer power (in the photovoltaic case) should be retained in their shipping boxes for added radiation shielding, several tasks remain to be accomplished at geosynchronous orbit when the modules arrive. These are summarized for the photovoltaic system in Figure 3.2.4-11. Analogous tasks exist for the thermal engine, except that since it is not as sensitive to radiation, all thermal engine equipment is deployed at LEO prior to initiating the transfer. In either case, the crew size for the GEO base is approximately 60.

GEO Bases for GEO Construction

The GEO construction base has also been sized to construct a satellite in one year and consequently is of the same overall size as the LEO construction base. The photovoltaic GEO base and its support LEO base are illustrated in Figure 3.2.4-12.

Indexing the satellite construction facility in two directions rather than one is required. This has been judged to be more cost effective than having a full width facility and additional construction equipment with the equipment idle half of the time. The mass difference for the GEO construction base, compared to the base for LEO construction, primarily reflects the additional mass required for crew shielding protection against solar flares. Other significant differences in the GEO construction base are the outriggers on the satellite facility to allow lateral direction indexing in addition to the movement of the antenna facility from one end of the satellite to the other.

The staging depot located in LEO in this construction option is sized to support the construction of one satellite per year, and accordingly requires one SPS component OI flight per day, based on a five day a week launch and flight schedule. As such, the depot must provide accommodations for three launch vehicle payloads: the SPS components and two propellant tankers used to refuel the

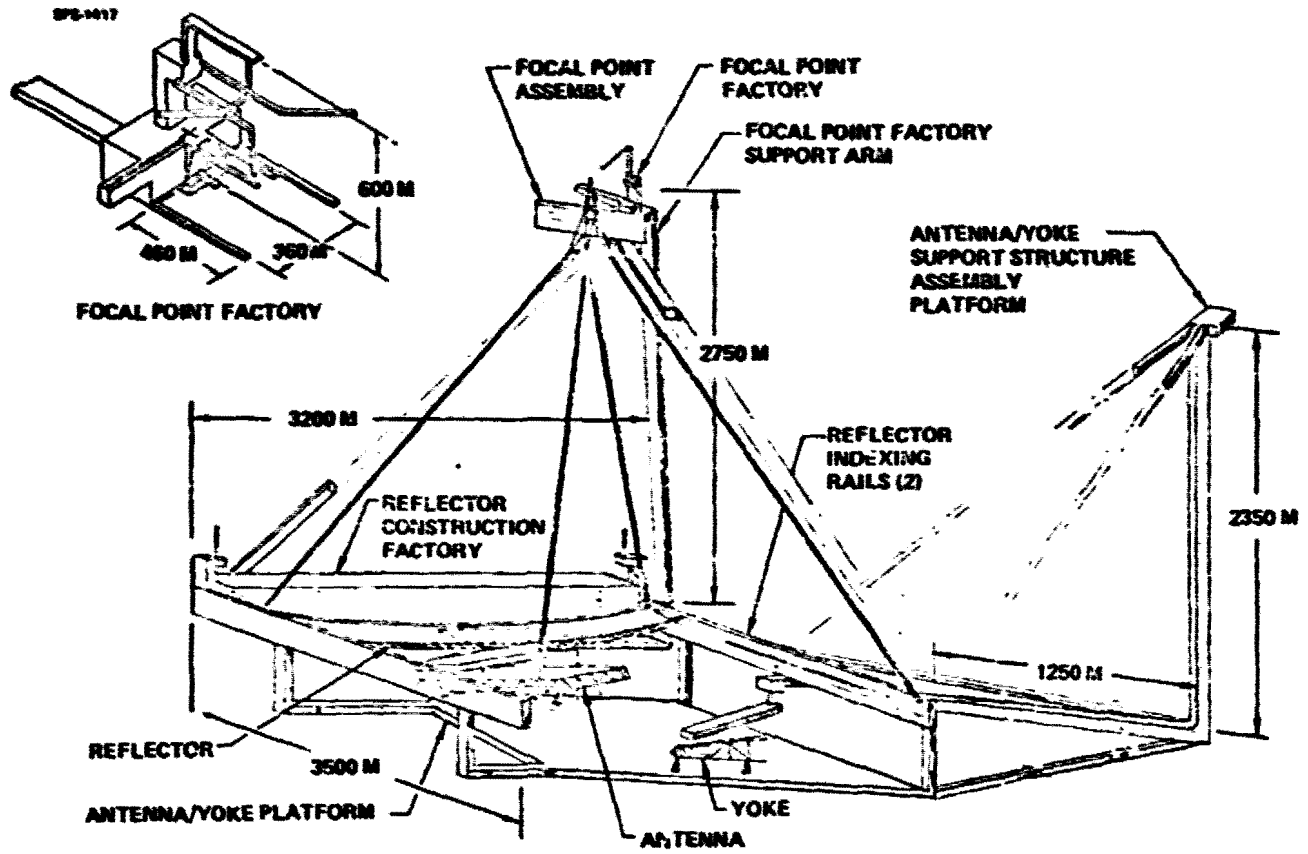


Figure 3.2.4-10 LEO Construction Base Thermal Engine Satellite

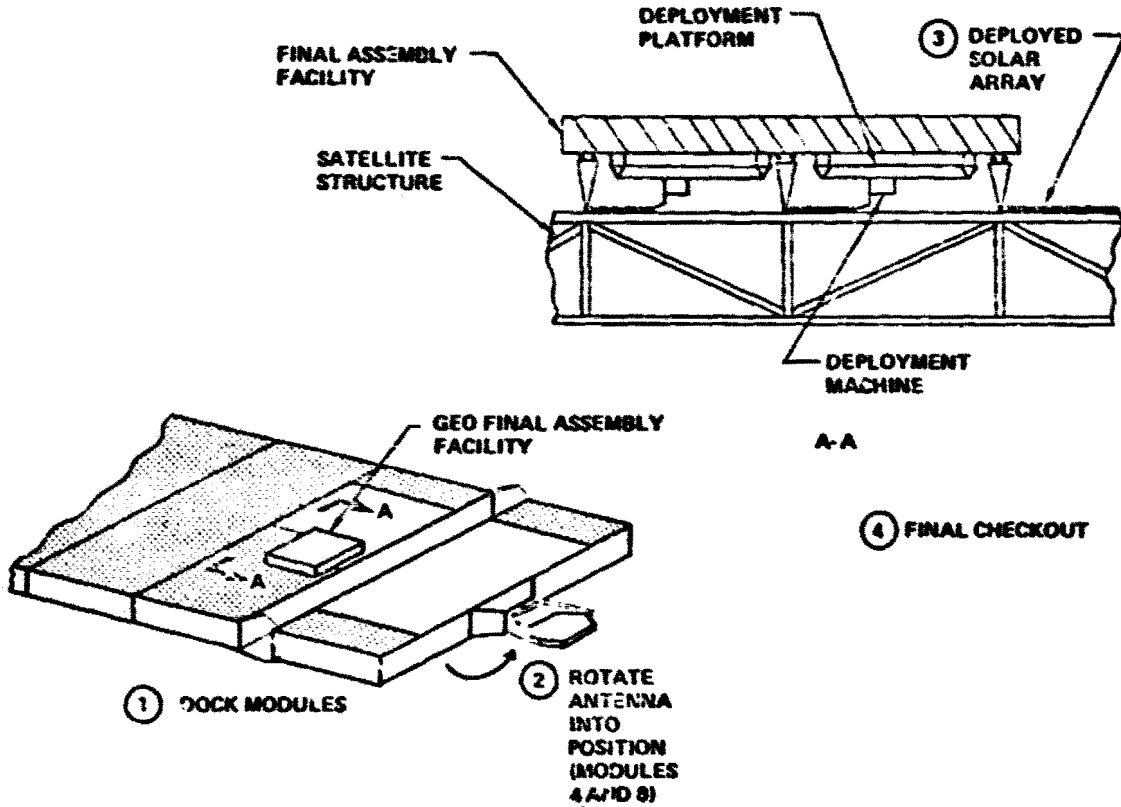


Figure 3.2.4-11 GEO Base Construction Tasks

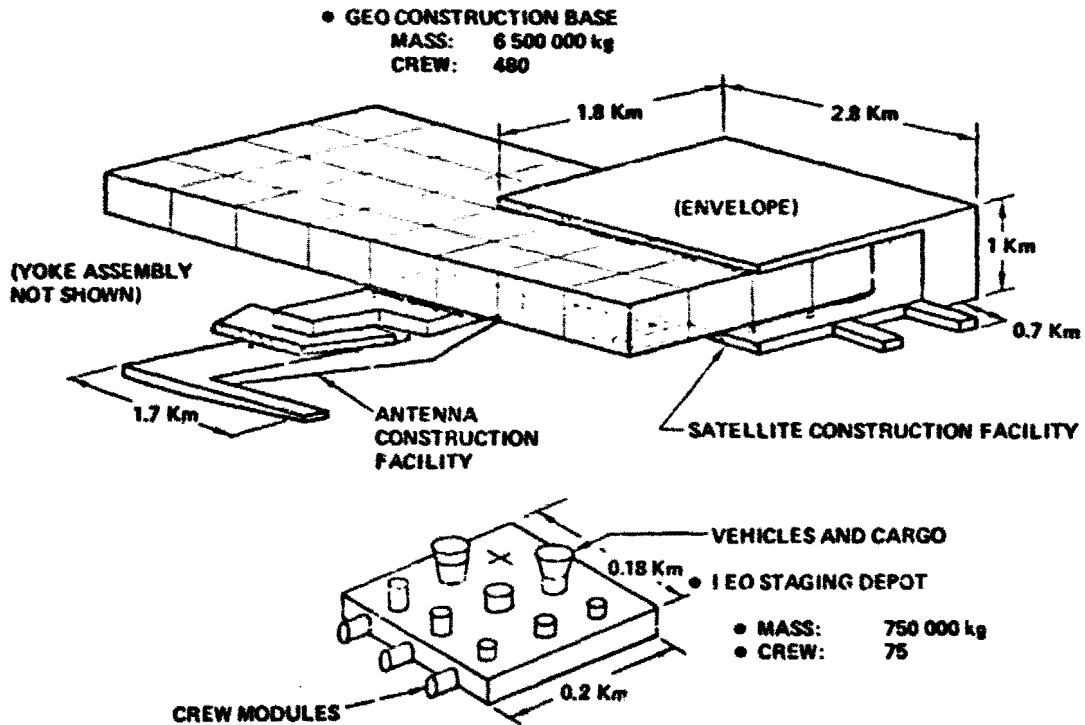


Figure 3.2.4-12 Orbital Bases GEO Construction

orbit transfer vehicles. Since the orbit transfer vehicle propellant loading requires slightly more propellant than can be provided by two tankers, a storage tank is also provided at the staging depot and is refueled every fourth OTV flight. Other docking accommodations are provided for a dedicated OTV used for GEO crew rotation/resupply on a once per month basis. This operation also requires docking for supply modules and crew transfer vehicles. The operational crew size for the staging depot is 75. They can be accommodated in one module similar to the crew modules used in the GEO construction base. A transient crew quarters module is also provided to accommodate the 160 personnel rotated with each crew flight to the GEO base. A maintenance module is included at this base for repair work on the transportation systems and base equipment.

3.2.4.5 Construction Equipment

The major construction equipment items associated with the photovoltaic satellite are illustrated in Figure 3.2.4-13 and Figure 3.2.4-14, along with key characteristics such as quantity, mass and dimensions. The beam machine shown is configured to allow two beam machines to form all the main structure. Accordingly, it has both translation and rotational capability. The dimensions and mass indicated are for the segmented beam approach although machines fabricating thermally formed continuous chord structure could be attached to the same frame and used in a similar manner.

Crane/manipulator systems are primarily used to form the structural beam joints. Although the size shown is most common, several 250 meter units are also required in the construction of the antenna yoke as well as several 20 meter cranes. Two-man control cabins with manipulators are located at the end of the crane which is itself attached to a moving platform.

The principal difference between the solar array deployment machine described here and those illustrated in previous documents is that the gantry itself is located approximately 50 meters below the facility beams since that is the location of the upper surface of the satellite.

The most significant unique piece of equipment used for antenna construction is the subarray installer shown in Figure 3.2.4-14. Long-boom manipulators are used to string the power leads from the power processors through the antenna structure to the subarrays.

Construction equipment requirements were also determined for the thermal engine option and are described in Volume V of this report. Because of the greater complexity of the thermal engine, about twice as many kinds of equipment are needed.

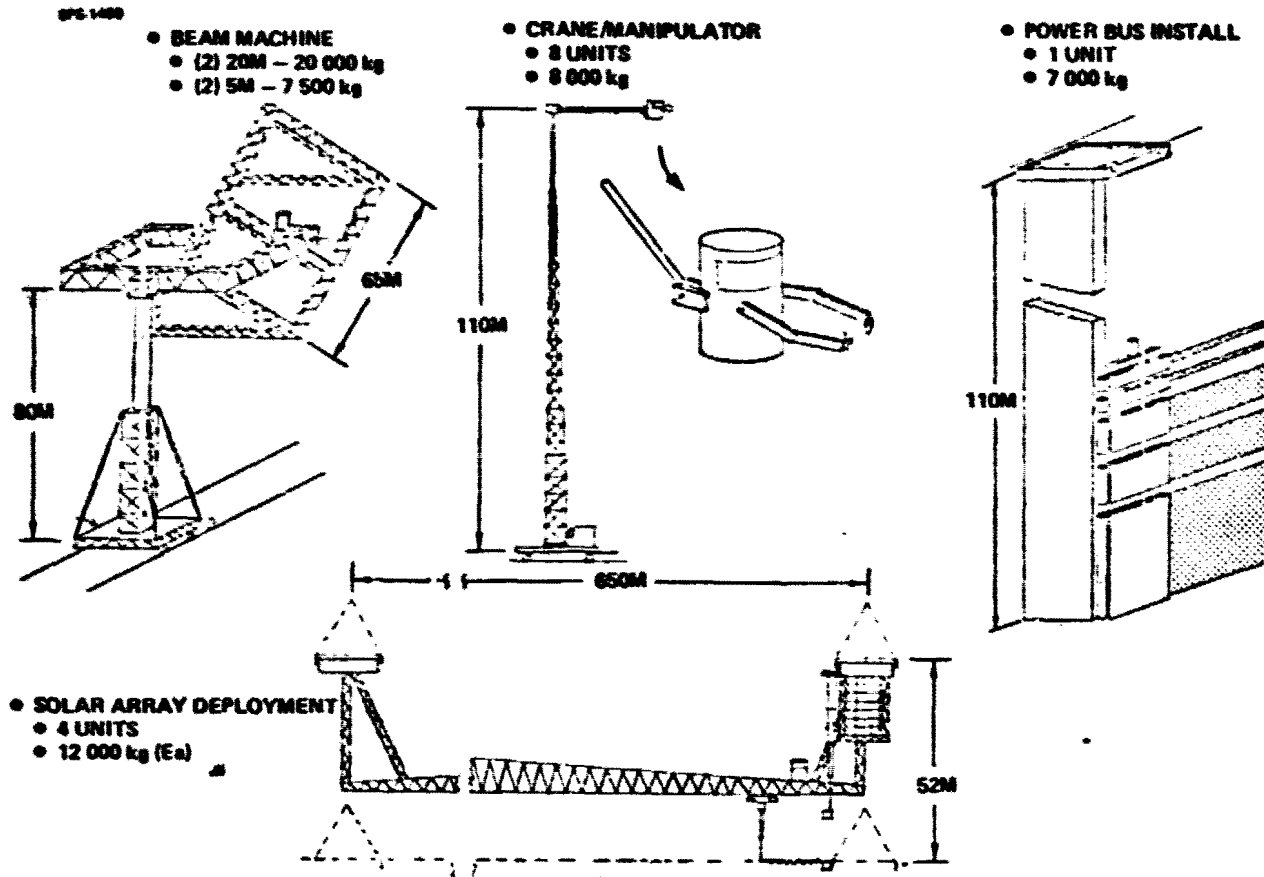


Figure 3.2.4-13 Major Construction Equipment Photovoltaic Satellite

SPS-1099

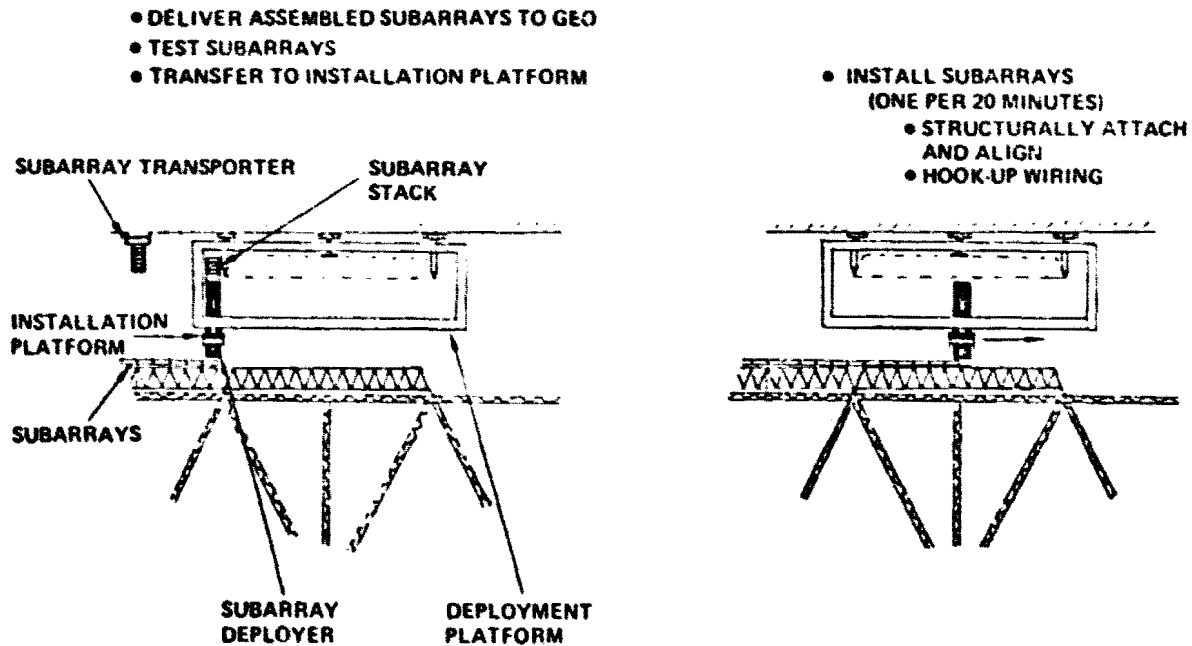


Figure 3.2.4-14 Antenna Subarray Installation Construction Operations

3.2.4.6 Representative Construction Sequence

The photovoltaic LEO construction sequence is presented here. Sequences for all four options (LEO and GEO, photovoltaic and thermal engine) were developed and are presented in Volume V of this report.

The module construction sequence for the structure, solar array and power buses begins with building the first end frame of the structure. This completed end frame is indexed forward one structural bay length. Machines can then form the remainder of the structure in each of the bays. The first row of four bays is then indexed forward to allow construction of the fifth structural bay in parallel with installation of solar arrays in bay 1 through 4. This sequence is shown in Figure 3.2.4-15. Solar array installation and construction of structure occurs simultaneously across the width of the module, although neither operation depends on the other. At the completion of the 16 bays (four rows of bays in length) the power buses and propellant tanks are installed. Construction of the structure and installation of solar arrays of the remaining four bay lengths of the module are done in a similar manner to that previously described. Thruster modules for the self-power system are attached to each of the four corners of the module.

Construction of the antenna takes place in parallel with module construction. The first antenna is completed during construction of the fourth module; the second antenna is completed with the eighth module.

As shown in Figure 3.2.4-16 the yoke for the antenna is constructed in the module construction facility because of its large dimensions. This requires the yoke to be made between the third and fourth module and between the seventh and eighth modules. Following yoke construction, it is moved to the side of the module facility. At that time either the fourth or the eighth module will be constructed. During the construction of these modules, the antenna is completed so that it can then be attached to the yoke. After five bays of either the fourth or eighth module have been completed, the antenna/yoke combination can then be attached to the module in its required location. Construction of two more rows of bays pushes the antenna outside the facility where it then can be hinged under the module for its transfer to GEO.

The first operation to occur once the modules reach GEO is that of the berthing (or docking) of the modules. In the case of the photovoltaic satellite, the modules are berthed along a single edge as indicated in Figure 3.2.4-17. The major equipment used to perform these berthing operations are shown. The concept employs the use of four docking systems with each involving a crane and three control cables. Variations in the applied tension to the cables allows the modules to be pulled in, provide stopping control and provides attitude control capability. Also required in this concept is an attitude control system involving thrusters which are not shown.

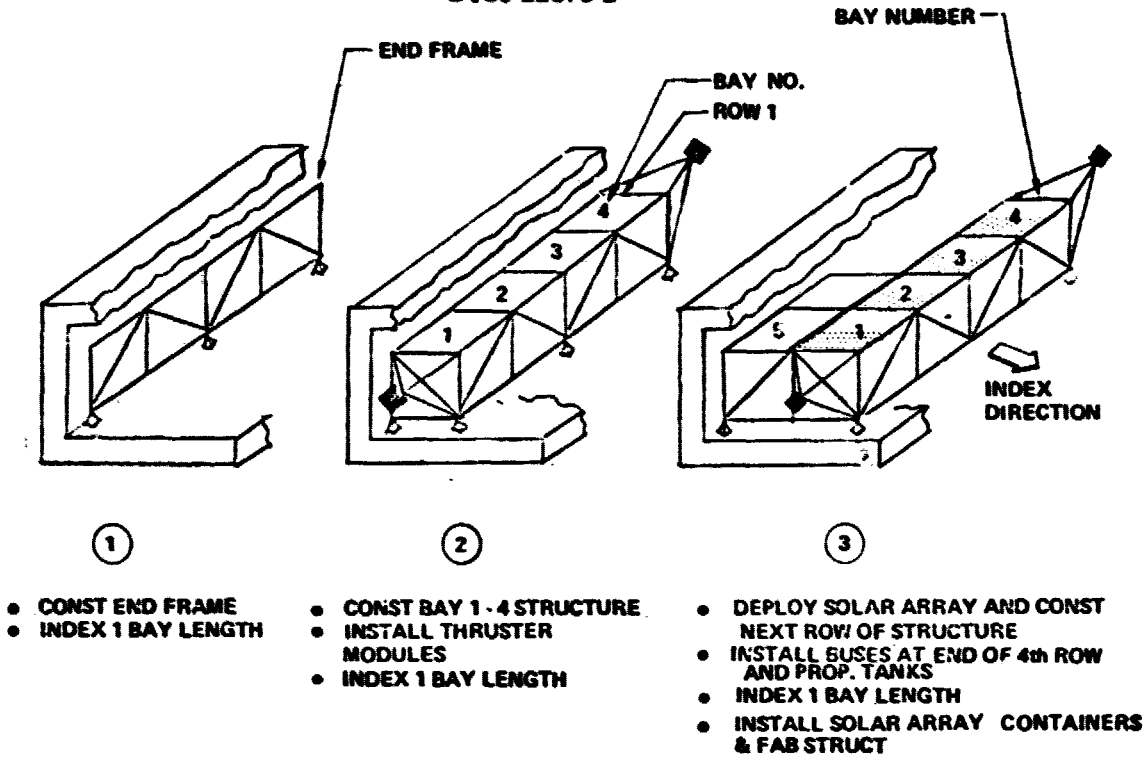


Figure 3.2.4-15 Module Construction Sequence Photovoltaic Satellite

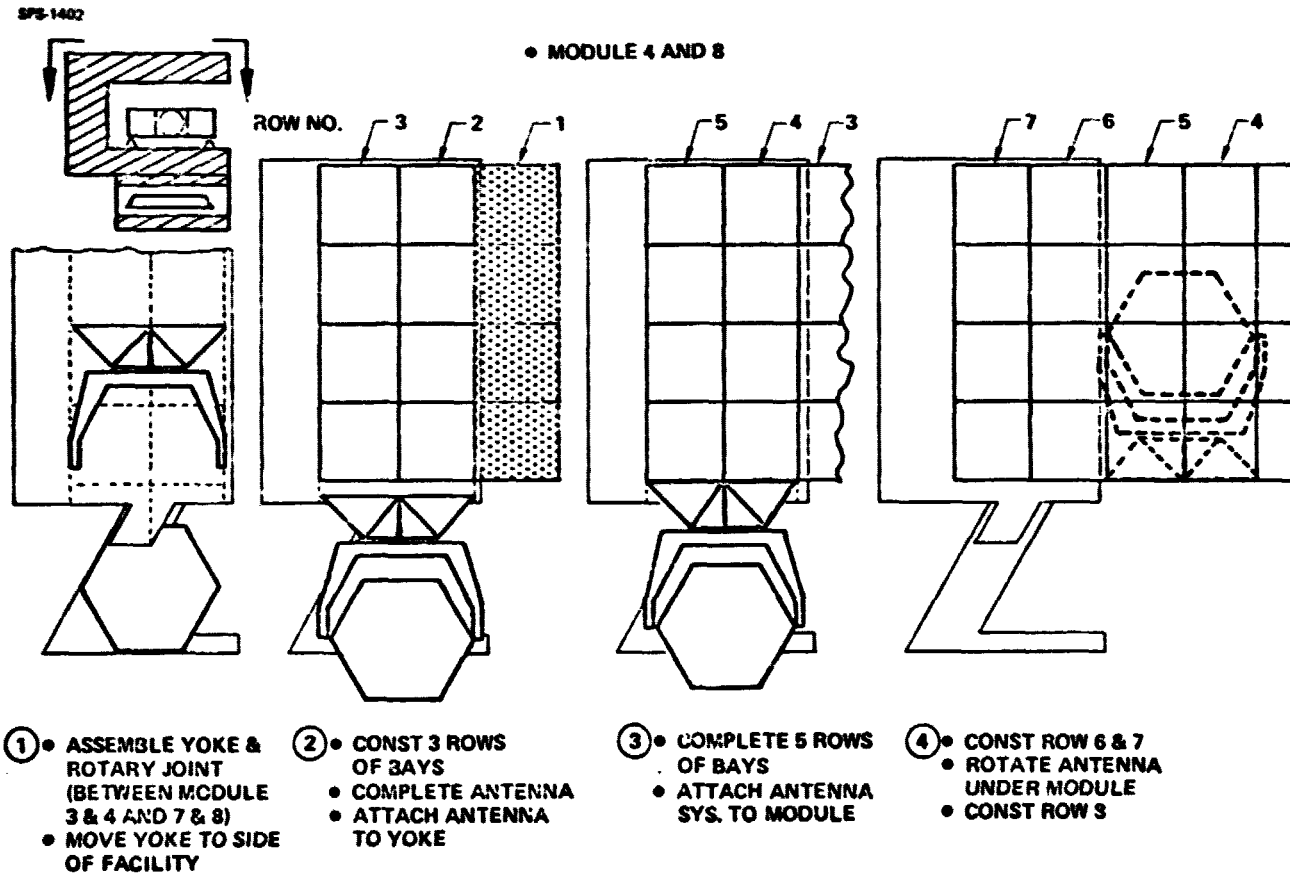


Figure 3.2.4-16 Antenna/Yoke/Module Assembly Photovoltaic Satellite

SP-002

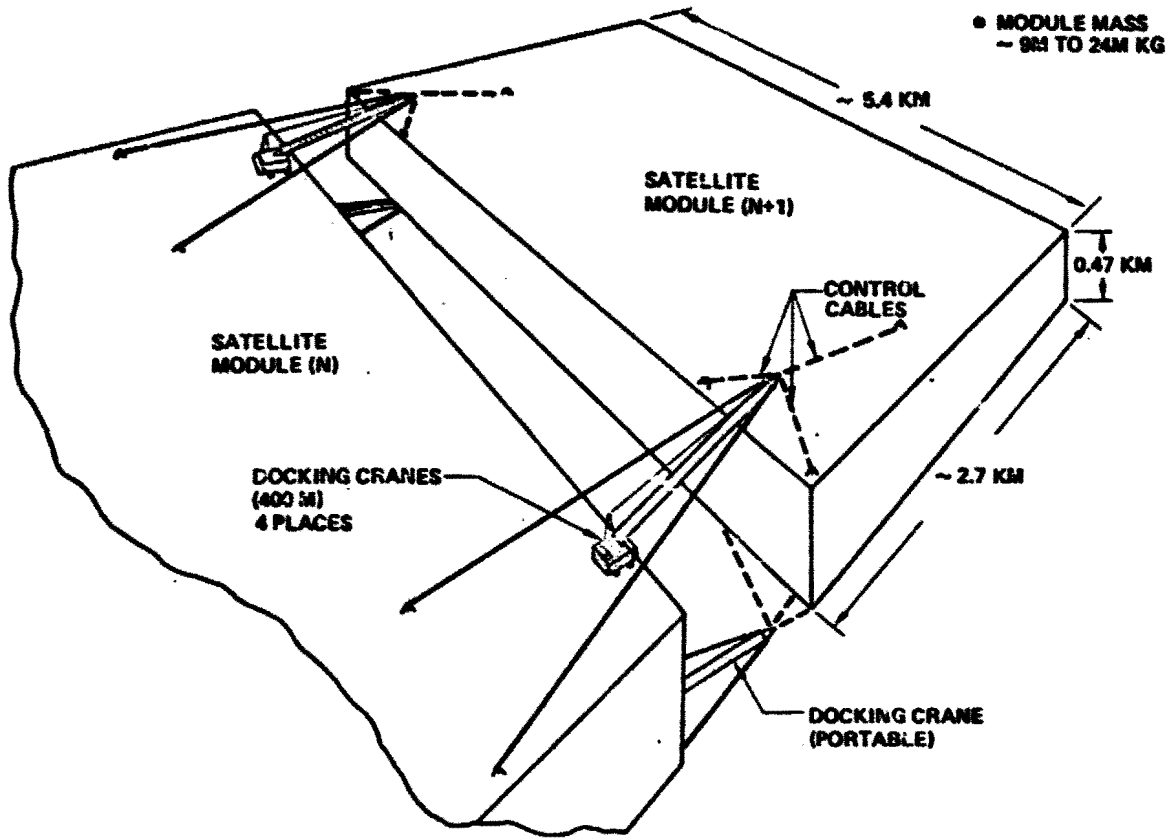


Figure 3.2.4-17 GEO Berthing Concept Photovoltaic Satellite

In its shipment position the antenna is attached below the module with a single hinge line. Once GEO is reached, the antenna is rotated into position followed by the final structural and electrical connections, as indicated by Figure 3.2.4-18.

The overall integrated construction and transportation timeline for this sequence is given in Figure 3.2.4-19. Detailed supporting timelines are presented in Volume V of this report.

3.2.4.7 SPS Options Construction Comparison

The difference in crew size and distribution of crew is compared in Figure 3.2.4-20 for the two satellite concepts. The photovoltaic satellite requires approximately 300 fewer crew, with all this difference occurring in the low Earth orbit construction base. The reason for the larger crew requirements for the thermal engine satellite is the more complex construction operations. This contributes to the construction indirect personnel and support personnel manloadings.

There are no significant differences in crew size between LEO and GEO construction. The difference is in the location of the majority of crew reflecting in differences in transportation requirements.

Figure 3.2.4-21 presents ROM mass estimates for the construction bases as well as crew rotation/resupply comparing the photovoltaic and thermal engine options. In the case of the LEO construction bases, the photovoltaic satellite base is lighter by approximately 3 million kilograms. The major contributors to the greater mass of the thermal engine construction base are the large foundation (structure) along with three extra crew modules for the 300 additional people and, as previously described, additional construction equipment. The GEO final assembly bases are approximately equal. Differences in the annual crew rotation resupply requirements reflects the 300 difference in crew size. Base mass differences between LEO and GEO construction are not significant although the locations result in significant differences for transportation.

The comparison of the unit cost of the first set of construction bases in Figure 3.2.4-22 indicates over a 4 billion, dollar savings for the photovoltaic satellite. These values include a 90% learning factor applied to each major end item. (Transportation costs are not included.) The principal difference in the facility cost is the three extra crew modules and the large difference in construction equipment quantity. The differences in construction base cost and crew size were one of the significant factors in the determination that the photovoltaic system represents the preferred SPS concept.

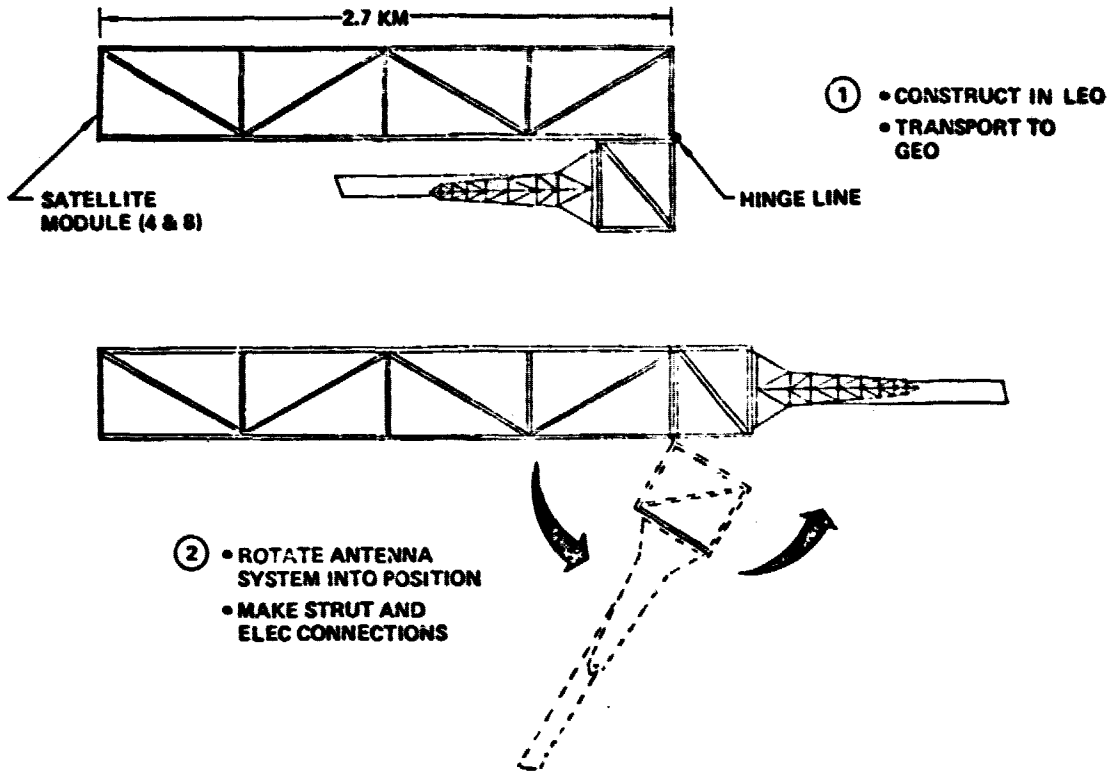


Figure 3.2.4-18 Antenna Final Installation Photovoltaic Satellite

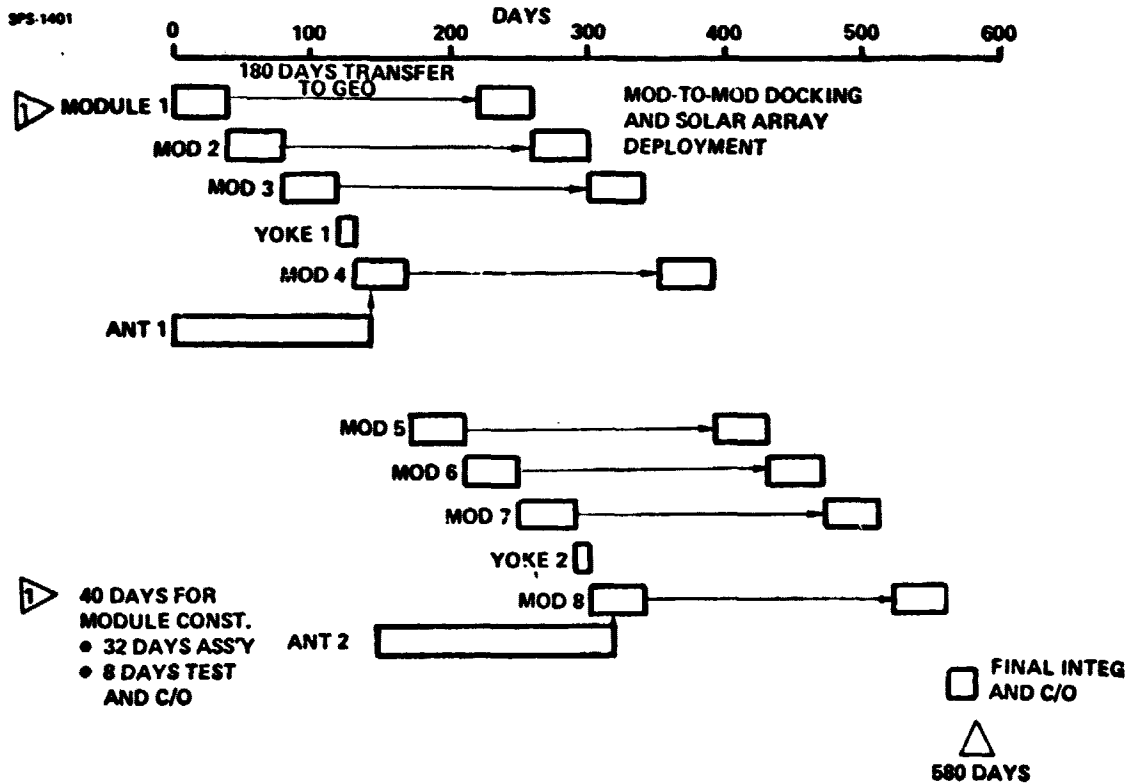


Figure 3.2.4-19 Photovoltaic Satellite LEO Construction Timeline

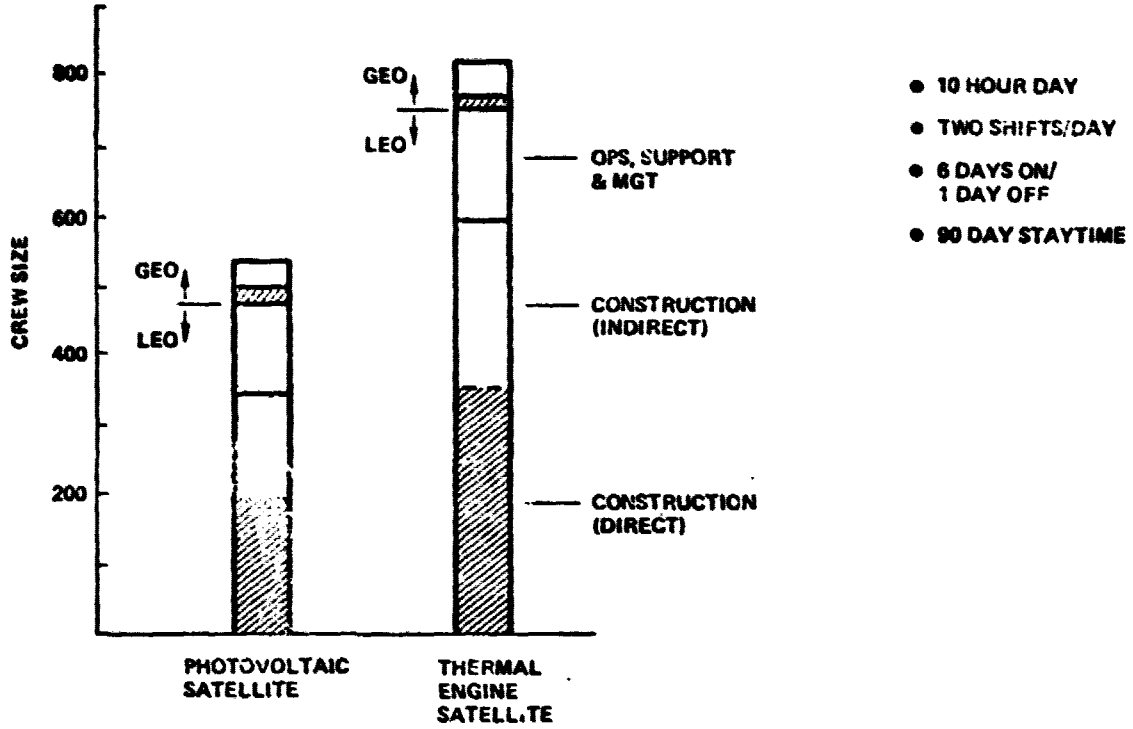


Figure 3.2.4-20 Crew Size and Distribution LEO Construction

● LEO CONSTRUCTION

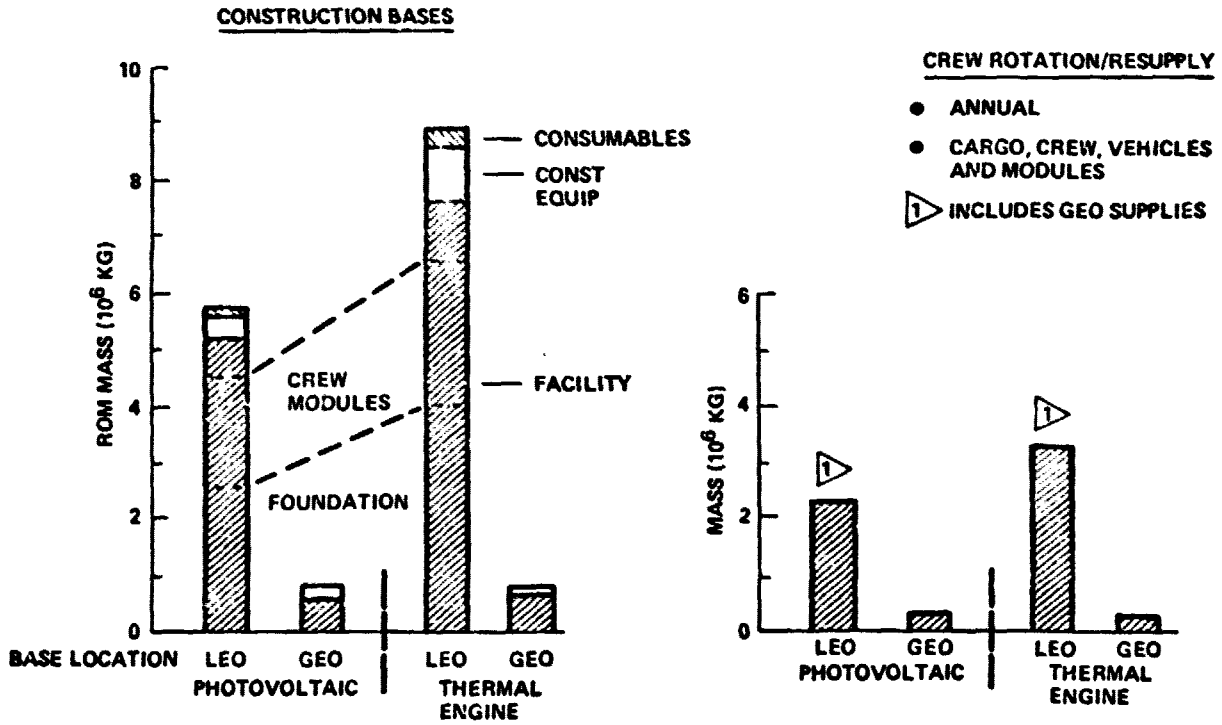


Figure 3.2.4-21 Construction Mass Summary

SPS-1000

- 1 SATELLITE PER YEAR
- 90% LEARNING

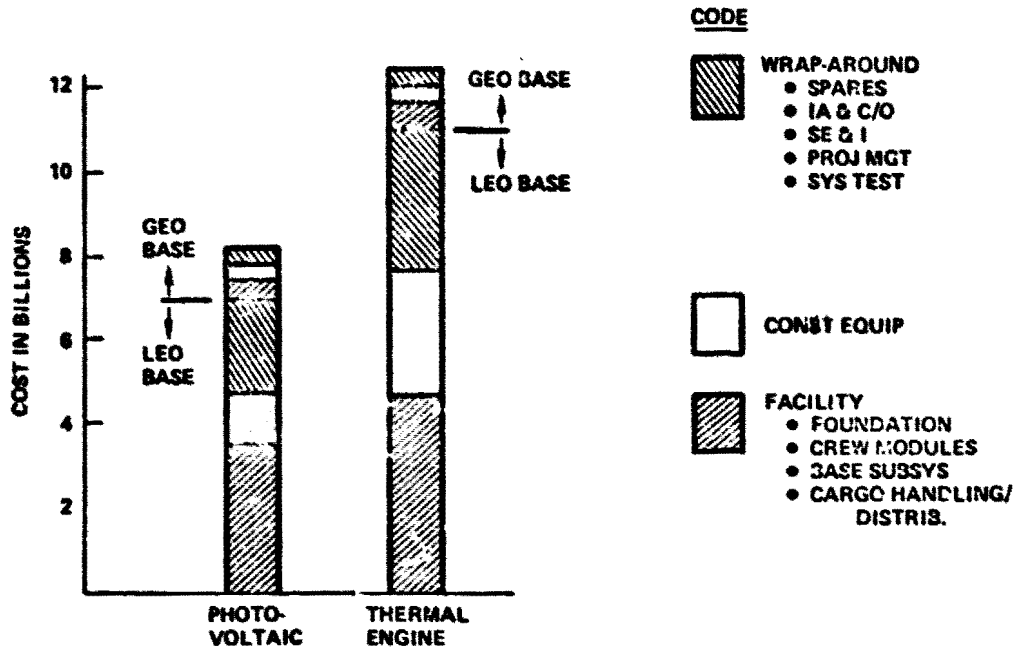


Figure 3.2.4-22 Construction Base ROM Cost First Set

3.2.4.8 Transportation Systems Background

Some of the earliest studies of SPS's assumed that the space shuttle would be the primary means of transportation to low Earth orbit. These early studies were more or less concurrent with studies of two-staged fully reusable shuttles then predicted to deliver payloads to orbit (on a shuttle traffic model) at about \$220/kg (\$100/lb). Costs to GEO would have fallen in the \$660-\$880/kg (\$300-\$400/lb) range. At these high transportation costs (take \$800/kg as representative) SPS's could have no more mass than 1.25 kg/kw_e to bring the transportation cost even as low as \$1000/kw_e. This is just about the figure quoted for SPS's by the early studies; it was necessary to invoke advanced technology or optimistic design assumptions to offer any hope of achieving masses this low.

This was, in effect, placing all of the burden of technology advance on the SPS, assuming that the space shuttle, designed for a very different job, would be the best space transportation available to an SPS program.

In 1974, during the early phases of the Future Space Transportation Systems Analysis Study sponsored by JSC, estimates were made that with a more plausible SPS technology, transportation costs would need to be as low as \$45/kg (\$20/lb) to make SPS's economically feasible. It was also recognized that an SPS traffic model would represent at least 100 times the annual payload to low Earth orbit extant in the then current 60 flights/year shuttle traffic model. An investigation of design trends by D. Gregory quickly indicated that vehicles aimed at such a market would be larger, fully reusable, would emphasize payload delivery with little or no return capability, and would not have too much difficulty attaining the \$45/kg target.

Subsequently, the Heavy Lift Launch Vehicles study, sponsored by JSC and later managed by MSFC, confirmed these results, predicting \$33/kg (\$15/lb) for the vehicle depicted in Figure 3.2.4-23. Subsequent more detailed operations analyses, under a continuation of the same study, confirmed this figure. During this time (circa 1976) it was believed that SPS payloads would be very low in density, as low as 20 kg/m³. Accordingly, the vehicle illustrated had a large expendable shroud. The shroud, which had to be replaced for each flight, contributed \$3.8 million to the cost of each flight

As payload packaging and packaging density analyses evolved during the current study, an average payload density of 75 kg/m³ appeared achievable through mixing of different payload types. This increase was largely due to the increase in structural density afforded by beam machines.

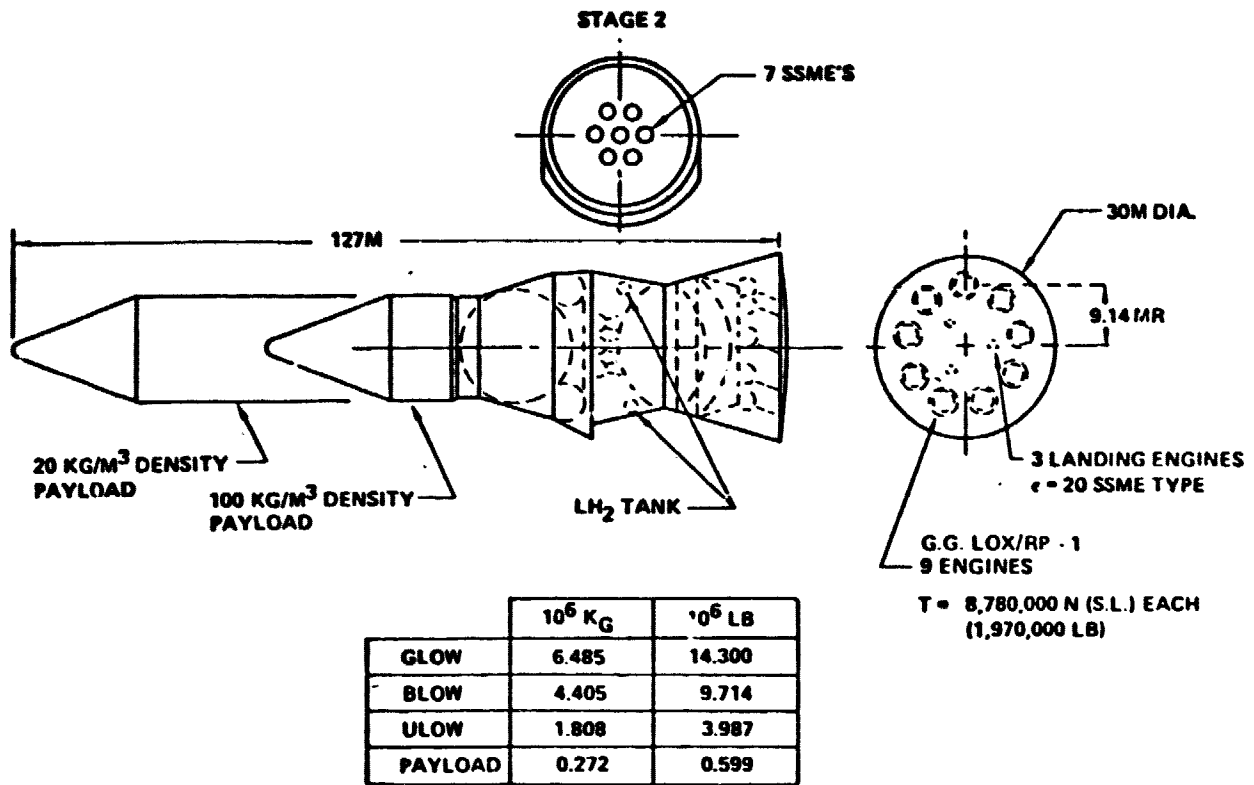


Figure 3.2.4-23 HLLV Two-Stage Configuration

3.2.4.9 Transportation Requirements Summary

As a part of the current study, a significant effort was made to understand and document SPS transportation requirements. The results were presented in Volume IV of the Part I report. A synopsis of those requirements most important to vehicle design and selection follows:

Cargo Launch Vehicles (Heavy Lift Launch Vehicles, HLLV's)

These vehicles have the primary function of delivering heavy cargo to low Earth orbit. Most of this cargo will be SPS hardware and orbit transfer propellant. Low cost per unit payload mass delivered to low Earth orbit is an overriding requirement. The following general vehicle requirements were identified:

- Recurring cost should be minimized. Accordingly, the vehicles should be completely reusable, with a design life of at least 300 flights, capable of fast recycle after use, employ low-cost propellants and minimize propellant energy consumption.
- A large payload volume capability should be provided. A payload density of 75 kg/m³ is needed to allow mass-limited launch operations.
- Large payload mass is desirable. Vehicles in the range 100 to 400 (metric) tons payload capability were studied. The high end of this range is desirable for a mature program; the smaller vehicles may be adequate in a developmental or early commercial phase.
- Vehicles and their launch facilities should be capable of sustaining high launch rates, reaching about 10 flights per day after several years' operations and should allow salvo launches of two to five vehicles at roughly 1-minute intervals.
- The upper stage of the vehicle (or the entire vehicle, if a single-stage system) should be capable of flying to an operation base in low earth orbit to deliver its payload. Payloads will be palletized. A change of the launch vehicle from payload configuration to tanker configuration should be possible at the launch site without major disruption of launch processing operations.
- The design reference launch site is KSC. The design reference orbit is 478 km altitude at 31° inclination.
- The vehicle should be designed for minimum environmental impact. This includes (1) selection of propellants, engine cycles and flight profiles that minimize atmosphere pollution and (2) remote launch and recovery operations to the degree necessary to control noise.
- In the event of an abort, recovery of the vehicle is given priority over recovery of the payload.

- The vehicles should have a return payload capability of roughly 10% of delivery capability to allow for return of empty tankers and payload pallets.

Personnel Launch Vehicles:

The personnel launch vehicle was assumed to be an updated shuttle with the payload bay converted to be capable of carrying 75 passengers. A liquid booster was assumed to replace the solids to reduce cost per flight and atmosphere pollution.

Orbit Transfer Vehicles

Orbit transfer vehicles (OTV's) serve to transfer crews and cargo between low earth orbit and geosynchronous orbit. Orbit transfer vehicle requirements are summarized as follows:

- Low cost is paramount. Accordingly, the orbit transfer vehicle should use liquid oxygen and liquid hydrogen as propellants, should be completely reusable, should be staged to improve efficiency, should permit fast turnaround, and should be capable of at least 50 reuses.
- Space-basing is desirable. The vehicle should be designed for efficient on-orbit propellant transfer from tanker. Services such as propellant transfer pumping may be provided by an operations base.
- Mission duration capability should be a minimum of 7 days.
- It should be a design goal to eliminate all fluids requirements except LO_2 and LH_2 , in order to simplify on-orbit servicing.
- The OTV should be matched to the cargo launch vehicle in the sense of having the capability to deliver an entire cargo payload to GEO without repacking at the LEO base. No cargo return payload is required for this mission case.
- For crew rotation missions, a crew module will be provided as a payload for the OTV. Round trip capability is required for this payload.
- The OTV shall be designed for crew safety. The OTV flight profile shall avoid, even as a transient condition, state vectors that do not represent a stable earth orbit from which a rescue can be accomplished.

Electric Propulsion Orbit Transfer System

The study indicated that minimum SPS system cost could be realized if SPS modules are constructed in low earth orbit and transferred to GEO under their own power using electric propulsion. Electric propulsion hardware must be fitted to the modules for this purpose. General requirements are as follows:

D180-22876-2

- **Low cost is paramount. Therefore the electric propulsion hardware should be efficient (to minimize power consumption and resultant design scar on the SPS modules). It may be desirable to avoid the necessity for return of the electric propulsion hardware to low earth orbit for reuse. Therefore, this hardware should be designed for low production cost and minimum consumption of critical materials.**
- **The propellant should be plentiful and non-polluting, e.g. argon.**
- **The thrusting system should be capable of large gimbal angles as required by flight control.**
- **The system shall provide power processing as necessary to minimize total cost, including design/mass scars on the SPS modules.**
- **The system shall provide chemical thrust capability (total impulse and thrust level TBD) as necessary to control SPS module attitude when module power is not available. Up to 90 minutes chemical thrust operation shall be possible without module power.**
- **The system Isp shall be selected for minimum overall SPS cost. Depending on SPS characteristics, Isp's in the range 2500 sec to 7500 sec may be desired.**
- **The system shall be capable of at least 5000 hours operation without entering the wearout regime of failures.**
- **The system shall provide its own services, e.g. thermal control, drawing only unprocessed power and possibly control signals from the SPS module.**

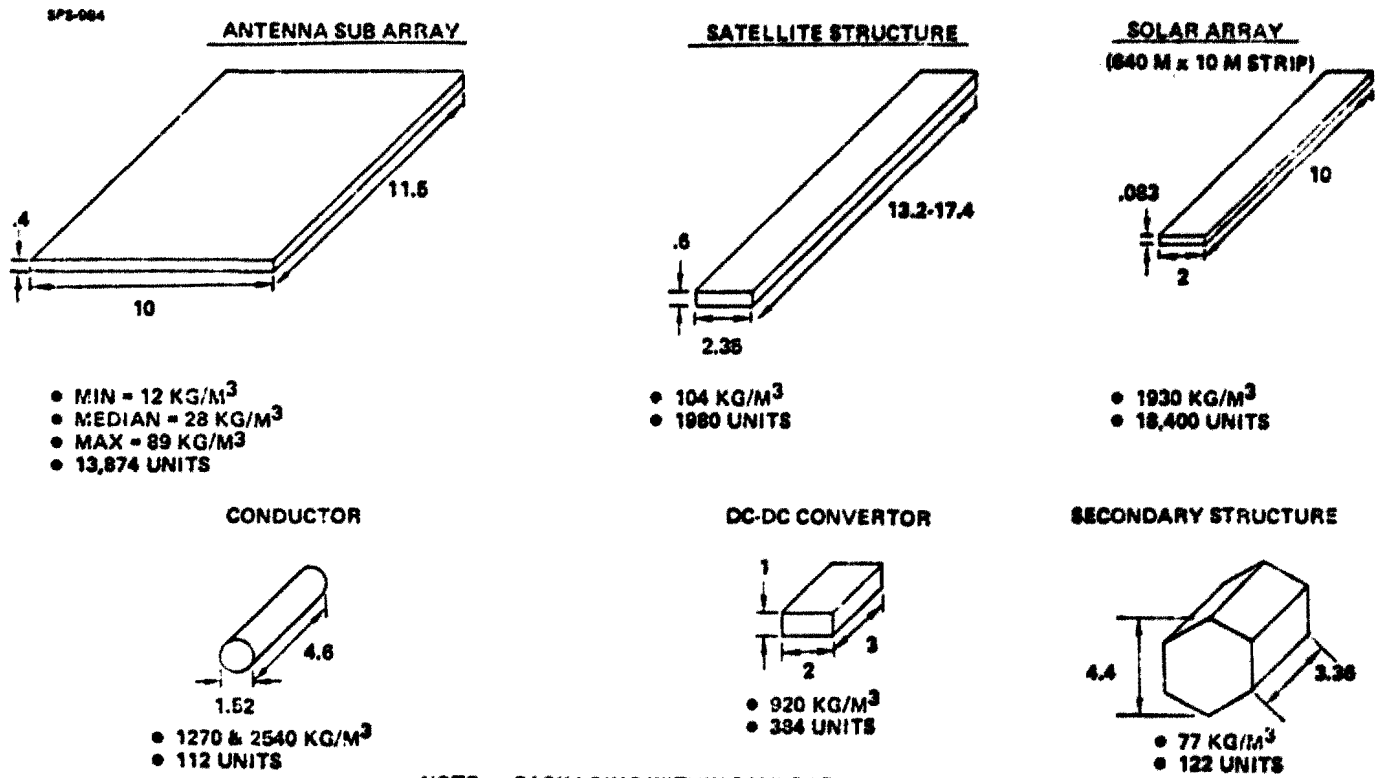
3.2.4.10 Payload Packaging

Payload packaging considerations affect both construction and transportation operations. The packaging analysis for the photovoltaic satellite reflects the structure fabrication approach (beam machines) and the first definition of the antenna. Packaging density and the number of units are presented in Figure 3.2.4-24 for the major components. The component presenting the greatest problem is the antenna subarrays with a median packaging density of only 28 kilograms per cubic meter. The payload shroud requirement had previously been set at 75 kilograms per cubic meter. Analysis has shown that since actual payloads have irregular shapes, the effective density of the payload within the shroud will be less than the average of individual component densities.

An estimate for the mixing of the various components for delivery to LEO is illustrated in Figure 3.2.4-25. The number of flights indicated are for the mix of components and are not meant to be indicative of the actual launch sequence. The dominating item was the antenna subarrays included in 246 out of 247 total flights (of identifiable hardware). Fortunately, the high density solar arrays can be used to offset the lower density subarrays during most of their launches. Unlike the Part I analysis where only about 25 to 30% of the payload shroud was used (antenna undefined), a more complete understanding of the antenna and desire to deliver subarrays fully assembled has resulted in using the entire volume of the payload shroud in order to achieve a mass-limited launch condition. The component density for the photovoltaic satellite reaches average density of approximately 95 kilograms per cubic meter is indicated. The reference 23 meter by 17.5 meter payload envelope with a volume utilization factor of 0.7 requires a component density of 93 kilograms per cubic meter in order to reach a mass limited condition.

The thermal engine satellite component density is approximately 66 kilograms per cubic meter primarily due to the low density of radiators, reflecting facets and antenna subarrays. Should the antenna subarrays be divided into a waveguide/structure section and klystron tube section, the density would go up to 76 kilograms per cubic meter. This, however, requires assembly of the subarrays in orbit which is deemed undesirable. Consequently, the thermal engine concept presents a difficult case for achieving mass limited launch conditions.

The number of flights shown in Figure 3.2.4-26 for the photovoltaic satellite reflect mass limited launch conditions. The thermal engine case is shown for both an expendable shroud large enough to reach a mass limited condition and a reusable shroud option. Launch cost for these options are compared in the third set of bars in the figure. For the thermal engine system, the expendable shroud shows approximately a 300 million dollar savings per satellite as compared with a reusable shroud due to the low cost (2 million dollars) for the expendable shroud when large quantities are procured. It should be noted that the thermal engine satellite will also utilize reusable shrouds for the delivery of crew and supplies and delivery of construction requirements.



NOTE: PACKAGING WITHIN PAYLOAD SHROUD TENDS TO REDUCE COMPONENT DENSITY

Figure 3.2.4-24 Component Packaging Characteristics

D180-22876-2

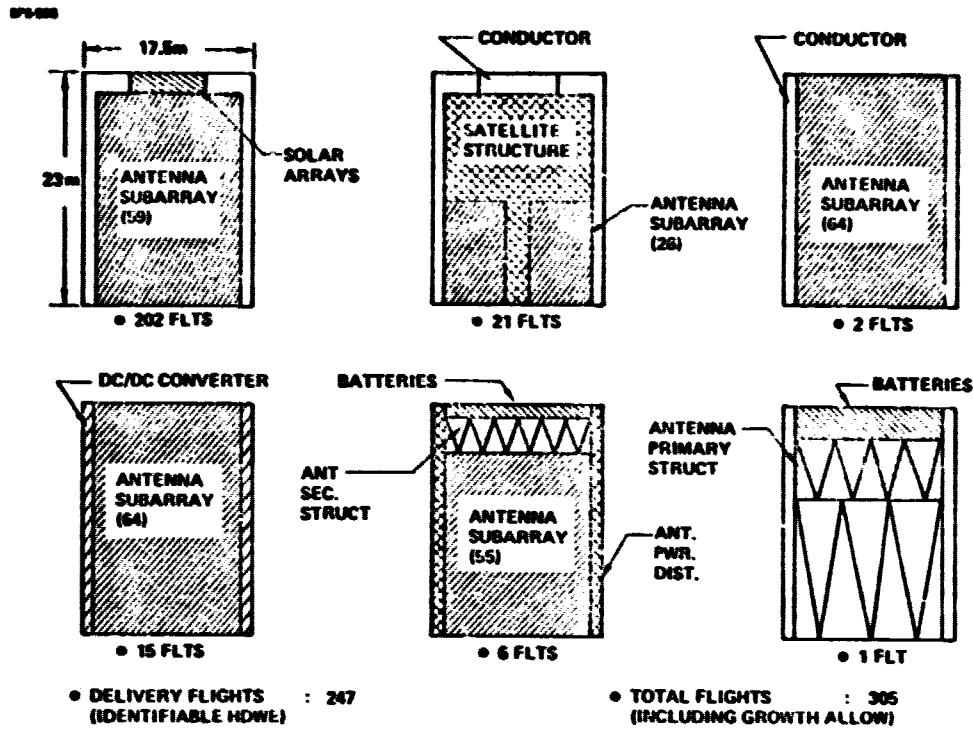


Figure 3.2.4-25 Component Mix Per Delivery Flight

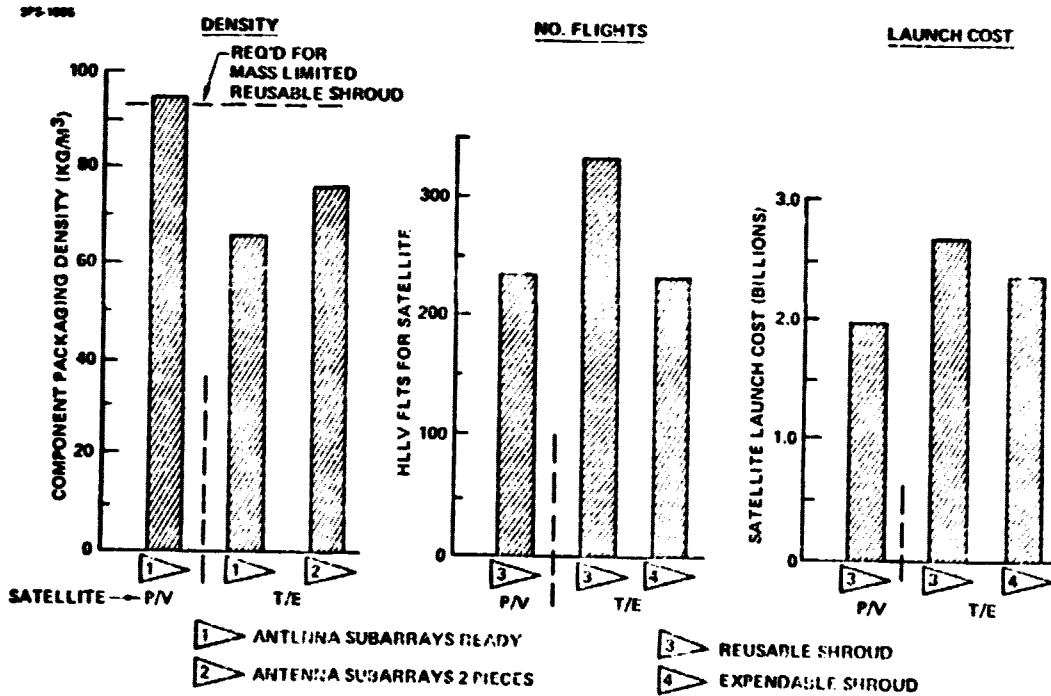


Figure 3.2.4-26 Component Packaging Density Impact

The most important conclusions from the packaging and payload density studies were:

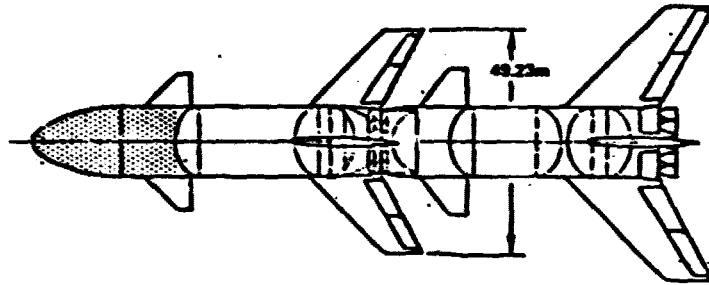
- Payload volume requirements are a major design consideration for the transportation system, especially Earth launch vehicles. A payload bay computed density greater than 75 kg/m^3 is likely to result in volume limited launches with attendant cost penalties. Payload physical sizes are large. Penalties associated with smaller payload bays have not been adequately assessed, but diameters of at least 15 m appear to be highly desirable.
- Achievement of adequate payload packaging densities requires mixing of component types for most launches. This means that (1) a payload unpacking area and crew will be required at the construction base; (2) some warehousing will be required at the construction base; (3) antenna and energy conversion elements of the SPS construction activity must be served by the same logistics network.
- When payload packaging is taken into account, transportation costs favor the photovoltaic SPS over the thermal engine option.

3.2.4.11 Transportation Vehicles and Systems

Two primary launch system options were characterized, a ballistic two-stage heavy lift vehicle and a winged two-stage heavy lift vehicle. The differences in performance between these two options were well within the uncertainty of performance estimation.

Figure 3.2.4-27 compares the HLLV options. The principal issue between the two systems is sea landing versus land landing. The sea landing mode requires restart of some of the rocket engines (or start of special landing engines) for the powered letdown into the water and the hardware is exposed to the sea saltwater environment. There is also some uncertainty associated with landing loads to be experienced upon water contact. The winged land landing vehicle avoids these issues. Because of the sonic boom profiles for ascent and reentry of the vehicles, and because the winged booster requires down range land landing, the winged system introduces significant launch and recovery siting issues. No suitable down range land landing sites are available for KSC launch. Potentially usable sites, with regions of significant sonic boom overpressure being under government control, exist in the southwestern United States. These sites are further north than KSC and introduce additional performance penalties associated with the plane change required to achieve a zero-inclination geosynchronous orbit. Other alternative sites have not been identified.

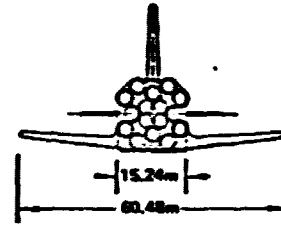
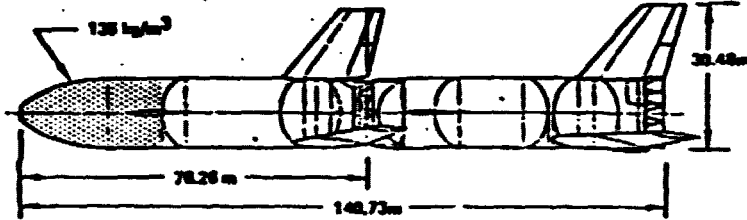
Both vehicles described have a liftoff mass of about 10,000 metric tons (more than 3 times the Saturn V lunar rocket), and a payload slightly less than 400 tons to the reference 478 km, 31° orbit. The winged vehicle does not meet currently-recognized payload bay volume requirements. Both vehicles have a calculated cost per flight in the \$8 million range at high launch rates. Cost per flight calculations are described in more detail in Section 3.2.6.3.3. Detailed vehicle descriptions are provided in Volume V of the Part I Final Report.



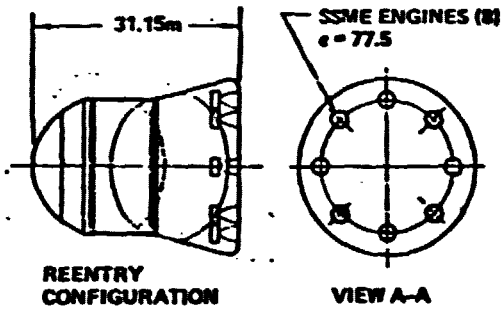
VEHICLE CHARACTERISTICS

- GLOW - 9.566×10^6 kg
- BLOW - 8.445×10^6 kg
- W_{P1} - 5.696×10^6 kg
- ULOW - 2.739×10^6 kg
- W_{P2} - 2.306×10^6 kg
- PAYLOAD - 0.391×10^6 kg
- T/W AT LIFTOFF - 1.30
- MAIN PROPULSION

STAGE	NUMBER & TYPE	c	THRUST/ENG. (10 ⁶ N VAC)	I_{sp} - Sec
1st	18-LO ₂ /RP-1	42.5	8.278	298.7
2nd	14-SSME	77.5	2.691	495.2



2-Stage Winged Launch Vehicle



GLOW	10.472×10^6 kg	(23,087 x 10 ⁶ lbrm)					
BLOW	8.243×10^6 kg	(18,173 x 10 ⁶ lbrm)					
W_{P1}	7.456×10^6 kg	(16,437 x 10 ⁶ lbrm)					
ULOW	1.838×10^6 kg	(4,051 x 10 ⁶ lbrm)					
W_{P2}	1.479×10^6 kg	(3,261 x 10 ⁶ lbrm)					
PAYLOAD	0.391×10^6 kg	(0.863 x 10 ⁶ lbrm)					
T/W AT LIFTOFF 1.30							
MAIN PROPULSION							
STAGE	c	NUMBER/TYPE	THRUST/ENGINE (PAYLOAD)		EXHAUST VELOCITY		I_{sp} - SEC
			10 ⁶ N	10 ⁶ Lb	MPS	FTS	
1ST	42.5	18-LO ₂ /RP-1	8.288	2.827	3401	11280	298.7
2ND	77.5	14-SSME	2.691	0.670	6400	14000	495.2

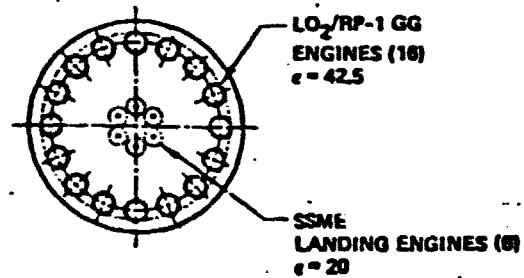
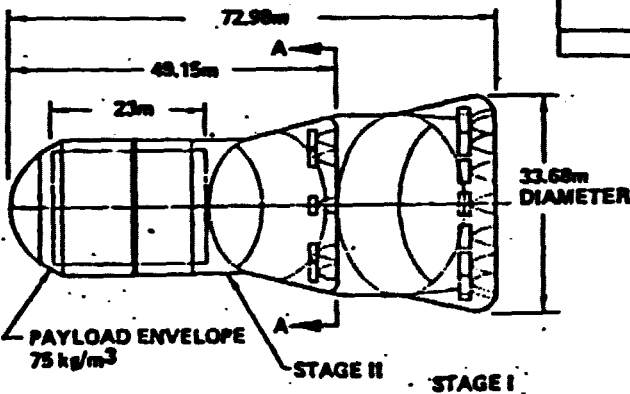


Figure 3.2.4-27. SPS Launch Vehicle-Cargo Version

The shuttle, with the addition of suitable crew accommodations in the payload bay and a new liquid propellant booster to reduce cost and atmosphere pollution, has been selected throughout the SPS studies as the basic crew launch and recovery vehicle. This modified shuttle capable of carrying 50 to 75 people to orbit and back is shown in Figure 3.2.4-28.

SPS-541

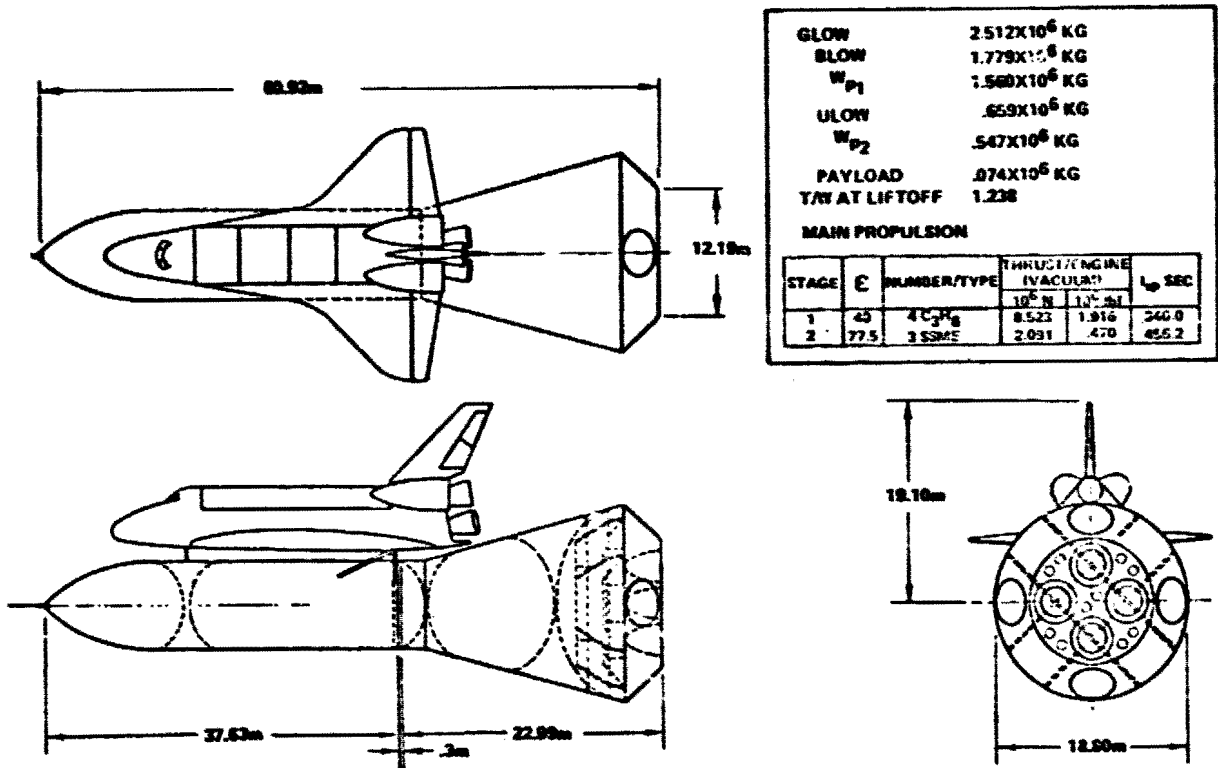


Figure 3.2.4-28 Personnel Launch Vehicle

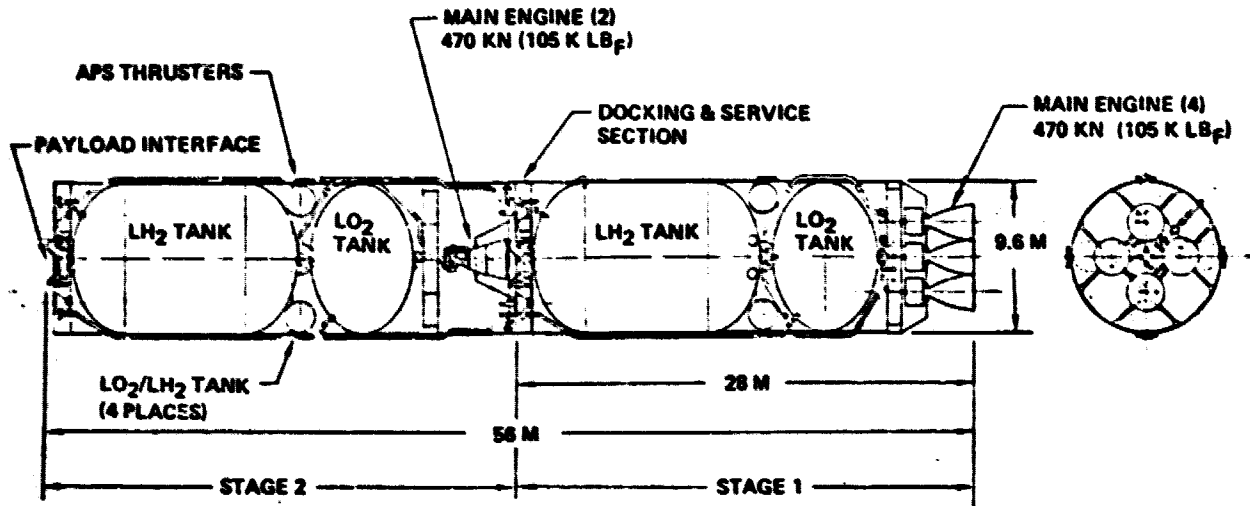
Crew/Cargo Orbit Transfer Systems

Transportation operations may be required to support construction operations either at low Earth orbit (LEO) or geosynchronous orbit (GEO), depending on which construction location is finally selected. In either case an orbit transfer vehicle system is needed to carry crews, crew resupply logistics and priority cargo to geosynchronous orbit. Earlier studies has investigated a variety of orbit transfer vehicle options and selected the configuration illustrated in Figure 3.2.4-29 as representative of a cost-optimal system. It is a space-based oxygen-hydrogen reusable 2-stage rocket system refueled by tankers brought to LEO by the heavy lift launch system. This vehicle serves to deliver crews and cargo to GEO from the LEO base. Up to 160 crew can be carried from LEO to GEO and returned by this vehicle, with a large crew module as payload.

Both stages have identical propellant capacity. The first stage provides approximately 2/3 of the delta V requirement for boost out of low earth orbit at which point it is separated for return to the low earth orbit as well as providing the remainder of the other delta V requirements to place the payload at GEO, and the required delta V to return the stage to the LEO staging depot for reuse. Subsystems for each stage are identical in design. The primary difference is the use of four engines in the first stage compared to two in the second due to thrust-to-weight requirements of approximately 0.15. The second stage requires additional auxiliary propulsion due to its maneuvering requirements in the docking of the payload to the construction base at GEO. The OTV shown has been sized to deliver a payload taken directly from the launch vehicle (400 000 kg). As a result, the OTV startburn mass is approximately 890 000 kg with the vehicle having an overall length of 56 meters. Main engines use a staged-combustion cycle at about 14 MPa (2000 psi) chamber pressure and deliver an Isp of 470 seconds with an area ratio of 400. Auxiliary propulsion uses a thermally-expelled pressure-fed O_2/H_2 system with a chamber pressure of about 700 kpa (100 psi) and a delivered Isp of about 400 seconds.

During Part I of this study, the natural question arose, "why not make the tanker into an orbit transfer vehicle and operate Earth-based?". This was investigated, and it was found that the space-based vehicle had about 15% better performance, yielding lower costs. There are two primary reasons: 1) the space-based vehicle need not be structurally designed to withstand launch loads with full propellant tanks; 2) the inert mass of engines and other subsystems needed to make the tanker into a vehicle need not be hauled back and forth from Earth to LEO. Concurrent with this SPS study, an orbital propellant depot study by General Dynamics has identified practical means of propellant transfer with minimal losses. The space-based system was selected as the preferred option.

If the SPS is constructed in low Earth orbit in a modular fashion, the electric generating capability of the modules may be used to drive electric propulsion systems to effect the orbit transfer. Each module is equipped with electric propulsion installations, propellant tanks and the other subsystems necessary to convert it into a powered spacecraft. A joint cost optimization of Isp and trip time resulted in selection of a 180-day transfer at 7500 seconds electrical ISP. The cost of invested capital has a significant influence on the optimization as illustrated in Figure 3.2.4-30. This occurs because



- PAYLOAD CAPABILITY = 400,000 KG
- OTV STARTBURN MASS = 890,000 KG
- STAGE CHARACTERISTICS (EACH)
 - PROPELLANT = 415,000 KG
 - INERTS = 29,000 KG (INCLUDING NONIMPULSE PROPELLANT)
- 280 OTV FLIGHTS PER SATELLITE

Figure 3.2.4-29 Space Based Common Stage OTV GEO Construction

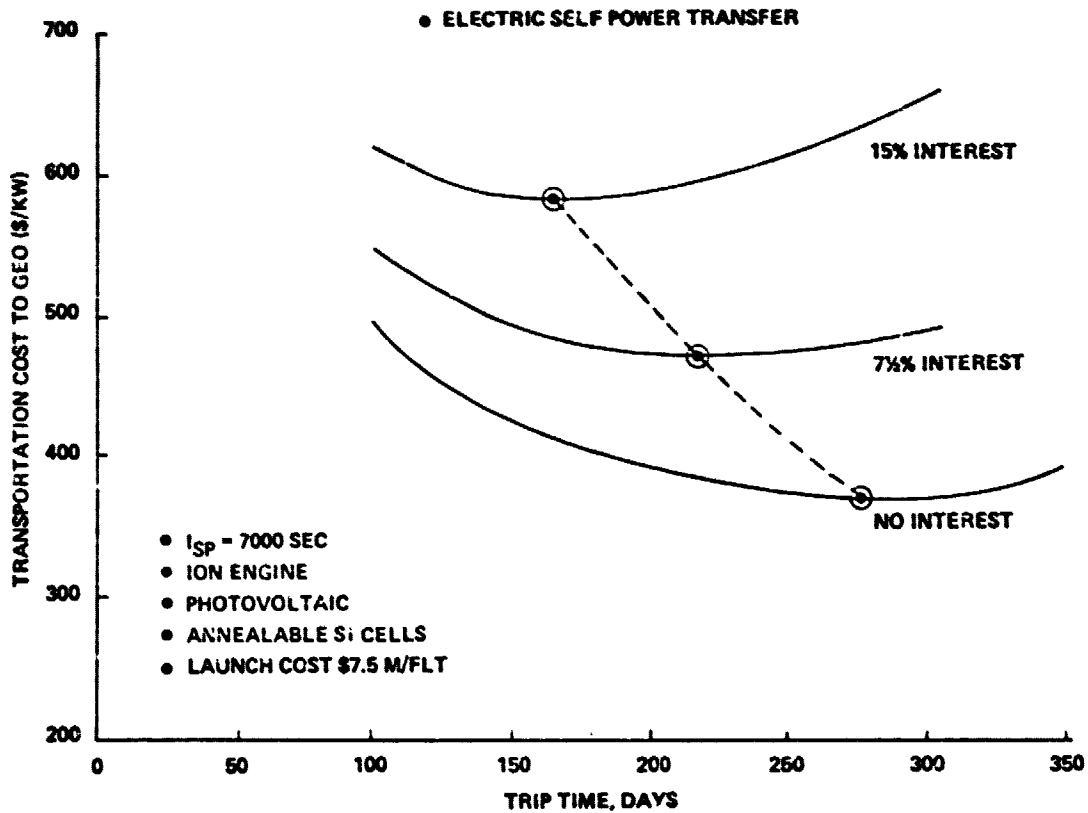


Figure 3.2.4-30 Transportation Cost Sensitivity Interest Rate

the transfer time causes a delay in the SPS entering service. Consequently, interest costs on investment in the SPS accumulate during the transfer: these costs trade against the reduction in thrust level (and therefore installed propulsion hardware cost) that occurs with acceptance of longer trip times.

The effective Isp of the orbit transfer system, after accounting for losses for attitude control thrusting and the use of chemical propulsion during transits of the Earth's shadow, is about 3000 seconds. This high effective specific impulse provides a major reduction in total freight delivery to low Earth orbit. The LO_2/LH_2 orbit transfer vehicle requires about 2.1 kg of propellant per kg of payload delivered to GEO. The high-specific-impulse option requires about 0.25 kg of propellant per kg of payload delivered. The net effect is a 50% reduction in the required number of heavy lift launches from Earth. There are a number of negative factors associated with the high specific impulse "self-powered" mode, but taken in the aggregate they exhibit considerably less cost than the savings in Earth launches.

The arrangement of a photovoltaic SPS module as a powered spacecraft is shown in Figure 3.2.4-31. One-quarter of the solar blankets are used for the transfer; the remainder are deployed from their shipping boxes after the module reaches geosynchronous orbit. The blankets used for propulsion power will be degraded by van Allen belt radiation absorbed during the transfer. They will be annealed during the final checkout and preparation process. The antennas are also built at LEO, and are transported by two of the eight modules.

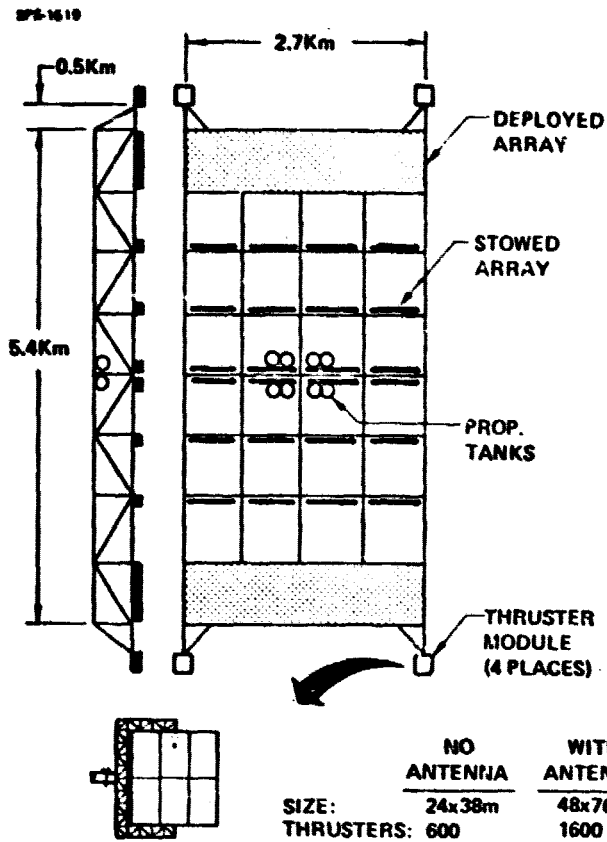
3.2.4.12 LEO/GEO Operations Comparison Summary

There is little difference in orbital crew size between the two construction location concepts, although the distribution of personnel is considerably different as shown in Figure 3.2.4-32. Staging depot and final assembly manning requirements were also found to be nearly the same.

Several key environmental factors should be considered when comparing the two construction location options.

One of the main differences between the two construction location options is the large amount of solar flare shielding which must be provided for all crew modules located at GEO. Steady-state radiation would make EVA at GEO considerably worse than at LEO although only a bare minimum of suit EVA is anticipated in either case.

Occultations of the construction base at LEO occur 15 times a day, while a base at GEO is only occulted 88 times per year. The principal effects of occultation are on the electrical power supply and thermal aspects of the structure. The GEO option requires less power. Less array power is needed to recharge the nickel-hydrogen batteries used for occultation periods. The penalty for the larger power system is relatively small with low mass, low cost solar arrays. Although a GEO base is



GENERAL CHARACTERISTICS

- 5% OVERSIZING (RADIATION)
- TRIP TIME = 180 DAYS
- ISP = 7000 SEC

MODULE CHARACTERISTICS

	NO ANTENNA	WITH ANTENNA
• NO. MODULES	6	2
• MODULE MASS (10^6 KG)	8.7	23.7
• POWER REQ'D (10^6 Kw)	0.3	0.81
• ARRAY %	13	36
• OTS DRY (10^6 KG)	1.1	2.9
• ARGON (10^6 KG)	2.0	5.6
• LO_2/LH_2 (10^6 KG)	1.0	2.8
• ELEC THRUST (10^3 N)	4.5	12.2
• CHEM THRUST (10^3 N)	12.0	5.0

	NO ANTENNA	WITH ANTENNA
SIZE:	24x38m	48x76m
THRUSTERS:	600	1600

Figure 3.2.4-31 Self Power Configuration Photovoltaic Satellite

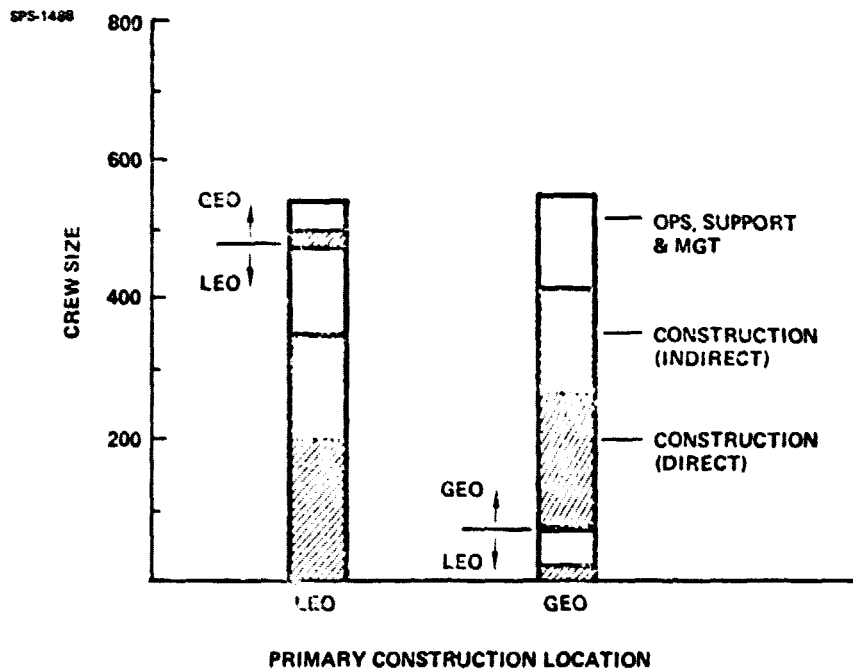


Figure 3.2.4-32 Crew Size and Distribution

more continuously illuminated, the construction base itself produces shadows. Consequently, both construction locations require a large amount of power for lighting purposes. Use of graphite/epoxy structure in both the satellite as well as the construction base structure should minimize the impact of thermal effects.

Most construction concepts will orient the construction base so it is passively stable for attitude control and minimize gravity gradient torque. Although the LEO construction case required considerably more orbit keeping/attitude control propellant per day, it still results in less than one HLLV launch per year for this propellant makeup.

Orbiting debris from man-made space systems has resulted in some concern regarding collisions during LEO construction. (The flux of objects is much greater at LEO than at GEO.) The analysis conducted has indicated the potential collision problem is greater with construction in LEO, however, simple avoidance maneuvers can reduce the probability of being hit to near zero.

The collision analysis was done for an environment predicted for the year 2000 including an addition of 500 objects per year since 1975. Results of this analysis indicated that the LEO construction approach could have forty additional collisions if no preventive action is taken. However, rescheduled orbit altitude corrections can essentially eliminate the problem of collision with little or no additional penalty, as illustrated in Figure 3.2.4-33. Thrust modulation or termination during orbit transfer can also be used to prevent collisions. There should be no difference between the two construction locations regarding the number of collisions. The LEO construction approach does require slightly different operations, including the use of debris tracking and warning systems.

The design impact on the satellite for the case of LEO construction and self-power has been described earlier in the description of the photovoltaic satellite. A summary of the key items is presented in Table 3.2.4-1. Solar array oversizing of 5 percent has been included to compensate for the inability to completely anneal out all the damage to the cells caused by radiation occurring during transfer and for the mismatch in voltage and current output between the damaged and undamaged cells.

The structural impact includes both that of modularity and oversizing. Modularity includes additional vertical members used around the perimeter of the satellite module and lateral beams at the end of the modules as well as the penalties for the transfer of the 15 million kg antenna supported underneath the module. (It should be noted that all module structure has been sized to that dictated by the modules used to transfer the antenna.)

The power distribution penalty is related to the additional length of bus caused by the oversizing of the array. The total mass penalty for a LEO-constructed satellite is approximately 4.2 million kg

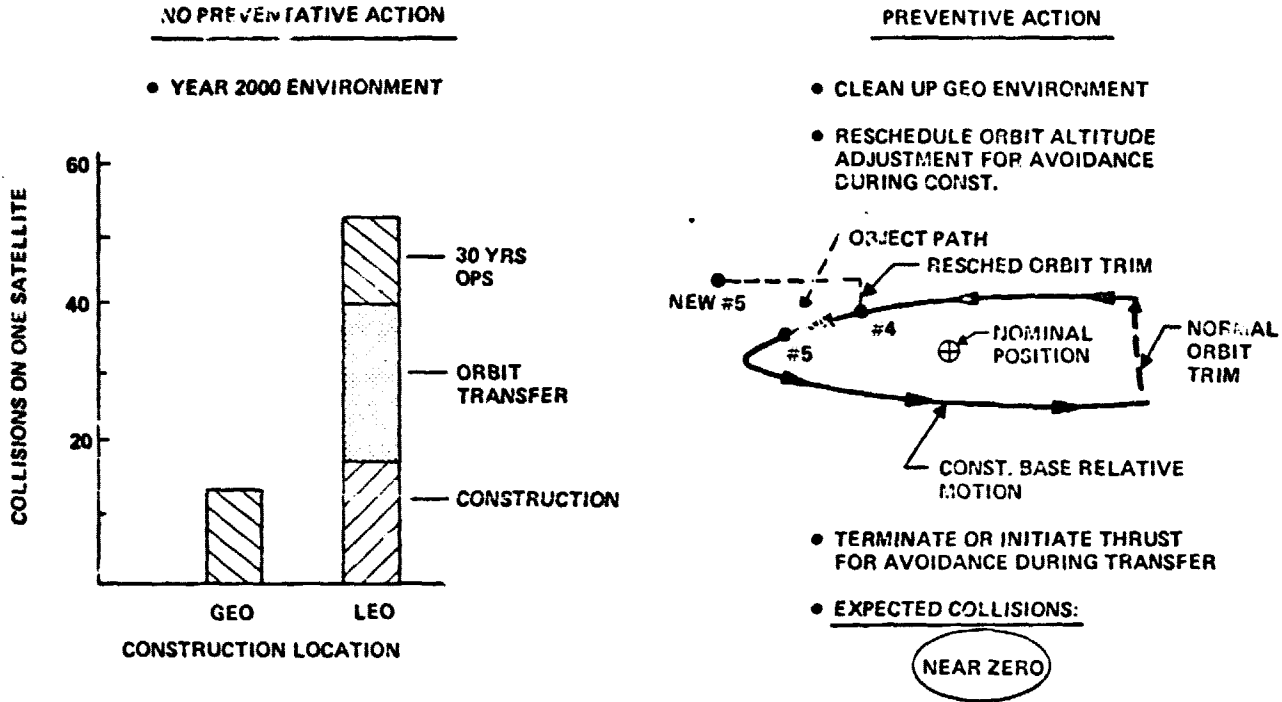


Figure 3.2.4-33 Collisions with Man Made Objects

Table 3.2.4-1 Satellite Design Impact Summary LEO Construction

SPS-1620

SELF POWER TRANSFER		
IMPACT	REASON	PENALTY
• POLAR ARRAY	• OVERSIZING FOR RADIATION DEGRADATION	• 2.75M Kg 
• STRUCTURE	• MODULARITY • OVERSIZING	• 1.07M Kg • 0.34M Kg 
• POWER DISTRIBUTION	• EXTRA LENGTH DUE TO OVERSIZING	• 0.07M Kg 

 FUNCTION OF SELF POWER PERFORMANCE CHARACTERISTICS

for the selected self-power transportation system. It should be noted that the array oversizing and power distribution penalty depend on the particular performance characteristics selected for the self-power system.

Transportation requirements associated with the payloads of each construction location concept are shown in Figure 3.2.4-34; no OTV propellant mass is included.

The difference in satellite mass reflects the structural mass penalty of the additional vertical and lateral members and loads caused by transfer of the antenna. Oversizing and power distribution penalties are all a function of orbit transfer characteristics and consequently are chargeable to the orbit transfer system itself.

Differences in crew and supply requirements delivered to LEO primarily reflect additional orbit keeping/attitude control propellant requirements. The key difference, however, is in the mass which must be delivered to GEO.

Facility transportation requirements reflect the initial placement task as well as, in the case of the GEO bases (both options), that mass that must be moved to the longitude location where the next satellite is to be constructed. The principal difference in the two main construction bases is that the six crew modules in the GEO concept each have approximately 115 000 kg of additional mass for solar flare shelters.

A most significant factor in the comparison is the difference in the number of launches required to support each construction location option. The number of flights indicated in Figure 3.2.4-35 are only those relating to the delivery of satellite components and orbit transfer provisions for the satellite and are for the case of constructing four satellites per year. As would be expected from the transportation requirements presented earlier, the LEO construction option requires only half as many Earth launches as the GEO construction option.

Total transportation cost for the three major system elements is presented in Figure 3.2.4-36. Cost is related to that associated with one satellite, but reflect rates associated with four satellites per year. The Earth-LEO bar increments reflect the cost of getting payloads to LEO. Accordingly, the LEO-GEO increment relates to cost of refueling orbit transfer vehicles and their unit cost. In the case of satellite delivery, the interest increment relates to the self-power trip time of 180 days and the additional interest accrued. (Note: Revenue is not lost, only delayed 180 days—the same revenue period still exists.)

The dominating factor in this comparison is that satellite transportation with LEO construction using self-power provides a \$2 billion (33% savings) over the GEO construction approach. Crew rotation, resupply transportation cost are also \$150 million (36%) lower for the LEO construction concept along with a \$200 million savings for the initial placement of the construction bases.

● PHOTOVOLTAIC SATELLITE

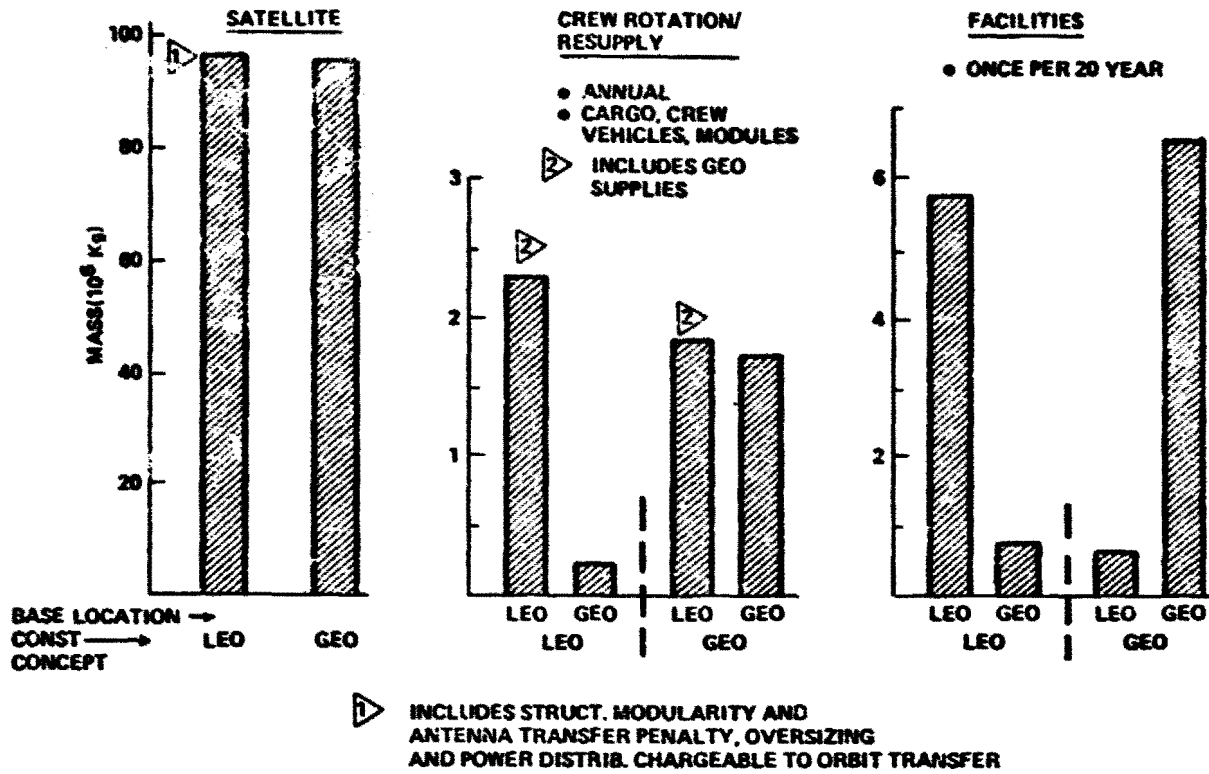


Figure 3.2.4-34 Transportation Requirements LEO vs GEO

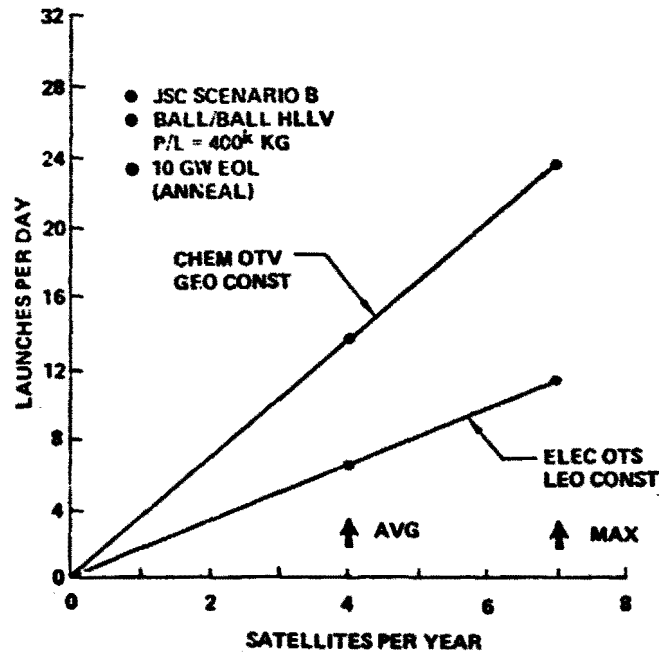


Figure 3.2.4-35 Number of HLLV Launches

SPS-1007

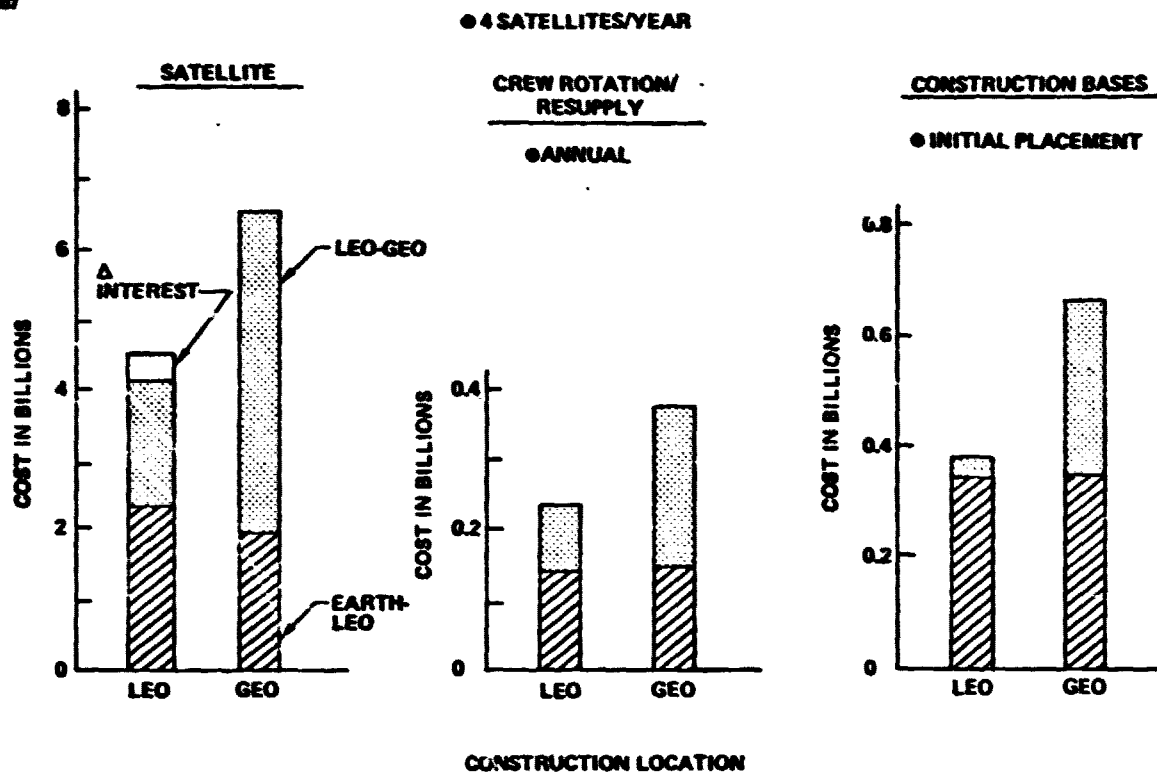


Figure 3.2.4-36 Transportation Cost LEO vs GEO

3.2.5 Uncertainty Analyses

One of the important objectives of the study was reduction of uncertainty in mass and cost for the SPS systems. Assessment of the attainment of this objective required a formalized uncertainty analysis.

Performance (efficiency in the case of SPS) and mass are the primary technical measures of uncertainty. Cost uncertainty tends to follow; there are additional cost uncertainty factors not directly associated with performance or mass.

History records a dismal record of mass and cost growth in all manner of projects. Curiously, some of the worst cost overruns have occurred on relatively mundane projects such as construction of domed stadiums. (One wonders what the cost overrun was on the Roman Colosseum.) Enough examples of mass growth have been collected for aerospace programs to allow some statistical measures to be taken. Figure 3.2.5-1 presents a statistical prediction of mass growth for various classes of systems in aerospace systems. Included in the "new concepts" statistics are systems such as the Concorde SST and the Apollo lunar spacecraft, the latter are also included in the manned spacecraft statistics. The SPS should presumably be classed as a new concept; it can be seen that history would suggest a probable 25% mass growth with appreciable risk that much greater growth would occur.

Three potential types of contributors to mass growth were identified:

- Program uncertainties, i.e., the likelihood that program requirements might change.
- Concept uncertainties, the likelihood that the design concept will change.
- Design uncertainties, the actual uncertainty in specific system design parameters or in mass estimates for given items.

It has been a general belief that mass growth results primarily from the first two of these contributors rather than the third. The former, however, cannot be adequately treated by a technical uncertainty analyses, e.g., if we knew why a program requirement would change in the future, we would change it now. The uncertainty analysis performed under this study considered only design uncertainties.

It is pertinent to discuss at this point a design phenomenon often called internal escalation. Airplane designs are notorious for internal escalation, which goes something like this: A subsystem mass growth item increases the aircraft mass, wing area must be added to compensate, further increasing mass, more fuel is needed to maintain range; more wing to carry the fuel, and so forth. These effects are positive feedbacks that amplify the effect of any elemental mass change. Manned spacecraft have internal escalation comparable to aircraft. The SPS has little of it.

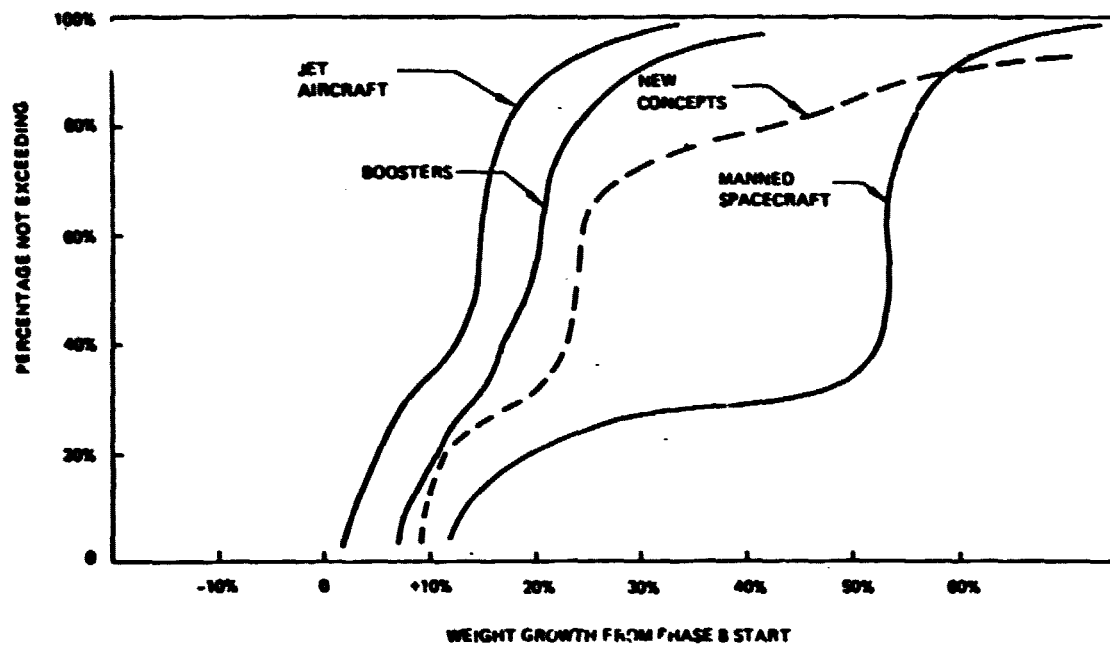


Figure 3.2.5-1. Past Program Growth Distribution

The uncertainty analysis methodology employed was newly developed for the study and included the principal steps indicated in Figure 3.2.5-2. The basis for the uncertainty analyses was itemized estimates in the uncertainties of component performance, masses and cost. A typical example would be the uncertainty in solar cell efficiency and degradation. This is an example of the case where correlation exists between the two factors: i.e., more efficient cells tend to experience somewhat greater degradation because the greater efficiency tends to be associated with greater thickness and experimental data indicate thicker cells degrade more. In developing the statistics in size, mass and cost, these kinds of correlations were taken into account through use of a bivariate normal distribution probability model.

Also providing input data to the uncertainty analyses was a conventional mass property analyses for the systems with estimated uncertainties in such factors as structural crippling criteria, solar cell thickness and turbomachinery unit masses. Additional uncertainties were developed in system costs, such as uncertainty in solar cell cost per unit area and uncertainties in machinery costs. These uncertainties were coupled with the cost analyses discussed later to prepare the cost statistics. Size statistics and mass statistics were combined to develop a joint mass/size uncertainty estimate and mass statistics and cost statistics were combined to generate combined cost/mass uncertainties. The bivariate normal distribution model was used to statistically combine the uncertainties, with recognition of correlations between component uncertainties where significant correlations were determined to exist.

It is a necessary and important consequence of the bivariate normal distribution model that the most probable value for a design parameter is the mean of the estimated extremes. The normal distribution model is believed to be the most appropriate for this type of uncertainty analysis - law of large numbers and all that - and the assumptions inherent in it were largely responsible for the nature of the results.

The significance of the central mean characteristics is evident in Table 3.2.5-1, and efficiency/size worksheet for the photovoltaic system. Note the significant difference between the most probable size (124 km^2) and the nominal size (108 km^2). Because of this central-mean modeling characteristic, the uncertainty analysis - in addition to estimating uncertainties, produced the unexpected result of predicting mass growth equivalent to that predicted by historical correlations. It had been believed that mass growth was the result of unpredictable variables, e.g. changes in program requirements. The outcome of this uncertainty analysis suggests that growth is more predictable than formerly believed and in fact results largely from the natural tendency to set point design parameters on the optimistic side of the actual uncertainty range.

The uncertainty analyses for the photovoltaic resulted in the relative efficiency uncertainty contributions illustrated in Figure 3.2.5-3. Also shown are the statistical combinations of all energy conversion effects and all power transmission effects. The energy conversion effect is slightly less than the power transmission effect because a significant correlation between solar cell efficiency and radiation degradation reduces the combined effect of these two parameters considerably below

SP8-1386

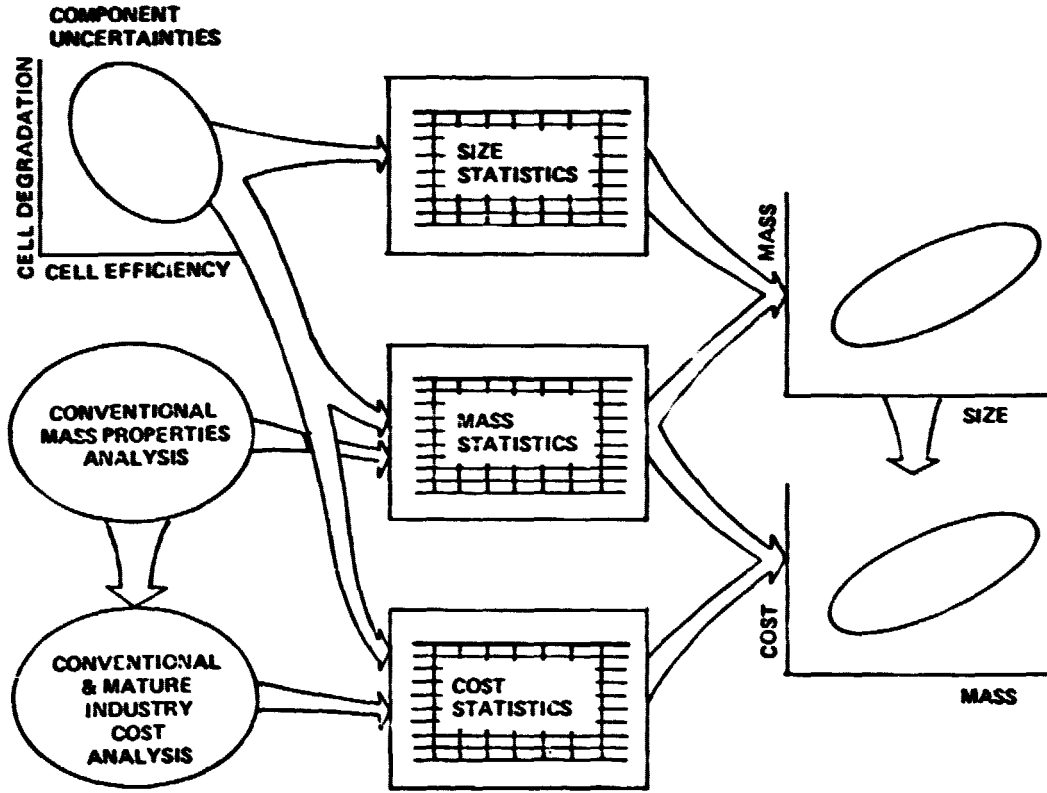


Figure 3.2.5-2 Uncertainty Analysis Methodology

Table 3.2.5-1 Photovoltaic End-To-End Efficiency Worksheet

SPS-1389

ITEM	NOMINAL	MINIMUM	MAXIMUM	LOG MIN	LOG MAX	LOG MEAN	σ	Correlations
Summer Solstice Factor	.9675	.9675	.9675	-.0330	-.0330	-.0330	0	} -0.6 (-.0009076)
Cosine Loss (POP)	.919	.919	.919	-.0845	-.0845	-.0845	0	
Solar Cell Efficiency	.173	.148	.18	-1.9105	-1.7147	-1.8126	.0326	
Radiation Degradation	.97	.90	1.0	-.1393	0	-.06963	.0232	
Temperature Degradation	.954	.954	.954	-.0471	-.0471	0.0471	0	
Cover UV Degradation	.956	.956	1.0	-.0450	0	-.0225	.00750	
Cell-to-Cell Mismatch	.99	.99	.99	-.01005	-.01005	-.01005	0	
Panel Lost Area	.961	.961	.961	-.0398	-.0398	-.0398	0	
String I ² R	.998	.995	.999	-.00501	-.001	-.00301	.00067	
Bus I ² R	.934	.91	.961	-.0943	-.0398	-.0670	.0091	
Rotary Joint	1.0	1.0	1.0	0	0	0	0	
Antenna Power Distr	.97	.95	.98	-.0513	-.0202	-.0357	.0052	
DC-RF Conversion	.85	.80	.86	-.223	-.1508	-.1870	.0121	
Waveguide I ²	.985	.985	.985	-.0151	-.0151	-.0151	0	
Ideal Beam	.965	.965	.99	-.0356	-.0100	-.0228	.0043	
Inter-Subarray Errors	.956	.88	.97	-.1278	-.0305	-.0791	.0162	} -0.3 (-.0000366)
Intra-Subarray Errors	.981	.97	.99	-.0304	-.010	-.0203	.0034	
Atmosphere Absorp.	.98	.98	.98	-.0202	-.0202	-.0202	0	} -0.5 (-.0000361)
Intercept Efficiency	.95	.90	.98	-.1054	-.0202	-.0629	.0142	
Ractenna RF-DC	.848	.79	.92	-.2357	-.0834	-.1596	.0254	
Grid Interfacing	.97	.96	.98	-.0408	-.0202	-.0305	.0034	
Products/Sums	.0679	.0383	.095			-2.822	Sums σ =	
Sizes (Km ²)	108.8	193	77.8				.00306	

3σ Max = $\exp(-2.822 + 3 \times .042) = .0675$ size = 109.5
 3σ Min = $\exp(-2.822 - 3 \times .042) = .0524$ size = 141.0

$\eta = .0595$ size = 124.0
 Correlation prod sum = -.00131
 $Net \sigma = \sqrt{.00306 - .00131} = .042$

150

D180-22876-2

ORIGINAL PAGE IS
OF POOR QUALITY

SPS-1672

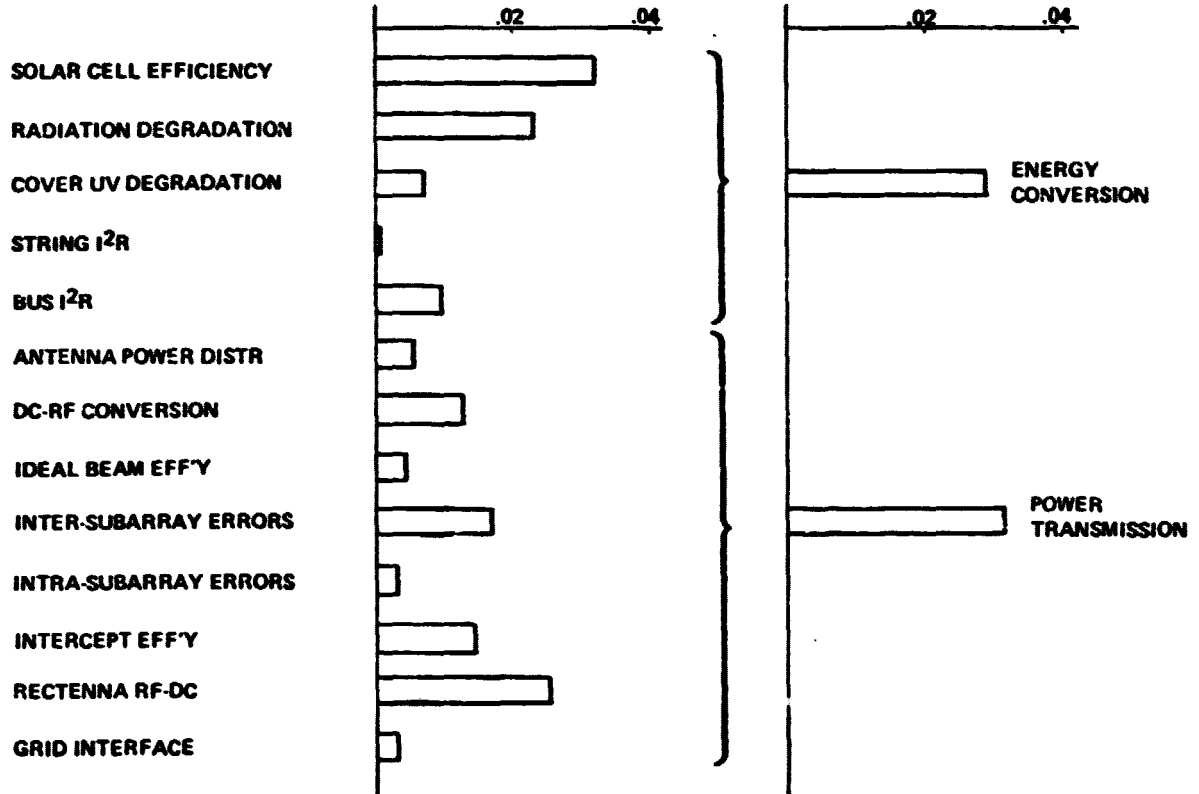


Figure 3.2.5-3 Photovoltaic SPS Efficiency:
Relative Uncertainty Contributions

and radiation degradation reduces the combined effect of these two parameters considerably below what a simple root sum square would indicate. The uncertainty in power transmission link efficiency is a principal driver on overall system mass and cost uncertainty because it influences more of the system than does solar blanket performance.

Figure 3.2.5-4 compares the statistically-derived result for the photovoltaic SPS with the worst-on-worst and best-on-best results defined by combining all the most optimistic component uncertainties and all the most pessimistic component performances. As increased detail is developed in this kind of analysis, the worst-on-worst and best-on-best extremes will continue to become further apart, while the statistical uncertainties will tend to change little and will approach a representation of true uncertainties. Significantly, the reference point design was outside the projected 3 sigma range for mass and size. This resulted primarily because the efficiency chain assigned to the reference design was more optimistic than the most probable efficiency chain defined by the statistical analyses.

Figure 3.2.5-5 presents an uncertainty estimate for the thermal engine comparable to the previous one for the photovoltaic system. Because the technology of the thermal engine system is somewhat more mature, it would be expected to project somewhat less mass growth and that turned out to be the case. An additional factor in the reduced mass growth projection is that a significant part of the size escalation is associated with the size of the concentrator which is a low-mass component of the thermal engine system.

With costs included in the uncertainty analyses, it is necessary to discriminate between the 1 SPS per year case and the 4 SPS per year case. For the 4 SPS per year case, an estimate was made that about 60% of the predicted mass growth could be removed by product improvement. This is believed to be a reasonable assumption since most of the mass growth resulted from increased size (reduced efficiency) stemming from component efficiency variances. Product improvement efforts can improve component efficiencies without changes in the overall system design. As was true for the size and mass estimates, the reference design trended towards the optimistic side of the median of the cost uncertainties as shown in Figure 3.2.5-6. Consequently, one sees first a cost escalation at the reference design point and then a further cost growth associated with the mass growth projection. Note the very high correlation between cost and mass uncertainties. This corresponds to the historical indications that cost growth is frequently associated with mass growth, and especially with the compensation for (or removal of) mass growth in a system when performance requirements dictate that mass growth be limited to predetermined values.

SPS-1679

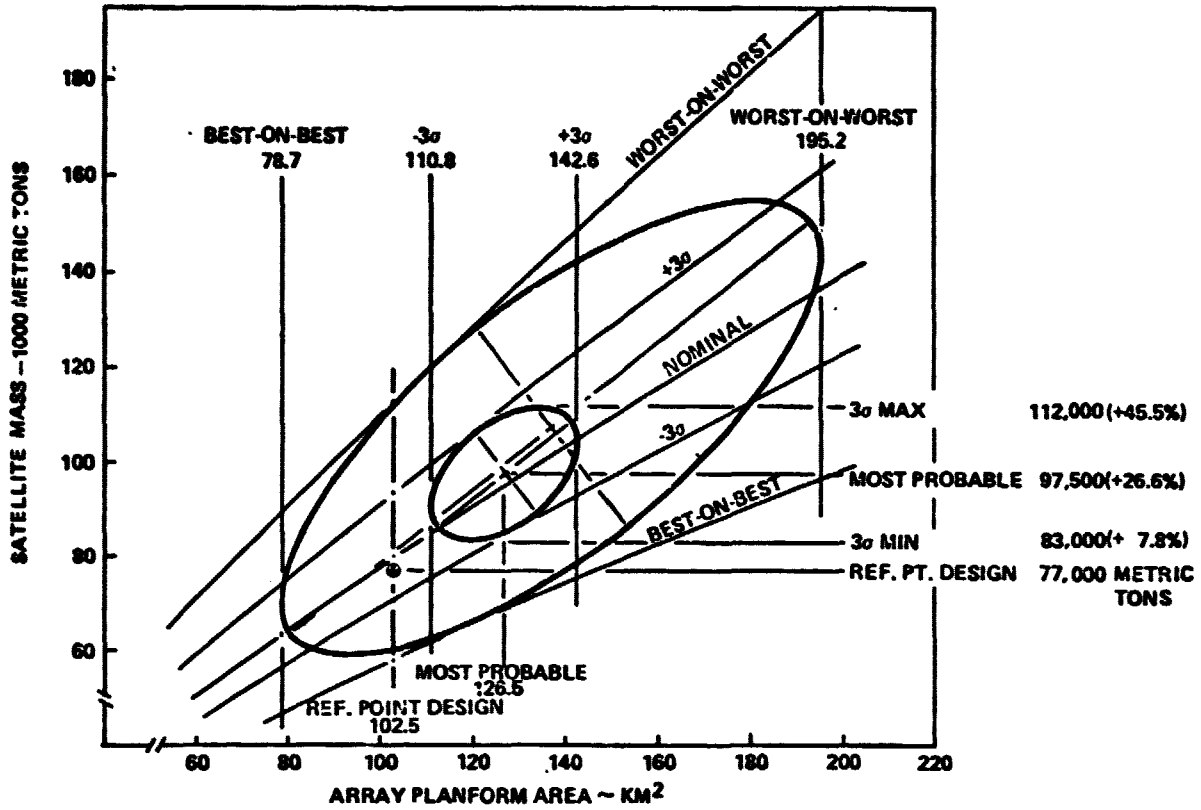


Figure 3.2.5-4 Photovoltaic SPS Mass/Size Uncertainty Analysis Results

SPS-1685

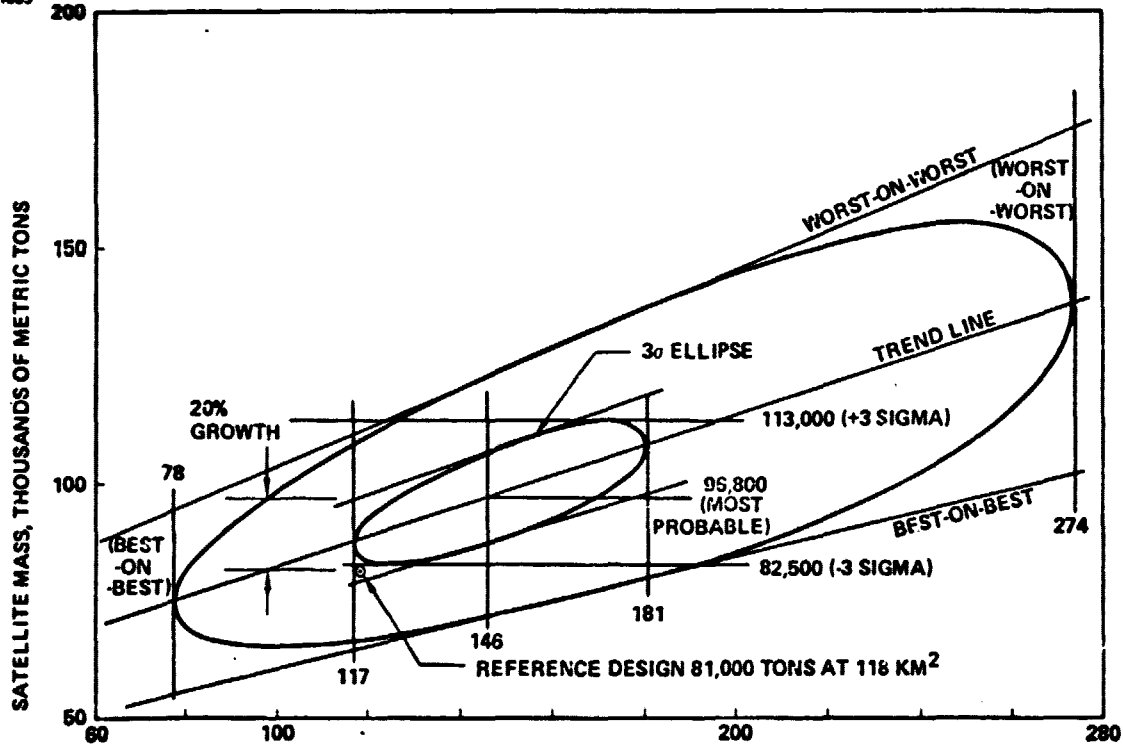


Figure 3.2.5-5 Rankine Thermal Engine Size/Mass Uncertainty Analysis Results

SPS-1680

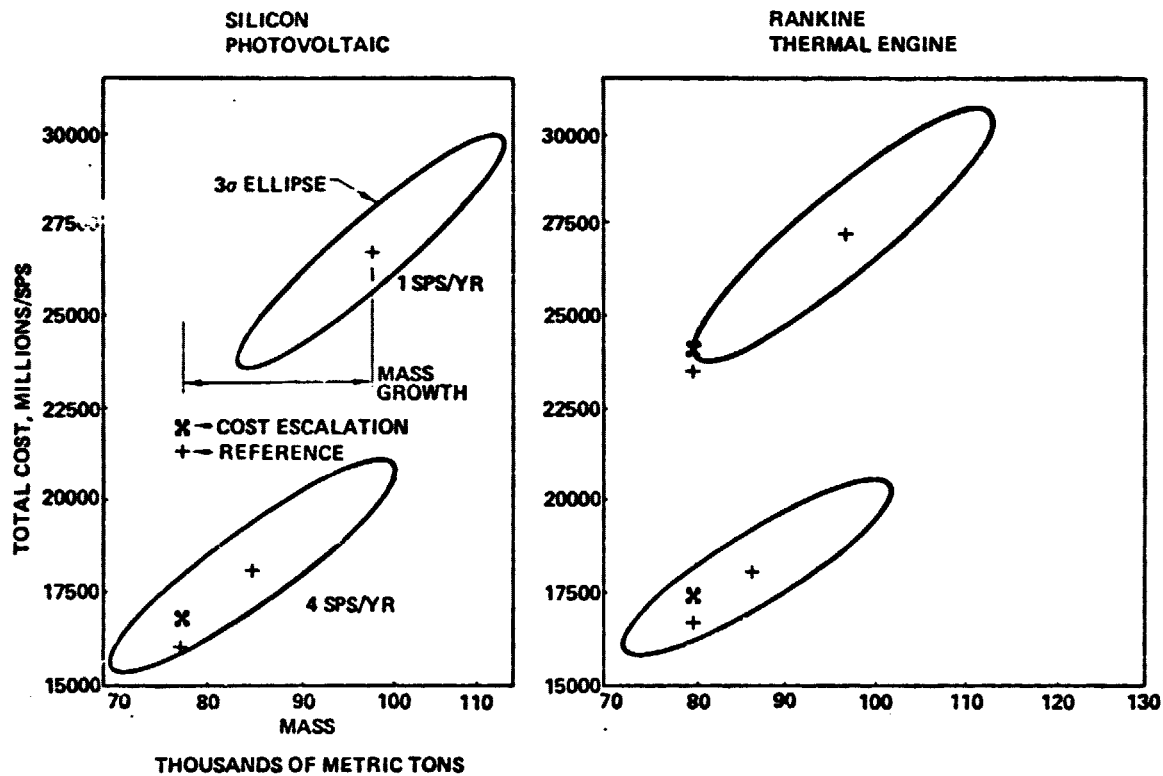


Figure 3.2.5-6 Mass/Cost Uncertainty Analysis Results

3.2.6 SPS Costs

3.2.6.1 General

One of the significant areas of emphasis of current SPS studies has been system costs, especially recurring (production) costs of SPS units to utilities. The present estimates of capital cost range from \$1700 to \$2700 per installed kilowatt (of useful ground output) for a modest-technology SPS system using silicon solar cells or potassium vapor Rankine heat engines (the latter, of course, employing solar concentrators). Since the installed kilowatts are baseload power rather than peaking or intermediate, the comparison with ground solar costs is potentially quite favorable.

These cost estimates may seem surprising. Since it is hardly obvious that putting a power plant in space will do anything to reduce cost, some amplification is in order. Otherwise the critical reader may well be justified in considering the estimates as frivolous.

Cost ultimately derives from the cost of materials, of energy, and of value added during production and installation. The SPS scores well on the first and the last of these, and on energy investment, scores a little better than typical nuclear systems.

Constructed and operated in space where design loads are virtually absent, a typical 10,000 megawatt SPS larger in area than Manhattan Island will have a total mass of 100,000 metric tons, about the displacement mass of a large aircraft carrier. Over 60% of the mass, be it a thermal engine or solar cell SPS, will be energy collection and conversion equipment with the balance being supporting structure, power transmitters, flight controls, and so forth. The energy conversion equipment produces several times as much output per unit area as a ground solar unit due to the continuous availability in space of sunlight of higher intensity.

Our SPS designs have employed very little in the way of exotic materials and are, except for their large size, relatively simple. The receiving antennas are also simple designs using ordinary materials (mostly concrete). With the receiving antennas included, the total materials required per kilowatt for an SPS are very similar to those for a conventional Earth-based plant; much less than for an Earth-based solar plant.

Energy

Lifetime energy investment to produce, install and operate an SPS is less than for most energy alternatives even if the latent energy in fuel for the alternatives is not counted. The energy cost of rocket propellant for space transportation has been calculated to be from 2000 to 4000 kwh_{th} per kwe installed; therefore, the payback time for rocket propellant is less than six months; less than two months if energy grade is included in the calculation.

Value Added

SPS systems and their receiving antennas are primarily made of simple, highly repetitive elements: billions of solar cells (or hundreds of thermal engine turbomachines); hundreds of thousands of standardized structural parts; tens of thousands of RF power tubes and associated circuitry; hundreds of standardized electrical switchgear units and power processors; billions of receiver dipole elements on the ground receiving antenna. All of these repetitive elements are well suited to highly automated mass production. This mass producibility is one of the keys to making SPS's at acceptable cost. Further, assembly of the SPS structure in space provides the unique opportunity to perform the assembly, even of this very large area structure, in a semi-automated production line manner. This is true because the lack of gravity and wind loads allows moving the SPS with respect to the assembly facility with relative ease.

3.2.6.2 Cost Analysis Approach

In view of the mass production potentials, we adopted a dual costing approach: For those items needed at production rates typical of aerospace products, we have used aerospace cost estimating practices. For those items needed at mass production rates, we have used mass production cost estimating. The relationships are illustrated in Figures 3.2.6-1 and 3.2.6-2. Aerospace cost experience follows a "learning" or improvement curve. (Most of the improvement comes from learning how to make the production plan work. Mechanics learn quickly.) Typical experience is an 85% curve: unit #2N will cost 85% of unit #N. 727 jetliner production experience shows that this type of projection is good well beyond the 1000th unit. Aerospace estimates are based on historical correlations of manhours, element physical characteristics, and complexity. They are made at the subsystem or subassembly level. Despite a contrary reputation, the basic estimating procedures are accurate. Aerospace cost variances can generally be traced to pricing and procurement practices, and most significantly to requirements and design changes, rather than to inability to estimate cost.

A mass production process is facility and equipment intensive rather than labor intensive. It does not follow an aerospace-type improvement curve. Historical correlations indicate a labor intensiveness relationship as shown in Figure 3.2.6-2. A mass production process reaches its labor cost plateau during the process shakedown period and then improves no further unless the process is changed.

The overall mature industry cost analysis methodology developed for the study is shown in Figure 3.2.6-3. It begins with mass estimates and system descriptions for the reference systems. The system descriptions allow selection of cost estimating relationships. These are used to exercise the Boeing parametric cost model to generate an aerospace cost estimate for DDT&E and first unit cost. The aerospace first unit costs are then run through a mature industry analysis that applies production

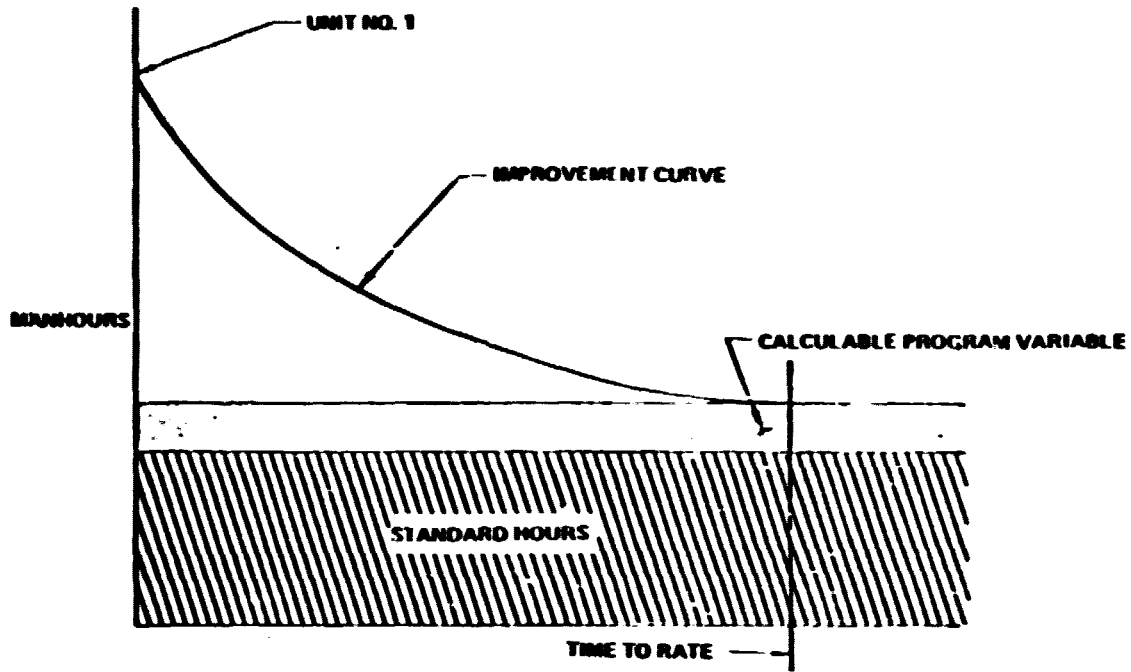


Figure 3.2.6-1 Program Cost Baseline

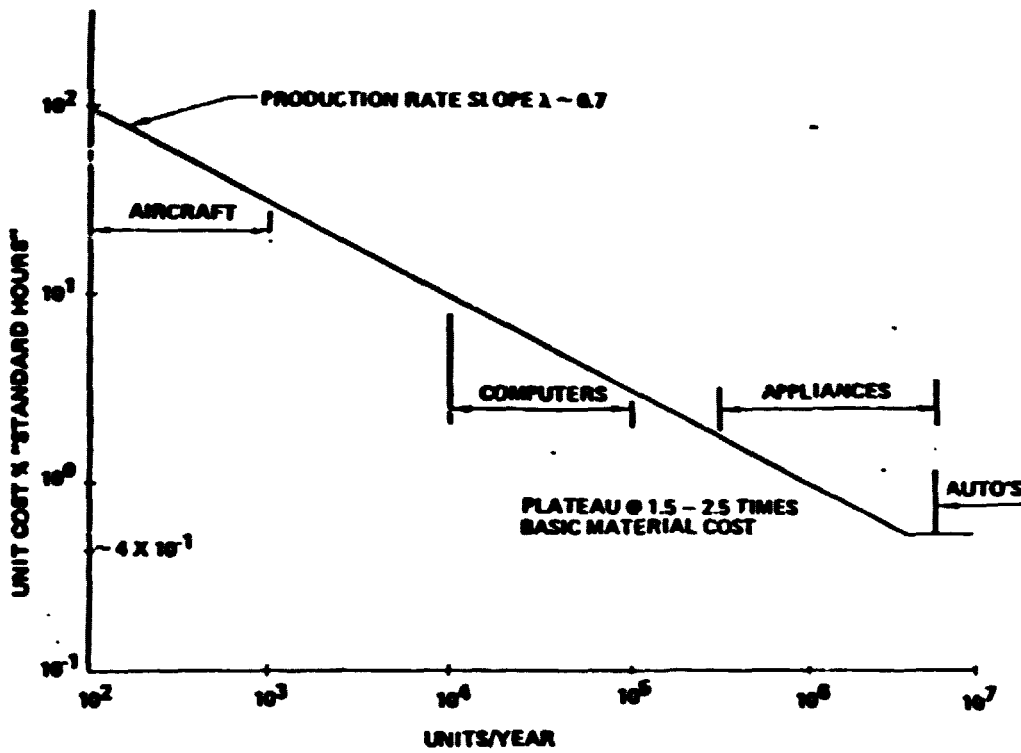


Figure 3.2.6-2 Mature Industry: Production Rate Curve

ORIGINAL PAGE 1
OF POOR QUALITY

SP5-1082

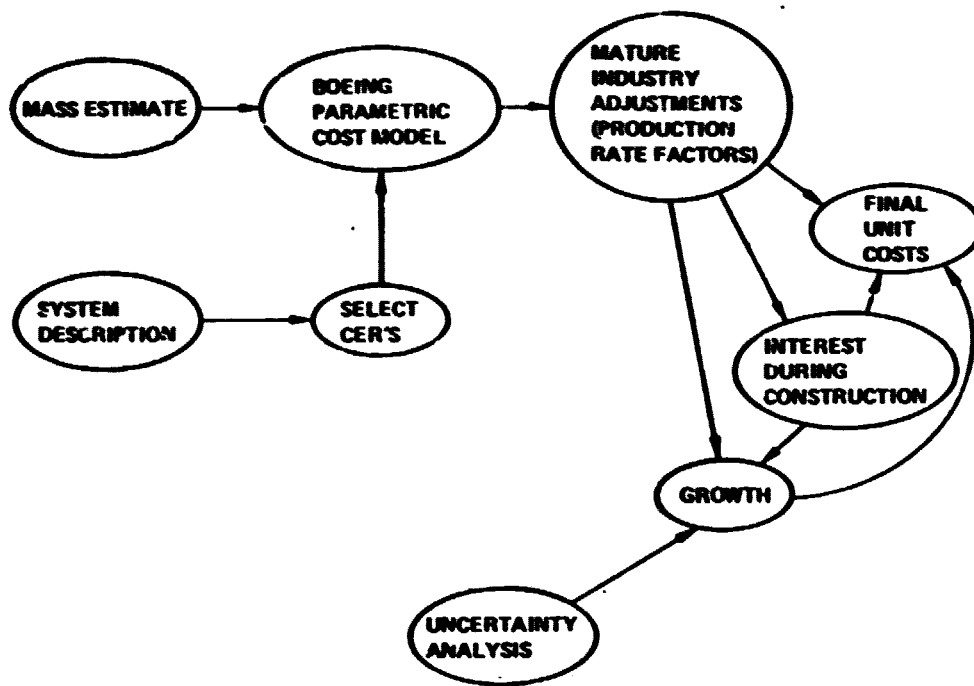


Figure 3.2.6-3 Cost Analysis Methodology

rate factors according to the production rate required for each system element. The totaled mature industry estimates are then adjusted for interest during construction and for cost growth corresponding to mass growth as predicted by the uncertainty analyses. These provide the final production unit costs for 1 SPS per year 4 SPS's per year.

The mature industry costing approach was developed by Dr. Joe Gauger based on information developed during IR&D analyses of design-to-cost, experienced costs for commercial aircraft and other systems, and statistical correlations for financial and production factors for a wide variety of commercial industries. It was judged to be desirable to spot-check the mature industry predictions. A total of five spot checks were made as indicated in Table 3.2.6-1. These included solar blankets, graphite composite structures, klystrons, potassium vapor turbines, and electromagnetic liquid potassium feed pumps. In all cases, the mature industry projection was well within the uncertainties that would be expected for the kind of cost estimates being made. Based on these examples, we believe the mature industry methodology to be an appropriate cost estimating procedure for SPS systems.

3.2.6.3 Specific Cost Results

The SPS cost estimates are collected according to the following high-level work breakdown structure:

Solar Power Satellite

- Multiple/Common Use Equipment, e.g., structure
- Energy Collection System
- Energy Conversion System
- Electric Power Distribution System
- Power Transmission System

Ground Receiving Station

- Land
- Receiving Equipment
- Power Collection & Processing
- Construction Costs

Space Flight Operations

- Transportation
- Construction

SPS-1003

Table 3.2.6-1 Mature Industry Methodology Confirmation

	<u>MATURE INDUSTRY PROJECTION</u>	<u>INDUSTRY ESTIMATES</u>
SOLAR BLANKETS	\$22 to \$37/m²	\$25 to \$50/m² (RCA, TI, GE, MOTOROLA)
GRAPHITE EPOXY STRUCTURE	\$80/kg	\$80/kg (BOEING)
KLYSTRONS	\$300/TUBE	\$1750 to \$2700/TUBE (VARIAN)
TURBINES	\$40 to \$50/kg	\$82/kg (GE)
PUMPS	\$75 to \$150/kg	\$80/kg (GE)

Primary emphasis in the current study effort has been directed to production and installation costs. Future efforts will investigate maintenance costs; the very preliminary estimates that have been made indicate that maintenance cost contribution to electric power cost will be comparable to that for conventional ground power plants.

Volume VI of this report presents cost estimating details and calculations.

3.2.6.3.1 Solar Power Satellite

In the multiple/common use equipment, the main structure is the principal cost driver. This structure is a graphite tubular truss, with individual tubular elements roughly 0.4 meters in diameter and 0.5 mm in wall thickness. These individual elements are arranged in triangular truss beams which are in turn arranged in the overall SPS planar truss structure. The mass of the entire structure is about 6×10^6 kg. Mature industry correlations predicted about \$60/kg for this hardware (ready to ship to space). Subsequent manufacturing analyses for automated production of these structural elements, including joints and fittings, estimated \$47 to \$57 per kg.

Solar cells and blankets are the cost driver for the photovoltaic SPS energy conversion system (at concentration ratio 1, there is no energy collection system). Solar cell costs were analyzed in three ways: (1) Mature industry projection; (2) Review of manufacturer's projections; (3) Energy cost check and review of production methods. Results are summarized in Table 3.2.6-2.

Current terrestrial array costs are at about \$10-\$12 per watt, about a factor of about 50 above the projections. Current annual production is about 0.7 MW_c. The production rate correlation described above predicts 10¢/watt at 5000 MW_c per year. These rate projections must be used with caution, as they will tend to predict costs below material and energy costs at high rates.

Therefore, a basic energy cost analysis was made:

Solar cells are very energy intensive. Presented in Figure 3.2.6-4 are representative energy costs in kilowatt hours per kilogram of cells. The energy payback for solar cells as a function of this energy cost is also shown on two scales (SPS and ground applications). Pricing the energy at 40 mills per kilowatt hour, the actual cost of the energy is shown on the outside scale.

The main reason today's cells are so intensive is that yields are very poor. Most of the silicon, in which a great deal of energy is invested, ends up as waste (saw kerfs and trimming). Continuous processes can probably reach a yield range of 60% to 80%, making the payback very attractive. Energy cost is a basic factor in the cost of solar cells, like materials cost in building hardware. If the energy cost is below 10 cents/watt one might be reasonably confident that cells in the 20 cents/watt range, made by an automated production process, would be possible. The development of solar cell

Table 3.2.6-2 Solar Cell/Blanket Costs

(1) J. Gauger's Mature Industry Correlation

8¢ to 17¢/Watt = 13.60 to 28.90/M² (Cells Only)
 = 22.00 to 37/M² (Array Panels)

(2) Manufacturers Estimates

10¢ to 25¢/Watt (Cells Only)
 = 17.00 to 42.50/M² (Cells Only)
 = \$25.00 to \$50/M² (Array Panels)

(3) Production Rate

Today \$10,000/M² for 50 kw
 Then $(17e6/50)^{1/2} = .0017 \times 10,000$ (70% Curve)
 = \$17.00/M²
 Energy Cost = \$17/M² for \$34/M² @ 1 SPS/YR

(4) Denman's Estimate - \$40/M² (Median)

Average of these values is \$35/M² @ 1 SPS/YR; use \$25/M² for 4 SPS/YR

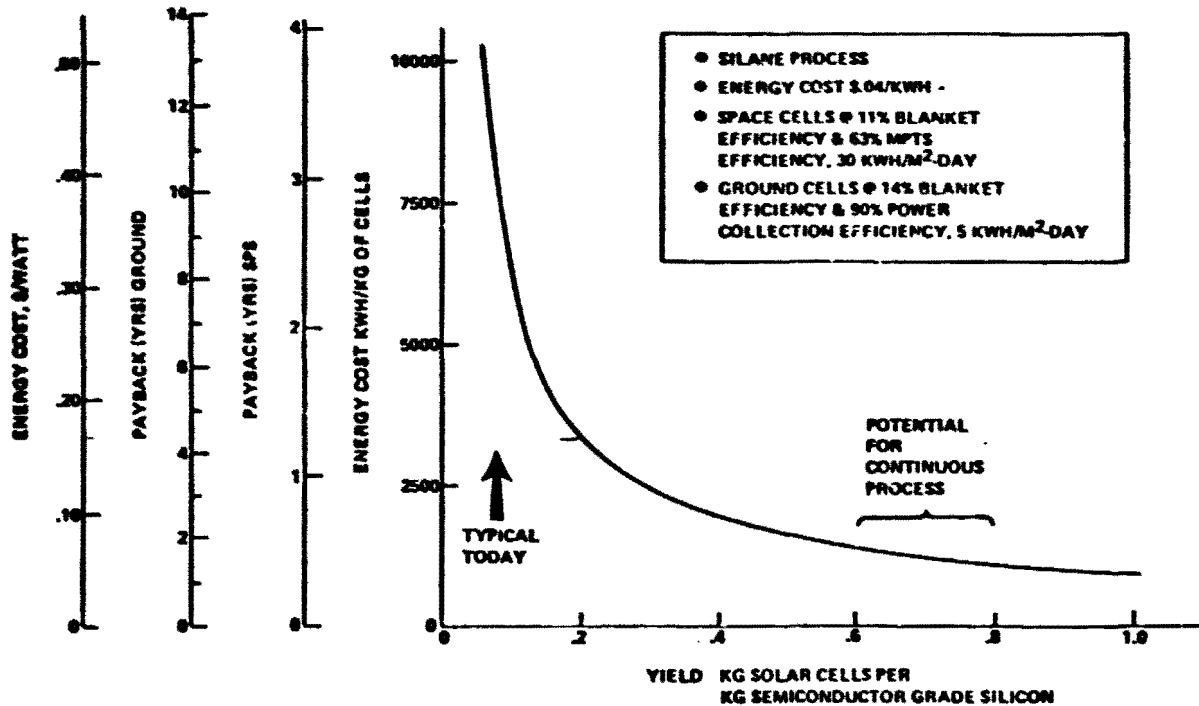


Figure 3.2.6-4 Energy Costs and Payback for Silicon Solar Cells

production technology is a competition between the existing technology and potential new technologies (Figure 3.2.6-5). Although the existing technology of growing single crystal boules and sawing them into wafers seems ill-suited to low cost production, an analogy to the internal combustion engine may exist. Although the IC engine seems ill-suited to propelling an automobile, the "more logical" technologies have never caught up. Similarly, improvements in sawing techniques (such as 0.1 MM saws) currently being introduced, and automation of the process may keep the Czochralski process competitive for longer than is often supposed.

Because of the uncertainty and controversy regarding solar blanket cost projections, the sensitivity of the photovoltaic system to solar blanket cost is important. Shown in Figure 3.2.6-6 are the study median projections for one SPS per year and four SPSs per year compared to the Department of Energy 1985 goal and Department of Energy post-1990 projections. Influence on SPS total system cost is shown for each case. Also shown are the comparative thermal engine system costs which indicate at what point an increase in solar blanket cost would motivate a change to the thermal engine system. This change occurs long before an unacceptable cost level is reached.

If solar cells exceed 20¢/watt by very much (an upper limit is probably 30¢/watt), the cost advantages of thermal engine energy conversion become compelling. SPS thermal engines were costed based on similar equipment presently in production, such as aircraft jet engines. Turbomachine cost estimates were provided by General Electric. The thermal engine system includes additional hardware in the concentrator, thermal cavity absorber, and waste heat radiators. The cost data base for this type of hardware is comparatively strong.

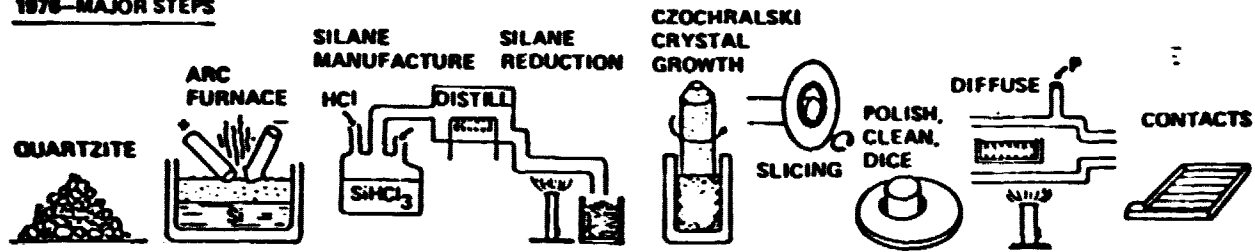
Considerable engineering effort was invested in power distribution analysis since large amounts of power are to be handled and power distribution mass/cost/efficiency optimization is important. Power distribution system elements were found to be well within the state of the art and the cost not very significant.

The dominating cost driver in the power transmission system was found to be the 70 KW_{RF} klystrons, of which nearly 200,000 are needed. A detailed manufacturing cost estimate was developed by Varian under subcontract, confirming a mature industry correlation estimate of about \$3000 per tube. Varian's results are a function of production rate as shown in Figure 3.2.6-7. The physical size of this klystron is about 0.2 m diameter by 1 m length.

3.2.6.3.2 Ground Receiving Station

Surprisingly, the ground receiving station has been subject to larger variances in cost projection than the flight hardware.

1976-MAJOR STEPS



IDEAL PROCESS-1987

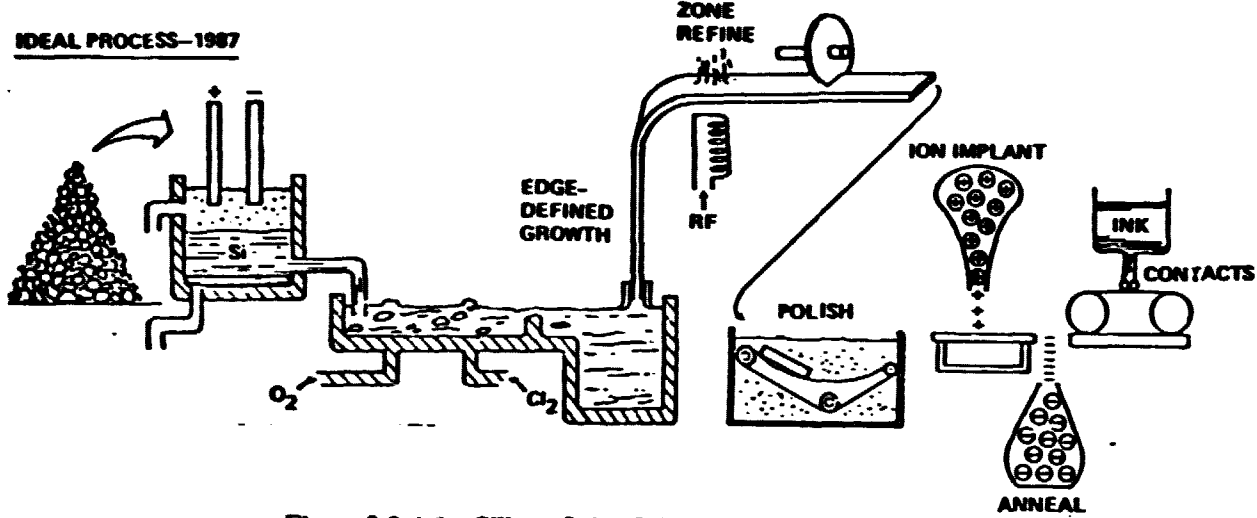


Figure 3.2.6-5 Silicon Solar Cell Manufacture

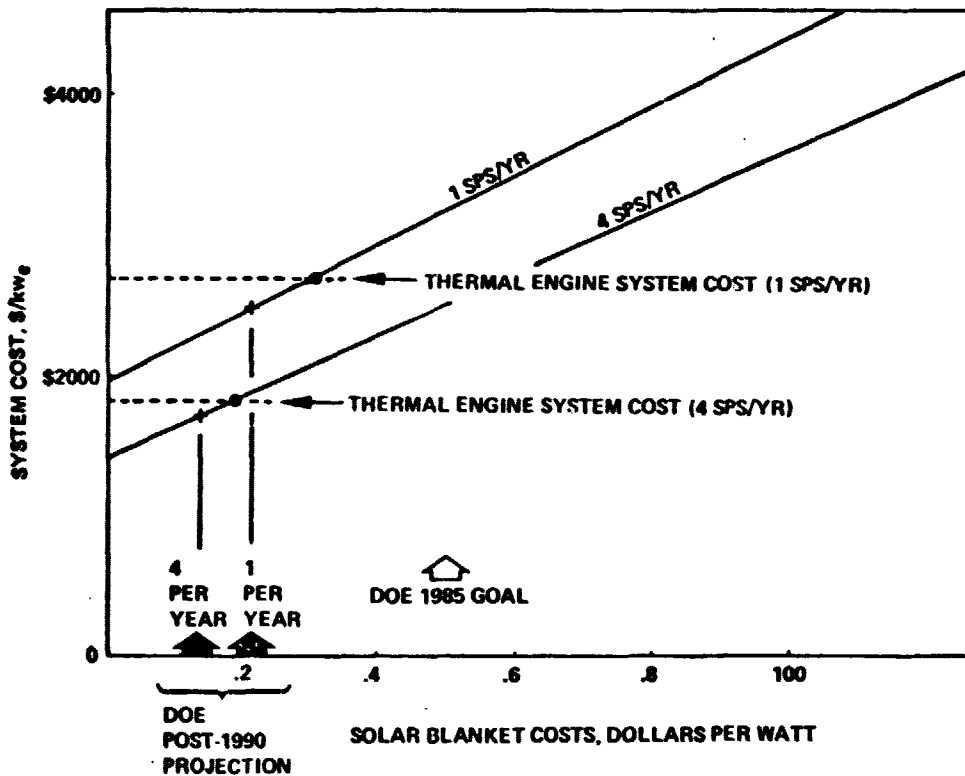


Figure 3.2.6-6 Photovoltaic Preference is Sensitive to Solar Blanket Costs

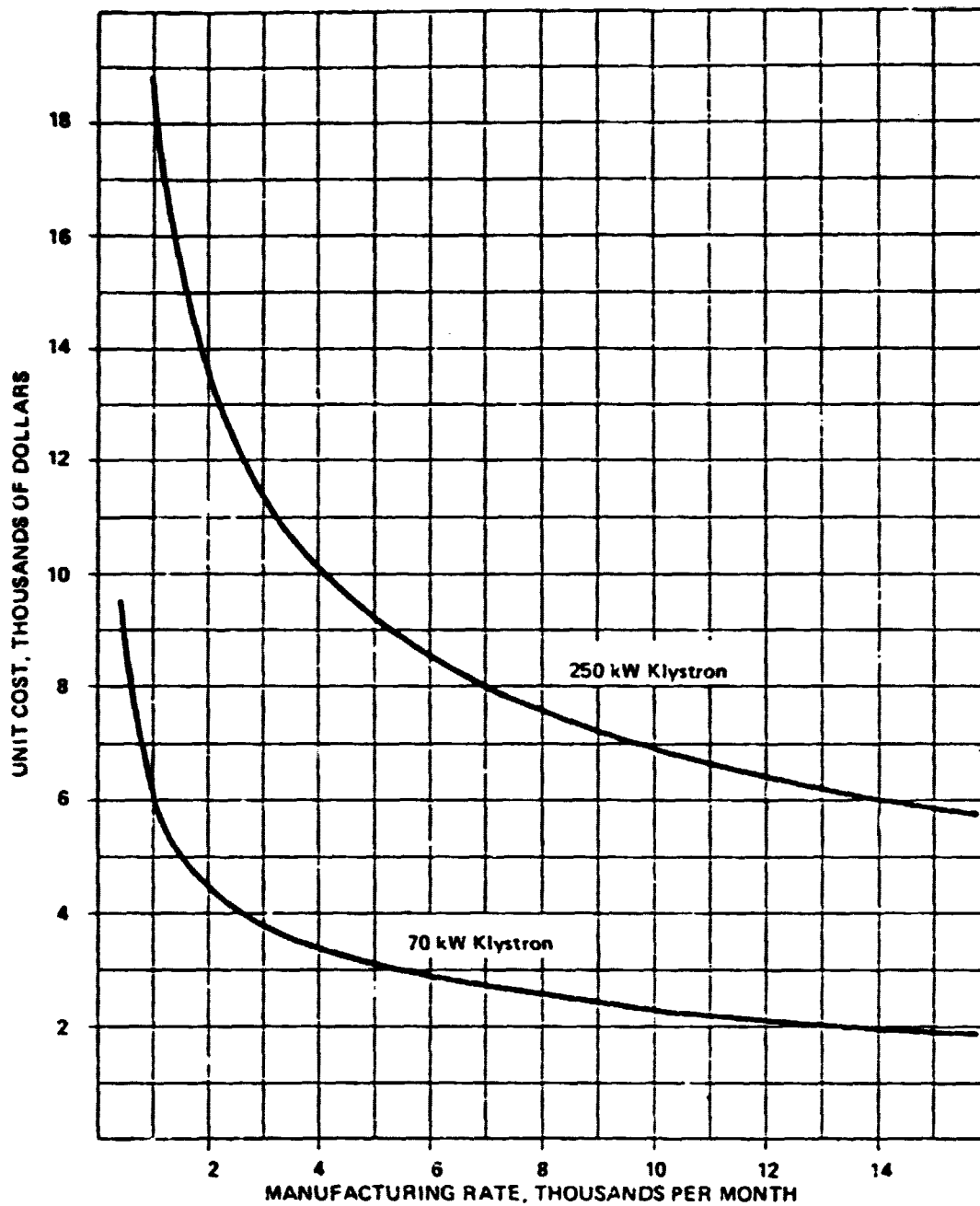


Figure 3.2.6-7 Unit Klystron Cost vs Manufacturing Rate for Large Volume Manufacture

Until recently, receiving antenna (rectenna) costs had received comparatively little attention. Because it was a ground system, it was taken for granted that it would not exhibit a very significant cost. However, the receiving antenna covers a lot of ground area, 50 to 100 km², and therefore is more important than was thought.

The most detailed study of the rectenna has been by the Raytheon Company. They have developed a design for the basic dipole-diode-filter element that is well suited for automated manufacturing and have evolved a semi-automated rectenna construction procedure as illustrated in Figure 3.2.6-8. Raytheon's current cost estimates are approximately \$12.00 per square meter. A more probable median estimate was also constructed at \$21.00 per square meter of ground area. If the receiving antenna is made large enough to fill the entire main beam, rectenna costs are a major cost contributor to system costs as shown in the rectenna cost comparison chart, Figure 3.2.6-9.

The outer part of the beam, however, is very low in intensity. The energy in this part of the beam costs more to collect than it is worth. Accordingly, a rectenna size optimization is possible, as illustrated in Figure 3.2.6-10. The final estimate for the optimal rectenna is summarized in Table 3.2.6-3.

3.2.6.3.3 Space Flight Operations

As a principal issue regarding SPS costs, space flight operations costs have received particularly careful attention.

Transportation Cost

For the most part, aerospace estimating techniques have been used for transportation cost as the production rate for vehicles is not large enough for mass production costs to be applicable. Costs are accrued in three primary and roughly equal categories: amortization of fleet investment plus expendable hardware costs; operations direct and indirect labor costs; and propellant (i.e., energy) costs.

Minimization of fleet investment requires the development of completely reusable launch vehicles. This must be traded against the development investment required to achieve the reusability. In earlier programs, the traffic projections have never justified the development expense. The space shuttle, for example, provides an approximately optimized level of reusability for its projected traffic level. The large traffic projections for a commercialized SPS, however, thoroughly justify a completely reusable space freighter. This is not so much new technology as it is a new market. (Engineering development of the SPS can be accomplished using the Shuttle. The new vehicle is needed for commercialization.)

Operations direct and indirect labor costs for SPS transportation were estimated based on detailed manpower requirements analyses for all task categories; these in turn were derived from Space Shuttle operations plans. Difference factors appropriate to differences in vehicle design, size and launch rate were applied.

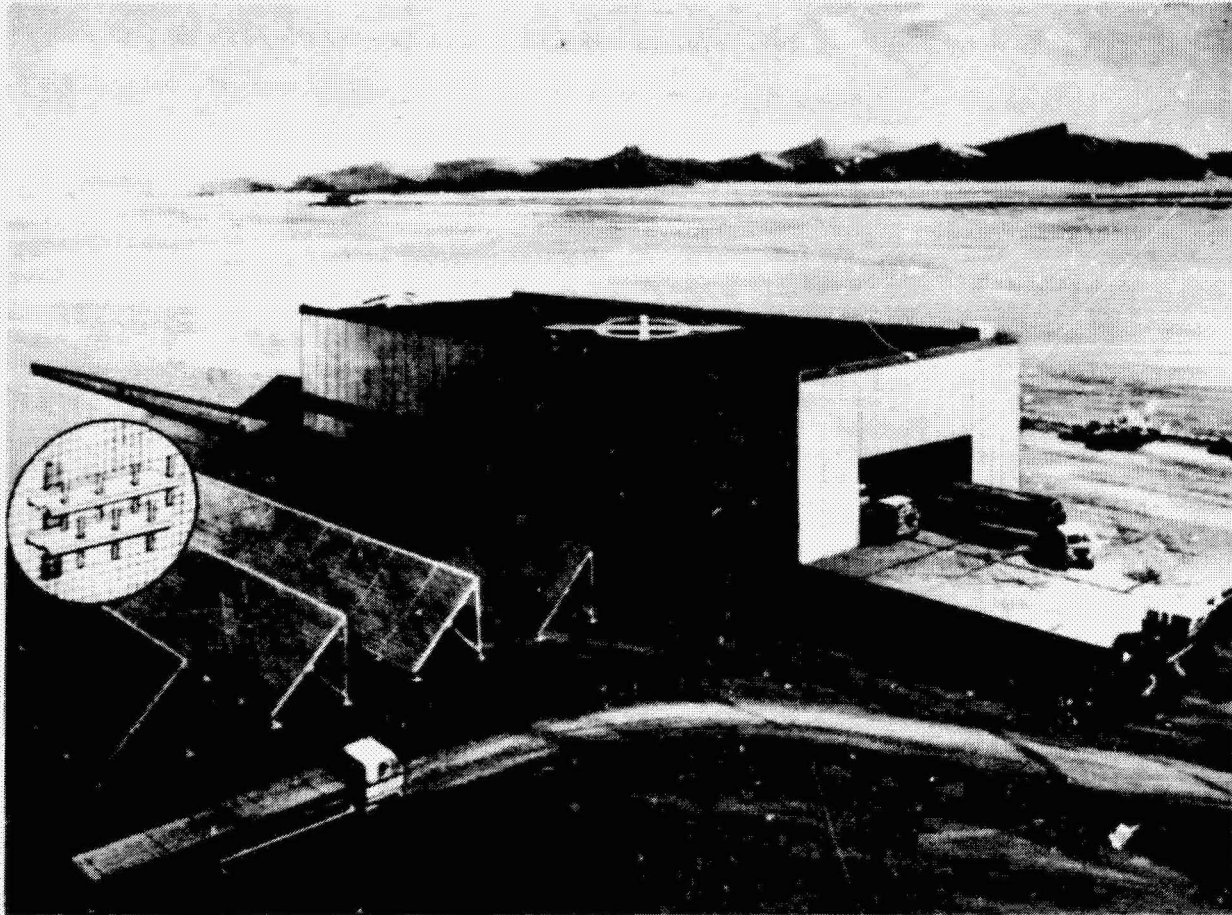
ORIGINAL PAGE IS
OF POOR QUALITY

Figure 3.2.6-8 Artists' concept of a moving rectenna factory. Materials brought in at one end of factory are basic ingredients to high speed automated manufacture and assembly of rectenna panels which flow continuously from other end of factory. Panels are placed on footings also placed in the ground by the moving factory.

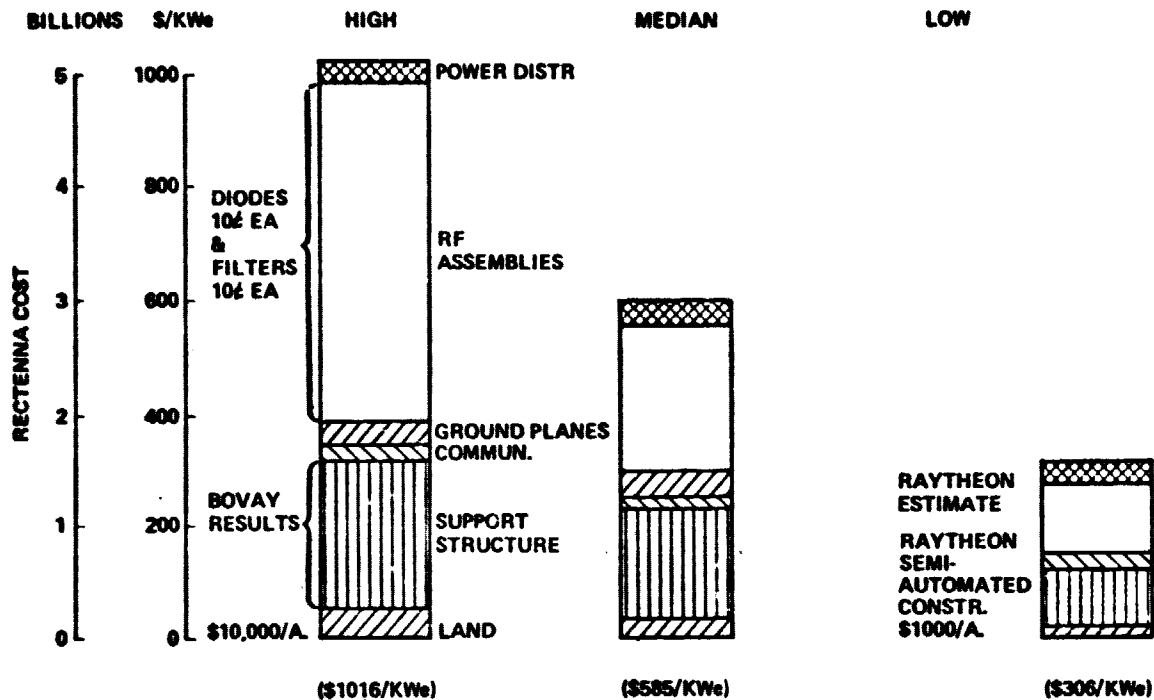
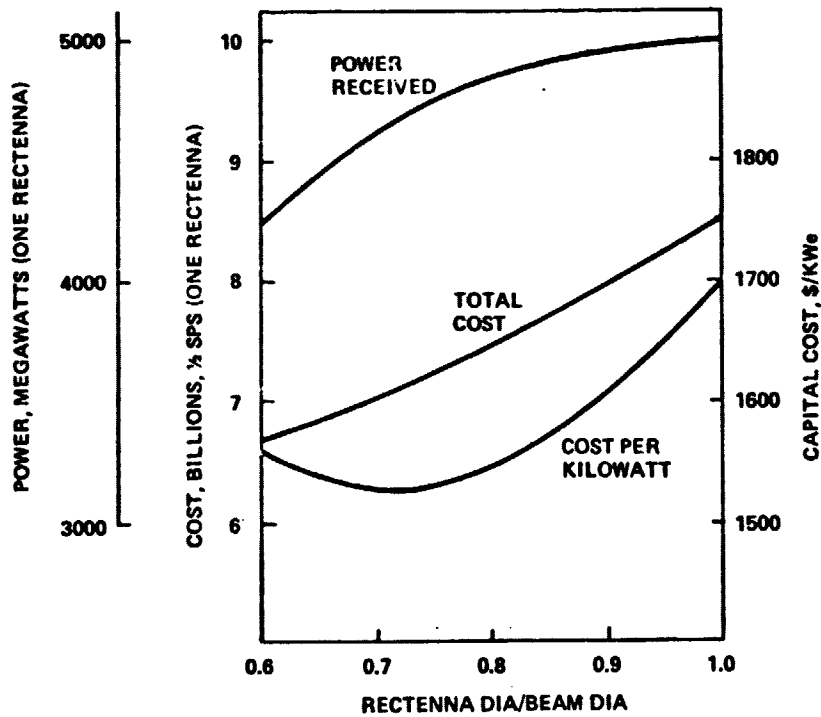


Figure 3.2.6-9 Rectenna Cost Estimates Span Wide Range



(Note: Beam diameter is the entire main lobe to the first null.)

Figure 3.2.6-10 Rectenna Size Optimization

Table 3.2.6-3 Rectenna Nominal Cost Estimate @ 1 SPS/Yr

BEAM DIAMETER	13 KM
RECTENNA INTERCEPT DIAMETER	9.36 KM
RECTENNA GROUND AREA	105 KM ²
RECTENNA PANEL AREA	68.8 KM ²
TOTAL CONTROLLED AREA (LAND AQUIS)	204 KM ² = 50.400 ACRES

WBS	ITEM	ESTIMATING FACTOR	NUMBER	COST/MILLIONS
1.02				
1.02.00	Mult/Common			
1.02.00.01	Land	\$5,000/Acre Acquis & Prep	50,400 Acres	252
1.02.00.02	Prim Structure	\$10/M ²	68.8 KM ²	688
1.02.00.03	Control	\$1,000/Subunit	500 Subunits	0.5
1.02.00.04	Commun			50
1.02.01	Energy Coll/Conv			
1.02.01.00	Support Str/ Gnd Plane	\$3/M ²	68.8 KM ²	206
1.02.01.01	Dipole/Diode/ Filter Units	0.08 Ea @ 70 CM ² /Element	0.983 x 10 ¹⁰	787
1.02.02	Power Distr. Sys.			
1.02.02.01	Busses	Satellite Value		7
1.02.02.02	Processors	\$50/KWe	4.65 x 10 ⁶ KWe	233
				2,223
				= 4,446 for 2 Rectennas

Energy costs can be accurately calculated from propellant quantities determined by flight performance analyses. As noted earlier, the energy cost is 2000 to 4000 kWh_{th} per SPS kw_e installed. Thermal energy from synthetic fuels has been estimated to be as expensive as $2¢/\text{kWh}_{\text{th}}$ about the turn of the century. (OPEC oil is presently about half of that.) At $2¢/\text{kWh}_{\text{th}}$ the worst case energy cost is $\$80/\text{kw}_e$.

Total transportation cost estimates are shown in Figure 3.2.6-11, in terms of cost per flight, for the winged launch vehicle. These figures represent about $\$20/\text{kg}$ to low Earth orbit; $\$45$ to $\$80/\text{kg}$ to geosynchronous orbit, or $\$450$ to $\$800$ per kw_e for SPS installation (propellant costs used in the figure include amortization of propellant production and handling facilities). Two modes of transport from low orbit to geosynchronous orbit were evaluated. Solar-electric self-propulsion yields the lower of the two figures; the higher figure is associated with the use of conventional rockets all the way to geosynchronous orbit.

Cost per flight analyses used the work breakdown structure shown in Table 3.2.6-4. This structure is patterned after the shuttle user charge cost analyses but includes two principal differences: (1) Because the large traffic model will wear out many vehicles, the production of vehicles and their spares is amortized in the cost per flight; (2) Production rates required will demand several shipsets of tooling. The tooling required to achieve the required rates is also amortized against cost per flight.

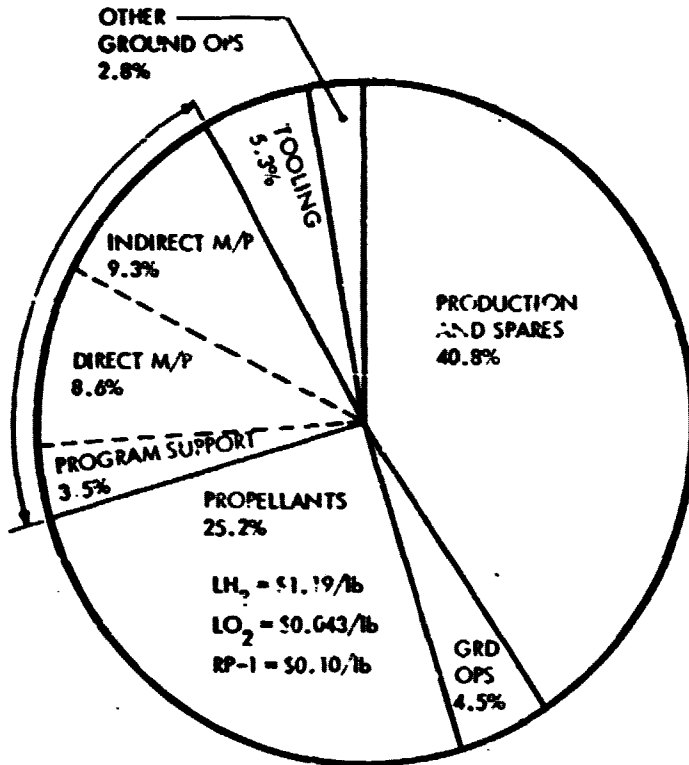
Since vehicle production is the most important component of space transportation costs, it is important to compare the estimates to other similar systems. Shown in Figure 3.2.6-12 are costs in terms of dollars per pound for several aerospace vehicles including commercial aircraft and launch vehicles, as well as the calculated costs for the second stage and first stage of the winged launch vehicle systems. All costs here are expressed as the average costs over 300 units with learning curves applied as appropriate. The commercial aircraft are similar in complexity to the launch vehicles, but a significantly smaller fraction of the overall investment is in propulsion. The S-IC Saturn booster stage is comparable in complexity to the first stage of the wing-wing vehicle. Shuttle costs are seen to be somewhat higher than would be expected from the cost estimates here.

The main cost difference between the shuttle orbiter and the SPS vehicles is that shuttle production uses prototype tooling. Historical data shows manufacturing with prototype tooling to be $1\frac{1}{2}$ times as expensive as with production tooling. However, even if shuttle unit costs were used, the cost of payload transportation would be increased less than $\$2/\text{lb}$.

Manpower cost estimates for conducting the SPS transportation operations were made on a detailed task/timeline/headcount basis including all indirect and direct tasks. The estimates are summarized in Figure 3.2.6-13. They were derived from analogies and extensions of the cost estimating base used to derive space shuttle user charges. In this illustration they are compared with the manpower requirements and fleet sizes for major domestic airlines. The level of overall operations is seen not

ORIGINAL PAGE IS
OF POOR QUALITY

SP-4188



TOTAL COST/FLIGHT = \$7.934M

COST/LB OF PAYLOAD = \$9.20

Figure 3.2.6-11 LEO Transportation Costs for 14 Year Program at 4 Satellites/Year

SP-4190

Table 3.2.6-4 Cost/Flight WBS

WBS ELEMENT
OPERATIONS COST
PROGRAM DIRECT
PROGRAM SUPPORT
PRODUCTION AND SPARES
STAGE 1
AIRFRAME
ENGINES
STAGE 2
AIRFRAME
ENGINES
TOOLING
STAGE 1
STAGE 2
GROUND OPS/SYS
GROUND OPS
GROUND SYS
GSE SUSTAINING ENGR
GSE SPARES
PROPELLANT
OTHER
DIRECT MANPOWER
CIVIL SERVICE
SUPPORT CONTRACTOR
INDIRECT MANPOWER
CIVIL SERVICE
SUPPORT CONTRACTOR

ORIGINAL PAGE IS
OF POOR QUALITY

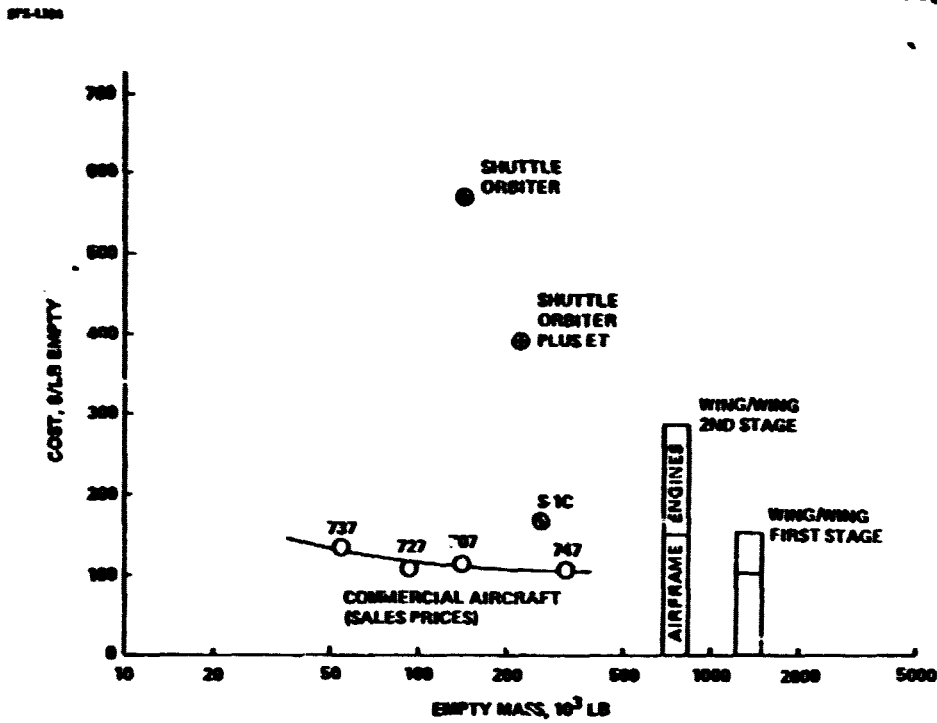


Figure 3.2.6-12 Flight Vehicle Production Hardware Costs

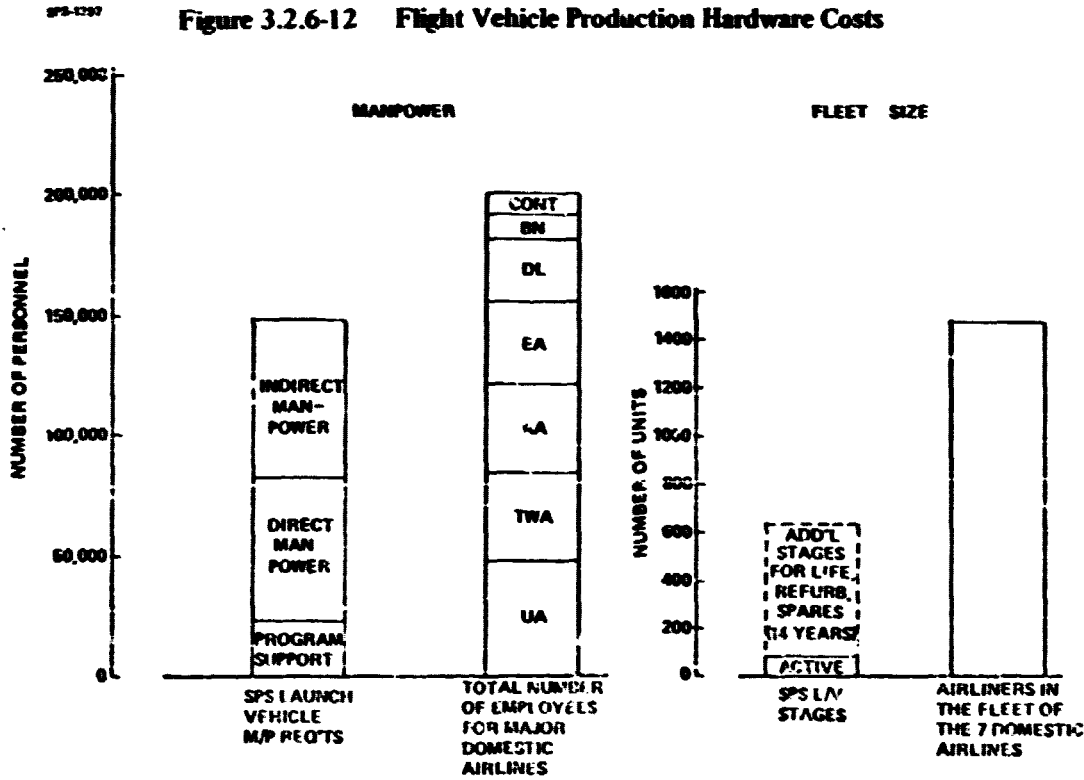


Figure 3.2.6-13 Major Manpower Cost Data and Comparisons

to be beyond the experience of commercial aerospace vehicle operators today and the fleet size active at any one time is very small by comparison to commercial airline operations. The vehicles, of course, are larger, but even if the left-hand bar is scaled according to vehicle size, the comparison of manpower and fleet size between the SPS operations and commercial airlines indicates the manpower allocations for SPS transportation to be quite generous.

Propellant costs are energy costs and, therefore, are of considerable significance in SPS transportation costs. At the left side of Figure 3.2.6-14 are shown the propellant mass and cost distributions for the SPS vehicles. On the right hand side, the SPS propellant cost estimates used are compared with more recent data arrived from Boeing and JSC studies of large-scale propellant cost production. Significantly, the propellant cost estimates used were higher than the more recent estimates, except in the case of RP-1, where the cost was commensurate with production of RP-1 from oil. In the timeframe considered, it may be necessary to use synthetic hydrocarbons produced from coal. This might increase the RP-1 cost significantly, but the RP-1 cost contribution to overall propellants was relatively small and this low estimate is more than compensated by the higher estimates for the other two propellants. Further, if synthetic propellants are employed, a synthetic hydrocarbon such as methane or propane can be produced at lower cost than a synthetic heavy hydrocarbon, such as RP-1.

The cost per flight for the heavy lift launch vehicle is dependent upon annual launch rate, being lower at high launch rates. Actual cost for the SPS systems used the parametric cost per flight data shown in Figure 3.2.6-15. Values ranged from about 13 million dollars per flight for the one SPS per year case with LEO construction to about 7½ million dollars per flight for the four SPS per year case with GEO construction.

Construction

Construction costs have two primary parts: cost of supporting the crew in space and amortization of the construction facilities in space. Crew support costs have been estimated based on the use of a modified shuttle for crew transportation. This is conservative in that a more advanced vehicle might profitably be used, and in that the seating capacity was very conservatively estimated at 75 people (an airline interior in the shuttle cargo bay would easily seat over 100 people). Construction facility and construction equipment must also be amortized into SPS costs.

3.2.6.4 Cost Results Summary

The costs described are summarized in Table 3.2.6-5 and shown in bar chart fashion in Figure 3.2.2-3.2.2-16. Costing details are presented in Volume VI of this report.

The bar chart shows results for eight combinations of energy conversion system, production rate, and construction location. The silicon photovoltaic system has a modest cost advantage over the thermal engine and low Earth orbit construction has a significant cost advantage over geosynchronous construction. The most important cost change occurs with the production rate increase from 1 SPS per year early in the program, to 4 SPS's per year in a more mature operation. Principal cost

SPS-1244

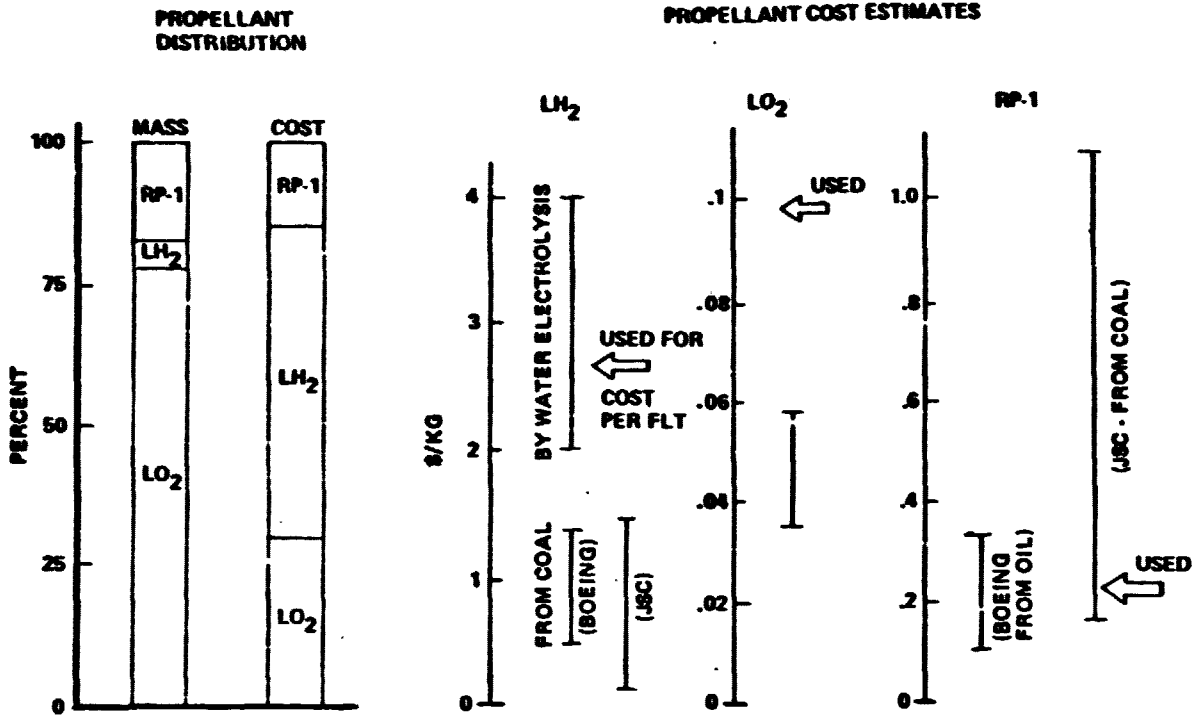


Figure 3.2.6-14 Propellant Cost Basis

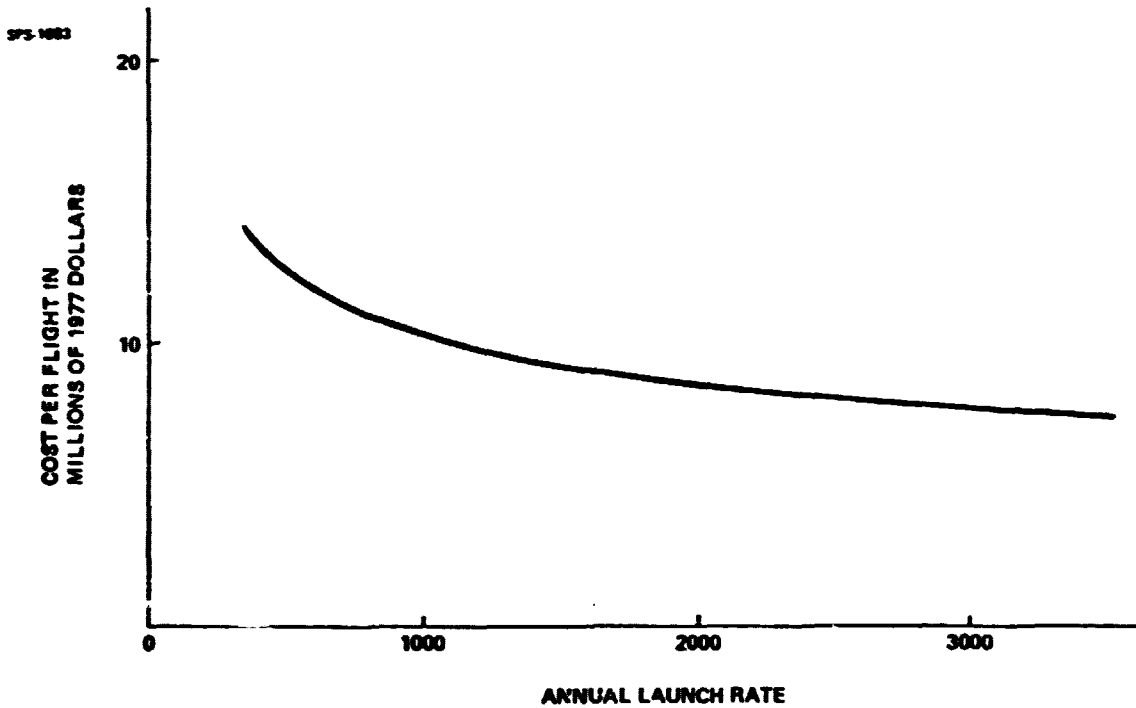


Figure 3.2.6-15 HLLV Launch Costs

Table 3.2.6-5 Cost Summary

	Silicon Photovoltaic				Rankine Thermal Engine			
	1 SPS/yr		4 SPS/yr		1 SPS/yr		4 SPS/yr	
	LEO	GEO	LEO	GEO	LEO	GEO	LEO	GEO
Satellite	7442	7190	5587	5378	7987	7987	5284	5284
Ground Receiver	4446	4446	4000	4000	4446	4446	4000	4000
Construction & Space Support	1109	1126	1109	1126	1716	1768	1716	1768
Space Transportation	6445	9780	4188	6522	7425	11,182	4678	7275
Interest During Construction	1864	1388	1154	851	2068	1563	1215	916
Growth	3450	4034	938	1094	2946	3489	755	903
TOTAL	24,756	27,964	16,976	18,971	26,888	30,435	17,648	20,146

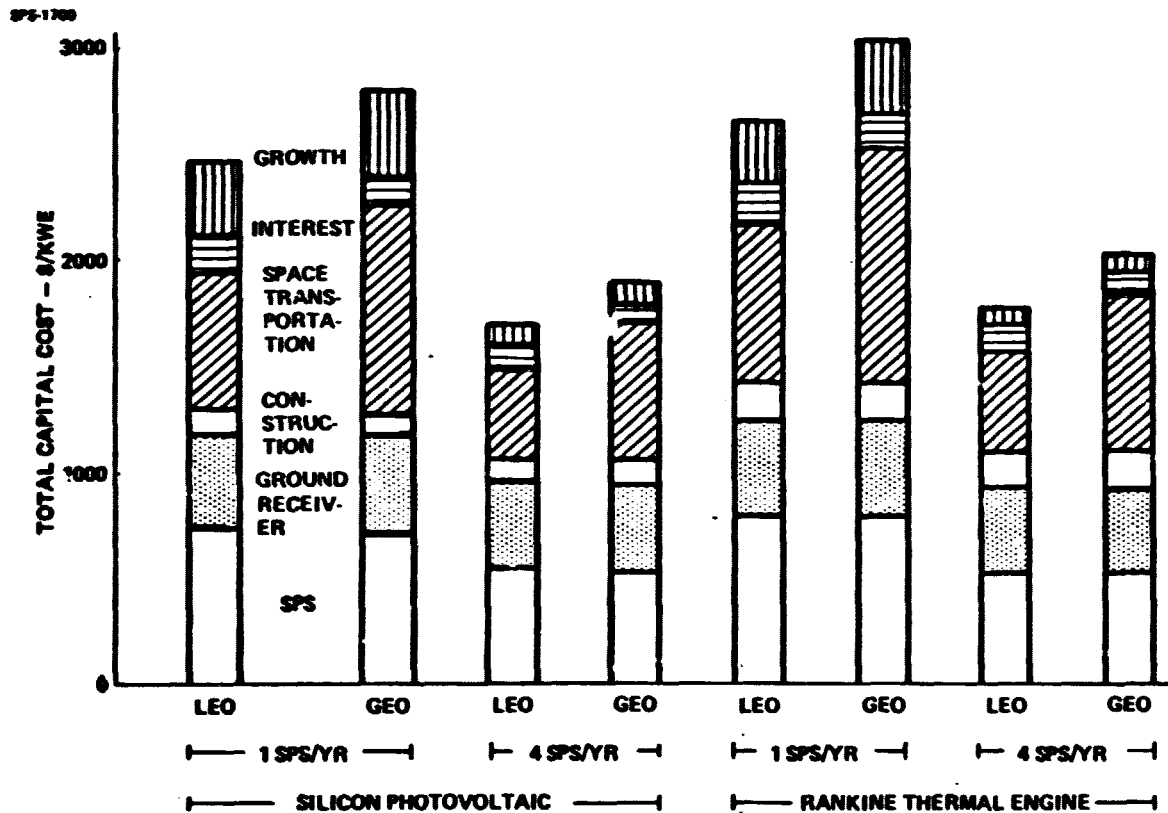


Figure 3.2.6-16 Production Cost Results Summary

reductions with system maturity occur in SPS hardware production, space transportation, and projected product improvement. The lowest capital cost is achieved with the silicon photovoltaic system at 4 SPS's per year with LEO construction. The figure is approximately \$1,700 per kilowatt electric including interest during construction and projected growth. Still lower figures might be projected for advanced systems, such as thin film gallium arsenide.

Achievement of the projected silicon photovoltaic costs is critically dependent on the development of a satisfactory mass production technology for single crystal silicon solar cells and blankets. This mass production technology may require continuous growth processes, but as discussed earlier, recent indications of improvements in the technology presently used for solar cell manufacture, indicate that automation of this technology may provide greater cost reduction than commonly supposed.

The construction time of two years is quite different than the typical terrestrial figure of 8-12 years. This is because building an SPS is a production line operation. Detailed timelines support a period slightly less than two years from beginning to fill the pipeline with SPS parts to beginning of power transmission from space.

The entire process of acquisition of an SPS by a utility would probably take longer. The process of acquisition of land for the receiving site would involve basically the same steps as are required for any other kind of power plant and would undoubtedly take just as long. But essentially all the construction costs are associated with the SPS hardware and space flight operations; this major investment need not begin until about two years before the plant is to go on line.

3.2.6.5 Cost of Electric Power

The bottom line for an SPS system is its capability to produce power at an acceptable cost. The result shown in Figure 3.2.6-17 represents the final result of the costing and uncertainty analyses. Uncertainties for busbar power costs include the uncertainties in unit costs as well as uncertainties in the appropriate capital charge factor to be applied and the plant factor at which the SPS can operate. Capital charge factors from 12-18 percent were considered and the plant factor uncertainty was taken as 70%-90% at one SPS per year and 85%-95% for four SPS's per year. These uncertainties were statistically combined with the cost uncertainties derived by the cost uncertainty analyses.

A study of energy and power costs conducted on IR&D provided the projection of increases in electrical power costs illustrated as the left-hand band of Figure 3.2.6-18. Results from this study are plotted as the right-hand band. This indicates that even with a relatively vigorous program to develop solar power satellites, by the time production installations could begin, the SPS's would be competitive with alternative energy sources.

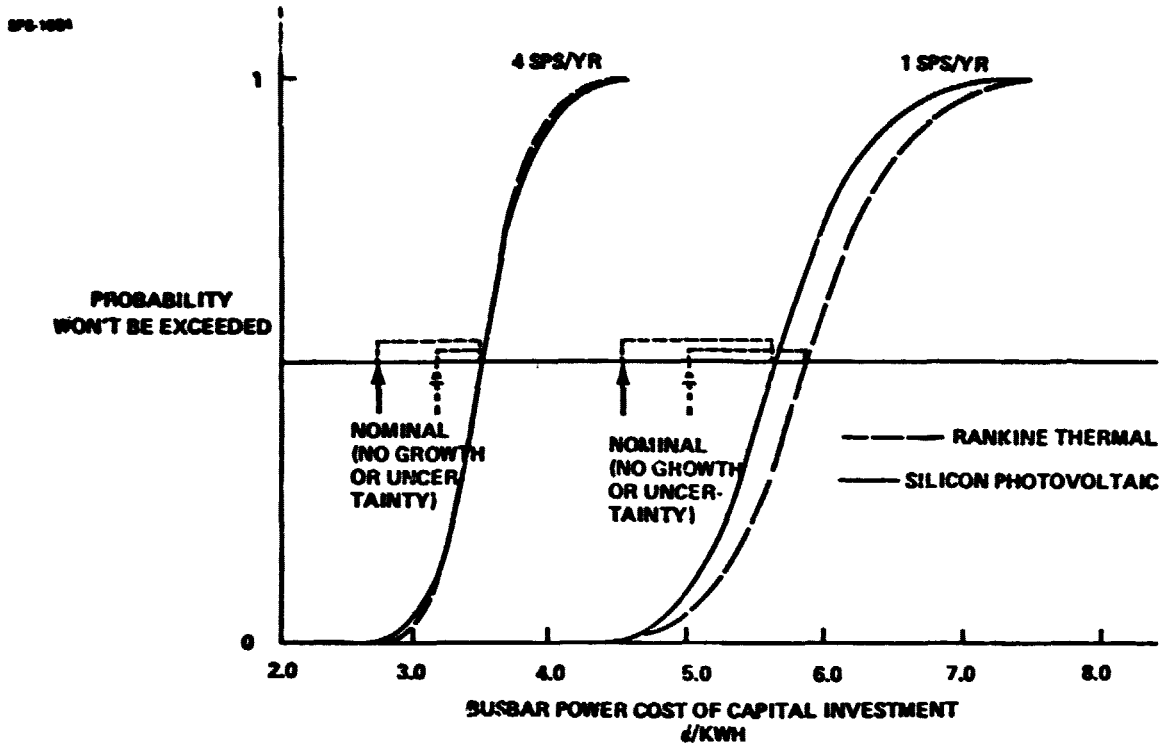


Figure 3.2.6-17 Predicted Busbar Power Cost & Uncertainties

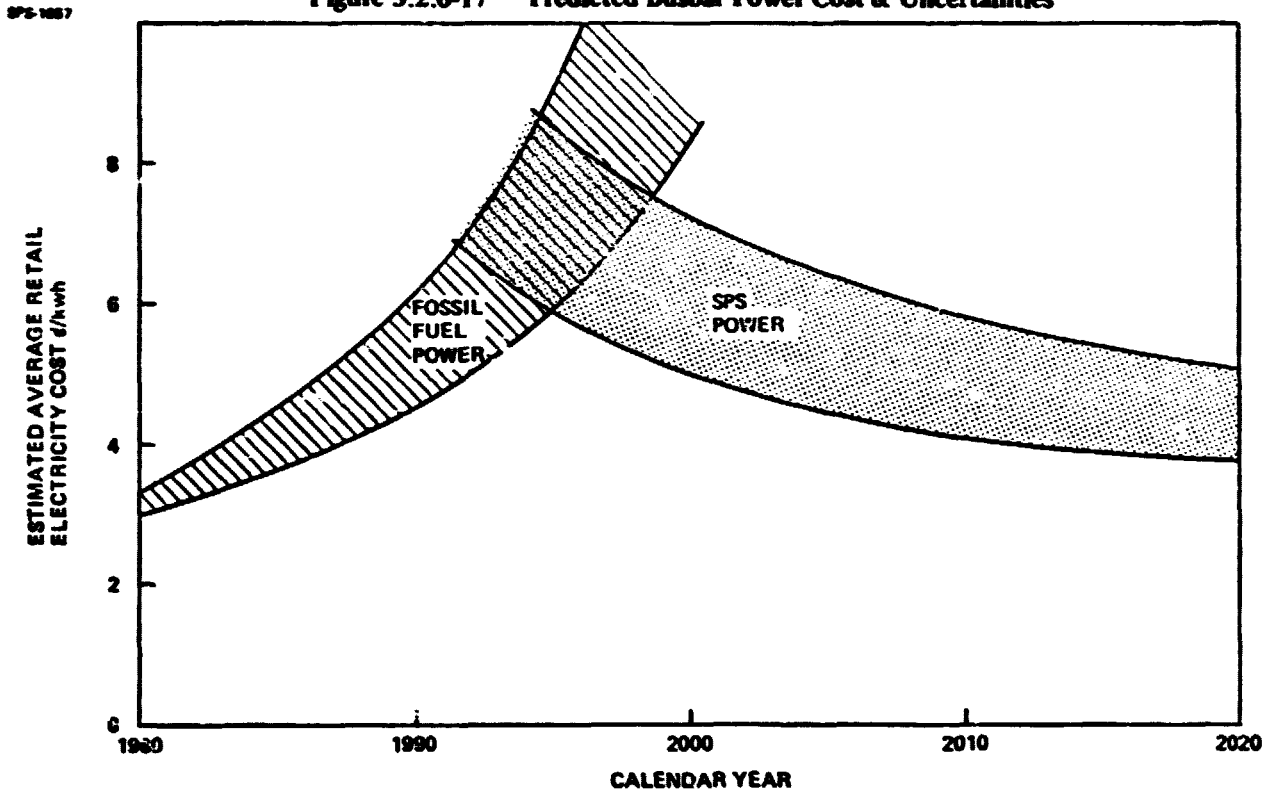


Figure 3.2.6-18 Projections Indicate SPS Power will be Economically Attractive

3.2.6.6 Nonrecurring Costs

An estimate was made of the nonrecurring costs required to construct the first SPS. In order to accomplish this estimate, it was necessary to invoke certain programmatic assumptions. These do not represent conclusions or recommendations as to how an SPS program should be conducted. There are of course many possible program options; no systematic analysis and comparison has been conducted. The assumptions for nonrecurring cost were:

- o After a technology verification program, involving ground and flight programs but no new space vehicles, development of the 10,000 megawatt SPS, and its associated systems begins.

- o The production capacity initially developed is sized for a production rate of one SPS per year.

Figure 3.2.6-19 shows an estimate through the first photovoltaic SPS for LEO construction. (Figures for GEO would be slightly higher.) The cost for the initial SPS was derived by deleting that part of costs for 1 SPS/year associated with amortization of facilities and vehicles to avoid double bookkeeping, and applying a 1.5 prototype factor to the balance. The thermal engine total was also estimated and is about \$8 billion higher, primarily due to the more expensive construction bases.

Note that the cost of SPS development as such is a small portion of the total. Most of the costs are associated with establishing the 10,000 megawatts per year production capability and with development of the associated space flight operations systems. The number 1 SPS itself is also a large cost item.

SPS-1040

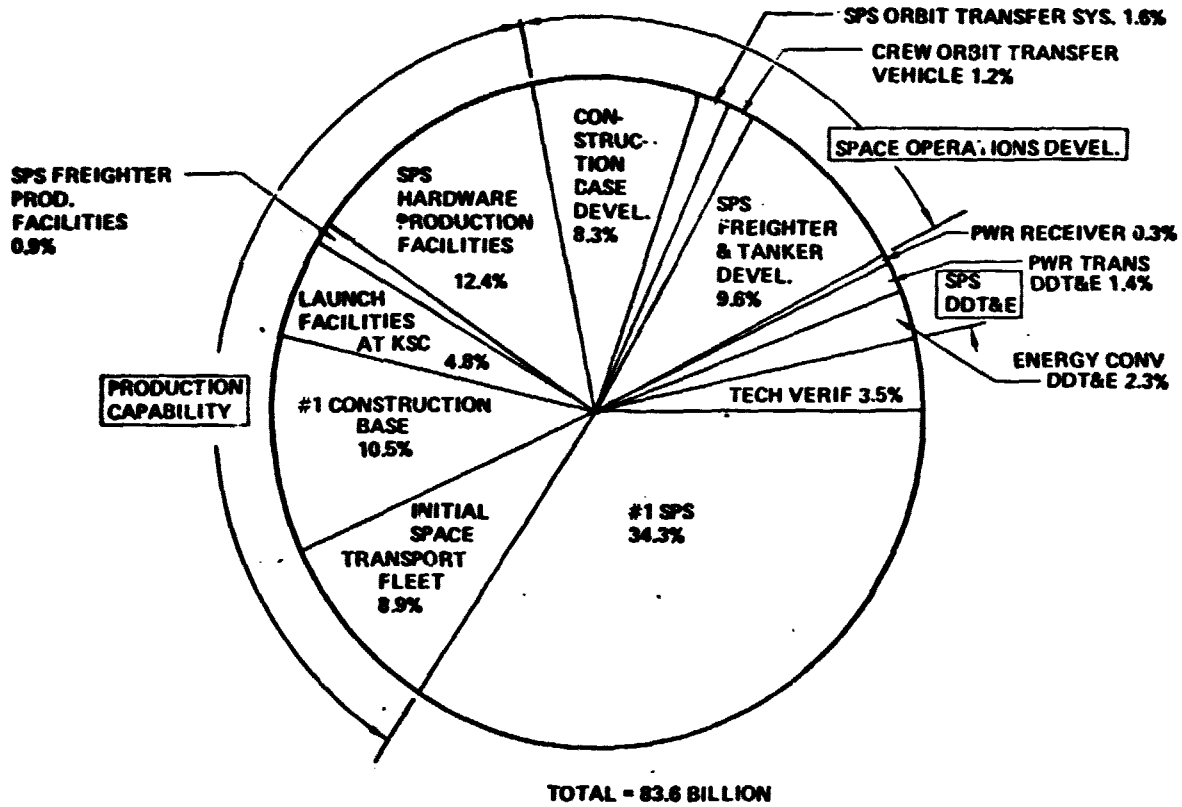


Figure 3.2.6-19. Total Costs Through #1 SPS Photovoltaic System

4.0 TECHNOLOGY VERIFICATION NEEDS

Establishment of firm designs, performance levels, cost expectations, development requirements, and environmental acceptability, depends on the achievable characteristics of several critical technologies. Although overall success of SPS development is possible over a range of performance of these technologies, establishment of specific attainable performance levels is important to establishment of designs and system specifications. Accordingly, technology verification can presently be regarded as a key schedule constraint for potential availability of SPS-derived energy. Because of this importance of technology verification, detailed recommendations have been developed:

4.1 GROUND-BASED (NON-FLIGHT) TECHNOLOGY VERIFICATIONS

General areas include energy conversion, materials, structures, electrical systems, RF systems, flight control, space transportation, space construction operations, and space environment effects.

Energy Conversion

If sufficiently low costs can be achieved, solar cells are preferred for energy conversion. Recommended solar blanket technology efforts include automated cell production by conventional and novel means, automated blanket assembly, development of prototype blanket element designs, radiation effects investigations and solar cell annealing, high voltage array operation, and advanced solar blanket (e.g., gallium arsenide) development.

These technology developments will confirm solar cell and blanket design parameters, performance and production methods and increase confidence in costs, providing a sufficient knowledge base to allow preparation of solar blanket hardware design specifications appropriate to an SPS program. Recommended funding in the first year is 2.5 million with aggregate over a five year program of 16 million.

Until near-term low cost production of photovoltaic solar blankets is assured, it is prudent to carry a backup technology program for the thermal engine energy conversion option. Recommended efforts include engine design studies and critical component testing, automated space welding/brazing techniques, solar concentrator model testing, meteoroid penetration testing, zero-g heat transfer investigations, and lightweight generator technology development. Most of these technology areas are applicable to SPS design and development even if thermal engine SPS's are never built.

These activities will establish design parameters, subsystem performance, and provide a sufficient knowledge base to allow preparation of thermal engine and other design specifications appropriate to an SPS program. Recommended funding in the first year is 2.5 million and the aggregate over five years is 16 million. Given early success in the photovoltaics effort, the thermal engine technology effort could be reduced in scope.

Materials

Materials testing and development are recommended in the areas of plastics and composites, life and properties in the space environment, bonding and fastening techniques for space construction, moderate-to-high temperatures composites, thermal control and other coatings, and special-purpose alloy development.

These technology items are required for selection of materials, setting of allowable stresses and other design conditions, and detailing of space assembly processes, appropriate to achievement of SPS designs suitable for 30 to 100 years' operating life. Recommended funding in the first year is 1.5 million and the aggregate over five years is 10 million.

Structures

Fabrication and tests of representative structural elements and joining devices should be conducted to establish confidence in prediction methods for structural strength and dynamics for these thin gage lightweight structural elements. Tests and analyses are also needed to improve predictions of structural thermal response and precision in the operating environment. Achievement of very small structural responses to thermal fluctuations can greatly simplify SPS design, especially in the power transmitter. Recommended funding in the first year is 0.75 million; the aggregate over five years is 8.75 million.

Electrical Systems

Electrical systems technology items include fast switchgear and components for RF amplifier arc suppression, high efficiency lightweight power processors (about 15% of the SPS onboard power requires processing), conductors, high-temperature semiconductors, high-power slip rings and lightweight electric power storage. These activities are needed to select and establish electrical power distributions and processing design parameters and to permit preparation of design specifications. Recommended funding in the first year is 1.5 million, the aggregate over five years is 12 million.

RF Systems

The power transmission system is at the heart of the SPS system. Its performance and operating characteristics are critical to establishment of the overall system design parameters as well as cost estimates. The design of the power transmitter requires integration of interacting structural, electrical, RF, thermal control, and flight control parameters. Although there is considerable design flexibility in the RF system in terms of altering design parameters to adapt to component/subsystem performance level, successful operation of a design, once the parameters are set, is dependent on achieving specified component/subsystem performances. Therefore, technology verification in this area is particularly important.

Specific items include development of laboratory prototype RF amplifier tubes, phase control circuitry, and antenna subarray hardware, leading to a prototype integrated subarray, supplemented by

ionosphere heating tests, radio frequency interference testing and design standards development, exploratory development of high efficiency, high temperature solid state amplifiers, and development of receiving antenna elements. The recommended verification program will provide the knowledge base for subsystem/component specifications and for selecting system design parameters. Recommended funding in the first year is 6 million dollars; the aggregate over five years is 37 million.

Flight Control Systems

A development effort on theory, algorithms, and software is needed to add confidence to the techniques appropriate to control of the large, flexible SPS spacecraft. A small effort on sensors is also appropriate. Recommended funding in the first year is 0.5 million, with an aggregate of 4 million over the five-year period.

Space Transportation

Achieving projected low costs for space transportation is important to economic attractiveness of SPS power. Studies have verified, to the extent possible by study, these low costs. Key technology verification needs include zero-g propellant transfer, a new booster engine, high-power electric propulsion, fully reusable (e.g., watercooled) launch vehicle heat shields, oxygen/hydrogen-fueled auxiliary propulsion, and on-orbit servicing of vehicles. (The recommended work on the last item involves design studies for checkout, maintenance, and hardware changeout equipment and techniques.) The booster engine will be the schedule limiter for the advanced launch vehicle system. Upper stages can use the Space Shuttle Main Engine. The recommended technology effort will support the initiation of development of the low-cost transportation system. Recommended first-year funding is 4 million with a five-year total of 36 million.

Space Construction

Construction of SPS's will involve the operation of a final assembly factory in space. Critical technologies include automated fabrication of space structures, closed life-support systems, means of in situ structure integrity verification, docking and berthing of large space systems, development of construction operator accommodations and provisions, and construction base onboard logistics systems. These activities will provide technology verification support development of construction bases and their equipment inventory. Recommended first-year funding is 3 million and the five-year aggregate is 22.5 million.

Space Environment

A modest study and analysis effort to improve knowledge and predictability of space environment effects is needed. Included are meteoroid, plasma and fields, and energetic radiation. Recommended first-year funding is 2 million for a five-year total of 11 million.

Totals

The total ground based technology verification program is summarized in Table 4-1. The first-year total is about 25 million with a five-year total of 170 million. Table 4-2 presents a more detailed description of the specific recommended technology items. Priorities indicated have the following meanings:

- (1) Very important to an SPS program decision.
- (2) Could probably be accommodated within a development effort, but precursor technology program would significantly reduce risk.
- (3) These technology items would support development of advanced SPS's with improved performance and reduced cost. Their leverage is great enough to merit early technology efforts.

4.2 FLIGHT TEST TECHNOLOGY VERIFICATION

The recommended flight program is presented below. It includes an interferometer spacecraft experiment, shuttle sortie flights, and a solar power technology demonstrator in the power range 250 kw to 1000 kw, constructed and tended in low Earth orbit by the space shuttle. Costs for this program are less well defined; estimated totals are 50 to 100 million for the interferometer spacecraft, 675 million for shuttle sorties, and 2.1 billion for the solar power demonstrator including design, development, launches, construction, and the complete experiment program.

Fabrication Tests

Objective Demonstrate in the space environment all critical fabrication processes to be used in the space construction of SPS's:

Specific Tests--

- Structure (beam) fabricators
- Mechanical fastening
- Fusion welding and brazing
- Ultrasonic welding of composites
- Bonding

Implementation Shuttle sortie flights.

Environment

Objective --Improve definition of space environmental factors important to SPS construction, operation, and life.

Specific Tests

- Metals, plastics, and composites outgassing and properties changes under representative SPS conditions.

Table 4-1 SPS 5 Year Technology Development Plan*

TECHNOLOGY AREA	YEARS					TOTAL
	1	2	3	4	5	
o SOLAR CELLS	2.5	3.6	3.85	3.7	2.6	16.25
o THERMAL ENGINES & THERMAL SYSTEMS	2.5	3.5	3.75	3.5	2.5	15.75
o MICROWAVE POWER TRANSMISSION SYSTEM	6.0	7.5	8.75	8.5	6.5	37.25
o SPACE STRUCTURES	0.75	2.0	2.2	2.0	1.8	8.75
o MATERIALS	1.5	2.0	2.5	2.0	2.0	10.0
o FLIGHT CONTROL SYSTEMS	0.5	0.8	1.0	0.9	0.8	4.0
c CONSTRUCTION SYSTEMS	3.0	4.0	4.5	5.5	5.5	22.5
o TRANSPORTATION SYSTEMS	4.5	7.5	8.75	7.5	7.5	35.75
o POWER DISTRIBUTION AND CONTROLS	1.5	2.0	2.5	3.5	2.5	12.0
o SPACE ENVIRONMENTAL FACTORS	2.0	2.6	2.45	2.2	2.0	11.25
TOTALS	24.75	35.50	40.25	39.3	33.7	173.5

* Does not include any required space testing
Funding in millions of dollars

Table 4-2 Recommended Technology Studies

AREA	IMPORTANCE	SUGGESTED ANNUAL FUNDING	PRIORITY
SOLAR CELLS			
o Continuous Growth Processing (Work With ERDA Program)	Solar Cell costs are a significant SPS cost driver. Cell efficiency has the greatest effect on SPS size of any identified parameter.	\$1M	1
o Automated Blanket Assembly	SPS size (approx. 100 square kilometers) requires large quantity of cell blanket. Automation required to achieve low cost and high production.	\$1M	1
o Prototype Blanket Dev.	Materials compatibility in space environment must be identified. Radiation degradation and annealing must be quantified.	\$0.25M	1
o Radiation Effects & Annealing	Radiation Effects are the largest identified Photovoltaic SPS performance degradation parameter. Annealing offers method of recovery from radiation degradation.	\$0.25M	1
o High Voltage Arrays with Voltage Switching & Regulation	High voltage array design data is lacking. Voltage regulation at the array level simplifies power processing requirements.	\$0.25M	1
o Thin-Film GaAs Cells	The use of GaAs solar cells offers the potential for significantly reducing SPS size and mass. Gallium reserves are finite. Thin-film cells reduce Gallium usage.	\$0.5M	3
TOTAL		\$3.25M	

Table 4-2 Continued

<u>AREA</u>	<u>IMPORTANCE</u>	<u>ESTIMATED APPROXIMATE FUNDING</u>	<u>PRIORITY</u>
<u>THERMAL ENGINES & THERMAL SYSTEMS</u>			
o Engine Detail Design Studies & Critical Component Testing	The development of thermal engines with 30 year + life is required. System weight reduction is strongly affected by peak cycle temperature.	\$1.0M	2
o Automated or Semi-Automated Pipe Welders for Space Use	Large numbers of fluid tight joints are required. Automated pipe welders will greatly increase construction rate and decrease orbital construction personnel requirements.	\$0.5M	1
o Hi-Volume Production of Heat Pipes	T/E SPS radiators require huge quantities of heat pipes. Problem similar to P/V SPS solar cell production.	\$0.5M	1
o Concentrator Test Models	A change in concentrator efficiency of 1% affects SPS size by 1%. Concentrator test models will provide performance data scalable to SPS size.	\$0.15M	2
o Meteoroid Penetration Testing	T/E SPS contain large areas of pressurized piping for which meteoroid penetration protection is required. Techniques for weight minimization of meteoroid penetration protection require testing.	\$0.1M	1
o Ceramic Heat Exchangers	Successful development of a ceramic heat exchanger technology would allow raising gas cycle temperatures to 1000, resulting in reduced mass and increased efficiency.	\$0.5M	1
o Zero G Heat Transfer	Assessment of the disturbing forces resulting from a variety of heat transfer devices operating over a range of heat transfer conditions is required.	\$0.15M	2
o Generators	Development of highly efficient, lightweight, generators required to minimize generator and radiation cooling system mass.	\$0.25M	2
<u>MATERIALS</u>		<u>TOTAL</u>	
		\$3.15M	
o Plastics & Composites Life & Properties in Space Environment	Radiation degradation effects on thin-film reflectors and composite structures impact SPS size and mass. Effects on 30 year life must be ascertained.	\$0.3M	1
o Bonding & Fastening Processes for Space Use	typical bonding and fastening processes is required for applications ranging from basic structural elements to thin sheet aluminum conductors	\$0.3M	1
o High Temperature Composites	The HPTS antenna requires an extremely stable flat surface over a variety of thermal conditions including various sun angles and ecliptic response.	\$1M	1
o Thermal Control & Other Coatings	The compatibility of thermal control surfaces with a space plasma/charging environment is not known. Applications range from sheet conductors to heat pipes.	\$0.1M	2
o Alloy Development	Present peak cycle thermal engine temperatures are limited by available alloys. Weight reduction can be effected by increasing peak cycle temperature.	\$0.3M	2
<u>STRUCTURES</u>		<u>TOTAL</u>	
		\$2M	
o Design Allowables and Practices for Space Structures	Current technology must be advanced to provide capability for analysis of elastic-plastic stresses in a complex stress field for thin gauge metals and composites. Building block element technology is required.	\$1M	1
o Joints & Fasteners	Candidate joining and fastening techniques applicable to SPS construction must be developed and analyzed for strength, electrical conductance and/or other properties.	\$0.25M	1
o Structural Response & Precision Under Operating Environments	Correlation is required for analysis and test results of SPS structure to the operating environment including loads, ecliptic response, sun angle variation, etc.	\$0.5M	1
<u>TOTAL</u>		\$1.75M	

Table 4-2 Continued

<u>AREA</u>	<u>IMPORTANCE</u>	<u>SUGGESTED ANNUAL FUNDING</u>	<u>PRIORITY</u>
<u>ELECTRICAL - (Ground & Space)</u>			
o Fast Switchgear & Components	Klystron mass optimization and failure protection requires very fast switch gear operation to prevent damage to tubes.	\$0.5M	2
o Super-Efficient, Lightweight power Processors & Components	Approximately 15% of all SPS power requires processing; Processors are a major SPS weight item. Efficient processors will reduce power generation and radiator mass.	\$1M	2
o Thin Film Sheet Conductors	Thin film sheet conductors optimize conductor mass in the space environment. Data base needs developing for installation techniques, thermal control, and response to induced loads.	\$0.25M	2
o High Temperature Components	Radiators for SPS power processors are very large due to temperature limits of silicon semiconductors. Development of gallium arsenide semiconductors will allow for higher temperature operation with a concomitant radiator size reduction.	\$0.25M	3
o Rotary Joints	High current transfer at high voltage required across rotary joint. Brush/slip ring combinations required. Design for 30 year life.	\$0.25M	1
o Induced Electric Power Storage	Storage of large quantities of energy is required for periods of occultation and maintenance. Improvement in specific weight and charge/discharge cycle life would reduce SPS mass.	\$0.25M	3
TOTAL		\$2.45M	
<u>RF SYSTEMS</u>			
o Prototype Klystron a. Efficiency, noise, & general performance b. Heat-pipe cooling c. Production technology	Klystron efficiency is directly proportional to SPS size. Large quantities required per SPS. Long life required to minimize maintenance. Integral cooling simplifies MPTS thermal control.	\$2M	1
o Amplitrons - Same	(Same as Klystron above)	\$2M	1
o Phase Control Methods & Circuitry incl. tests	The total phase control system will be complex and sophisticated. Phase control affects both the antenna steering and propagation pattern.	\$1.5M	1
o Environmental Effects a. Ionosphere heating b. RFI	Present limits on RF power density is based on theoretical ionosphere heating limits. RFI impacts on global communications and navigation systems and radio astronomy are not well defined. These interactions must be assessed.	\$1M	1
o Subarray Hardware a. Waveguides-tolerances & losses b. Overall precision c. Rfr. Techniques	Waveguide efficiencies directly affect SPS size. Tolerances are extremely small in order to achieve good patterns. Manufacturing techniques must be developed for either earth or space fabrication of antenna sub-arrays.	\$0.5M	1
o Hi-Temp. Hi-Eff'y Transistor RF Amp.	Transistorized RF-DC converters offer an attractive alternate to klystrons and amplitrons particularly with regard to service life since cathode erosion is not a problem with solid state devices.	\$0.15M	3
o Antenna Elements	The rectenna is a major SPS cost element. Rectenna elements (diodes, filters, dipoles, etc.) must be mass produced at low cost while retaining performance characteristics of present lab hardware.	\$0.3M	2
TOTAL		\$7.45M	

D180-22876-2

Table 4-2 Continued

AREA	IMPORTANCE	SUGGESTED ANNUAL FUNDING	PRIORITY
<u>INTERFEROMETER S/C</u>	Many questions with regard to PPTS performance can be answered using an interferometer spacecraft. Some items are ionospheric effects, phase control atmospheric perturbations, antenna steering, and mechanical tolerances.	\$10M (peak)	1
<u>FLIGHT CONTROL SYSTEMS</u>			
• Theory, Algorithms, & Software	Attitude control of the SPS will require filtering the motions caused by the flexibility of the main spacecraft. The initial tools for incorporating a realistic flexible model into the flight control system must be developed.	\$9.4M	1
• Sensors	High accuracy, long life sensors are required for attitude reference of large flexible spacecraft. Antenna pointing requirements impose extremely accurate correlation of SPS and rectenna locations.	\$0.4M	2
<u>TRANSPORTATION</u>	TOTAL	\$0.6M	
• Propellant Transfer	SPS Leo-Geo orbit transfer schemes (self-powered COTV, or POTV) require propellant transfer from HLLV to orbit transfer vehicles. Propellant transfer effects and techniques for large scale operations must be determined.	\$0.25M	1
• Booster Engines	In order to maximize payload and minimize recurring costs, advances are required in areas of specific impulse improvement, weight reduction, and service life. Transportation costs are major SPS satellite cost driver.	\$2M	2
• Space Engine (existing program is adequate)	(Same as Booster Engines above)	(existing program)	2
• Electric Propulsion Thrusters Processors Flt. Control	Significant payload and performance benefits accrue through use of this technology for application in LEO-Geo orbit transfer and SPS station keeping.	\$2M \$1M \$0.15M	1
• Advanced Heat Shields	The development of reusable space transportation system will require the use of lightweight heat shields capable of multiple flights in order to lower recurring costs.	\$0.5M	2
• Residuals Utilization	For single-stage-to-orbit and the upper stage of multi-stage transportation vehicles, propellant residual allowance is directly related to payload.	\$0.25M	2
• LO ₂ /LH ₂ APS	The use of only two consumable propellants will simplify orbital operations. The use of monopropellants for APS adds another propellant plus a pressurizing medium.	\$0.5M	2
• On-orbit servicing	The development of operations scenarios must be established for orbital based launch complexes. Check-out, maintenance, engine changeout techniques, etc. must be established.	\$0.5M	1
<u>CONSTRUCTION</u>	TOTAL	\$7.15M	
• Automated Fabrication of Structure	The area of the SPS is approximately 100 square kilometers. Construction requires automated fabrication of all elements to the fullest extent possible. Reduction of transportation cost requires that payload densities exceed those achievable with pre-fabricated or deployable structures.	\$2M	1
• Closed Life Support Systems	Closed cycle life support systems will reduce the quantity of consumables replenishment thereby reducing construction costs. The use of expendables rather than regenerable systems for long duration missions result in high logistics costs.	\$2M	2
• Structure Integrity Verification	Concepts must be developed to verify or "proof test" large scale light weight structural elements or "building blocks" used in SPS system structural design.	\$0.5M	1
• Large System Docking	A concept for SPS construction proposes modular construction of the SPS with docking and attachment of large modules. Modules must be maneuvered into position and attached. The concept allows smaller construction bases.	\$0.5M	2
• Construction Operator Provisions (Cam, Controls, Displays, LSS)	Development of construction techniques with remote operators will influence SPS design. Remote operator controls, displays, and life support systems must be designed for both manufacturing and quality assurance.	\$1M	2
• On-Base Transportation	Large scale construction base operations require the movement of large quantities of construction materials, equipment, and personnel between warehousing and hotels and work areas on the construction base.	\$0.5M	2
	TOTAL	\$1.5M	

Table 4-2 Continued

<u>AREA</u>	<u>IMPORTANCE</u>	<u>SUGGESTED ANNUAL FUNDING</u>	<u>PRIORITY</u>
<u>SPACE ENVIRONMENT</u>			
o Plasma Effects	SPS solar cell arrays, thermal control surfaces, power distribution systems, and other elements contain a large number of dielectric materials in the space environment. There is evidence of adverse interactions of these materials with the space/plasma environment.	\$0.5M	1
o Meteoroid Environment Model Improvement	The size of the SPS makes it vulnerable to meteoroid damage. The meteoroid model needs improvement to better predict meteoroid damage, assess protection requirements, or determine preferential orientations available to minimize collision probability.	\$0.25M	1
o Radiation Environment Definition, Effects, & Shielding	SPS system elements are susceptible to radiation damage. Solar cells and reflecting membranes suffer loss of performance when exposed to radiation. Radiation effects on personnel have been investigated. SPS operational and construction radiation environment require better definition in order that proper protection can be provided to sensitive items and personnel.	\$1M	2

D180-22876-2

Implementation—Shuttle sorties and geosynchronous long duration exposure facility (LDEF). The latter could be placed at GEO by an IUS and samples later retrieved by a manned GEO sortie when the latter capability is developed.

- Space plasma and radiation environments—emphasis on better definition of low to moderate energy radiation environments and plasma effects.

Implementation—Measurements aboard suitable spacecraft. Existing programs such as SCATHA and ISEE can provide much of the needed information.

- RF/microwave propagation—Signal-power-level simulation of power transmitter beam steering and phase control over actual geosynchronous range.

Implementation—Shuttle/IUS-launched geosynchronous microwave interferometer spacecraft. The spacecraft concept is shown in Figure 4-1. RF transponders on the boom tips would simulate the large aperture of the power transmitter. The transponders would be synchronized and phase controlled by methods being tested for power transmitter application. Ground measurements of the interference patterns produced by the interferometer transponders would determine the performance of the phase control techniques.

SPS Power Generation and Power Transmission

Objective—Demonstrate critical technology applications and operation in the space environment.

Specific Tests

- Power generation—operate large solar arrays at moderate to high voltage.
- Power transmission—operate prototype klystron modules in space conditions. Test open and closed envelope tubes. Measure and assess RF arcing problems in evacuated waveguides under various temperature and outgassing conditions.
- Electric propulsion—test high power (≈ 100 kw) thrusters. Measure thruster plasma/solar array interactions.
- Space-based solar cell annealing tests.

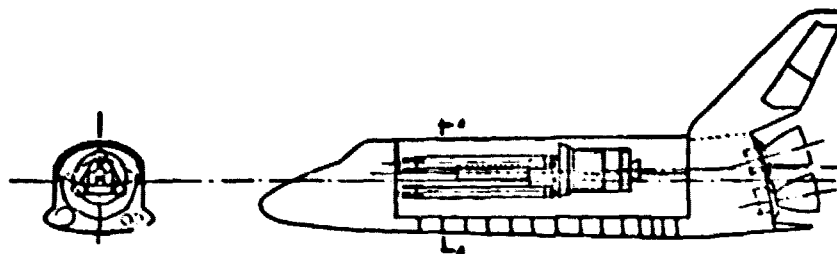
Implementation—

Initial—Shuttle sortie flights.

Final—Large Power Module: Up to 1000 kw of solar-electric power at LEO.

(Thermal environment tests may require operation of up to nine 70 kw klystron modules requiring about kw_e .) Array voltage switchable up to 3000 volts. "Test bench" configuration to allow conduct of various power generation, power transmission and propulsion tests.

Annealing tests could be preceded by electric-propelled LPM sortie into lower van Allen belts with return to 450-500 km orbit for tests.



SPACECRAFT & IUS PACKAGED IN SHUTTLE

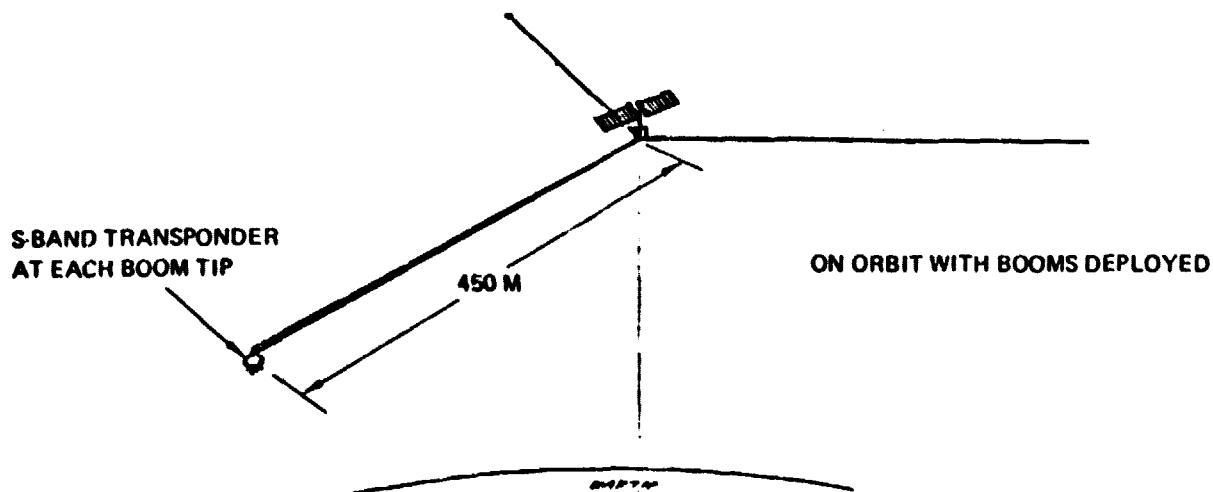
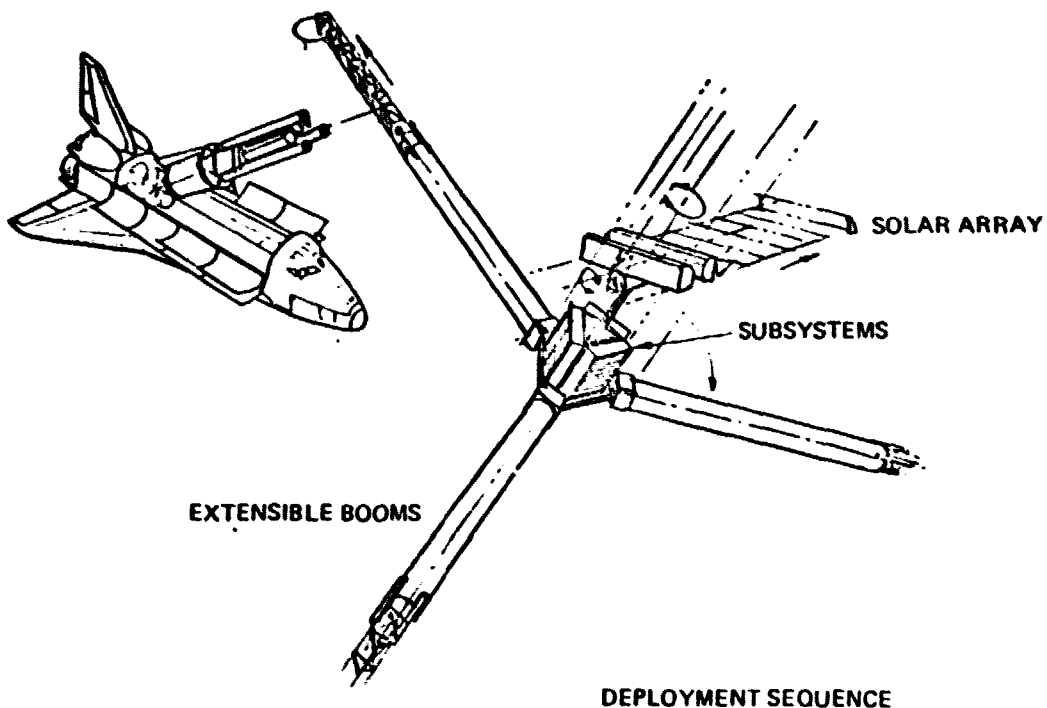


Figure 4-1 Interferometer Spacecraft Concept

LPM test program primarily automated with support by periodic shuttle sortie flights.

The total ground and flight program is summarized in Figure 4-2.

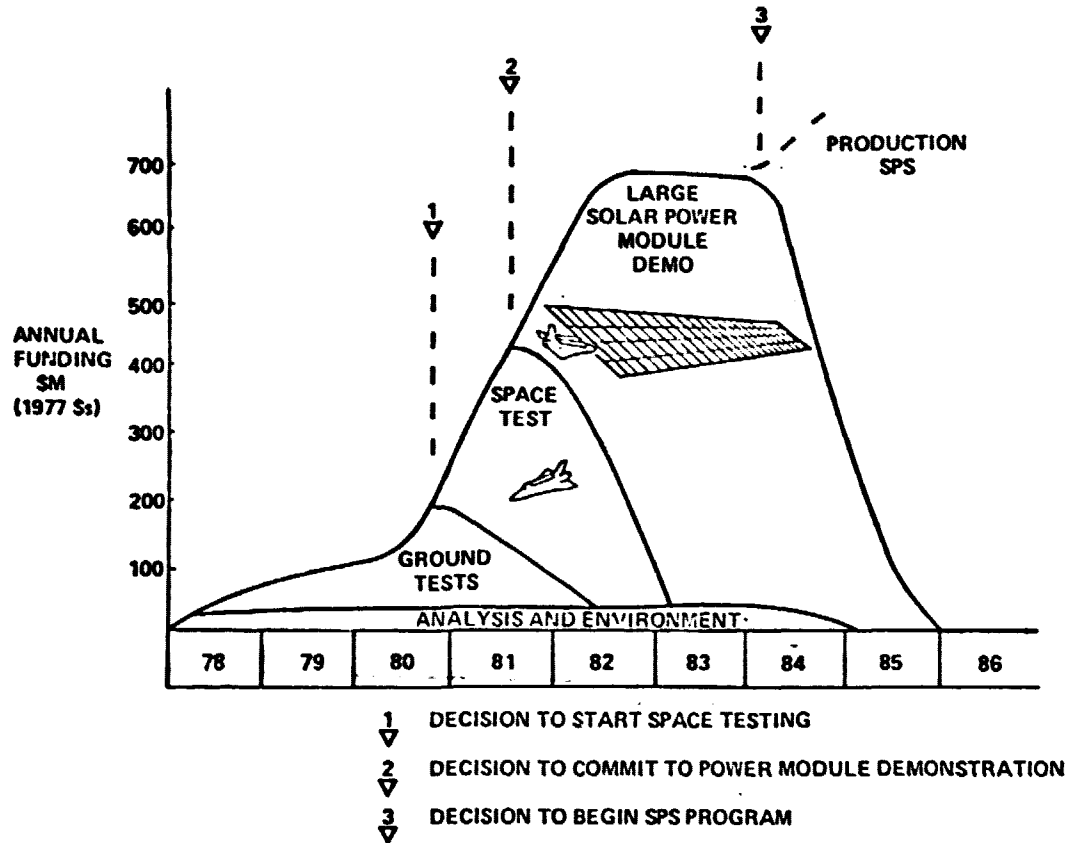


Figure 4-2 The Verification Phase: First Step to SPS

5.0 DISCUSSION OF SPS PLANNING ISSUES

This section presents a discussion of the SPS planning issues that were appended to the NASA Statement of Work for the SPS System Definition Study.

A. Subprogram Area: Systems Definition

SPS Objective—Define the candidate Solar Power Satellite (SPS) systems which are capable of supplying a significant portion of the future United States electrical energy requirements at costs equal to or less than alternative nondepleting sources.

- (1) What is the mass, acquisition cost, operating cost, and reliability of a SPS network built utilizing the technology available now, in 1980, 1985, and 1990, respectively?

Answer

This study emphasized the definition of SPS systems utilizing base technology generally available now to 1980. Several areas of technology verification and refinement were identified as discussed in Section 4 of this volume. Also discussed in Section 3.2.6 of this volume are the masses, acquisition cost, operating cost, and availability estimates. The principal technology advancements expected to become available in the next 10 years that would significantly influence SPS mass and cost are those in advanced photovoltaics, such as thin film gallium arsenide. An advanced high efficiency, thin-film photovoltaic technology could reduce system cost by 10 to 15%. It should be noted that the greatest cost leverages appear to be in the development of production and operations technologies appropriate to large scale installation of SPS's. It is believed that these technologies will mature as a result of the development and deployment of SPS systems.

- (2) What is the confidence level of each of the technology forecast utilized in answering the first question? What are the impacts upon basic feasibility and costs of over or under estimation of the figures of merit of each parameter of the technology forecasts? Which of those forecasts may be in error without significant impact?

Answer

Confidence levels were addressed by the uncertainty analyses. Relative significances of the uncertainties and elemental technologies were discussed as a part of the uncertainty analyses discussion in Section 3.2.5 of this volume. Power transmission system link efficiency, space operations cost, and receiving antenna costs, appear to have the greatest leverage on overall system cost and feasibility. Sensitivity of the SPS's to solar cell cost was less than suspected. This sensitivity is discussed in Section 3.1.3.

D180-22876-2

- (3) What is the expected change in each candidate SPS concepts' mass and cost characteristics as a multiple-decade program matures? Can ongoing research and development be applied to improve the characteristics of the later satellites and their ground complex? What is the extent of improvement given a R&D activity parallel to operational deployment constrained only by talent and facilities? What fraction of this unconstrained R&D effort appears to be cost effective? In what areas should the effort be concentrated?

Answer

Expected changes in the candidate SPS concepts, mass and cost characteristics during the early to middle parts of an SPS program were discussed under the cost analyses section of this volume. The nature of the SPS system is such that continuing research and development will be highly effective in accomplishing product improvement and cost reduction. Detailed analyses of parallel product improvement programs were not conducted. Again, the major leverages appear to be in power transmission link efficiency, space operations costs, and receiving antenna costs.

- (4) Are there natural limits to growth of an SPS network? What present or planned activities of terrestrial society might be adversely impacted by placement of such a network? How may these impacts be ameliorated?

Answer

Limits to the growth of an SPS network appear to be sufficiently far removed to be of little practical interest at this time. Numbers of satellites greater than 1,000 would certainly be feasible. Sociological impact analyses were beyond the scope of this study.;

- (5) What are the alternative paths which might be pursued in establishing an SPS network? What are the details of the technology advancement phase, prerequisite to commitment to large scale experimental satellites? When must major decisions be reached in order to begin commercial power generation (1000 MW or more) by 1988? by 1992? by 1996? What are the issues to be resolved in order for each major decision to be reached? What are the criteria for proceeding? For stopping?

Answer

Alternative paths were not investigated. The technology verification phase was specifically characterized and is described in Section 4 of this document. The minimum length of a program reaching commercial power generation appears to be 12 to 15 years. Development of the basic space operations technology could occur in about the length of time required to accomplish the manned lunar landing, that is, roughly 8 years. However, once this technology is operational, about 4 years would be required to establish the construction base in space and construct the first SPS. The technology verification plan addressed the technical issues to be resolved; other issues such as environmental and sociological impact were outside the scope of this study.

D180-22876-2

- (6) What management, ownership and responsibility structure is suitable for each phase of an SPS program? What involvement is appropriate of non-government groups in the conduct of each phase? Are there issues which require intergovernmental activity?

Answer

This question was not investigated.

- (7) What are the favorable and adverse impacts to society which may be consequent to a technology advancement phase of an SPS program? Of a pilot plant or demonstrator unit? Of a small network? Of the limiting case (or very large) network? How may these impacts be handled to maximize benefits, minimize penalties and permit progress to continue?

Answer

This question was not investigated.

B. Subprogram Area: Microwave Energy Technology

SPS Objective—To transmit 5×10^6 kw over a distance of 3.6×10^4 km by means of a pilot-signal steered phased array antenna at an overall DC-DC efficiency of 65-70%.

- (1) What performance characteristics of key components including DC-RF converter noise and efficiency and rectenna efficiency were assumed in the system studies? Are these attainable? What technology is needed to meet system requirements?

Answer

Performance characteristics of the components are discussed in brief in Section 3.2.1 of this volume and in detail in Volume 4. Detailed study of the critical performance characteristics indicated little doubt that these characteristics could be obtained by the technology verification program discussed in Section 4 of this volume.

- (2) Can an adaptive phase control system that electronically positions the microwave beam to within one arc-second be realized? What technology is required?

Answer

Several approaches to adaptive phase control have been identified by the various studies. Two of these are discussed in some detail in volume 4. Study results indicate that the desired performance can be achieved by appropriate application of existing base technology. The performance requirements, however, are demanding and a technology verification effort is needed to confirm predictions and techniques.

D180-22876-2

- (3) What candidate antenna waveguide and structural materials were assumed in the system studies? Can these materials satisfy the mechanical and thermal constraints, including thermal cycling? What technology is needed to meet the requirements?

Answer

Graphite composites were assumed because they can satisfy the constraints and requirements. The graphite composite waveguides would be metal plated on the inside to reduce losses. This information is discussed in more detail in Volume 4.

- (4) What are the mechanical tolerances that can be maintained in the fabrication of 10-20 meter long, thin-walled waveguides?

Answer

Mechanical tolerances are discussed in detail in Volume 4 with an analysis of the errors resulting from the various mechanical tolerances. These errors were included in the link efficiency analyses.

- (5) What antenna structural configurations and subarray segmenting techniques will satisfy the requirement of maintaining mechanical alignment to several mm over the one km diameter array?

Answer

Structural configurations for the antenna are discussed in Volume 4. These appear to be adequate to meet the mechanical alignment needs. Mechanical alignment to several millimeters is not literally required since electronic phase control can compensate for large-scale mechanical error. The principal tolerance and precision requirements are at the subarray level. The radiating face of the subarray for example, must be flat to within a few millimeters and it is highly desirable to have an overall antenna configuration that is relatively unaffected by thermal changes.

- (6) What are the effects of the interaction of GEO plasma, ionosphere plasma and the Earth's atmosphere on a 5 to 10 gigawatt power beam and the pilot steering beam?

Answer

This question was not investigated. An experimental program is needed to define these interactions. Such experimental programs are discussed under the technology verification section of this volume.

C. Subprogram Area: Environmental Effects

SPS Objective—Assure acceptable impacts on the ground, in the atmosphere, and in space, when steadily delivering 500-2000 GW of electric power to the ground by microwave beams that originate from 100-200 satellite power stations located in geosynchronous orbit.

- (1) What types of vehicles and propellants did the system studies assume for launch to low Earth orbit, operations there, transfer from LEO to GEO, and stationkeeping, attitude control, and operations in GEO? What types of emissions are produced by these vehicles using these propellants? For a system of 100-200 power satellites, each delivering 5-10 GW of power on the ground, what total mass of exhaust pollutants and chemical reaction products per year are produced on the ground, in the atmosphere, and in space during (a) buildup of the system, and (b) steady operation?

Answer

Transportation system characteristics, propellants, types of emissions, and quantities of emissions are discussed in Volume 5 of Part 1 of this study and Volume 5 of Part 2.

- (2) What microwave frequency was assumed in the system studies for power transmission to the ground? What analyses and experiments are needed to assess potential interference (RFI) with other users of the radio frequency spectrum?

Answer

The microwave frequency is 2.45 gigahertz. Analyses and experiments required are discussed in the technology verification section of this document.

- (3) What power density levels and distributions in the microwave beam did the system studies assume (a) at the transmitting antenna, and (b) at the rectenna on the ground? What are the power densities during beam passage through the ionosphere? What analyses and experiments are needed to assess the effects on the ionosphere of 1, 100, and 200 such microwave beams? What analyses and experiments are needed to estimate the microwave field on the ground near to and far from the rectenna due to taper of the main beam and due to the sidelobes, for a system of 100-200 satellite power stations and total ground power levels of 500-2000 GW? How can the impact on man be assessed due to (a) acute exposure to the main beam and (b) chronic exposure to low intensity microwave fields? How can long term ecological effects be assessed?

Answer

Power density level at the transmitter was no greater than 23 kw/m² because of thermal limitations. At the receiving antenna on the ground the peak beam intensity was limited to 23 mw/cm². Ionosphere densities are essentially the same as the ground level densities. Limited

D180-22876-2

information on ionosphere effects of these beams can be obtained by ground based ionosphere heating tests. Analysis of farfield microwave intensities for multiple satellite systems were not investigated. These fields can be predicted by analysis and further investigation is needed. Environmental impacts were outside the scope of this study.

- (4) If the rectenna is 85-90 percent efficient, 10-15 percent of the energy in the beam may be released as waste heat. What analyses and experiments are needed to assess potential heat island effects, flora and fauna impacts, and potential land utilization?

Answer

Heat release from the receiving antenna was not investigated by this study. (A heat release analysis was performed by JSC and effects were estimated to be negligible.)

D. Subprogram Area: Space Structures

SPS Objective—Very large area, minimum weight, controllable structures configured for construction in space.

- (1) What candidate structural materials are candidates for the system studies? Can these materials satisfy the lifetime requirements and mechanical and thermal constraints, including thermal cycling?

Answer

The primary structural material assumed was graphite composite because of its indicated ability to satisfy mechanical and thermal constraints including thermal cycling. Additional information on the lifetime of this material in the space environment is needed. This can be obtained by appropriate technology verification activities as recommended in Section 4 of this volume.

- (2) What structural configurations will satisfy the conflicting requirements of minimizing weight while maximizing rigidity?

Answer

Tubular truss structures can meet these requirements. Various means of producing tubular truss structures have been investigated and appear feasible.

- (3) What is the feasibility and cost-effectiveness of manufacturing structural modules in space?

D180-22876-2

Answer

The packaging density of these structures is so low as to make necessary either assembly of the structures from nested elements, or production of these structures by structure fabrication devices commonly called "beam machines." Either approach appears to be feasible and cost effective.

- (4) What thermal control problems are present in SPS structures? How can thermal control be provided?

Answer

The best thermal control approach is to utilize a structural material that is insensitive to thermal changes.

- (5) What is the optimum balance between earth and space assembly operations?

Answer

A complete analysis of this question was not made. The answer appears to be that earth assembly is preferred to the extent it can be accommodated while still operating the space transportation system in a mass limited mode. The cost of volume-limited launches is so great that space assembly operations are probably preferable. This places a considerable premium on large volume payload bays for launch vehicles.

- (6) What structural configurations, consistent with mechanical and thermal requirements, are adaptable to automated assembly in space?

Answer

A number of structural configurations were investigated and all were adaptable to automated assembly in space. Either continuously-formed beams or assembled beams made of nestable elements are feasible.

E. Subprogram Area: Power Conversion (Including power processing & distribution)

SPS Objective—Multi-gigawatt power conversion systems, configured for assembly in space and designed for 30-year life, with a very low mass per unit area and a cost of several hundred dollars per kilowatt.

- (1) What performance characteristics of key power conversion components and subsystems were assumed in the system studies? Are these characteristics attainable? What technology is required?

Answer

Performance characteristics of the power conversion components are discussed in this volume, in Volume 3 and in Volume 6. These characteristics were determined to be attainable by the technology verification program described in Section 4 of this volume.

- (2) What overall performance characteristics of candidate power conversion systems have been assumed in the SP5 system studies? What technology is needed to achieve such overall performance?

Answer

Overall performance characteristics are similarly described.

- (3) Which of the candidate power conversion systems is most attractive for this application from the viewpoints of performance, feasibility, reliability and cost?

Answer

The power conversion system that presently seems to be most attractive is single crystal silicon photovoltaic, as discussed in this volume.

- (4) What are the design tradeoffs required to accommodate high voltage/plasma interactions and electrical charging of large structures in geosynchronous orbit?

Answer

This question was not specifically addressed. Design procedures to accommodate electrical charging appear to be available and basically consist of making the entire system sufficiently conductive to avoid excessive charge differential buildups.

- (5) What is the optimum balance between earth and space assembly operations?

Answer

The answer was given under question 5 of the previous subprogram area.

- (6) How can power transfer be accomplished across the power system/antenna interface?

Answer

An electrical rotary joint employing slip ring technology is well within the state of the art. The slip ring design is discussed in Volume 3 of this report.

- (7) How can the power turn-on, turn-off transients best be handled in the switching, circuit protection and voltage regulation areas?

Answer

Systems were designed to handle these transients by incorporating switch gear and circuit breakers in the power collection system and in the power processing and regulation system on the transmitting antennas.

- (8) What are acceptable techniques for power collection, regulation, switching and protection which satisfy the rectenna/load interface requirements?

Answer

The designs developed for power collection, regulation, switching, and protection satisfy the rectenna and load interface requirements as presently understood. These are discussed in Volume 3.

F. Subprogram Area: Attitude Control and Stationkeeping

SPS Objective—(a) Stationkeep and mechanically point a 1-km diameter microwave transmitting antenna to within ± 1 minute of arc in geosynchronous orbit. (b) Stationkeep and mechanically point a very large solar array to within ± 1 degree of arc in geosynchronous orbit. (c) Stationkeep and attitude control the structures during assembly, and control them during orbit transfer.

- (1) What types of control devices (e.g., ion thrusters) did the system studies investigate? What performance levels were assumed for the devices? Should alternate types of devices and performance levels be evaluated? Are the assumed or alternate devices available? Is technology advancement required? Are the technology requirements affected by:
- (a) the structure characteristics (rigidity or flexibility, integral modular construction, inertia, vibrational modes)?
 - (b) thermal deformations of the structure during steady state and during the transients arising from short period orbits in LEO and recurrent eclipses in GEO?
 - (c) steady, pulsed, or commanded operational modes?
 - (d) the 30-year lifetime requirement of the satellite?
 - (e) the need to minimize pollutant emission?
 - (f) the need to minimize system weight?
 - (g) other factors?

Answer

The principal control device investigated was ion thrusters for the overall SPS configuration. The accumulated momenta appeared to be too large for practical momentum exchange devices. Magnetic torquing is conceivable but might be unreliable in the variable magnetic environment at geosynchronous orbit. Momentum exchange devices appear to be entirely practical for aiming the antenna and can be unloaded by applying torque to the antenna from the SPS. The momentum unloading then is accomplished by the ion thrusters on the SPS

D180-22876-2

itself. The principal area of technology advance required is scaling up of existing ion thrusters to larger size and developing the high power processors. Control system analyses indicated that simple control techniques and software are adequate, that the structural dynamics can be maintained at a high enough frequency so that they do not intermix with control responses. Ion thruster ISP's were selected in order to minimize weight. Because of the long system lifetime, it is expected that maintenance of the attitude control system will be required. An additional factor is the need to establish control authority and correct the satellite attitude in an instance where control has been temporarily lost and the satellite is not sun-facing. Under such a circumstance, a backup chemical thrust system is needed and was included in the system definition.

- (2) What types of data sensing, data processing, and device actuation and control systems did the satellite system studies postulate? What performance levels were assumed? Should alternate data sensing, processing, actuation, and device control systems, and performance levels be investigated? Are the assumed or alternate systems available? Is technology advancement required? Are the technology requirements affected by:
- (a) requirements on response times and accuracies?
 - (b) automated response requirement?
 - (c) sensor and electronic interface with the antenna phase front control system?
 - (d) other factors?

Answer

Analysis of data sensing was confined primarily to measurement lists. The nature of the lists does not indicate any serious problem in meeting the requirements by the data processing capabilities presently under development.

- (3) What requirements exist on satellite tracking and data acquisition? What technology advancements are needed?

Answer

Satellite orbit maintenance should be based on determination of the satellite ephemeris by the interaction of the satellite and its ground station in order to minimize requirements on separate tracking networks. No unusual data acquisition needs were identified except for the potential total processing load requirements resulting from many satellites being in place. Again, most of this requirement should be handled between each satellite and its ground station to minimize need for separate networks.

- (4) What requirements for materials and structure technology are implied?

Answer

No specific requirements were identified other than those identified by other investigations.

G. Subprogram Area: Transportation

SPS Objective—Transportation of all goods and personnel necessary to construct and emplace an operational space power station network at the least possible total program cost. Preliminary analyses indicate that transportation costs in the \$50 to \$20/Kg range may be achieved. The former target cost is needed if the SPS mass is near the upper bounds of the preliminary estimates while the latter cost may be acceptable for the lighter weight SPS concepts.

(1) HLLV

- (a) What are the expected RDT&E and TFU costs of candidate HLLV configurations ranging in size from 150 to 1000 metric tons of payload per launch?
- (b) What are the expected recovery and refurbishment costs of the vehicle stages (1 or 2) comprising each candidate HLLV concept? Comparison of winged and ballistic recovery, water and land touchdown, and flyback or ground traverse of stages.
- (c) What are the anticipated personnel staff sizes required for each concept to perform pre-launch and launch ground operations, mission planning, flight control and support (including sustaining engineering)? How do these manpower levels vary with launch rates consistent with the placement of 100×10^3 to 2500×10^3 metric tons per year into LEO?
- (d) What are the facility acquisition and operational costs to support the flux rate of (c)?
- (e) What are the propellant requirements of the candidate HLLV's to fulfill (c), including those fluids consumed at the launch site but not launched? What is the energy budget to produce these fluids in the quantities required? What are the environmental impacts of their expenditure in the biosphere, including pre-launch, launch and entry/recovery/servicing mission phases?
- (f) What requirements are placed upon the national material resource/refining/ground transportation structure to acquire and operate the fleet of HLLV's for the SPS program? Can material conservation/substitution programs reduce dependence upon scarce or imported resources?
- (g) What new/innovative technology may be developed, for use in the 1990-2025 interval (may be several stages, time phased) to enhance the cost-effectiveness or decrease any adverse effects of the launch activity of (c)?
- (h) What are the consequent costs per flight and costs/kg of payload of the candidate concepts as a function of size and launch rate? What confidence is present in these estimates? What graceful fallback positions are available for each area capable of jeopardizing either program technical success or cost targets?

Answer

All of these questions are addressed in Volume 5 of Part 1 and Part 2 of the study, respectively, with the exception of item (g). New technology was not specifically addressed, but one area of significant contribution would be an advanced space shuttle for personnel transportation.

D180-22876-2

(2) OTV – Independently-powered

- (a) What are the expected RDT&E and TFU (Theoretical First Unit) costs of candidate independent cargo OTV's ranging in size from 250 to 1000 metric tons of payload delivered to GEO from LEO?
- (b) To what extent can reflight preparation be accomplished in LEO? What are the facility/manpower/material requirements necessary to achieve reflight?
- (c) How many reflights may be accomplished with each candidate OTV? What changes in reflight costs and mission-completion reliability accrue as the vehicle approaches end-of-life? What is to be the disposition of units which have completed their service life?
- (d) What are the sizes of the staffs required in LEO and on Earth to support the cargo OTV operations (see 1c). How do these manpower levels and costs vary with annual payload to GEO over the range of 40×10^3 to 150×10^3 metric tons per year? How do the LEO facility requirements change over this same range?
- (e) What operational issues emerge consequent to the orbital transfer operations over the range of 2d. above? Launch windows, communication rendezvous and docking requirements, abort, safety, mission planning and control, LEO inventory management all require consideration and development of the associated costs.
- (f) What technical issues emerge for propellant handling and conservation in LEO? Is new technology required or advantageous? What losses may be anticipated of the fluids delivered to LEO?
- (g) What requirements are placed upon the national material resource/refining/ground transportation structure to acquire and operate the fleet of HLLV's for the SPS program? Can material conservation/substitution programs reduce dependence upon scarce or imported resources?
- (h) What new/innovative technology may be developed for use in the 1990-2025 interval (may be several stages, time phased) to enhance the cost-effectiveness or decrease any adverse effects of the launch activity of (1)c).
- (i) What are the presently-expected performance/cost/refurbishment parameters of candidate electrical propulsion thrusters, power conditioners, and power sources? Confidence?

Answer

This question is addressed by Volumes 4 and 5 of Part 1 of the study and Volume 5 of Part 2.

(3) OTV - Dependent Upon SPS Power

- (a) What requirements does the OTV impose upon the SPS (or power producing modules thereof) to permit utilization of the available electrical power for the LEO-GEO transit? Power conditioning, distribution, storage, control, attitude control, structural response and other requirements must be addressed.

D180-22876-2

- (b) What are the developments and unit costs associated with thrusters, dedicated power conditioners, propellant supply and avionic systems if the units are to be:
 - (1) Expended
 - (2) Remain with the SPS and serve as the attitude/orbit maintenance subsystem
 - (3) Recovered to LEO for reuse
- (c) What is necessary to perform the mission from LEO, considering earth occultation? Departure time, date, inclination altitude and thruster system thrust decay power-off all interact.
- (d) Same series of staff level/facility questions as other vehicles.
- (e) Same series of propellant/environmental impact question as others.

Answer

This question is addressed by Volume 5 of Part 1 and Part 2 of the study. Staff levels were not specifically addressed. The space construction facility in low Earth orbit includes capability to install the thrusting system.

(4) Personnel Launch Vehicle

- (a) What can be done to configure the space shuttle orbiter as a personnel launch vehicle? How many passengers? How soon can the shuttle system mature sufficiently to permit this use? At what cost? Is a dedicated orbiter or mission-bit approach preferred?
- (b) What new concepts (SSTO, new shuttle boosters, etc.) compete with the shuttle for this role? What are the cost trade-offs vs. level of activity and time?
- (c) What are the inter-project interfaces with the space evaluation facility (space station) and the PLV? Inter-project issues include safety, rescues, rendezvous docking, etc.

Answer

Item (a)–The space shuttle orbiter in a personnel launch vehicle configuration was discussed in Volume 5 of Part 1 of the study. A passenger capacity of 75 was assumed. It is indicated that a dedicated orbiter would be the preferred approach. Items (b) and (c) under Question 4 were not specifically addressed. Several other studies have addressed new concepts that may compete with the shuttle in this role.

(5) Personnel OTV

- (a) What are the candidate configurations, their technical characteristics and programmatic factors? Can the personnel compartment be the same unit as the personnel compartment of the PLV?
- (b) What are the abort and mission safety considerations?

Answer

Item (a) is addressed in Volume 5 of Part 1 of the study; Item (b) is addressed in Volume 4 of Part 1 of the study.

H. Subprogram Area: Operations

SPS Objective—Achieve the construction in orbit, placement and activation, and maintain the productive capability for 30 years or more, of an operational space power station network in a manner that assures reliable power availability to the ground network at minimum cost to the power consumer.

- (1) What are the construction/assembly/activation/maintenance tasks to be considered for LEO and GEO performance?
- (2) What are the required input of man-hours to perform these tasks? IVA? EVA? Ground support?
- (3) What facilities are required at the construction site to perform the tasks?
- (4) What tools/equipment/consumables are required?
- (5) What is the potential for malfunction/accident during construction? Recovery/work around/salvage?
- (6) What costs are involved in 2, 3, and 4?
- (7) What is the potential for manufacturing SPS components and subassemblies in orbit more productively than on Earth? Crystals, thin film, solid state electronic devices, structural and reflector elements, etc.?
- (8) What are the staffing requirements in orbit and on Earth for representative SPS construction/operations scenario for:
 - (a) LEO construction?
 - (b) GEO construction?
 - (c) LEO construction of modules assembled/deployed at GEO?
- (9) What are the operational considerations of the large manned orbital activities?
 - (a) Personnel support in orbit
 - (b) Personnel support on Earth
 - (c) Communications and data handling
 - (d) Natural and induced environments and protection
 - (e) Induced effects upon the SPS under construction due to operations in orbit? Upon the biosphere?
 - (f) Mission and career constraints upon personnel due to radiation and other factors typical career progression (e.g., what to do with five year men)?
 - (g) Training/simulation/certification/annual check for personnel
 - (h) Costs of all of the above
- (10) What provisions must be made for receipt and disbursement of supplies, expendables, tools, etc. What facility and staff implications are inherent to the large-scale logistics tasks?
- (11) What provisions are necessary for mobility of personnel, equipment, and construction elements? Are these provisions consistent with the work schedule/day-night cycle/SPS vulnerability (to rocket exhausts, torques, etc.)?

D180-22876-2

- (12) What will be the data traffic in orbit—local and remote—how handled?
- (13) What are the key elements of the orbital operations process of the mature SPS which *must* be developed/demonstrated/refined by Earth-orbital precursor projects? How do the shuttle, extended duration (up to 180 days) spacelab, space station, pilot plant contribute to help meet these needs? What funding is needed to support these Earth-orbital precursor projects?
- (14) What ground operations are associated with the rectenna? What operations are needed at the interface with the user?

Answer

Most of the questions under operations are addressed by Volume 3 of Part 1 of the study and Volume 5 of Part 2. The following were specifically not addressed: Question 5, Question 7, Question 9.e, Question 9.f, Question 9.g. Additional work is recommended on Questions 10 and 11. Question 12 was not addressed. Question 13 is addressed under the technology verification program discussed in Section 4 of this volume. Question 14 was not addressed.

I. Subprogram Area: Orbital Technology Verification

SPS Objective—To assure dependable, long-lived operation in the space environment, at viable energy costs to the user.

Pertinent questions derive from the need to operate in the space environment, which has characteristics that include the following:

- (a) Gravity fields of low magnitudes, significant gradients
 - (b) Low absolute pressure, low sink temperature
 - (c) Radiation (particles, photons, ionizing, non-ionizing)
 - (d) Low density plasma
 - (e) Meteoroids
 - (f) Perturbing forces and torques (in addition to the gravity effects) on Earth orbiting bodies
 - (g) Periodic occultation of sun by Earth, when viewed by an Earth orbiting body
- (1) What are the impacts of these (and other relevant) properties of the space environment on SPS design in the nine SPS subprogram areas? Which of these effects can be verified only in space and not on the ground?
- (2) What technology advancements are needed relative to the effects that can be verified only in space?
- (3) What is the impact of the (space-verifiable) effects on the costs of system development and operations?

Answer

The orbital technology verification program is included in the technology verification programs described under Section 4 of this volume.